ISSN 1007-9327 (print)
ISSN 2219-2840 (online)

World Journal of *Gastroenterology*

World J Gastroenterol 2024 April 14; 30(14): 1934-2067

Published by Baishideng Publishing Group Inc

World Journal of Gastroenterology

Contents

Weekly Volume 30 Number 14 April 14, 2024

EDITORIAL

REVIEW

MINIREVIEWS

ORIGINAL ARTICLE

Retrospective Study

Observational Study

World Journal of Gastroenterology

Weekly Volume 30 Number 14 April 14, 2024

Contents

World Journal of Gastroenterology

Weekly Volume 30 Number 14 April 14, 2024

Contents

NAME OF JOURNAL
World Journal of Gastroenterology

ISSN
ISSN 1007-9327 (print) ISSN 2219-2840 (online)

LAUNCH DATE
October 1, 1995

FREQUENCY
Weekly

EDITORS-IN-CHIEF
Andrzej S Tarnawski

EXECUTIVE ASSOCIATE EDITORS-IN-CHIEF
Xian-Jun Yu (Pancreatic Oncology), Jian-Gao Fan (Chronic Liver Disease), Hou-Bao Liu (Biliary Tract Disease)

EDITORIAL BOARD MEMBERS
http://www.wjgnet.com/1007-9327/editorialboard.htm

PUBLICATION DATE
April 14, 2024

COPYRIGHT
© 2024 Baishideng Publishing Group Inc

PUBLISHING PARTNER
Shanghai Pancreatic Cancer Institute and Pancreatic Cancer Institute, Fudan University
Biliary Tract Disease Institute, Fudan University

INSTRUCTIONS TO AUTHORS
https://www.wjgnet.com/bpg/gerinfo/204

GUIDELINES FOR ETHICS DOCUMENTS
https://www.wjgnet.com/bpg/GerInfo/287

GUIDELINES FOR NON-NATIVE SPEAKERS OF ENGLISH
https://www.wjgnet.com/bpg/gerinfo/240

PUBLICATION ETHICS
https://www.wjgnet.com/bpg/GerInfo/288

PUBLICATION MISCONDUCT
https://www.wjgnet.com/bpg/gerinfo/208

POLICY OF CO-AUTHORS
https://www.wjgnet.com/bpg/GerInfo/310

ARTICLE PROCESSING CHARGE
https://www.wjgnet.com/bpg/gerinfo/242

STEPS FOR SUBMITTING MANUSCRIPTS
https://www.wjgnet.com/bpg/GerInfo/239

ONLINE SUBMISSION
https://www.f6publishing.com

PUBLISHING PARTNER's OFFICIAL WEBSITE
https://www.shca.org.cn
https://www.zs-hospital.sh.cn

World Journal of Gastroenterology

Submit a Manuscript: https://www.f6publishing.com

World J Gastroenterol 2024 April 14; 30(14): 1934-1940

DOI: 10.3748/wjg.v30.i14.1934

ISSN 1007-9327 (print) ISSN 2219-2840 (online)

EDITORIAL

Topic highlight on texture and color enhancement imaging in gastrointestinal diseases

Osamu Toyoshima, Toshihiro Nishizawa, Keisuke Hata

Specialty type: Gastroenterology and hepatology

Provenance and peer review: Invited article; Externally peer reviewed.

Peer-review model: Single blind

Peer-review report's scientific quality classification

Grade A (Excellent): 0
Grade B (Very good): B
Grade C (Good): 0
Grade D (Fair): 0
Grade E (Poor): 0

P-Reviewer: Altonbary AY, Egypt

Received: November 30, 2023
Peer-review started: November 30, 2023
First decision: February 2, 2024
Revised: February 3, 2024
Accepted: March 25, 2024
Article in press: March 25, 2024
Published online: April 14, 2024

Osamu Toyoshima, Department of Gastroenterology, Toyoshima Endoscopy Clinic, Tokyo 157-0066, Japan

Toshihiro Nishizawa, Department of Gastroenterology and Hepatology, International University of Health and Welfare, Narita Hospital, Narita 286-8520, Japan

Keisuke Hata, Department of Gastroenterology, Nihonbashi Muromachi Mitsui Tower Midtown Clinic, Tokyo 103-0022, Japan

Corresponding author: Osamu Toyoshima, MD, PhD, Director, Doctor, Department of Gastroenterology, Toyoshima Endoscopy Clinic, 6-17-5, Seijo, Setagaya-ku, Tokyo 157-0066, Japan. t@ichou.com

Abstract

Olympus Corporation developed texture and color enhancement imaging (TXI) as a novel image-enhancing endoscopic technique. This topic highlights a series of hot-topic articles that investigated the efficacy of TXI for gastrointestinal disease identification in the clinical setting. A randomized controlled trial demonstrated improvements in the colorectal adenoma detection rate (ADR) and the mean number of adenomas per procedure (MAP) of TXI compared with those of white-light imaging (WLI) observation (58.7% *vs* 42.7%, adjusted relative risk 1.35, 95%CI: 1.17-1.56; 1.36 *vs* 0.89, adjusted incident risk ratio 1.48, 95%CI: 1.22-1.80, respectively). A cross-over study also showed that the colorectal MAP and ADR in TXI were higher than those in WLI (1.5 *vs* 1.0, adjusted odds ratio 1.4, 95%CI: 1.2-1.6; 58.2% *vs* 46.8%, 1.5, 1.0-2.3, respectively). A randomized controlled trial demonstrated non-inferiority of TXI to narrow-band imaging in the colorectal mean number of adenomas and sessile serrated lesions per procedure (0.29 *vs* 0.30, difference for non-inferiority -0.01, 95%CI: -0.10 to 0.08). A cohort study found that scoring for ulcerative colitis severity using TXI could predict relapse of ulcerative colitis. A cross-sectional study found that TXI improved the gastric cancer detection rate compared to WLI (0.71% *vs* 0.29%). A cross-sectional study revealed that the sensitivity and accuracy for active *Helicobacter pylori* gastritis in TXI were higher than those of WLI (69.2% *vs* 52.5% and 85.3% *vs* 78.7%, respectively). In conclusion, TXI can improve gastrointestinal lesion detection and qualitative diagnosis. Therefore, further studies on the efficacy of TXI in clinical practice are required.

Key Words: Endoscopy; Texture and color enhancement imaging; White-light imaging;

Narrow-band imaging; Colorectal neoplasm; Gastric cancer; Adenoma; Ulcerative colitis; Helicobacter infections; Colonoscopy

Core Tip: Olympus Corporation has developed texture and color enhancement imaging (TXI) as a novel image-enhancing endoscopy technique. This highlights a series of hot-topic articles investigating the usefulness of TXI for gastrointestinal disease diagnosis in clinical practice. TXI showed improvement compared with white-light imaging (WLI) and non-inferiority compared with narrow-band imaging in detecting colorectal neoplasia. TXI observation can predict the relapse of ulcerative colitis. TXI improved gastric cancer detection and diagnostic accuracy for active *Helicobacter pylori* gastritis compared to WLI. In conclusion, TXI can improve detection and qualitative diagnosis.

Citation: Toyoshima O, Nishizawa T, Hata K. Topic highlight on texture and color enhancement imaging in gastrointestinal diseases. *World J Gastroenterol* 2024; 30(14): 1934-1940
URL: https://www.wjgnet.com/1007-9327/full/v30/i14/1934.htm
DOI: https://dx.doi.org/10.3748/wjg.v30.i14.1934

INTRODUCTION

Image-enhanced endoscopy (IEE) improves the diagnosis of gastrointestinal lesions that are challenging in conventional white-light imaging (WLI). Narrow-band imaging (NBI) developing as an IEE modality is effective in diagnosing gastrointestinal disease[1-3]. Following NBI, blue-light imaging and linked color imaging (LCI) have been developed as our new IEE modalities. The utility of BLI and LCI has also been reported extensively[4-6]. Texture and color enhancement imaging (TXI), which is a novel technique to enhance images, was developed in the new endoscopy system EVIS X1 (Olympus Corporation, Tokyo, Japan) in 2020. TXI enhances three image factors, namely texture, brightness, and color, in WLI. This enhancement helps to define subtle tissue differences by applying the retinex-based method. TXI has two modes (*i.e.*, modes 1 and 2). TXI mode 2 is composited with brightness adjustment in dark regions and texture enhancement for subtle contrast. Additionally, TXI mode 1 applies color enhancement to define slight color contrasts more clearly[7,8]. Representative endoscopic images of colonic neoplasm are shown in Figure 1.

Many studies investigating the visibility and color differences of TXI have been published. For example, visibility scores and color differences of TXI for colorectal neoplasia[9-12], gastric neoplasia[13-18], gastritis[13,19], Barrett's esophagus[20,21], pharyngeal and esophageal cancer[22], duodenal neoplasia[23], and the papilla of Vater[24] have been assessed. However, few studies have evaluated the detection and diagnosis of lesions using TXI. Therefore, this study highlights recent reports. We selected six comparative studies that examined the effects of TXI on neoplasia detection, disease prognosis, and diagnostic accuracy (Table 1).

TXI FOR DETECTION OF COLORECTAL NEOPLASIA

Two randomized controlled trials (RCTs) examined the utility of TXI in colorectal neoplasia detection. Antonelli *et al*[25] conducted an international multicenter RCT (Italy, Germany, and Japan) assessing colorectal adenoma detection using TXI compared to WLI. Patients were randomly assigned to two arms, those who underwent colonoscopy using TXI or WLI. A total of 747 patients were enrolled (mean age 62.3 years; 50.2% male). Adenoma detection rate (ADR) was higher in the TXI group compared with the WLI group (58.7% *vs* 42.7%; adjusted relative risk 1.35, 95%CI: 1.17-1.56, $P = 0.001$). The detection rate of adenomas < 10 mm was higher with TXI than with WLI (37.1% *vs* 24.5%). The TXI group had a higher proportion of patients with high-risk polyps compared to the WLI group (26.7% *vs* 19.9%, 1.31, 1.01-1.71, $P = 0.046$). High-risk polyps were defined as at least one adenoma ≥ 10 mm or with high-grade dysplasia, or at least five adenomas, or any serrated polyp ≥ 10 mm or with dysplasia, according to the most recent European Society of Gastrointestinal Endoscopy guideline[26]. The mean number of adenomas per procedure (MAP) with TXI was larger than that with WLI (1.36 *vs* 0.89; adjusted incident risk ratio 1.48, 95%CI: 1.22-1.80, $P < 0.001$). This is the first RCT to compare colorectal neoplasia detection using TXI and WLI. Researchers demonstrated that TXI had a higher ADR than WLI and was useful for colorectal adenoma detection. They also reported that TXI increased the detection rate of small adenomas. Furthermore, TXI provided a larger MAP and a higher high-risk polyp detection rate, indicating that a different surveillance interval after colonoscopy is recommended compared to WLI.

Yoshida *et al*[27] performed a multicenter RCT evaluating the efficacy of an additional 30-s (Add-30-s) observation of the right-sided colon (*i.e.*, cecum to ascending colon) using TXI compared with NBI observation. Patients were assigned to either the TXI or NBI group. The right colon was first observed with WLI in both groups; then, the right colon was examined with Add-30-s observations using either TXI or NBI. Three-hundred fifty-eight patients were enrolled (mean age 68.3 years, 63.4% male). This study showed the non-inferiorities of TXI to NBI (0.29 *vs* 0.30, difference for non-

Table 1 Topic studies on texture and color enhancement imaging

Ref.	Publication year	Study design	Country	No. of patients	Endpoint	Comparison	Main result
Antonelli *et al*[25]	2023	Randomized control study	Italy, Germany, and Japan	747	Detection of colorectal neoplasia	TXI *vs* WLI	Improvement
Yoshida *et al*[27]	2023	Randomized control study	Japan	381	Detection of colorectal neoplasia	TXI *vs* NBI	Non-inferiority
Sakamoto *et al*[28]	2023	Cross-over study	Japan	470	Detection of colorectal neoplasia	TXI *vs* WLI	Improvement
Hayashi *et al*[29]	2023	Cohort study	Japan	146	Relapse of ulcerative colitis	TXI score 2 *vs* TXI scores 0-1	Predictable
Kemmoto *et al*[30]	2024	Cross-sectional study	Japan	13440	Detection of gastric cancer	TXI (mode 2) *vs* WLI	Improvement
Kitagawa *et al*[31]	2023	Cross-sectional study	Japan	60	Diagnostic accuracy for active *Helicobacter pylori* gastritis	TXI (mode 1) *vs* WLI	Improvement

TXI: Texture and color enhancement imaging; WLI: White-light imaging; NBI: Narrow-band imaging.

inferiority -0.01, 95%CI: -0.10 to 0.08, P = 0.02) in the mean number of adenomas and sessile serrated lesions per procedure (MASP). The difference in MAP between TXI and NBI groups was also significant for non-inferiority (0.23 *vs* 0.24, -0.01, -0.09 to 0.007, P = 0.01). Multivariable analyses showed no significant differences in MASPs and MAPs between the TXI and NBI groups, regardless of bowel preparation, endoscopes, and endoscopist level. Increases in the ADR, adenoma and sessile serrated lesion detection rate, and polyp detection rate for the right colon from WLI to TXI were 10.2%, 13.0%, and 15.3%, respectively, and from WLI to NBI were 10.5%, 12.7%, and 13.8%, respectively. The increases in the TXI and NBI groups were not significantly different. This is the first non-inferiority RCT comparing TXI and NBI for colorectal neoplasia detection. The authors recommend that either TXI or NBI be used for Ad-30-s observation.

Sakamoto *et al*[28] conducted a retrospective cross-over study that compared colorectal neoplasia detection using TXI and WLI. They repeated the right colon observation twice with WLI or TXI as the first observation in the WLI and TXI groups, respectively. Then, the right-sided colon was re-examined as a second look using TXI or WLI, whichever was not used for the first observation. The remaining colorectal mucosa was examined using the first observation method. This study included 470 patients (mean age 64.0 years, 64.0% male). Multivariable analyses showed that the MAP and ADR in the TXI group were higher than those in the WLI group (1.5 *vs* 1.0, adjusted odds ratio 1.4, 95%CI: 1.2-1.6, P < 0.001; 58.2% *vs* 46.8%, 1.5, 1.0-2.3, P = 0.044), regardless of patient demographic characteristics, withdrawal time, bowel preparation, and endoscopes. TXI detected more adenomas in the ascending colon with a non-polypoid morphology and a size of 6-9 mm. Fewer non-polypoid lesions were missed in the TXI group than in the WLI group (16.6% *vs* 30.6%). This cross-over study indicated that TXI was more suitable than WLI for the detection of adenomas, especially small non-polypoid adenomas, in the ascending colon.

TXI FOR ULCERATIVE COLITIS

A cohort study established a score using the TXI as a predictor of ulcerative colitis (UC) relapse and investigated its usefulness. Hayashi *et al*[29] did a prospective single-center, single-arm cohort study. They developed the TXI scores as follows: Score 0 = no accentuated redness; score 1 = accentuated redness; and score 2 = accentuated redness and poor visibility of deep vessels. The endoscopic images of 146 patients with UC in remission were reviewed. Patients with a TXI score of 2 had lower UC relapse-free rates than those with TXI scores of 0 and 1 (log-rank test, P < 0.01). When pathologic remission was defined as Matts grade ≤ 2, the rate of pathologic remission decreased with higher TXI scores (TXI score 0, 95.2%; TXI score 1, 67.8%; TXI score 2, 40.0%, respectively, P = 0.01). In multivariate analysis, TXI score 2 was associated with UC relapse (hazard ratio 4.16, 95%CI: 1.72-10.04, P < 0.01), whereas the Mayo endoscopic subscore (MES) was not. Furthermore, the relapse-free rate was lower in MES 1 with a TXI score of 2 than in MES 0 or MES 1 with a TXI score of 0 or 1. The authors concluded that TXI could identify populations with poor prognosis in MES 1, for whom treatment intensification has been controversial.

TXI FOR GASTRIC CANCER AND GASTRITIS

Two studies have investigated the efficacy of TXI in treating gastric lesions. Kemmoto *et al*[30] performed a cross-sectional study analyzing gastric cancer (GC) detection during gastroscopic screening. They compared the GC detection rate in TXI mode 2 with that of the WLI observations. A total of 13440 patients (median age 57 years; 60.6% male) were

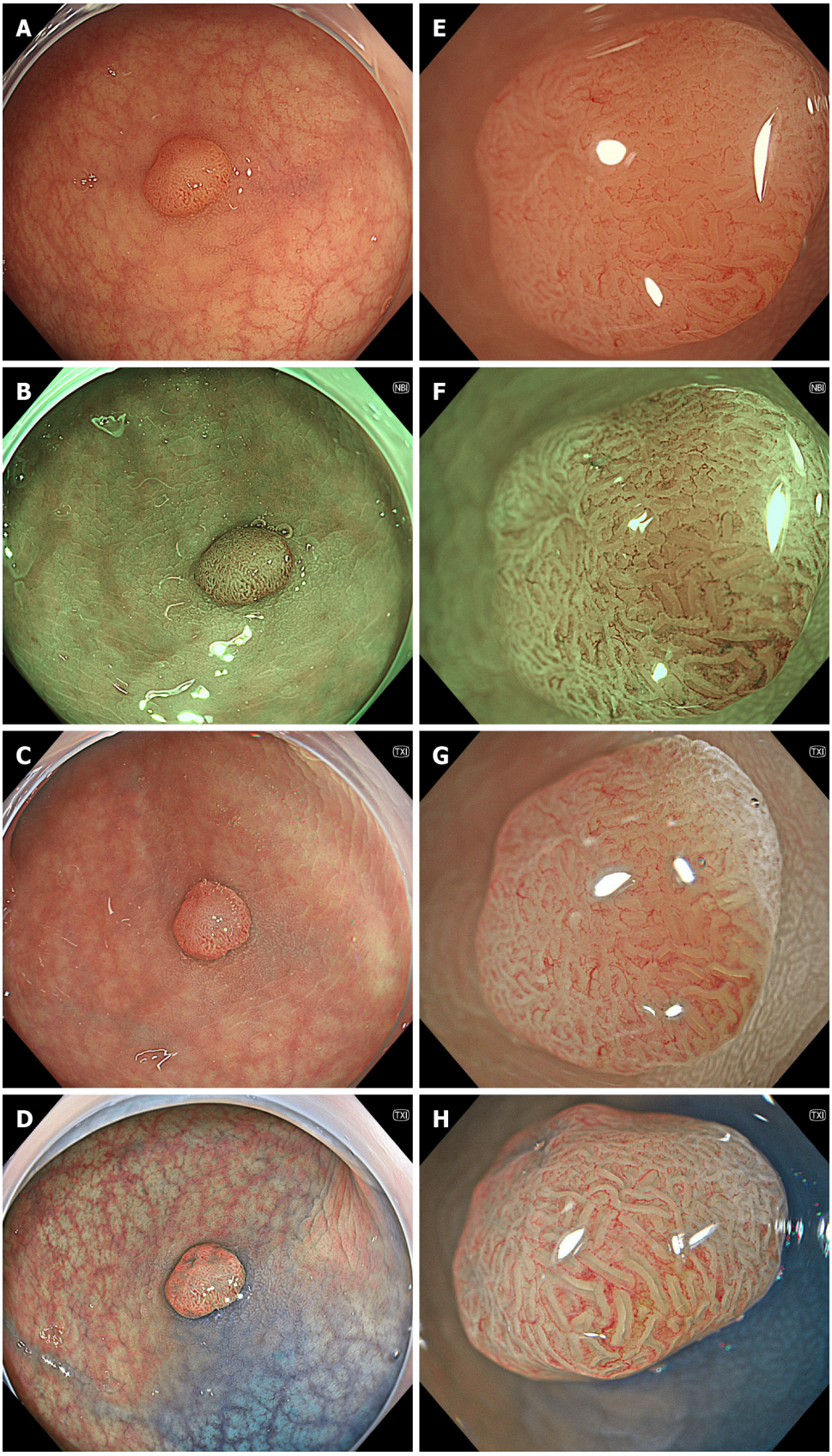

Figure 1 Representative endoscopic images of a colonic adenoma. A-D: Conventional view; E-H: Magnifying view. A and E: White-light imaging; B and F: Narrow-band imaging; C and G: Texture and color enhancement imaging; D and H: Texture and color enhancement imaging with indigo carmine. An Olympus' X1 system and a CF-XZ1200 scope were used.

included in this study. The GC detection rate was higher in the TXI group than in the WLI group (0.71% *vs* 0.29%), especially among patients who had undergone *Helicobacter pylori* (*H. pylori*) eradication (1.36% *vs* 0.43%). The positive predictive value of GC on biopsy was higher in the TXI group than in the WLI group (11.0% *vs* 4.9%). Furthermore, the Expert-WLI group, which was limited to patients who underwent WLI by three endoscopists with the highest GC detection rates, was compared with the TXI group. The detection rates of GC after *H. pylori* eradication in the lower stomach, with 0-IIc endoscopic morphology according to the Paris classification, and with the histologically differentiated type were higher in the TXI group than in the Expert-WLI group (0.87% *vs* 0.17%, 1.36% *vs* 0.43%, and 1.36% *vs* 0.52%, respectively). The authors concluded that TXI mode 2 improved the detection of GC after *H. pylori* eradication in the L-region with superficially depressed and differentiated types. This study demonstrated the usefulness of TXI observation in GC screening.

Kitagawa *et al*[31] examined the diagnostic accuracy of *H. pylori* infections in the stomach. The patients were divided into three groups based on *H. pylori* infection status: Current, past, and non-infection. The diagnostic accuracy for *H. pylori* infection status was compared in TXI with WLI observation. Endoscopic images of 60 patients (median age 73 years; 68.3% male) were reviewed. The sensitivity and accuracy for current *H. pylori* infection in TXI were higher than those of WLI (69.2% *vs* 52.5%, $P = 0.012$; 85.3% *vs* 78.7%, $P = 0.034$). The diagnostic odds ratio of diffuse redness for current infection, map-like redness for past infection, and regular arrangement of collecting venules for non-infection in TXI observation were higher than those in WLI observation (56.21 *vs* 22.00, 10.97 *vs* 6.29, and 42.25 *vs* 25.24, respectively). TXI may be useful for diagnosing *H. pylori* infection during gastroscopy.

CONCLUSION

We have highlighted recent reports examining the usefulness of TXI for gastrointestinal diseases in clinical practice (Table 1). For colorectal neoplasia, an RCT and a cross-over study demonstrated that TXI had a higher ADR and MAP than WLI, and an RCT showed that TXI had non-inferiority to NBI in terms of MASP and MAP. A scoring system using the TXI was shown to be useful in predicting UC relapse in a cohort study. For the stomach, TXI was reported to improve GC detection and diagnostic accuracy of active *H. pylori* gastritis compared to WLI. TXI can selectively enhance brightness in dark areas of an endoscopic image and highlight subtle tissue differences, such as slight morphological or color changes, without over-enhancement[7]. These characteristics of TXI may aid in making more accurate diagnoses.

Further validation of the detection of neoplastic and inflammatory lesions using TXI is required. Furthermore, investigations on whether the use of TXI endoscopy is associated with better patient prognosis are desirable. Studies have shown that endoscopy with magnification, dye spraying[9,10,32,33], and artificial intelligence[34-36] is useful for diagnosing neoplasia and inflammation, and validation of these modalities in combination with TXI is expected. Therapeutic applications of TXI are expected in the future[37]. The two modes of TXI have different features, so they should be separately described in future studies. There have been many reports from Japan, and further international research is required. In conclusion, TXI can improve the detection and qualitative diagnosis of gastrointestinal lesions.

FOOTNOTES

Author contributions: Toyoshima O, Nishizawa T, and Hata K contributed to this paper; Toyoshima O contributed to the design, writing of the manuscript, and review of literature; Nishizawa T and Hata K contributed to the design, discussion, and editing the manuscript.

Conflict-of-interest statement: All the authors report no relevant conflicts of interest for this article.

Country/Territory of origin: Japan

ORCID number: Osamu Toyoshima 0000-0002-6953-6079; Toshihiro Nishizawa 0000-0003-4876-3384; Keisuke Hata 0000-0003-4064-8701.

S-Editor: Li L
L-Editor: A
P-Editor: Yuan YY

REFERENCES

1 **Muto M**, Minashi K, Yano T, Saito Y, Oda I, Nonaka S, Omori T, Sugiura H, Goda K, Kaise M, Inoue H, Ishikawa H, Ochiai A, Shimoda T, Watanabe H, Tajiri H, Saito D. Early detection of superficial squamous cell carcinoma in the head and neck region and esophagus by narrow band imaging: a multicenter randomized controlled trial. *J Clin Oncol* 2010; **28**: 1566-1572 [PMID: 20177025 DOI: 10.1200/JCO.2009.25.4680]

2 **Kobayashi S**, Yamada M, Takamaru H, Sakamoto T, Matsuda T, Sekine S, Igarashi Y, Saito Y. Diagnostic yield of the Japan NBI Expert Team (JNET) classification for endoscopic diagnosis of superficial colorectal neoplasms in a large-scale clinical practice database. *United European Gastroenterol J* 2019; **7**: 914-923 [PMID: 31428416 DOI: 10.1177/2050640619845987]

3 **Cho JH**, Jeon SR, Jin SY, Park S. Standard vs magnifying narrow-band imaging endoscopy for diagnosis of Helicobacter pylori infection and gastric precancerous conditions. *World J Gastroenterol* 2021; **27**: 2238-2250 [PMID: 34025076 DOI: 10.3748/wjg.v27.i18.2238]

4 **Suzuki T**, Hara T, Kitagawa Y, Takashiro H, Nankinzan R, Sugita O, Yamaguchi T. Linked-color imaging improves endoscopic visibility of colorectal nongranular flat lesions. *Gastrointest Endosc* 2017; **86**: 692-697 [PMID: 28193491 DOI: 10.1016/j.gie.2017.01.044]

5 **Fujiyoshi T**, Miyahara R, Funasaka K, Furukawa K, Sawada T, Maeda K, Yamamura T, Ishikawa T, Ohno E, Nakamura M, Kawashima H, Nakaguro M, Nakatochi M, Hirooka Y. Utility of linked color imaging for endoscopic diagnosis of early gastric cancer. *World J Gastroenterol* 2019; **25**: 1248-1258 [PMID: 30886507 DOI: 10.3748/wjg.v25.i10.1248]

6 **Cheema HI**, Tharian B, Inamdar S, Garcia-Saenz-de-Sicilia M, Cengiz C. Recent advances in endoscopic management of gastric neoplasms. *World J Gastrointest Endosc* 2023; **15**: 319-337 [PMID: 37274561 DOI: 10.4253/wjge.v15.i5.319]

7 **Sato T**. TXI: Texture and Color Enhancement Imaging for Endoscopic Image Enhancement. *J Healthc Eng* 2021; **2021**: 5518948 [PMID: 33880168 DOI: 10.1155/2021/5518948]

8 **Wang Y**, Sun CY, Scott L, Wu DD, Chen X. Texture and color enhancement imaging for detecting colorectal adenomas: Good, but not good enough. *World J Gastrointest Endosc* 2022; **14**: 471-473 [PMID: 36051993 DOI: 10.4253/wjge.v14.i7.471]

9 **Nishizawa T**, Toyoshima O, Yoshida S, Uekura C, Kurokawa K, Munkhjargal M, Obata M, Yamada T, Fujishiro M, Ebinuma H, Suzuki H. TXI (Texture and Color Enhancement Imaging) for Serrated Colorectal Lesions. *J Clin Med* 2021; **11** [PMID: 35011860 DOI: 10.3390/jcm11010119]

10 **Toyoshima O**, Nishizawa T, Yoshida S, Yamada T, Odawara N, Matsuno T, Obata M, Kurokawa K, Uekura C, Fujishiro M. Texture and color enhancement imaging in magnifying endoscopic evaluation of colorectal adenomas. *World J Gastrointest Endosc* 2022; **14**: 96-105 [PMID: 35316981 DOI: 10.4253/wjge.v14.i2.96]

11 **Tamai N**, Horiuchi H, Matsui H, Furuhashi H, Kamba S, Dobashi A, Sumiyama K. Visibility evaluation of colorectal lesion using texture and color enhancement imaging with video. *DEN Open* 2022; **2**: e90 [PMID: 35310754 DOI: 10.1002/deo2.90]

12 **Hiramatsu T**, Nishizawa T, Kataoka Y, Yoshida S, Matsuno T, Mizutani H, Nakagawa H, Ebinuma H, Fujishiro M, Toyoshima O. Improved visibility of colorectal tumor by texture and color enhancement imaging with indigo carmine. *World J Gastrointest Endosc* 2023; **15**: 690-698 [PMID: 38187913 DOI: 10.4253/wjge.v15.i12.690]

13 **Ishikawa T**, Matsumura T, Okimoto K, Nagashima A, Shiratori W, Kaneko T, Oura H, Tokunaga M, Akizue N, Ohta Y, Saito K, Arai M, Kato J, Kato N. Efficacy of Texture and Color Enhancement Imaging in visualizing gastric mucosal atrophy and gastric neoplasms. *Sci Rep* 2021; **11**: 6910 [PMID: 33767278 DOI: 10.1038/s41598-021-86296-x]

14 **Abe S**, Yamazaki T, Hisada IT, Makiguchi ME, Yoshinaga S, Sato T, Nonaka S, Suzuki H, Oda I, Saito Y. Visibility of early gastric cancer in texture and color enhancement imaging. *DEN Open* 2022; **2**: e46 [PMID: 35310718 DOI: 10.1002/deo2.46]

15 **Kawasaki A**, Yoshida N, Nakanishi H, Tsuji S, Takemura K, Doyama H. Usefulness of third-generation narrow band imaging and texture and color enhancement imaging in improving visibility of superficial early gastric cancer: A study using color difference. *DEN Open* 2023; **3**: e186 [PMID: 36439990 DOI: 10.1002/deo2.186]

16 **Koyama Y**, Sugimoto M, Kawai T, Mizumachi M, Yamanishi F, Matsumoto S, Suzuki Y, Nemoto D, Shinohara H, Ichimiya T, Muramatsu T, Kagawa Y, Matsumoto T, Madarame A, Morise T, Uchida K, Yamaguchi H, Kono S, Naito S, Fukuzawa M, Itoi T. Visibility of early gastric cancers by texture and color enhancement imaging using a high-definition ultrathin transnasal endoscope. *Sci Rep* 2023; **13**: 1994 [PMID: 36737509 DOI: 10.1038/s41598-023-29284-7]

17 **Shijimaya T**, Tahara T, Uragami T, Yano N, Tokutomi Y, Uwamori A, Nishimon S, Kobayashi S, Matsumoto Y, Nakamura N, Okazaki T, Takahashi Y, Tomiyama T, Honzawa Y, Fukata N, Fukui T, Naganuma M. Usefulness of texture and color enhancement imaging (TXI) in early gastric cancer found after Helicobacter pylori eradication. *Sci Rep* 2023; **13**: 6899 [PMID: 37106009 DOI: 10.1038/s41598-023-32871-3]

18 **Futakuchi T**, Dobashi A, Horiuchi H, Furuhashi H, Matsui H, Hara Y, Kobayashi M, Ono S, Tamai N, Gomisawa K, Yamauchi T, Suka M, Sumiyama K. Texture and color enhancement imaging improves the visibility of gastric neoplasms: clinical trial with image catalogue assessment using conventional and newly developed endoscopes. *BMC Gastroenterol* 2023; **23**: 389 [PMID: 37957560 DOI: 10.1186/s12876-023-03030-9]

19 **Sugimoto M**, Kawai Y, Morino Y, Hamada M, Iwata E, Niikura R, Nagata N, Koyama Y, Fukuzawa M, Itoi T, Kawai T. Efficacy of high-vision transnasal endoscopy using texture and colour enhancement imaging and narrow-band imaging to evaluate gastritis: a randomized controlled trial. *Ann Med* 2022; **54**: 1004-1013 [PMID: 35441573 DOI: 10.1080/07853890.2022.2063372]

20 **Sugimoto M**, Kawai Y, Akimoto Y, Hamada M, Iwata E, Murata M, Mizuno H, Niikura R, Nagata N, Fukuzawa M, Itoi T, Kawai T. Third-Generation High-Vision Ultrathin Endoscopy Using Texture and Color Enhancement Imaging and Narrow-Band Imaging to Evaluate Barrett's Esophagus. *Diagnostics (Basel)* 2022; **12** [PMID: 36553156 DOI: 10.3390/diagnostics12123149]

21 **Ikeda A**, Takeda T, Ueyama H, Uemura Y, Iwano T, Yamamoto M, Uchida R, Utsunomiya H, Oki S, Suzuki N, Abe D, Yatagai N, Akazawa Y, Ueda K, Asaoka D, Shibuya T, Hojo M, Nojiri S, Nagahara A. Comparison of Texture and Color Enhancement Imaging with White Light Imaging in 52 Patients with Short-Segment Barrett's Esophagus. *Med Sci Monit* 2023; **29**: e940249 [PMID: 37309104 DOI: 10.12659/MSM.940249]

22 **Dobashi A**, Ono S, Furuhashi H, Futakuchi T, Tamai N, Yamauchi T, Suka M, Sumiyama K. Texture and Color Enhancement Imaging Increases Color Changes and Improves Visibility for Squamous Cell Carcinoma Suspicious Lesions in the Pharynx and Esophagus. *Diagnostics (Basel)* 2021; **11** [PMID: 34829318 DOI: 10.3390/diagnostics11111971]

23 **Okimoto K**, Matsumura T, Maruoka D, Kurosugi A, Shiratori W, Nagashima A, Ishikawa T, Kaneko T, Kanayama K, Akizue N, Ohta Y, Taida T, Saito K, Kato J, Kato N. Magnified endoscopy with texture and color enhanced imaging with indigo carmine for superficial nonampullary duodenal tumor: a pilot study. *Sci Rep* 2022; **12**: 10381 [PMID: 35725752 DOI: 10.1038/s41598-022-14476-4]

24 **Miyaguchi K**, Mizuide M, Tanisaka Y, Fujita A, Jinushi R, Hiromune K, Ogawa T, Saito Y, Tashima T, Mashimo Y, Imaeda H, Ryozawa S. Distinguishing the papilla of Vater during biliary cannulation using texture and color enhancement imaging: A pilot study. *DEN Open* 2023; **3**: e125 [PMID: 35898835 DOI: 10.1002/deo2.125]

25 **Antonelli G**, Bevivino G, Pecere S, Ebigbo A, Cereatti F, Akizue N, Di Fonzo M, Coppola M, Barbaro F, Walter BM, Sharma P, Caruso A, Okimoto K, Antenucci C, Matsumura T, Zerboni G, Grossi C, Meinikheim M, Papparella LG, Correale L, Costamagna G, Repici A, Spada C, Messmann H, Hassan C, Iacopini F. Texture and color enhancement imaging versus high definition white-light endoscopy for detection of colorectal neoplasia: a randomized trial. *Endoscopy* 2023; **55**: 1072-1080 [PMID: 37451283 DOI: 10.1055/a-2129-7254]

26 **Hassan C**, Antonelli G, Dumonceau JM, Regula J, Bretthauer M, Chaussade S, Dekker E, Ferlitsch M, Gimeno-Garcia A, Jover R, Kalager M, Pellisé M, Pox C, Ricciardiello L, Rutter M, Helsingen LM, Bleijenberg A, Senore C, van Hooft JE, Dinis-Ribeiro M, Quintero E. Post-polypectomy colonoscopy surveillance: European Society of Gastrointestinal Endoscopy (ESGE) Guideline - Update 2020. *Endoscopy* 2020; **52**: 687-700 [PMID: 32572858 DOI: 10.1055/a-1185-3109]

27 **Yoshida N**, Inagaki Y, Inada Y, Kobayashi R, Tomita Y, Hashimoto H, Dohi O, Hirose R, Inoue K, Murakami T, Morimoto Y, Okuyama Y, Morinaga Y, Itoh Y. Additional 30-Second Observation of the Right-Sided Colon for Missed Polyp Detection With Texture and Color Enhancement Imaging Compared with Narrow Band Imaging: A Randomized Trial. *Am J Gastroenterol* 2023 [PMID: 37782280 DOI: 10.14309/ajg.0000000000002529]

28 **Sakamoto T**, Ikematsu H, Tamai N, Mizuguchi Y, Takamaru H, Murano T, Shinmura K, Sasabe M, Furuhashi H, Sumiyama K, Saito Y. Detection of colorectal adenomas with texture and color enhancement imaging: Multicenter observational study. *Dig Endosc* 2023; **35**: 529-537 [PMID: 36398944 DOI: 10.1111/den.14480]

29 **Hayashi Y**, Takabayashi K, Kato M, Tojo A, Aoki Y, Hagihara Y, Yoshida K, Yoshimatsu Y, Kiyohara H, Sugimoto S, Nanki K, Mikami Y, Sujino T, Mutaguchi M, Kawaguchi T, Hosoe N, Yahagi N, Ogata H, Kanai T. Usefulness of texture and color enhancement imaging in assessing mucosal healing in patients with ulcerative colitis. *Gastrointest Endosc* 2023; **97**: 759-766.e1 [PMID: 36460084 DOI: 10.1016/j.gie.2022.11.019]

30 **Kemmoto Y**, Ozawa SI, Sueki R, Furuya K, Shirose D, Wakao S, Shindo K, Nagata A, Sato T. Higher detectability of gastric cancer after Helicobacter pylori eradication in texture and color enhancement imaging mode 2 in screening endoscopy. *DEN Open* 2024; **4**: e279 [PMID: 37529380 DOI: 10.1002/deo2.279]

31 **Kitagawa Y**, Koga K, Ishigaki A, Nishii R, Sugita O, Suzuki T. Endoscopic diagnosis of Helicobacter pylori gastritis using white light imaging and texture and color enhancement imaging. *Endosc Int Open* 2023; **11**: E136-E141 [PMID: 36741344 DOI: 10.1055/a-2005-7486]

32 **Waki K**, Kanesaka T, Michida T, Ishihara R, Tanaka Y. Improved visibility of early gastric cancer by using a combination of chromoendoscopy and texture and color enhancement imaging. *Gastrointest Endosc* 2022; **95**: 800-801 [PMID: 34971670 DOI: 10.1016/j.gie.2021.12.016]

33 **Takabayashi K**, Kato M, Sugimoto S, Yahagi N, Kanai T. Texture and color enhancement imaging in combination with indigo carmine dye spraying to highlight the border of flat ulcerative colitis-associated neoplasia. *Gastrointest Endosc* 2022; **95**: 1273-1275 [PMID: 35181337 DOI: 10.1016/j.gie.2022.02.011]

34 **Joseph J**, LePage EM, Cheney CP, Pawa R. Artificial intelligence in colonoscopy. *World J Gastroenterol* 2021; **27**: 4802-4817 [PMID: 34447227 DOI: 10.3748/wjg.v27.i29.4802]

35 **Taghiakbari M**, Mori Y, von Renteln D. Artificial intelligence-assisted colonoscopy: A review of current state of practice and research. *World J Gastroenterol* 2021; **27**: 8103-8122 [PMID: 35068857 DOI: 10.3748/wjg.v27.i47.8103]

36 **Du RC**, Ouyang YB, Hu Y. Research trends on artificial intelligence and endoscopy in digestive diseases: A bibliometric analysis from 1990 to 2022. *World J Gastroenterol* 2023; **29**: 3561-3573 [PMID: 37389238 DOI: 10.3748/wjg.v29.i22.3561]

37 **Nabi Z**, Chavan R, Ramchandani M, Darisetty S, Reddy DN. Endoscopic submucosal dissection and tunneling procedures using novel image-enhanced technique. *VideoGIE* 2022; **7**: 158-163 [PMID: 35937197 DOI: 10.1016/j.vgie.2021.11.005]

World Journal of Gastroenterology

Submit a Manuscript: https://www.f6publishing.com

World J Gastroenterol 2024 April 14; 30(14): 1941-1948

DOI: 10.3748/wjg.v30.i14.1941

ISSN 1007-9327 (print) ISSN 2219-2840 (online)

EDITORIAL

Immune checkpoint inhibitor-associated gastritis: Patterns and management

Jing Lin, Zhong-Qiao Lin, Shi-Cheng Zheng, Yu Chen

Specialty type: Gastroenterology and hepatology

Provenance and peer review: Invited article; Externally peer reviewed.

Peer-review model: Single blind

Peer-review report's scientific quality classification
Grade A (Excellent): A
Grade B (Very good): 0
Grade C (Good): 0
Grade D (Fair): 0
Grade E (Poor): 0

P-Reviewer: Verma V, United States

Received: December 15, 2023
Peer-review started: December 15, 2023
First decision: February 19, 2024
Revised: February 23, 2024
Accepted: March 28, 2024
Article in press: March 28, 2024
Published online: April 14, 2024

Jing Lin, Yu Chen, Department of Medical Oncology, Clinical Oncology School of Fujian Medical University, Fujian Cancer Hospital, Fuzhou 350000, Fujian Province, China

Zhong-Qiao Lin, Phase I Clinical Trial Ward, Clinical Oncology School of Fujian Medical University, Fujian Cancer Hospital, Fuzhou 350000, Fujian Province, China

Shi-Cheng Zheng, School of Basic Medical Sciences, Fujian Medical University, Fuzhou 350000, Fujian Province, China

Corresponding author: Yu Chen, MD, Chief Doctor, Department of Medical Oncology, Clinical Oncology School of Fujian Medical University, Fujian Cancer Hospital, No. 420 Fumu Road, Jin'an District, Fuzhou 350000, Fujian Province, China. chenyu1980@fjmu.edu.cn

Abstract

Immune checkpoint inhibitors (ICIs) are widely used due to their effectiveness in treating various tumors. Immune-related adverse events (irAEs) are defined as adverse effects resulting from ICI treatment. Gastrointestinal irAEs are a common type of irAEs characterized by intestinal side effects, such as diarrhea and colitis, which may lead to the cessation of ICIs. Although irAE gastritis is rarely reported, it may lead to serious complications such as gastrorrhagia. Furthermore, irAE gastritis is often difficult to identify early due to its diverse symptoms. Although steroid hormones and immunosuppressants are commonly used to reverse irAEs, the best regimen and dosage for irAE gastritis remains uncertain. In addition, the risk of recurrence of irAE gastritis after the reuse of ICIs should be considered. In this editorial, strategies such as early identification, pathological diagnosis, management interventions, and immunotherapy rechallenge are discussed to enable clinicians to better manage irAE gastritis and improve the prognosis of these patients.

Key Words: Immunotherapy; Immune checkpoint inhibitor; Immune-related adverse events; Immune checkpoint inhibitor-related gastritis

Core Tip: Immune checkpoint inhibitor (ICI)-related gastritis is rare but may lead to serious complications such as gastrorrhagia. Biopsy under esophagogastroduodenoscopy is the gold standard for diagnosis. Specifically, this article discusses strategies for treating ICI-related gastritis, including early recognition, pathological diagnosis, management interventions, and rechallenge with immunotherapy, providing clinicians with valuable consultations to enable cancer patients to benefit early from treatment.

Citation: Lin J, Lin ZQ, Zheng SC, Chen Y. Immune checkpoint inhibitor-associated gastritis: Patterns and management. *World J Gastroenterol* 2024; 30(14): 1941-1948
URL: https://www.wjgnet.com/1007-9327/full/v30/i14/1941.htm
DOI: https://dx.doi.org/10.3748/wjg.v30.i14.1941

INTRODUCTION

Immunotherapy has been shown to have great efficacy in treatment of multiple kinds of cancers by inhibiting the downregulation of T-cell-mediated destruction and promoting the patient's immune system to target and destroy cancer cells. Immune checkpoint inhibitors (ICIs), which are programmed cell death protein 1/programmed cell death ligand 1 (PD-1/PD-L1) and cytotoxic T lymphocyte-associated protein 4 (CTLA-4) inhibitors, are common pharmacotherapeutics for immunotherapy and improve survival across a range of malignancies. While the inhibition of these proteins reinvigorates the host antitumor immune response, broad inhibition of these central immune regulators leads to a unique spectrum of immune-related adverse events (irAEs), and gastrointestinal (GI)-irAEs are among the most common toxicities of current ICIs. The side effects affecting the distal gastrointestinal tract, including colitis and diarrhea, are well recognized. However, gastritis induced by immune checkpoint inhibitors has also been described. Gastritis is a broad category of diagnosis that stems from inflammation to the gastric mucosa that can lead to nausea, vomiting, abdominal pain, and weight loss. This editorial focuses on early identification, pathological diagnosis, management interventions, and immunotherapy rechallenge of irAE gastritis to enable clinicians to better manage irAE gastritis and improve the prognosis of these patients.

INCIDENCE, TIME-TO-ONSET AND SEVERITY

Overall, GI-irAEs occurred in approximately 6.5% to 8.4% of patients receiving monotherapy ICIs[1,2]. ICI-related gastritis has a lower occurrence. Several retrospective studies based on large samples have reported an incidence of approximately 0.35%-1.46%[3-6]. The time-to-onset is highly variable, with a wide range of 2 wk to 156 wk, and the median time was calculated as 29.3 wk[7]. The incidence of GI-irAEs of ICI combined therapy occurred at 6-8 wk after the start of ICI treatment, which was much earlier than ICI monotherapy[8]. Furthermore, combined therapy with anti-PD1/PD-L1 and anti-CTLA-4 agents led to higher rates of GI-irAEs than anti-PD1/PD-L1 or anti-CTLA-4 monotherapy (15% *vs* 4% and 12%, respectively)[9-13]. There was also a positive association between increasing doses of ICIs and the incidence and severity of GI-irAEs, especially in anti-CTLA-4 monotherapy and combined therapy of anti-PD1/PD-L1 and anti-CTLA-4 agents[14-17]. The severity grades of ICI-related gastritis are based on the Common Terminology Criteria for Adverse Events (CTCAE)[18]. In patients with grade 1 gastritis, upper gastrointestinal symptoms are not obvious and are often detected inadvertently. ICI-related gastritis of CTCAE grade 2-3 has been reported most often (more than 75%), requiring the cessation of ICIs and steroid intervention[19].

Patients with a history of gastrointestinal disease are more likely to develop ICI-related gastritis after immunotherapy. One study revealed that in 54 patients with ICI-related gastritis, thirteen (24%) had a history of gastroesophageal and liver disorders, and nine of thirteen had former gastroesophageal reflux disease[4]. Previous medications that potentially damage the stomach should be assessed in patients with ICI-related gastritis. In a total of 25 patients with ICI-related gastritis, 3 (12%) patients had a history of nonsteroidal anti-inflammatory drug (NSAID) use, and 11 (44%) patients had received chemotherapy, radiation, or combined therapy[3]. A shorter onset time of 2.0 wk was observed in those patients, and they all had grade-2 or higher adverse events (AEs) that required prednisolone (PSL) therapy.

SYMPTOMS AND CLINICAL EXAMINATIONS

Clinical symptoms of ICI-related gastritis are diverse; they can be covered by the delayed or cumulative effect of previous treatment lines or can be neglected when coexisting with other lower GI tract toxicities, which makes diagnosis challenging. Nausea/vomiting and abdominal pain are most commonly seen in patients with ICI-related gastritis. High-dose, short-interval administration of pembrolizumab increases the frequency of nausea and vomiting[20]. Sometimes, nausea/vomiting may be the only discomfort, digestive discomfort may be absent, so the occurrence of ICI-related gastritis should be determined in patients receiving immunotherapy under this circumstance. Dyspepsia (38%) and bloating (25%) are also observed in patients with ICI-related gastritis. Compared with patients with concomitant

enteritis/colitis, patients with isolated gastritis were less likely to have diarrhea (13% *vs* 68%; $P < 0.001$) or abdominal pain (19% *vs* 47%; $P = 0.07$)[4].

In general, serological evidence is still insufficient. Laboratory findings for most patients were not clinically significant, or they had mild anemia and malnutrition. Elevated C-reactive protein (CRP) was observed in several patients, but their WBC counts were within normal limits. However, in two reported cases, patients with severe eosinophilia and increased IgE and IL-5 levels showed eosinophilic infiltration on histology. Several serum biomarkers have been shown to predict ICI-related colitis. An increase in the serum IL-17 concentration at baseline with an exponential elevation at six weeks is a good indicator for ICI-diarrhea/colitis, and an decrease in the serum IL-17 concentration correlates with the resolution of symptoms, making it a valuable indicatior of treatment response[21]. High sCTLA-4 serum levels might predict favorable clinical outcomes and greater risk of irAEs in MM patients treated with ipilimumab[22]. Currently, there is no specific index to demonstrate ICI-related gastritis in an early stage.

Abdominal computed tomography (CT) is often unremarkable, with only a few patients displaying thickening of the gastric wall[7]. PET-CT can reveal diffuse fluorodeoxyglucose accumulation in the stomach wall, but it is poorly distinguished from metastasis[23-25]. Esophagogastroduodenoscopy (EGD) can reveal gastritis, duodenitis [frequently without *Helicobacter pylori* (*H. pylori*) infection], esophageal or gastric ulcers, ileitis, or enterocolitis[11]. Erythema (64%-88%) and edema (46%-52%) of the gastric mucosa are typical findings under EGD[3,26]. In patients with grade-3 ICI gastritis, hemorrhagic and fragile mucosa, network-pattern erosion or ulcers in the antrum have also been observed[6,27]. However, histological examination or endoscopic ultrasonography may show prominent characteristics of autoimmune gastritis, although there are no typical gastroscopic characteristics or clinical symptoms. Some reports have indicated a weak correlation between gastroscopic and histological findings in PD-1-induced gastritis[28,29]. Approximately 10%-20% of patients have endoscopically normal gastric tissue despite biopsy–proven ICI-related gastritis[4]. Thus, in patients with suspected PD-1-induced gastritis, a complete workup is necessary for diagnosis, especially stomach biopsy. Furthermore, patients with isolated ICI-realted gastritis exhibit a trend toward greater endoscopic severity of gastric inflammation (erosions/ulcerations/severe erythema *vs* mild erythema/normal) than those with concurrent enteritis/colitis ($P = 0.12$)[4]. Gastric biopsies in patients with endoscopic lesions often show pathohistological manifestations of active gastritis or chronic active pangastritis. Lymphoplasmacytic and granulocytic infiltration with scattered eosinophils in the lamina propria and epithelium, diffuse inflammation and crypt abscesses are usually observed[23,26,27,30-32]. Further immunohistochemical analysis demonstrated that the infiltrating lymphocytes were positive for CD3, with CD8+ prevailing over CD4+ but negative for CD20, and PD-L1 was positive in immune cells and/or epithelial cells[6,33]. The involvement of limited areas of the GI tract, such as the duodenum, stomach, ileum, or colon, suggests an underlying immune mechanism directed toward epitopes specific to this location.

Autoimmune gastritis or ICI-induced autoimmune-like gastritis need to be differentiated. A marked reduction in acid-secreting cells and destruction of the glands in the background of diffuse lymphoplasmacytic infiltration are typical manifestations of autoimmune gastritis under EGD[34]. In addition, peripheral blood is positive for B-cell antibodies, with concomitant pernicious anemia. ICI-associated immune gastritis also needs to be distinguished from *H. pylori* gastritis and cytomegalovirus gastritis. Unlike ICI-associated gastritis, *H. pylori* gastritis is characterized by significantly lower numbers of intraepithelial lymphocytes, more lamina propria inflammation, and more lymphoid aggregates[35]. However, lymphocyte phenotyping of *H. pylori* gastritis and nivolumab gastritis showed no difference in the number of lamina propria CD4+ cells or CD8+ cells[35]. A C-13 or C-14 blow test is a noninvasive method for differentiation of *H. pylori* infection. Cytomegalovirus (CMV) gastritis after immunotherapy has been reported, and a CMV inclusion body inside the cytoplasm is a hallmark[36]. Notably, autoimmune gastritis may be concurrent with *H. pylori* and/or CMV infection. For patients in whom *H. pylori* gastritis and CMV gastritis are initially excluded but symptoms worsen after steroid therapy, another EGD should be performed to exclude opportunistic *H. pylori* or CMV infection. In addition, gastric metastases can be seen as hemorrhagic, ulcer and fragile mucosa, which need to be differentiated from gastritis[37,38], and pathological biopsy to find tumor cells is well suited for identification.

POSSIBLE MECHANISM

The detailed mechanisms underlying ICI-related gastritis are poorly understood. A common view is that ICIs increase T-cell activation and proliferation, abrogate Treg functions, and possibly boost humoral autoimmunity, which results in irAEs[39]. Moreover, CTLA-4 inhibitors increase the number of circulating Th17 cells, decrease the number of circulating Tregs and contribute to irAEs[40-42]. PD-1/PD-L1 inhibitors regulate Tregs *via* deficient differentiation from Th1 cells to Treg cells, reducing the immunosuppressive effect of Treg cells and enhancing T-cell activation[33,43]. All these imbalances result in enhanced CD4+ and CD8+ T-cell activation and drive destruction of normal cells[44]. Furthermore, CTLA-4 and PD-1/PD-L1 inhibition results in increased cytokine production, such as TNF, IFN-γ and IL-17, which further leads to T-cell proliferation and activation as well as proinflammatory effects[39].

A common histological feature is an increase in CD8+ T cells but a decrease in CD4+ T cells. Hence, there is a hypothesis that PD-1 inhibitors promote gastritis through weak expression of CD4+ Treg cells and disturbed immune tolerance; strong expression of CD8+ T cells enhances the effect of cytotoxic T lymphocytes in attacking autologous organs[33]. Additionally, as PD-L1 is expressed in immune cells and/or epithelial cells, a novel hypothesis is that T cells actively attack antigens present on gastric epithelial cells, which exacerbates gastritis, but this needs to be assessed in a case-control study[6].

TREATMENTS FOR ICI-RELATED GASTRITIS

Because of the scarcity of prospective trials on drug immunosuppression in the setting of ICI-related gastritis, no guidelines exist for management, and clinicians can only seek information from small series studies and case reports on how to handle these challenging cases. Treatment decisions for ICI-related gastritis are based on individual clinical presentations. A wait and watch approach can be used for patients with EGD without symptoms[45]. Immunotherapy is often stopped after ≥ grade 2 gastritis occurs[7,46]. In several patients with isolated gastritis, symptoms have improved after PPI treatment alone[4]. However, in most cases, steroids are the first-line empirical agent. Indeed, early use and high doses of prednisone (1-2 mg/kg/d) lead to a favorable prognosis, with only 16.7% clinical recurrence[19]. Steroids can attenuate the CD28 signaling pathway and CD80 co-stimulation that partly impairs T-cell function[47]. With ICI cessation, use of prednisone and proton pump inhibitors, symptoms of ICI-related gastritis can rapidly subside within a week, but complete resolution under EGD will take months[3,31,48,49], and the longest remission is reported at 66 wk [50]. The use of steroids, most commonly prednisone, begins to taper when clinical symptoms reduce to grade 1, and *Pneumocystis Carinii* pneumonia and *Fungal* infections should be necessarily prevented for long-term steroid therapy (≥ 4 wk)[51-53]. For patients who have concomitant CMV infection, symptom improvement can be achieved with active antiviral treatment[49]. If no improvement is noted within 2 to 3 d on intravenous steroids (1-2 mg/kg/d), immunosuppression agents, such as TNF-α (*e.g.*, infliximab) or integrin blockers (*e.g.*, vedolizumab), can be used for this type of steroid-resistant gastritis. Retrospective data from a large cohort study of cancer patients administered ipilimumab reported that 103 (35%) of 298 patients received corticosteroids to manage an irAE and that 29 (10%) of 298 needed additional immunosuppressive drugs[54]. Vedolizumab can be used in treating steroid-refractory GI-irAEs. One study showed that 24 of 28 patients with steroid-resistant ICI-related colitis who received vedolizumab achieved clinical remission; 12 patients with EGD monitoring had nonulcerative inflammation or no signs by the last repeat EGD[55]. Patients with GI-irAEs who were initiated on infliximab within 14 d of starting steroids had good resolution, and the average time to infliximab response was 17 d[56]. Infliximab has been reported to be effective against steroid-resistant gastritis in several case reports[23,26,57], such as one patient whose symptoms did not resolve after 6 d of high-dose steroid treatment but improved significantly after 2 doses of infliximab (2-wk regimen)[23]. The duration of therapy with a TNF-α blocker (infliximab) or an integrin blocker (vedolizumab) is not clearly defined. Evidence supports use of up to 3 doses (at weeks 0, 2, and 6) to reduce risk of recurrence and increase the likelihood of endoscopic/histologic remission [58]. In addition, active parenteral nutrition, such as water and electrolyte balance and energy supplementation, preventive anti-infection treatment when needed, and symptomatic management, are important.

Despite the lack of prospective data, retrospective studies have shown that the use of steroids and immunosuppressants after irAEs does not reduce the efficacy of ICIs[53]. In 54 patients with ICI-related gastritis, the overall response rate and disease control rate were 52% and 74%, respectively, after immunotherapy[4]. Patients who developed GI-irAEs experienced a better response to ICI therapy than those who did not develop GI-irAEs (41% *vs* 27%, $P = 0.003$)[32]. Development of GI-irAEs was also associated with better overall survival[5]. However, for ICI-related gastritis, it is still unclear whether the occurrence of ICI-related gastritis correlates positively with better outcomes. Nevertheless, there was no clear correlation between the endoscopic severity or extent of inflammation and the response to ICIs ($P = 0.85$ and $P = 0.44$, respectively)[4]. More evidence is needed for better support.

RECHALLENGING IMMUNE CHECKPOINT INHIBITORS

After the complete resolution of irAEs, resumption of immunotherapy is of crucial importance for treatment and patient prognosis, as is the risk of relapse of irAEs. The recurrence rate of all kinds of irAEs is reported to be 28.6% after anti-PD-1 monotherapy resumption, 47.4% after anti-CTLA-4 monotherapy resumption, and 43.5% after combination therapy resumption in patients with various cancers[59]. A retrospective study reported that a lower recurrence rate of GI-IrAEs was found in 23.1% (6/26) of patients receiving another course of ICIs, 95% (25/26) of patients treated with anti-PD-1 as second-line therapy had no relapse within 3 months, and 88% (23/26) of patients had no relapse within one year[8]. Among the six patients who relapsed with the second ICI, the recurrence severity was grade I for 2/6 (33%), grade II for 2/6 (33%) and grade IV for 2/6 (33%); the outcome was favorable with medical treatment[8]. However, the incidence of recurrent ICI-related gastritis remains uncertain. Two studies demonstrated that 5 patients who recovered from ICI-related gastritis restarted immunotherapy without any recurrence of irAEs[60,61]. There is also a report of two patients who experienced recurrence of ICI gastritis at 10 to 12 wk after rechallenge with anti-PD-1 monotherapy, and EGD findings indicated milder lesions than those occurred during the first time (erythematous and edematous vs. network-pattern erosion or ulceration and fragile mucosa)[6]. A high possibility is increased awareness of ICI-related gastritis and EGD performed at an earlier stage. Moreover, it should be noted that patients with irAEs may experience autoimmune damage in other systems after restarting immunotherapy. According to a pharmacovigilance database review, when rechallenged after ICI discontinuation for irAEs ≥ grade 2, 39% experienced another ≥ grade 2 irAE at relapse[62].

In general, whether and when to restart ICI treatment should be based on the conditions. Limited data are available to support clinicians' decisions. Available data on the timing of ICI resumption after the first irAE show that it ranges from a median of 14 d to 60 wk[63]. One study involving ten patients with ICI-related gastritis found a median time of 2.8 months (range: 1.0-35.8) between treatment discontinuation and resumption of ICIs[27]. However, as complete resolution of symptoms will require a couple of months and the longest duration for resolution of inflammation is reported to be 66 wk, a new EGD examination or biopsy needs to be performed for confirmation before resumption of ICI treatment. Furthermore, the duration of steroid tapering, severity of initial irAEs and use of additional immunosuppressants do not

predict toxicity upon rechallenge, but patients who remain on steroid therapy at the time of anti-PD-1 therapy resumption have high rates of toxicity (55% *vs* 31%, $P = 0.03$)[64]. Moreover, the time of the first appearance of irAEs may help to predict their recurrence. Compared with the nonrecurrent group, the recurrent group had a shorter average time to first irAEs (9 wk *vs* 15 wk)[65]. Fecal calprotectin and lactoferrin are good biomarkers for monitoring irAE-colitis with rechallenge ICI therapy, but there is no biomarker to predict recurrence of ICI-related gastritis at present[66].

CONCLUSION

In conclusion, ICI-related gastritis is rare and should be suspected in patients with recurrent upper gastrointestinal symptoms and a history of immunotherapy. Adopting a proactive monitoring strategy is expected to reduce the occurrence of severe immune gastritis. EGD examination and biopsy are needed to confirm ICI-related gastritis. Early and adequate glucocorticoids can improve prognosis, and recommendation for re-examination of EGD before restarting ICI therapy. Furthermore, proper management of severe irAEs requires the efficient response and concerted decision of multidisciplinary teams. Such efforts will ensure that patients with cancer benefit from the highest quality of care as immunotherapy continues to evolve.

FOOTNOTES

Co-first authors: Jing Lin and Zhong-Qiao Lin.

Author contributions: Lin J and Lin ZQ contributed equally to this work; Lin J designed the study and revised the manuscript; Lin ZQ performed the research and wrote the manuscript; Zheng SC wrote the manuscript and contributed on funding; Chen Y revised and supervised the manuscript, and contributed on funding; All authors have read and approve the final manuscript.

Supported by Joint Funds for the Innovation of Science and Technology, Fujian Province, China, No. 2021Y9227; Natural Science Foundation of Fujian Province, China, No. 2023J011254; The Science Foundation for The Excellent Youth Scholars of Fujian Provincial Health Commission, China, No. 2022ZQNZD009; The Special Research Funds for Local Science and Technology Development Guided by Central Government, Fujian Province, China, No. 2023L3020; and Fujian Medical University Student Innovation and Entrepreneurship Training Project, China, No. JC2023191.

Conflict-of-interest statement: All authors have no conflicts of interests.

Country/Territory of origin: China

ORCID number: Jing Lin 0000-0002-9025-1721; Zhong-Qiao Lin 0000-0002-5539-1526; Yu Chen 0000-0003-4293-1324.

S-Editor: Gong ZM
L-Editor: A
P-Editor: Yuan YY

REFERENCES

1 **Yamada K**, Sawada T, Nakamura M, Yamamura T, Maeda K, Ishikawa E, Iida T, Mizutani Y, Kakushima N, Ishikawa T, Furukawa K, Ohno E, Honda T, Kawashima H, Ishigami M, Furune S, Hase T, Yokota K, Maeda O, Hashimoto N, Akiyama M, Ando Y, Fujishiro M. Clinical characteristics of gastrointestinal immune-related adverse events of immune checkpoint inhibitors and their association with survival. *World J Gastroenterol* 2021; **27**: 7190-7206 [PMID: 34887637 DOI: 10.3748/wjg.v27.i41.7190]

2 **Thapa B**, Roopkumar J, Kim AS, Gervaso L, Patil PD, Calabrese C, Khorana AA, Funchain P. Incidence and clinical pattern of immune related adverse effects (irAE) due to immune checkpoint inhibitors (ICI). *J Clin Oncol* 2019; **37**: e14151-e14151 [DOI: 10.1200/JCO.2019.37.15_suppl.e14151]

3 **Farha N**, Faisal MS, Allende DS, Sleiman J, Shah R, Farha N, Funchain P, Philpott JR. Characteristics of Immune Checkpoint Inhibitor-Associated Gastritis: Report from a Major Tertiary Care Center. *Oncologist* 2023; **28**: 706-713 [PMID: 36905577 DOI: 10.1093/oncolo/oyad031]

4 **Haryal A**, Townsend MJ, Baskaran V, Srivoleti P, Giobbie-Hurder A, Sack JS, Isidro RA, LeBoeuf NR, Buchbinder EI, Hodi FS, Grover S. Immune checkpoint inhibitor gastritis is often associated with concomitant enterocolitis, which impacts the clinical course. *Cancer* 2023; **129**: 367-375 [PMID: 36377339 DOI: 10.1002/cncr.34543]

5 **Alomari M**, Al Ashi S, Chadalavada P, Khazaaleh S, Covut F, Al Momani L, Elkafrawy A, Padbidri V, Funchain P, Campbell D, Romero-Marrero C. Gastrointestinal Toxicities of Immune Checkpoint Inhibitors Are Associated With Enhanced Tumor Responsiveness and Improved Survival. *Gastroenterology Res* 2022; **15**: 56-66 [PMID: 35572476 DOI: 10.14740/gr1491]

6 **Sugiyama Y**, Tanabe H, Matsuya T, Kobayashi Y, Murakami Y, Sasaki T, Kunogi T, Takahashi K, Ando K, Ueno N, Kashima S, Moriichi K, Tanino M, Mizukami Y, Fujiya M, Okumura T. Severe immune checkpoint inhibitor-associated gastritis: A case series and literature review. *Endosc Int Open* 2022; **10**: E982-E989 [PMID: 35845030 DOI: 10.1055/a-1839-4303]

7 **Woodford R**, Briscoe K, Tustin R, Jain A. Immunotherapy-related gastritis: Two case reports and literature review. *Clin Med Insights Oncol* 2021; **15**: 11795549211028570 [PMID: 34290539 DOI: 10.1177/11795549211028570]

8 **de Malet A**, Antoni G, Collins M, Soularue E, Marthey L, Vaysse T, Coutzac C, Chaput N, Mateus C, Robert C, Carbonnel F. Evolution and recurrence of gastrointestinal immune-related adverse events induced by immune checkpoint inhibitors. *Eur J Cancer* 2019; **106**: 106-114 [PMID: 30476730 DOI: 10.1016/j.ejca.2018.10.006]

9 **Morganstein DL**, Lai Z, Spain L, Diem S, Levine D, Mace C, Gore M, Larkin J. Thyroid abnormalities following the use of cytotoxic T-lymphocyte antigen-4 and programmed death receptor protein-1 inhibitors in the treatment of melanoma. *Clin Endocrinol (Oxf)* 2017; **86**: 614-620 [PMID: 28028828 DOI: 10.1111/cen.13297]

10 **Osorio JC**, Ni A, Chaft JE, Pollina R, Kasler MK, Stephens D, Rodriguez C, Cambridge L, Rizvi H, Wolchok JD, Merghoub T, Rudin CM, Fish S, Hellmann MD. Antibody-mediated thyroid dysfunction during T-cell checkpoint blockade in patients with non-small-cell lung cancer. *Ann Oncol* 2017; **28**: 583-589 [PMID: 27998967 DOI: 10.1093/annonc/mdw640]

11 **Rajha E**, Chaftari P, Kamal M, Maamari J, Chaftari C, Yeung SJ. Gastrointestinal adverse events associated with immune checkpoint inhibitor therapy. *Gastroenterol Rep (Oxf)* 2020; **8**: 25-30 [PMID: 32104583 DOI: 10.1093/gastro/goz065]

12 **Collins M**, Michot J-M, Danlos F-X, Champiat S, Mussini C, Soularue E, Mateus C, Loirat D, Anthony B, Rosa I, Lambotte O, Laghouati S, Voisin AL, Soria JC, Marabelle A, Robert C, Carbonnel F. P315 Gastrointestinal immune related adverse events associated with programmed-Death 1 blockade. *J Crohns Colitis* 2017; **11**: S237-S237 [DOI: 10.1093/ecco-jcc/jjx002.440]

13 **Wolchok JD**, Chiarion-Sileni V, Gonzalez R, Rutkowski P, Grob JJ, Cowey CL, Lao CD, Wagstaff J, Schadendorf D, Ferrucci PF, Smylie M, Dummer R, Hill A, Hogg D, Haanen J, Carlino MS, Bechter O, Maio M, Marquez-Rodas I, Guidoboni M, McArthur G, Lebbé C, Ascierto PA, Long GV, Cebon J, Sosman J, Postow MA, Callahan MK, Walker D, Rollin L, Bhore R, Hodi FS, Larkin J. Overall Survival with Combined Nivolumab and Ipilimumab in Advanced Melanoma. *N Engl J Med* 2017; **377**: 1345-1356 [PMID: 28889792 DOI: 10.1056/NEJMoa1709684]

14 **Wolchok JD**, Neyns B, Linette G, Negrier S, Lutzky J, Thomas L, Waterfield W, Schadendorf D, Smylie M, Guthrie T Jr, Grob JJ, Chesney J, Chin K, Chen K, Hoos A, O'Day SJ, Lebbé C. Ipilimumab monotherapy in patients with pretreated advanced melanoma: a randomised, double-blind, multicentre, phase 2, dose-ranging study. *Lancet Oncol* 2010; **11**: 155-164 [PMID: 20004617 DOI: 10.1016/S1470-2045(09)70334-1]

15 **Hodi FS**, Chesney J, Pavlick AC, Robert C, Grossmann KF, McDermott DF, Linette GP, Meyer N, Giguere JK, Agarwala SS, Shaheen M, Ernstoff MS, Minor DR, Salama AK, Taylor MH, Ott PA, Horak C, Gagnier P, Jiang J, Wolchok JD, Postow MA. Combined nivolumab and ipilimumab versus ipilimumab alone in patients with advanced melanoma: 2-year overall survival outcomes in a multicentre, randomised, controlled, phase 2 trial. *Lancet Oncol* 2016; **17**: 1558-1568 [PMID: 27622997 DOI: 10.1016/S1470-2045(16)30366-7]

16 **Jiang Y**, Zhang N, Pang H, Gao X, Zhang H. Risk and incidence of fatal adverse events associated with immune checkpoint inhibitors: a systematic review and meta-analysis. *Ther Clin Risk Manag* 2019; **15**: 293-302 [PMID: 30858709 DOI: 10.2147/TCRM.S191022]

17 **Chang CY**, Park H, Malone DC, Wang CY, Wilson DL, Yeh YM, Van Boemmel-Wegmann S, Lo-Ciganic WH. Immune Checkpoint Inhibitors and Immune-Related Adverse Events in Patients With Advanced Melanoma: A Systematic Review and Network Meta-analysis. *JAMA Netw Open* 2020; **3**: e201611 [PMID: 32211869 DOI: 10.1001/jamanetworkopen.2020.1611]

18 **U.S. Department of Health and Human Services**. Common Terminology Criteria for Adverse Events (CTCAE) Version 5.0. National Institutes of Health, National Cancer Institute 2017. Available from: https://ctep.cancer.gov/protocoldevelopment/electronic_applications/docs/ctcae_v5_quick_reference_5x7.pdf

19 **Obeidat A**, Silangcruz K, Kozai L, Wien E, Fujiwara Y, Nishimura Y. Clinical Characteristics and Outcomes of Gastritis Associated With Immune Checkpoint Inhibitors: Scoping Review. *J Immunother* 2022; **45**: 363-369 [PMID: 35972801 DOI: 10.1097/CJI.0000000000000435]

20 **Patnaik A**, Kang SP, Rasco D, Papadopoulos KP, Elassaiss-Schaap J, Beeram M, Drengler R, Chen C, Smith L, Espino G, Gergich K, Delgado L, Daud A, Lindia JA, Li XN, Pierce RH, Yearley JH, Wu D, Laterza O, Lehnert M, Iannone R, Tolcher AW. Phase I Study of Pembrolizumab (MK-3475; Anti-PD-1 Monoclonal Antibody) in Patients with Advanced Solid Tumors. *Clin Cancer Res* 2015; **21**: 4286-4293 [PMID: 25977344 DOI: 10.1158/1078-0432.CCR-14-2607]

21 **Tarhini AA**, Zahoor H, Lin Y, Malhotra U, Sander C, Butterfield LH, Kirkwood JM. Baseline circulating IL-17 predicts toxicity while TGF-β1 and IL-10 are prognostic of relapse in ipilimumab neoadjuvant therapy of melanoma. *J Immunother Cancer* 2015; **3**: 39 [PMID: 26380086 DOI: 10.1186/s40425-015-0081-1]

22 **Pistillo MP**, Fontana V, Morabito A, Dozin B, Laurent S, Carosio R, Banelli B, Ferrero F, Spano L, Tanda E, Ferrucci PF, Martinoli C, Cocorocchio E, Guida M, Tommasi S, De Galitiis F, Pagani E, Antonini Cappellini GC, Marchetti P, Quaglino P, Fava P, Osella-Abate S, Ascierto PA, Capone M, Simeone E, Romani M, Spagnolo F, Queirolo P; Italian Melanoma Intergroup (IMI). Soluble CTLA-4 as a favorable predictive biomarker in metastatic melanoma patients treated with ipilimumab: an Italian melanoma intergroup study. *Cancer Immunol Immunother* 2019; **68**: 97-107 [PMID: 30311027 DOI: 10.1007/s00262-018-2258-1]

23 **Vindum HH**, Agnholt JS, Nielsen AWM, Nielsen MB, Schmidt H. Severe steroid refractory gastritis induced by Nivolumab: A case report. *World J Gastroenterol* 2020; **26**: 1971-1978 [PMID: 32390707 DOI: 10.3748/wjg.v26.i16.1971]

24 **Samonis G**, Bousmpoukea A, Molfeta A, Kalkinis AD, Petraki K, Koutserimpas C, Bafaloukos D. Severe Gastritis Due to Nivolumab Treatment of a Metastatic Melanoma Patient. *Diagnostics (Basel)* 2022; **12**: 2864 [PMID: 36428923 DOI: 10.3390/diagnostics12112864]

25 **Tomiyasu H**, Komori T, Ishida Y, Otsuka A, Kabashima K. Eosinophilic gastroenteritis in a melanoma patient treated with nivolumab. *J Dermatol* 2021; **48**: E486-E487 [PMID: 34151453 DOI: 10.1111/1346-8138.16036]

26 **Zhang ML**, Neyaz A, Patil D, Chen J, Dougan M, Deshpande V. Immune-related adverse events in the gastrointestinal tract: diagnostic utility of upper gastrointestinal biopsies. *Histopathology* 2020; **76**: 233-243 [PMID: 31361907 DOI: 10.1111/his.13963]

27 **Bresteau C**, Bonnet P, Robert C, Mussini C, Saiag P, Buecher B, Lebbe C, Allez M, Benamouzig R, Hagège H, Bécheur H, Meyer A, Carbonnel F. Serious immune-related upper gastrointestinal toxicity of immune checkpoint inhibitors: a multicenter case series. *J Gastroenterol Hepatol* 2023; **38**: 2104-2110 [PMID: 37710354 DOI: 10.1111/jgh.16349]

28 **Omotehara S**, Nishida M, Yamanashi K, Sakurai K, Katsurada T, Komatsu Y, Shimizu A, Shibuya H, Shinagawa N, Sugita J, Teshima T. A case of immune checkpoint inhibitor-associated gastroenteritis detected by ultrasonography. *J Clin Ultrasound* 2021; **49**: 605-609 [PMID: 33580597 DOI: 10.1002/jcu.22975]

29 **Yip RHL**, Lee LH, Schaeffer DF, Horst BA, Yang HM. Lymphocytic gastritis induced by pembrolizumab in a patient with metastatic melanoma. *Melanoma Res* 2018; **28**: 645-647 [PMID: 30256271 DOI: 10.1097/CMR.0000000000000502]

30 **Ferrian S**, Liu CC, McCaffrey EF, Kumar R, Nowicki TS, Dawson DW, Baranski A, Glaspy JA, Ribas A, Bendall SC, Angelo M. Multiplexed imaging reveals an IFN-γ-driven inflammatory state in nivolumab-associated gastritis. *Cell Rep Med* 2021; **2**: 100419 [PMID: 34755133 DOI: 10.1016/j.xcrm.2021.100419]

31 **Gaffuri P**, Espeli V, Fulciniti F, Paone G, Bergmann M. Immune-related acute and lymphocytic gastritis in a patient with metastatic melanoma treated with pembrolizumab immunotherapy. *Pathologica* 2019; **111**: 92-97 [PMID: 31748755 DOI: 10.32074/1591-951X-24-19]

32 **Gonzalez RS**, Salaria SN, Bohannon CD, Huber AR, Feely MM, Shi C. PD-1 inhibitor gastroenterocolitis: case series and appraisal of 'immunomodulatory gastroenterocolitis'. *Histopathology* 2017; **70**: 558-567 [PMID: 28000302 DOI: 10.1111/his.13118]

33 **Chen X**, Shi W. An unusual case of immune-related gastritis in one patient receiving toripalimab therapy. *Immunotherapy* 2023; **15**: 335-342 [PMID: 36852424 DOI: 10.2217/imt-2022-0270]

34 **Pennelli G**, Grillo F, Galuppini F, Ingravallo G, Pilozzi E, Rugge M, Fiocca R, Fassan M, Mastracci L. Gastritis: update on etiological features and histological practical approach. *Pathologica* 2020; **112**: 153-165 [PMID: 33179619 DOI: 10.32074/1591-951X-163]

35 **Irshaid L**, Robert ME, Zhang X. Immune Checkpoint Inhibitor-Induced Upper Gastrointestinal Tract Inflammation Shows Morphologic Similarities to, but Is Immunologically Distinct From, Helicobacter pylori Gastritis and Celiac Disease. *Arch Pathol Lab Med* 2021; **145**: 191-200 [PMID: 33501492 DOI: 10.5858/arpa.2019-0700-OA]

36 **Hulo P**, Touchefeu Y, Cauchin E, Archambeaud I, Chapelle N, Bossard C, Bennouna J. Acute Ulceronecrotic Gastritis With Cytomegalovirus Reactivation: Uncommon Toxicity of Immune Checkpoint Inhibitors in Microsatellite Instability-High Metastatic Colorectal Cancer. *Clin Colorectal Cancer* 2020; **19**: e183-e188 [PMID: 32703755 DOI: 10.1016/j.clcc.2020.04.006]

37 **Yuen T**, Liu E, Kohansal A. Gastric metastases from primary breast cancers: rare causes of common gastrointestinal disorders. *BMJ Case Rep* 2020; **13** [PMID: 32636223 DOI: 10.1136/bcr-2019-231763]

38 **Ushida Y**, Yoshimizu S, Horiuchi Y, Yoshio T, Ishiyama A, Hirasawa T, Tsuchida T, Fujisaki J. Clinicopathological Features of Metastatic Gastric Tumors Originating From Breast Cancer: Analysis of Eleven Cases. *World J Oncol* 2018; **9**: 104-109 [PMID: 30220947 DOI: 10.14740/wjon1112w]

39 **Ramos-Casals M**, Brahmer JR, Callahan MK, Flores-Chávez A, Keegan N, Khamashta MA, Lambotte O, Mariette X, Prat A, Suárez-Almazor ME. Immune-related adverse events of checkpoint inhibitors. *Nat Rev Dis Primers* 2020; **6**: 38 [PMID: 32382051 DOI: 10.1038/s41572-020-0160-6]

40 **von Euw E**, Chodon T, Attar N, Jalil J, Koya RC, Comin-Anduix B, Ribas A. CTLA4 blockade increases Th17 cells in patients with metastatic melanoma. *J Transl Med* 2009; **7**: 35 [PMID: 19457253 DOI: 10.1186/1479-5876-7-35]

41 **Pico de Coaña Y**, Poschke I, Gentilcore G, Mao Y, Nyström M, Hansson J, Masucci GV, Kiessling R. Ipilimumab treatment results in an early decrease in the frequency of circulating granulocytic myeloid-derived suppressor cells as well as their Arginase1 production. *Cancer Immunol Res* 2013; **1**: 158-162 [PMID: 24777678 DOI: 10.1158/2326-6066.CIR-13-0016]

42 **Knochelmann HM**, Dwyer CJ, Bailey SR, Amaya SM, Elston DM, Mazza-McCrann JM, Paulos CM. When worlds collide: Th17 and Treg cells in cancer and autoimmunity. *Cell Mol Immunol* 2018; **15**: 458-469 [PMID: 29563615 DOI: 10.1038/s41423-018-0004-4]

43 **Francisco LM**, Salinas VH, Brown KE, Vanguri VK, Freeman GJ, Kuchroo VK, Sharpe AH. PD-L1 regulates the development, maintenance, and function of induced regulatory T cells. *J Exp Med* 2009; **206**: 3015-3029 [PMID: 20008522 DOI: 10.1084/jem.20090847]

44 **Shivaji UN**, Jeffery L, Gui X, Smith SCL, Ahmad OF, Akbar A, Ghosh S, Iacucci M. Immune checkpoint inhibitor-associated gastrointestinal and hepatic adverse events and their management. *Therap Adv Gastroenterol* 2019; **12**: 1756284819884196 [PMID: 31723355 DOI: 10.1177/1756284819884196]

45 **Bello E**, Cohen JV, Mino-Kenudson M, Dougan M. Antitumor response to microscopic melanoma in the gastric mucosa mimicking ipilimumab-induced gastritis. *J Immunother Cancer* 2019; **7**: 41 [PMID: 30744698 DOI: 10.1186/s40425-019-0524-1]

46 **Choi J**, Lee SY. Clinical Characteristics and Treatment of Immune-Related Adverse Events of Immune Checkpoint Inhibitors. *Immune Netw* 2020; **20**: e9 [PMID: 32158597 DOI: 10.4110/in.2020.20.e9]

47 **Giles AJ**, Hutchinson MND, Sonnemann HM, Jung J, Fecci PE, Ratnam NM, Zhang W, Song H, Bailey R, Davis D, Reid CM, Park DM, Gilbert MR. Dexamethasone-induced immunosuppression: mechanisms and implications for immunotherapy. *J Immunother Cancer* 2018; **6**: 51 [PMID: 29891009 DOI: 10.1186/s40425-018-0371-5]

48 **Călugăreanu A**, Rompteaux P, Bohelay G, Goldfarb L, Barrau V, Cucherousset N, Heidelberger V, Nault JC, Ziol M, Caux F, Maubec E. Late onset of nivolumab-induced severe gastroduodenitis and cholangitis in a patient with stage IV melanoma. *Immunotherapy* 2019; **11**: 1005-1013 [PMID: 31304833 DOI: 10.2217/imt-2019-0077]

49 **Lu J**, Firpi-Morell RJ, Dang LH, Lai J, Liu X. An Unusual Case of Gastritis in One Patient Receiving PD-1 Blocking Therapy: Coexisting Immune-Related Gastritis and Cytomegaloviral Infection. *Gastroenterology Res* 2018; **11**: 383-387 [PMID: 30344812 DOI: 10.14740/gr1068w]

50 **Bazarbashi AN**, Dolan RD, Yang J, Perencevich ML. Combination Checkpoint Inhibitor-Induced Hemorrhagic Gastritis. *ACG Case Rep J* 2020; **7**: e00402 [PMID: 33062778 DOI: 10.14309/crj.0000000000000402]

51 **Schneider BJ**, Naidoo J, Santomasso BD, Lacchetti C, Adkins S, Anadkat M, Atkins MB, Brassil KJ, Caterino JM, Chau I, Davies MJ, Ernstoff MS, Fecher L, Ghosh M, Jaiyesimi I, Mammen JS, Naing A, Nastoupil LJ, Phillips T, Porter LD, Reichner CA, Seigel C, Song JM, Spira A, Suarez-Almazor M, Swami U, Thompson JA, Vikas P, Wang Y, Weber JS, Funchain P, Bollin K. Management of Immune-Related Adverse Events in Patients Treated With Immune Checkpoint Inhibitor Therapy: ASCO Guideline Update. *J Clin Oncol* 2021; **39**: 4073-4126 [PMID: 34724392 DOI: 10.1200/JCO.21.01440]

52 **Haanen J**, Obeid M, Spain L, Carbonnel F, Wang Y, Robert C, Lyon AR, Wick W, Kostine M, Peters S, Jordan K, Larkin J; ESMO Guidelines Committee. Electronic address: clinicalguidelines@esmo.org. Management of toxicities from immunotherapy: ESMO Clinical Practice Guideline for diagnosis, treatment and follow-up. *Ann Oncol* 2022; **33**: 1217-1238 [PMID: 36270461 DOI: 10.1016/j.annonc.2022.10.001]

53 **Thompson JA**, Schneider BJ, Brahmer J, Achufusi A, Armand P, Berkenstock MK, Bhatia S, Budde LE, Chokshi S, Davies M, Elshoury A, Gesthalter Y, Hegde A, Jain M, Kaffenberger BH, Lechner MG, Li T, Marr A, McGettigan S, McPherson J, Medina T, Mohindra NA, Olszanski AJ, Oluwole O, Patel SP, Patil P, Reddy S, Ryder M, Santomasso B, Shofer S, Sosman JA, Wang Y, Zaha VG, Lyons M, Dwyer M, Hang L. Management of Immunotherapy-Related Toxicities, Version 1.2022, NCCN Clinical Practice Guidelines in Oncology. *J Natl Compr Canc Netw* 2022; **20**: 387-405 [PMID: 35390769 DOI: 10.6004/jnccn.2022.0020]

54 **Horvat TZ**, Adel NG, Dang TO, Momtaz P, Postow MA, Callahan MK, Carvajal RD, Dickson MA, D'Angelo SP, Woo KM, Panageas KS, Wolchok JD, Chapman PB. Immune-Related Adverse Events, Need for Systemic Immunosuppression, and Effects on Survival and Time to Treatment Failure in Patients With Melanoma Treated With Ipilimumab at Memorial Sloan Kettering Cancer Center. *J Clin Oncol* 2015; **33**:

3193-3198 [PMID: 26282644 DOI: 10.1200/JCO.2015.60.8448]

55 **Abu-Sbeih H**, Ali FS, Alsaadi D, Jennings J, Luo W, Gong Z, Richards DM, Charabaty A, Wang Y. Outcomes of vedolizumab therapy in patients with immune checkpoint inhibitor-induced colitis: a multi-center study. *J Immunother Cancer* 2018; **6**: 142 [PMID: 30518410 DOI: 10.1186/s40425-018-0461-4]

56 **Brongiel S**, Rychalsky KL, Luon D, Johnson AR, Price C, Abdelghany O. Management of Steroid-Refractory Gastrointestinal Immune-Related Adverse Events. *Ann Pharmacother* 2023; **57**: 148-155 [PMID: 35656843 DOI: 10.1177/10600280221094330]

57 **Johncilla M**, Grover S, Zhang X, Jain D, Srivastava A. Morphological spectrum of immune check-point inhibitor therapy-associated gastritis. *Histopathology* 2020; **76**: 531-539 [PMID: 31692018 DOI: 10.1111/his.14029]

58 **Abu-Sbeih H**, Ali FS, Wang X, Mallepally N, Chen E, Altan M, Bresalier RS, Charabaty A, Dadu R, Jazaeri A, Lashner B, Wang Y. Early introduction of selective immunosuppressive therapy associated with favorable clinical outcomes in patients with immune checkpoint inhibitor-induced colitis. *J Immunother Cancer* 2019; **7**: 93 [PMID: 30940209 DOI: 10.1186/s40425-019-0577-1]

59 **Dolladille C**, Ederhy S, Sassier M, Cautela J, Thuny F, Cohen AA, Fedrizzi S, Chrétien B, Da-Silva A, Plane AF, Legallois D, Milliez PU, Lelong-Boulouard V, Alexandre J. Immune Checkpoint Inhibitor Rechallenge After Immune-Related Adverse Events in Patients With Cancer. *JAMA Oncol* 2020; **6**: 865-871 [PMID: 32297899 DOI: 10.1001/jamaoncol.2020.0726]

60 **Alhatem A**, Patel K, Eriksen B, Bukhari S, Liu C. Nivolumab-Induced Concomitant Severe Upper and Lower Gastrointestinal Immune-Related Adverse Effects. *ACG Case Rep J* 2019; **6**: e00249 [PMID: 32309466 DOI: 10.14309/crj.0000000000000249]

61 **Placke JM**, Rawitzer J, Reis H, Rashidi-Alavijeh J, Livingstone E, Ugurel S, Hadaschik E, Griewank K, Schmid KW, Schadendorf D, Roesch A, Zimmer L. Apoptotic Gastritis in Melanoma Patients Treated With PD-1-Based Immune Checkpoint Inhibition - Clinical and Histopathological Findings Including the Diagnostic Value of Anti-Caspase-3 Immunohistochemistry. *Front Oncol* 2021; **11**: 725549 [PMID: 34458154 DOI: 10.3389/fonc.2021.725549]

62 **Allouchery M**, Lombard T, Martin M, Rouby F, Sassier M, Bertin C, Atzenhoffer M, Miremont-Salame G, Perault-Pochat MC, Puyade M; French Network of Regional Pharmacovigilance Centers. Safety of immune checkpoint inhibitor rechallenge after discontinuation for grade ≥2 immune-related adverse events in patients with cancer. *J Immunother Cancer* 2020; **8** [PMID: 33428586 DOI: 10.1136/jitc-2020-001622]

63 **Allouchery M**, Beuvon C, Pérault-Pochat MC, Roblot P, Puyade M, Martin M. Safety of Immune Checkpoint Inhibitor Resumption after Interruption for Immune-Related Adverse Events, a Narrative Review. *Cancers (Basel)* 2022; **14** [PMID: 35205703 DOI: 10.3390/cancers14040955]

64 **Pollack MH**, Betof A, Dearden H, Rapazzo K, Valentine I, Brohl AS, Ancell KK, Long GV, Menzies AM, Eroglu Z, Johnson DB, Shoushtari AN. Safety of resuming anti-PD-1 in patients with immune-related adverse events (irAEs) during combined anti-CTLA-4 and anti-PD1 in metastatic melanoma. *Ann Oncol* 2018; **29**: 250-255 [PMID: 29045547 DOI: 10.1093/annonc/mdx642]

65 **Simonaggio A**, Michot JM, Voisin AL, Le Pavec J, Collins M, Lallart A, Cengizalp G, Vozy A, Laparra A, Varga A, Hollebecque A, Champiat S, Marabelle A, Massard C, Lambotte O. Evaluation of Readministration of Immune Checkpoint Inhibitors After Immune-Related Adverse Events in Patients With Cancer. *JAMA Oncol* 2019; **5**: 1310-1317 [PMID: 31169866 DOI: 10.1001/jamaoncol.2019.1022]

66 **Chennamadhavuni A**, Abushahin L, Jin N, Presley CJ, Manne A. Risk Factors and Biomarkers for Immune-Related Adverse Events: A Practical Guide to Identifying High-Risk Patients and Rechallenging Immune Checkpoint Inhibitors. *Front Immunol* 2022; **13**: 779691 [PMID: 35558065 DOI: 10.3389/fimmu.2022.779691]

World Journal of Gastroenterology

Submit a Manuscript: https://www.f6publishing.com

World J Gastroenterol 2024 April 14; 30(14): 1949-1957

DOI: 10.3748/wjg.v30.i14.1949

ISSN 1007-9327 (print) ISSN 2219-2840 (online)

EDITORIAL

Liver biopsy in the post-hepatitis C virus era in Japan

Yoshihiro Ikura, Takako Okubo, Yasuhiro Sakai

Specialty type: Gastroenterology and hepatology

Provenance and peer review: Invited article; Externally peer reviewed.

Peer-review model: Single blind

Peer-review report's scientific quality classification

Grade A (Excellent): 0
Grade B (Very good): B, B
Grade C (Good): 0
Grade D (Fair): 0
Grade E (Poor): 0

P-Reviewer: Jiang X, China; Jiang W, China

Received: December 26, 2023
Peer-review started: December 26, 2023
First decision: January 24, 2024
Revised: February 5, 2024
Accepted: March 25, 2024
Article in press: March 25, 2024
Published online: April 14, 2024

Yoshihiro Ikura, Takako Okubo, Department of Pathology, Takatsuki General Hospital, Takatsuki 569-1192, Osaka Prefecture, Japan

Yasuhiro Sakai, Department of Pathology, Kansai Medical University Medical Center, Moriguchi 570-8507, Japan

Corresponding author: Yoshihiro Ikura, DSc, MD, Chief Doctor, Professor, Department of Pathology, Takatsuki General Hospital, 1-3-13, Kosobecho, Takatsuki 569-1192, Osaka Prefecture, Japan. ikura@ajk.takatsuki-hp.or.jp

Abstract

In Japan, liver biopsies were previously crucial in evaluating the severity of hepatitis caused by the hepatitis C virus (HCV) and diagnosing HCV-related hepatocellular carcinoma (HCC). However, due to the development of effective antiviral treatments and advanced imaging, the necessity for biopsies has significantly decreased. This change has resulted in fewer chances for diagnosing liver disease, causing many general pathologists to feel less confident in making liver biopsy diagnoses. This article provides a comprehensive overview of the challenges and potential solutions related to liver biopsies in Japan. First, it highlights the importance of considering steatotic liver diseases as independent conditions that can coexist with other liver diseases due to their increasing prevalence. Second, it emphasizes the need to avoid hasty assumptions of HCC in nodular lesions, because clinically diagnosable HCCs are not targets for biopsy. Third, the importance of diagnosing hepatic immune-related adverse events caused by immune checkpoint inhibitors is increasing due to the anticipated widespread use of these drugs. In conclusion, pathologists should be attuned to the changing landscape of liver diseases and approach liver biopsies with care and attention to detail.

Key Words: Liver biopsy; Alteration; Post-hepatitis C virus era; Steatotic liver disease; Hepatic tumors; Immune checkpoint inhibitors

Core Tip: Over the past 30 years in Japan, liver biopsies for assessing hepatitis C virus (HCV) hepatitis and HCV-related liver cancer were common but declined due to advanced treatments and imaging. This shift decreased diagnostic opportunities and eroded general pathologists' confidence in conducting liver biopsies. This editorial outlines key challenges: Understanding steatotic liver diseases as independent conditions, caution in diagnosing nodular lesions to prevent misinterpretation, and addressing hepatic injuries caused by immune checkpoint inhibitors. It stresses the need for pathologists to adapt to evolving liver disease landscapes and approach biopsies meticulously.

Citation: Ikura Y, Okubo T, Sakai Y. Liver biopsy in the post-hepatitis C virus era in Japan. *World J Gastroenterol* 2024; 30(14): 1949-1957
URL: https://www.wjgnet.com/1007-9327/full/v30/i14/1949.htm
DOI: https://dx.doi.org/10.3748/wjg.v30.i14.1949

INTRODUCTION

I (Yoshihiro Ikura) started my career in pathology in Japan about 30 years ago, when abundant liver biopsies for interferon treatment for hepatitis C virus (HCV)[1,2] were submitted to pathology laboratories, day after day (Figure 1). Those who do not know about those days may think that it must have been very tough, but it was rather easy because all we had to do was to evaluate the severity of hepatitis and diagnose hepatocellular carcinoma (HCC).

In 2014, oral direct-acting antiviral agents (DAAs) were introduced[3,4], resulting in a steady decline of liver biopsies in Japan (Figure 2). Pretherapeutic histologic examination is not required for DAA administration[5], and most HCC cases can be treated based solely on radiological findings[6]. Consequently, the necessity of pathologic assessment of liver specimens is decreasing. This is a favorable change for minimizing patients' burden. However, opportunities for general pathologists to learn hepatic histopathology have decreased.

The changing landscape of liver diseases in Japan has caused many general pathologists to lack confidence in making liver biopsy diagnoses. This article categorizes the current issues surrounding liver biopsies in Japan and provides an overview of how to address them.

DIFFERENTIAL DIAGNOSIS CENTERED AROUND STEATOTIC LIVER DISEASES

Liver biopsies from patients with steatotic liver diseases (SLDs; either metabolic dysfunction-associated or alcoholic) and positive for autoantibodies are frequently submitted to our pathology laboratory as consultation cases. Figure 3A and B shows an example of such a case, where steatosis and inflammatory injury are evident, but the portal area remains almost unaffected (Figure 3A). I informed the physician that the patient had steatohepatitis, which is characterized by hepatocyte ballooning and lipogranulomas (Figure 3B), there being no findings of autoimmune hepatitis (AIH).

Figure 3C-E provides a contrasting example. The liver biopsy of a diabetic patient shows inflammatory changes associated with steatosis, similar to the previous case (Figure 3C). Additionally, the portal area exhibits inflammation and fibrosis, and most importantly, inflammatory bile duct damage (Figure 3D) with a small granuloma formation (Figure 3E). These findings are typical of primary biliary cholangitis. The patient's serological test confirmed a positivity for anti-mitochondrial antibodies. Complications of SLDs are apt to obscure the features of autoimmune liver diseases.

Currently, SLDs are estimated to affect 30% of the general adult population[7]. It should be noted that 30% of patients with autoimmune liver diseases, as well as those who are positive for autoantibodies but do not have autoimmune liver diseases, also have SLDs (Figure 4). Pathology reports should provide comments on whether SLDs are complicated by other liver diseases, rather than differentiating between them.

Figure 5 shows results of the comparative biopsy findings before and after HCV eradication with DAAs[8]. While inflammation, fibrosis and iron deposition have improved, steatosis appears to have worsened. This indicates that steatosis was an independent lesion, and not connected to HCV hepatitis. The data suggest that it is time to completely revise the conventional perspective of steatosis as a secondary change linked to various liver diseases.

DIAGNOSIS OF NODULAR LESIONS

The diagnosis of classical HCV-associated HCC was relatively easy because almost all cases had cirrhosis in the background and were observed as clearly demarcated atypical hepatocyte proliferation bordered by fibrous bundles (Figure 6). The histologic features of the current HCCs differ significantly from those of the classic HCCs. HCCs are increasingly developing in livers with only mild steatosis, without hepatitis or cirrhosis. Pathologists in Japan must abandon their previous understanding that HCC is usually associated with cirrhosis[9,10]. Diagnosing HCC has become increasingly challenging. Immunostaining, such as Glypican-3 and CD34, is recommended for cases where morphological diagnosis is difficult.

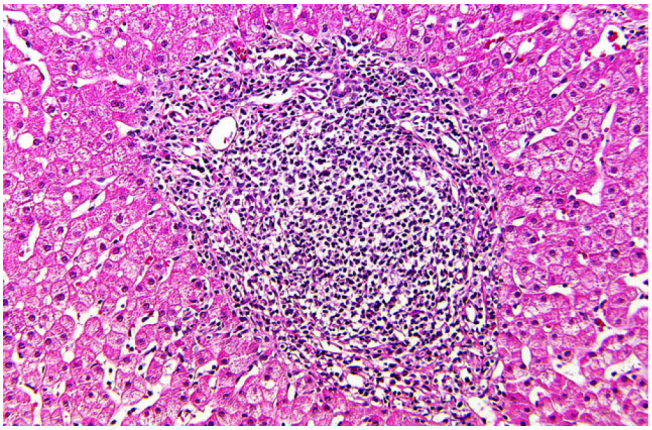

Figure 1 A typical histologic finding of chronic hepatitis C. A dense, follicle-like accumulation of lymphocytes is seen in the portal area. Hematoxylin-eosin, original magnification 200 ×.

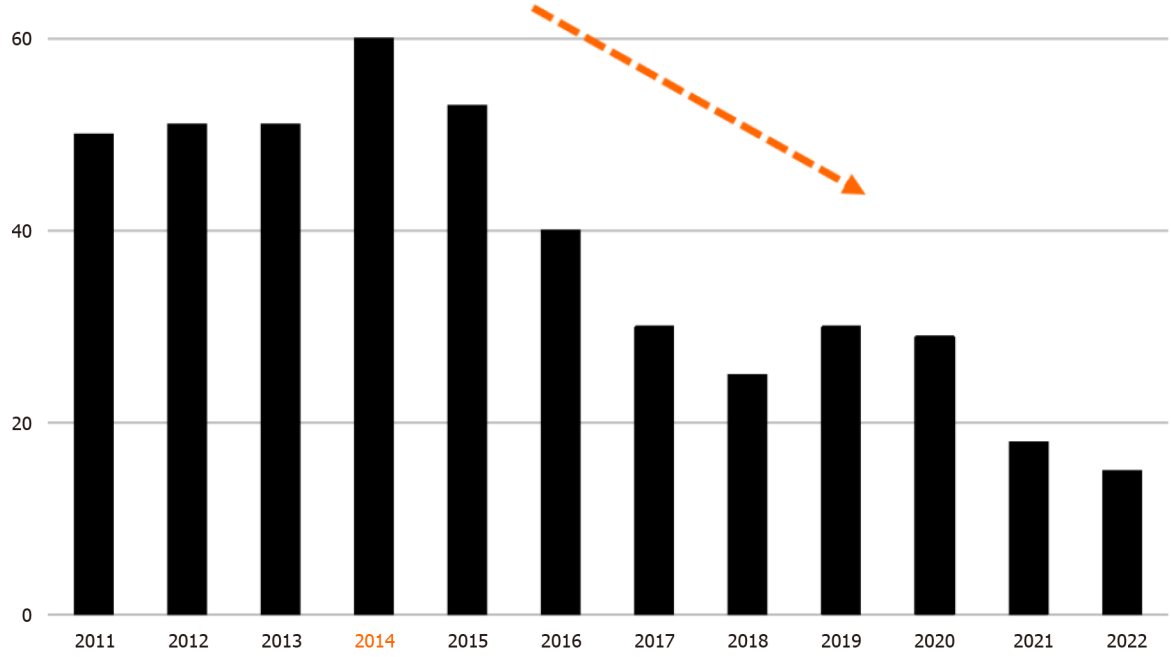

Figure 2 The number of liver biopsies conducted at Takatsuki General Hospital starting from 2011. In 2014, oral direct-acting antiviral agents were introduced, resulting in a steady decline of liver biopsies.

Among the biopsies for nodular lesions, the number of biopsies to diagnose HCC is decreasing. In addition to a certain percentage of tumor-free specimens, it is noteworthy that metastases and benign lesions have increased in recent years (Figure 7). Figure 8A-C shows a liver biopsy sent to our pathology laboratory as a consultation case, which originally had been diagnosed as HCC by biopsy a few years previously, then the tumor recurred repeatedly. The physician performed re-biopsy because of its unusual biological behavior inconsistent with HCC. No background cirrhosis was observed. The lesion consisted of cells with mild atypia and pale cytoplasm showing a cord-like arrangement. I couldn't accept the diagnosis of recurrent HCC, so I ordered immunostaining, which was positive for synaptophysin, and replied that it was probably a metastasis of a neuroendocrine tumor.

HEPATIC INJURY CAUSED BY DRUGS (INCLUDING IMMUNE CHECKPOINT INHIBITORS)

Drug-induced liver injury (DILI), including immune checkpoint inhibitors-related adverse effects (irAE), will become an increasingly important problem, and may require more detailed histologic assessment[11,12].

Figure 8D and E shows a liver biopsy from a patient clinically suspected of AIH, due to positive antinuclear antibody and abnormally elevated serum IgG. The liver tissue shows mild fibrosis, and the main site of injury being centrolobular, indicating acute injury. There are no findings such as hepatocyte rosettes or cobblestone-like arrangement that strongly suggest AIH. I recommended that the possibility of drug-induced injury should be considered first in terms of frequency.

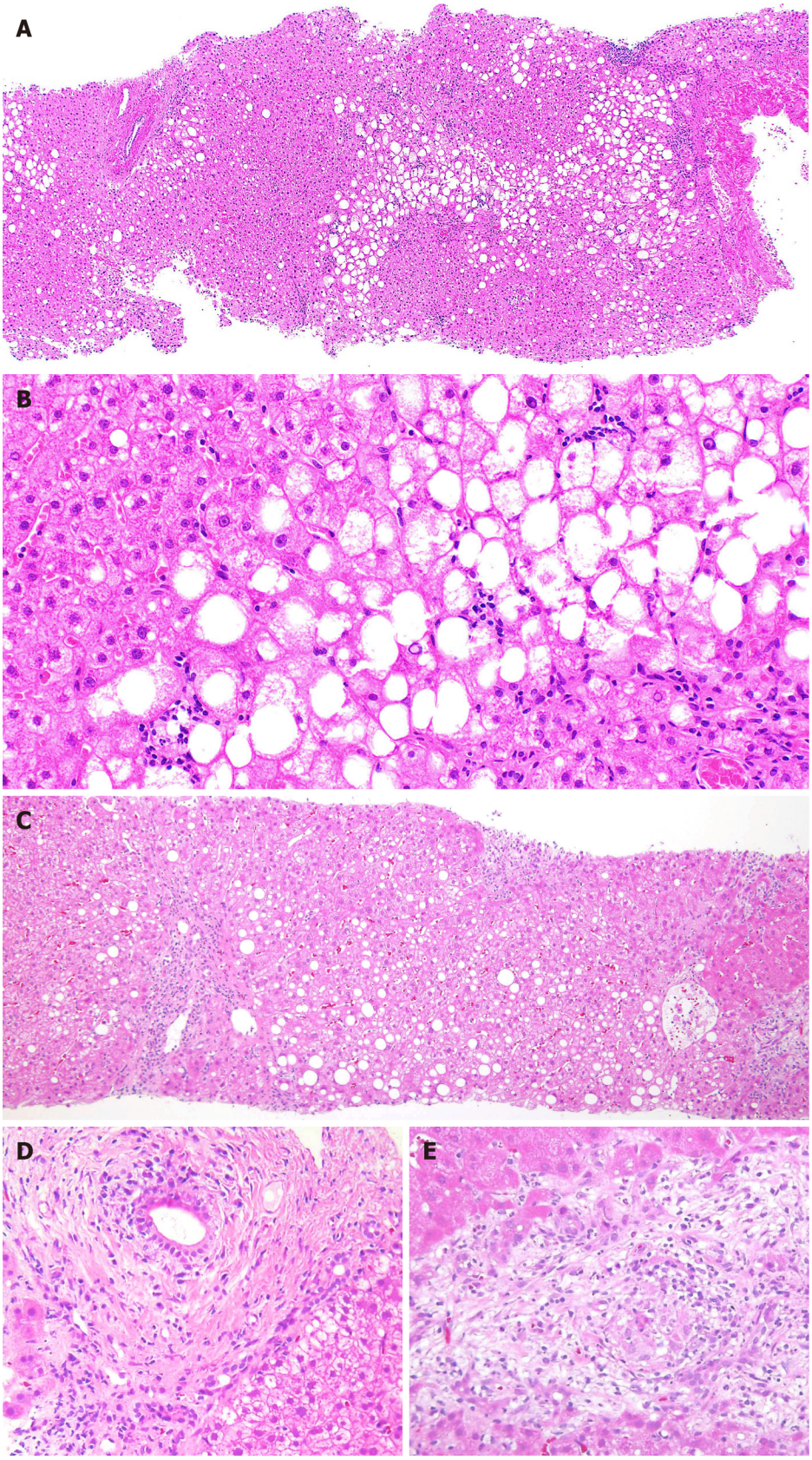

Figure 3 Biopsy from 2 patients. A and B: A liver biopsy from a 78-year-old male positive for antinuclear antibody. Hematoxylin-eosin (HE), original magnifications 40 × (A); HE, original magnifications 400 × (B); C-E: A liver biopsy from a 62-year-old male patient with diabetes mellitus. HE, original magnifications 100 × (C), 200 ×(D) and 200 ×(E).

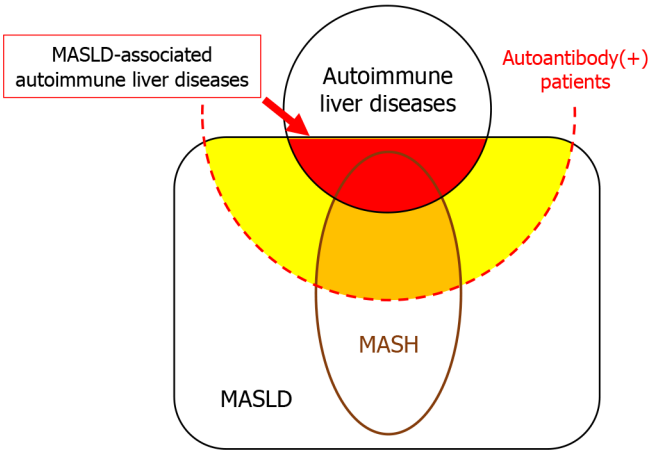

Figure 4 A schematic illustration indicating the relationships among metabolic-dysfunction associated steatotic liver disease, autoimmune liver diseases and autoantibody-positivity. MASLD: Metabolic-dysfunction associated steatotic liver disease; MASH: Metabolic-dysfunction associated steatohepatitis.

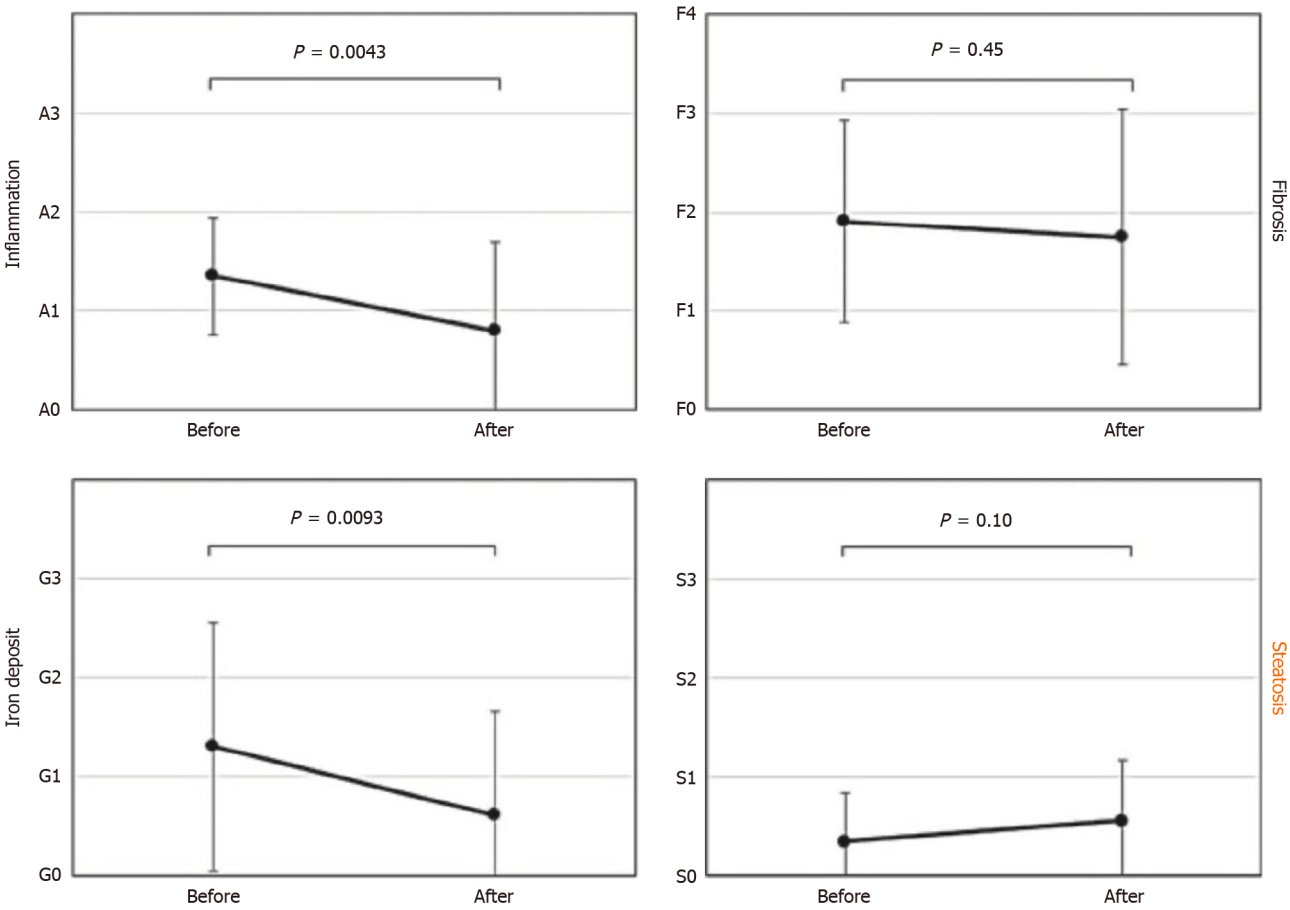

Figure 5 Findings of comparative biopsies before and after hepatitis C virus eradication with direct-acting antiviral agents. While inflammation, fibrosis and iron deposition have improved, steatosis has not changed and appears to have worsened[8].

The patient was later diagnosed with DILI, caused by one of the regular medications.

Figure 8F-I illustrates a case of bile duct injury that occurred three months after the initiation of nivolumab treatment for melanoma. Inflammatory cell infiltration and concentric fibrosis surround the interlobular bile ducts. The infiltrating cells were mostly CD3-positive T lymphocytes, with CD8-positive cells predominating over CD4-positive cells. CK7 staining clearly showed bile duct injury, which was ambiguous in the Hematoxylin & eosin slide. These pathologic changes were consistent with irAEs. After withdrawal of nivolumab, laboratory values returned to normal without the use of steroids.

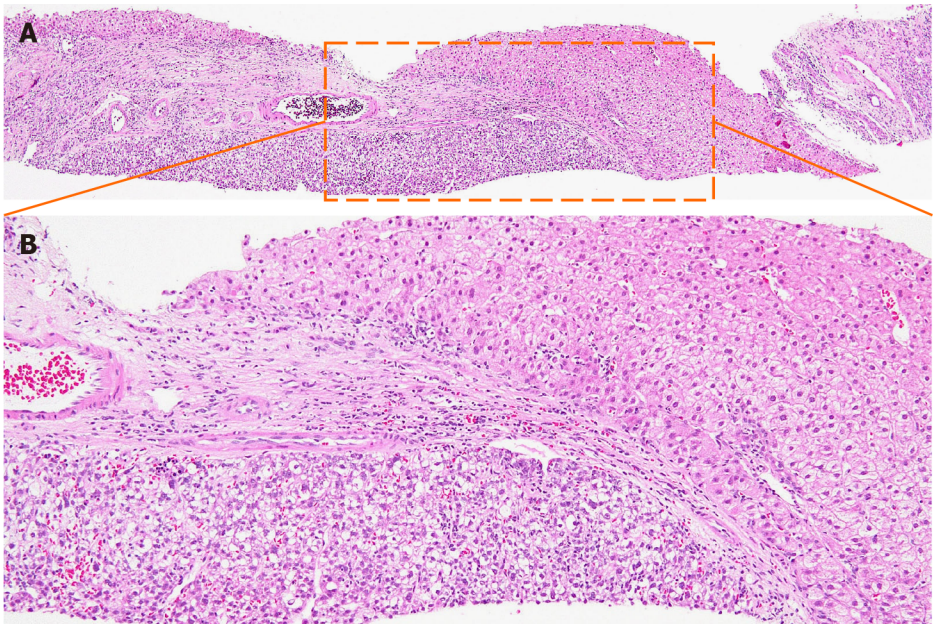

Figure 6 A typical case of hepatitis C virus-associated hepatocellular carcinoma. A: Hematoxylin-eosin (HE), original magnifications 20 ×; B: HE, original magnifications 100 ×.

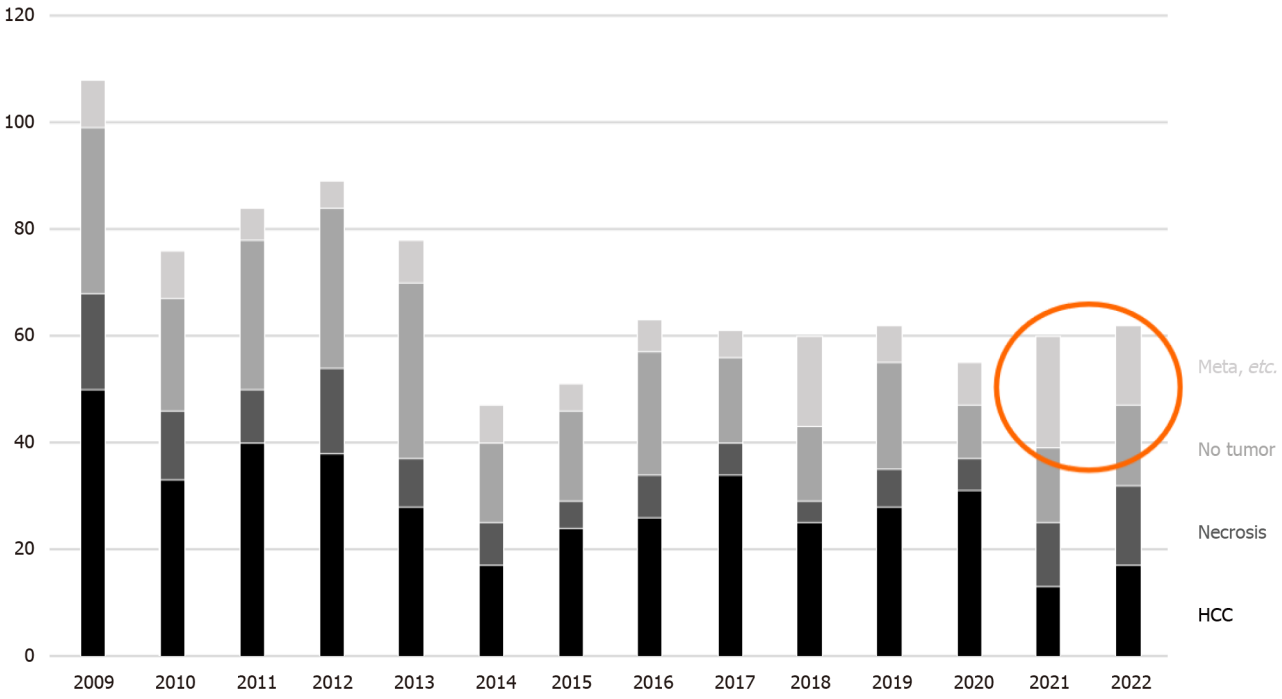

Figure 7 Trends in the number of tumor biopsies at Kansai Medical University Medical Center. Meta: Metastatic tumor; HCC: Hepatocellular carcinoma.

The histologic diagnosis of a liver biopsy requires careful evaluation, taking into account a detailed history of drug use.

CONCLUSION

In the post-HCV era, the number of liver biopsies is decreasing, but their variation is increasing. Pathologic diagnosis of liver biopsies needs appreciation of the changing landscape of liver disease.

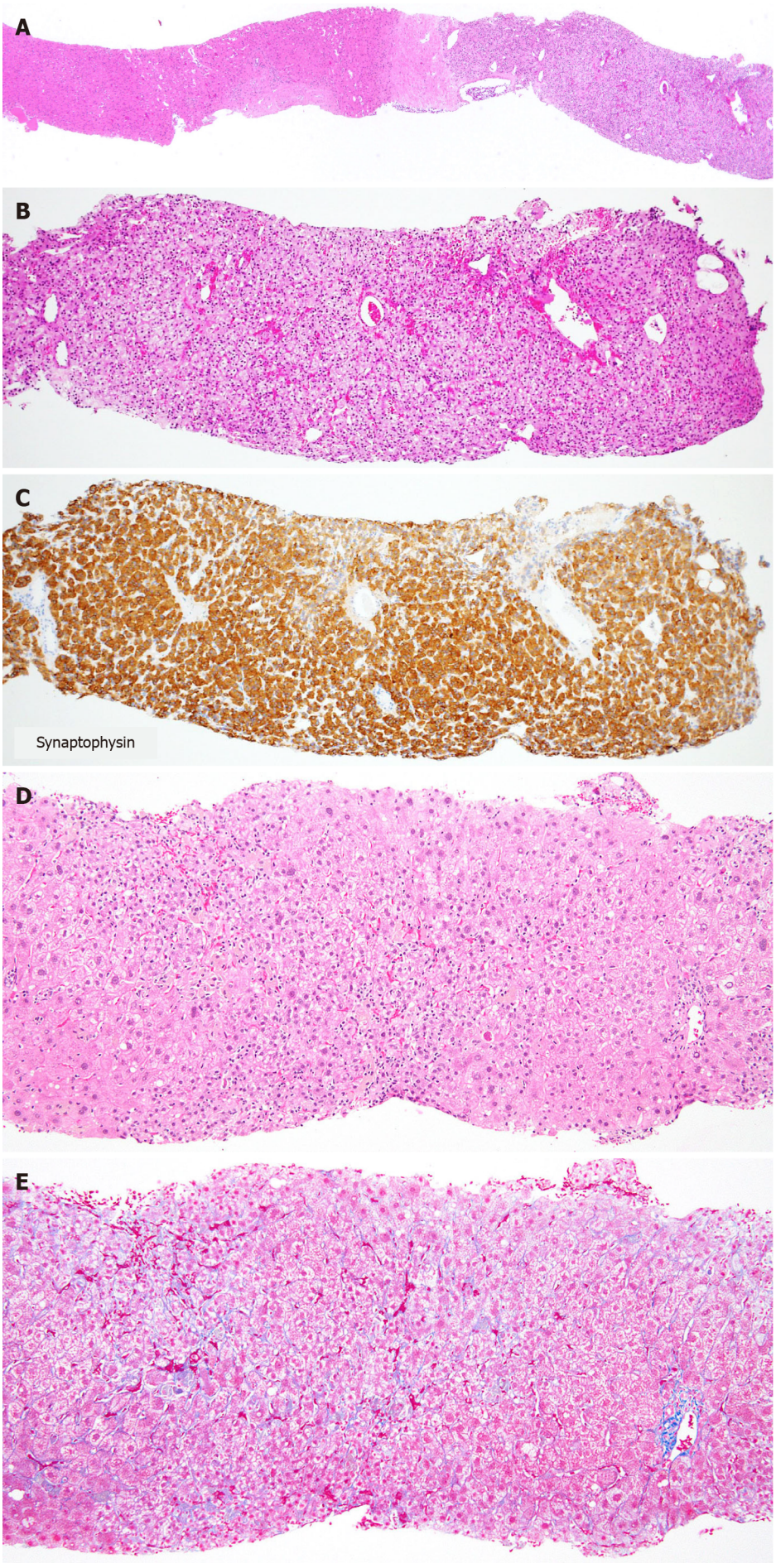
A
B
C
Synaptophysin
D
E

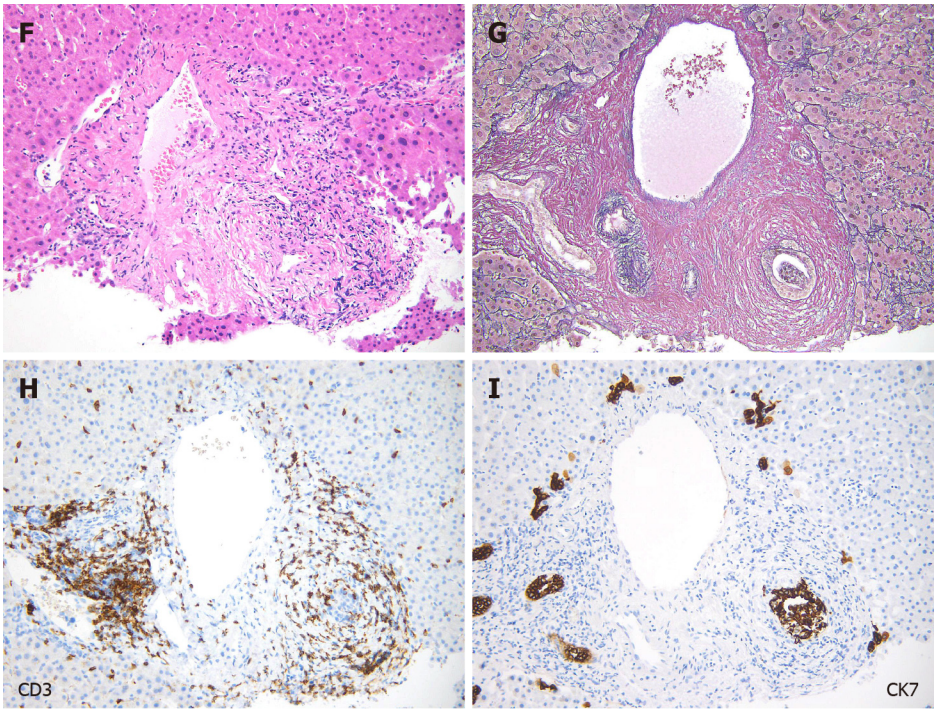

Figure 8 Liver biopsy from 3 patients. A-C: A biopsy of hepatic tumor from a 60-year-old female patient previously diagnosed as hepatocellular carcinoma. Hematoxylin-eosin (HE), original magnifications 20 × (A), 100 × (B); Immunostaining for synaptoophysin, original magnification 100 × (C); D and E: A liver biopsy from a 72-year-old female patient diagnosed as drug-induced liver injury. HE, original magnification 100 × (D); Azan-Mallory stain, original magnification 100 × (E); F-I: A liver biopsy from a 76-year-old male patient with bile duct injury due to inhibitors-related adverse effects. HE, original magnification 100 × (F); Elastica van Gieson, original magnification 100 × (G); Immunostaining for CD3 and cytokeratin 7, original magnification 100 × (H, I). CK7: Cytokeratin 7.

ACKNOWLEDGEMENTS

We thank Dr. Noriyo Yamashiki from Kansai Medical University for providing valuable comments on current clinical issues related to various liver diseases.

FOOTNOTES

Author contributions: Ikura Y contributed to the conception and drafting of the manuscript; Ikura Y, Okubo T, and Sakai Y contributed to critical revisions of the manuscript.

Conflict-of-interest statement: The authors declare that they have no conflicts of interest related to this article.

Country/Territory of origin: Japan

ORCID number: Yoshihiro Ikura 0000-0001-8599-2245; Takako Okubo 0009-0003-9651-4224; Yasuhiro Sakai 0000-0002-6159-782X.

S-Editor: Li L
L-Editor: A
P-Editor: Yuan YY

REFERENCES

1 **Hoofnagle JH**, Mullen KD, Jones DB, Rustgi V, Di Bisceglie A, Peters M, Waggoner JG, Park Y, Jones EA. Treatment of chronic non-A,non-B hepatitis with recombinant human alpha interferon. A preliminary report. *N Engl J Med* 1986; **315**: 1575-1578 [PMID: 3097544 DOI: 10.1056/NEJM198612183152503]

2 **Kakumu S**, Arao M, Yoshioka K, Ichimiya H, Murase K, Aoi T, Kusakabe A. Pilot study of recombinant human alpha-interferon for chronic

non-A, non-B hepatitis. *Am J Gastroenterol* 1989; **84**: 40-45 [PMID: 2521421]

3 **Poordad F**. Big changes are coming in hepatitis C. *Curr Gastroenterol Rep* 2011; **13**: 72-77 [PMID: 21063814 DOI: 10.1007/s11894-010-0153-9]

4 **Omata M**, Nishiguchi S, Ueno Y, Mochizuki H, Izumi N, Ikeda F, Toyoda H, Yokosuka O, Nirei K, Genda T, Umemura T, Takehara T, Sakamoto N, Nishigaki Y, Nakane K, Toda N, Ide T, Yanase M, Hino K, Gao B, Garrison KL, Dvory-Sobol H, Ishizaki A, Omote M, Brainard D, Knox S, Symonds WT, McHutchison JG, Yatsuhashi H, Mizokami M. Sofosbuvir plus ribavirin in Japanese patients with chronic genotype 2 HCV infection: an open-label, phase 3 trial. *J Viral Hepat* 2014; **21**: 762-768 [PMID: 25196837 DOI: 10.1111/jvh.12312]

5 **Trivedi HD**, Patwardhan VR, Malik R. Chronic hepatitis C infection - Noninvasive assessment of liver fibrosis in the era of direct acting antivirals. *Dig Liver Dis* 2019; **51**: 183-189 [PMID: 30553749 DOI: 10.1016/j.dld.2018.11.016]

6 **Marrero JA**, Kulik LM, Sirlin CB, Zhu AX, Finn RS, Abecassis MM, Roberts LR, Heimbach JK. Diagnosis, Staging, and Management of Hepatocellular Carcinoma: 2018 Practice Guidance by the American Association for the Study of Liver Diseases. *Hepatology* 2018; **68**: 723-750 [PMID: 29624699 DOI: 10.1002/hep.29913]

7 **Fujii H**, Suzuki Y, Sawada K, Tatsuta M, Maeshiro T, Tobita H, Tsutsumi T, Akahane T, Hasebe C, Kawanaka M, Kessoku T, Eguchi Y, Syokita H, Nakajima A, Kamada T, Yoshiji H, Kawaguchi T, Sakugawa H, Morishita A, Masaki T, Ohmura T, Watanabe T, Kawada N, Yoda Y, Enomoto N, Ono M, Fuyama K, Okada K, Nishimoto N, Ito YM, Kamada Y, Takahashi H, Sumida Y; Japan Study Group of Nonalcoholic Fatty Liver Disease (JSG-NAFLD). Prevalence and associated metabolic factors of nonalcoholic fatty liver disease in the general population from 2014 to 2018 in Japan: A large-scale multicenter retrospective study. *Hepatol Res* 2023; **53**: 1059-1072 [PMID: 37537735 DOI: 10.1111/hepr.13947]

8 **Enomoto M**, Ikura Y, Tamori A, Kozuka R, Motoyama H, Kawamura E, Hagihara A, Fujii H, Uchida-Kobayashi S, Morikawa H, Murakami Y, Kawada N. Short-term histological evaluations after achieving a sustained virologic response to direct-acting antiviral treatment for chronic hepatitis C. *United European Gastroenterol J* 2018; **6**: 1391-1400 [PMID: 30386612 DOI: 10.1177/2050640618791053]

9 **Tobari M**, Hashimoto E, Taniai M, Kodama K, Kogiso T, Tokushige K, Yamamoto M, Takayoshi N, Satoshi K, Tatsuo A. The characteristics and risk factors of hepatocellular carcinoma in nonalcoholic fatty liver disease without cirrhosis. *J Gastroenterol Hepatol* 2020; **35**: 862-869 [PMID: 31597206 DOI: 10.1111/jgh.14867]

10 **Kawada N**, Imanaka K, Kawaguchi T, Tamai C, Ishihara R, Matsunaga T, Gotoh K, Yamada T, Tomita Y. Hepatocellular carcinoma arising from non-cirrhotic nonalcoholic steatohepatitis. *J Gastroenterol* 2009; **44**: 1190-1194 [PMID: 19672551 DOI: 10.1007/s00535-009-0112-0]

11 **Peeraphatdit TB**, Wang J, Odenwald MA, Hu S, Hart J, Charlton MR. Hepatotoxicity From Immune Checkpoint Inhibitors: A Systematic Review and Management Recommendation. *Hepatology* 2020; **72**: 315-329 [PMID: 32167613 DOI: 10.1002/hep.31227]

12 **Remash D**, Prince DS, McKenzie C, Strasser SI, Kao S, Liu K. Immune checkpoint inhibitor-related hepatotoxicity: A review. *World J Gastroenterol* 2021; **27**: 5376-5391 [PMID: 34539139 DOI: 10.3748/wjg.v27.i32.5376]

World Journal of Gastroenterology

Submit a Manuscript: https://www.f6publishing.com

World J Gastroenterol 2024 April 14; 30(14): 1958-1962

DOI: 10.3748/wjg.v30.i14.1958

ISSN 1007-9327 (print) ISSN 2219-2840 (online)

EDITORIAL

Current status of liver transplantation for human immunodeficiency virus-infected patients in mainland China

Jian-Xin Tang, Dong Zhao

Specialty type: Gastroenterology and hepatology

Provenance and peer review: Invited article; Externally peer reviewed.

Peer-review model: Single blind

Peer-review report's scientific quality classification

Grade A (Excellent): 0
Grade B (Very good): B
Grade C (Good): 0
Grade D (Fair): 0
Grade E (Poor): 0

P-Reviewer: Majhi S, India

Received: December 28, 2023
Peer-review started: December 28, 2023
First decision: February 9, 2024
Revised: February 18, 2024
Accepted: March 21, 2024
Article in press: March 21, 2024
Published online: April 14, 2024

Jian-Xin Tang, Dong Zhao, Department of Liver Surgery and Organ Transplantation Center, Shenzhen Third People's Hospital, The Second Affiliated Hospital of Southern University of Science and Technology, National Clinical Research Center for Infectious Disease, Shenzhen 518000, Guangdong Province, China

Corresponding author: Dong Zhao, MD, Chief Doctor, Department of Liver Surgery and Organ Transplantation Center, Shenzhen Third People's Hospital, The Second Affiliated Hospital of Southern University of Science and Technology, National Clinical Research Center for Infectious Disease, No. 29 Bulan Road, Longgang District, Shenzhen 518000, Guangdong Province, China. zdong1233@126.com

Abstract

According to the report from the Chinese Center for Disease Control and Prevention, the prevalence of human immunodeficiency virus (HIV) infection exceeded 1.2 million individuals by the year 2022, with an annual increase of about 80000 cases. The overall prevalence of hepatitis B surface antigen among individuals co-infected with HIV reached 13.7%, almost twice the rate of the general population in China. In addition to the well-documented susceptibility to opportunistic infections and new malignancies, HIV infected patients frequently experience liver-related organ damage, with the liver and kidneys being the most commonly affected. This often leads to the development of end-stage liver and kidney diseases. Therefore, organ transplantation has emerged as an important part of active treatment for HIV infected patients. However, the curative effect is not satisfactory. HIV infection has been considered a contraindication for organ transplantation. Until the emergence of highly active anti-retroviral therapy in 1996, the once intractable replication of retrovirus was effectively inhibited. With prolonged survival, the failure of important organs has become the main cause of death among HIV patients. Therefore, transplant centers worldwide have resumed exploration of organ transplantation for HIV-infected individuals and reached a positive conclusion. This study provides an overview of the current landscape of HIV-positive patients receiving liver transplantation (LT) in mainland China. To date, our transplant center has conducted LT for eight end-stage liver disease patients co-infected with HIV, and all but one, who died two months postoperatively due to sepsis and progressive multi-organ failure, have survived. Comparative analysis with hepatitis B virus-infected patients during the same period revealed no statistically significant differences in acute rejection reactions, cytomegalovirus infection, bacteremia, pulmonary infections, acute kidney injury, new-onset cancers, or vascular and biliary complications.

Key Words: Liver transplantation; Human immunodeficiency virus; Infection; Hepatitis B virus; End-stage liver disease; Mainland China

Core Tip: In mainland China, human immunodeficiency virus (HIV) infection has long been considered an absolute contraindication for liver transplantation (LT). Until June 2004, Chinese scholars performed LT on two HIV patients, but these cases were only followed up for 24 and 22 months, respectively. Subsequently, there were no reported cases of LT in mainland China for patients with HIV infection until April 2019, when our transplant center performed ABO-incompatible LT for a patient with liver failure co-infected with HIV and hepatitis B virus. This study provides an overview of the current landscape of HIV-positive patients receiving liver transplantation in mainland China.

Citation: Tang JX, Zhao D. Current status of liver transplantation for human immunodeficiency virus-infected patients in mainland China. *World J Gastroenterol* 2024; 30(14): 1958-1962
URL: https://www.wjgnet.com/1007-9327/full/v30/i14/1958.htm
DOI: https://dx.doi.org/10.3748/wjg.v30.i14.1958

INTRODUCTION

Human immunodeficiency virus (HIV) remains a significant global health concern, with the latest data from the Joint United Nations Programme on HIV/acquired immunodeficiency syndrome (AIDS) indicating a staggering 38 million individuals infected worldwide in 2021. Approximately 4000 people contract HIV daily, resulting in an annual increase of 1.5 million new infections[1]. According to a report from the Chinese Center for Disease Control and Prevention, it is projected that by 2023, over 1.2 million individuals in China will be living with HIV, with an annual increment of around 80000 cases (https://www.chinacdc.cn. Accessed 30 November 2023). Since the advent of highly active antiretroviral therapy (HAART) in 1996, substantial progress has been made in controlling HIV infection, managing opportunistic infections, reducing mortality rates, and prolonging life expectancy among infected individuals[2]. HIV/AIDS has become a chronic, manageable condition. However, liver-related mortality remains a formidable challenge, particularly for HIV-positive individuals undergoing HAART, who are increasingly susceptible to complications associated with co-infections, notably hepatitis C virus (HCV) and hepatitis B virus (HBV), leading to hepatocellular carcinoma, end-stage liver disease (ESLD), or alcohol-related liver disease[3,4]. Given the shared transmission routes, co-infections with chronic HCV and chronic HBV are prevalent[5].

GLOBAL TRENDS IN LIVER TRANSPLANTATION FOR HIV-POSITIVE PATIENTS

Liver transplantation (LT) is the only effective method for treating various ESLDs. Initially, HIV-positive patients were excluded from LT due to concerns about their compromised immune system, potential acceleration of HIV progression with immunosuppressive drugs, and limited organ resources[6,7]. However, by the year 2000, as the number of HIV-positive patients requiring LT significantly increased, the focus shifted towards addressing ESLD and end-stage renal disease in these individuals. The United States and the United Kingdom initiated two pilot trials for LT in HIV-positive individuals, yielding favorable outcomes without evidence of immunosuppressive drugs exacerbating the progression of HIV[8]. Then, a prospective multicenter study confirmed that LT in HIV patients exhibited excellent patient and graft outcomes[9].

In 2020, a large retrospective study enrolling LT recipients from the Organ Procurement and Transplantation Network and the Scientific Registry of Transplant Recipients from 2008 to 2015 elucidated the survival trends and characteristics of HIV-infected LT recipients[10]. Among 73206 LT patients, 658 (0.9%) were HIV-infected. From 2008 to 2011, patients survival rates at 1 year and 3 years for the HIV-infected group were 78.2% and 64.1%, respectively. From 2012 to 2015, the 1-year and 3-year survival rates for the HIV-infected group improved significantly to 86.2% and 75.4%, respectively. The cumulative graft survival rates during 2012-2015 also showed substantial improvement, likely attributed to the rational use of anti-HIV drugs, immunosuppressants, and advancements in surgical techniques. Currently, LT outcomes and survival for HIV-positive recipients are comparable to those of HIV-negative recipients[11,12]. However, during the years 2012-2015, the 3-year graft survival rates for HIV-infected recipients with and without concurrent HCV infection were 62.6% and 84.7%, respectively, with similar results observed in patient survival rates. HIV/HCV co-infected recipients exhibited significantly lower survival rates than HCV mono-infected patients, possibly due to a higher rate of post-transplant HCV recurrence leading to graft failure and recipient mortality[13,14]. Cohort studies from France and Spain indicated a 5-year survival rate below 55% for HIV/HCV co-infected LT recipients[15,16]. Therefore, the question of whether LT should be pursued for this patient population remains contentious. To comprehensively evaluate the long-term postoperative survival of HIV-positive LT recipients, a retrospective cohort study with a follow-up exceeding 10

years examined 180 cases in the United States from 2002 to 2011[17]. At 5 years after transplantation (64.8% for HIV+/HCV- *vs* 51.8% for HIV+/HCV+, $P = 0.15$) and 10 years after transplantation (43.9% for HIV+/HCV- *vs* 44.1% for HIV+/HCV+, $P = 0.20$), there was no statistically significant difference in long-term survival rates between mono-infected (HIV+/HCV-) and co-infected (HIV+/HCV+) recipients. However, when compared to the general transplant population with HCV-positive recipients, the long-term survival and graft survival rates for HIV/HCV co-infected recipients after transplantation were suboptimal. Therefore, further research is necessary to investigate the long-term postoperative outcomes for HIV/HCV co-infected LT recipients.

In contrast to co-infection with HCV, HIV-infected patients concurrently affected by HBV appear to have a more favorable prognosis after LT when an appropriate HBV recurrence prevention strategy is implemented. Optimal prevention for recurrent HBV infection in HIV/HBV co-infected patients seems to involve the combination of antiviral therapy with hepatitis B immunoglobulin (HBIG)[18]. In a prospective multicenter study in the United States, with passive prophylaxis using HBIG and antiviral treatment, there was no significant difference in graft and patient survival rates between HIV/HBV co-infected and HBV mono-infected LT recipients, with 3-year survival rates reaching 85%[11]. Studies by Anadol *et al*[19] demonstrated a 5-year survival rate of 80% for HIV/HBV co-infected patients, with no clinically relevant HBV-related ESLD observed after LT. Tateo *et al*[20] reported a cumulative graft and patient survival rate of 100% at an average follow-up of 32 months for 13 HIV/HBV co-infected LT recipients. To assess the postoperative prognosis and the risk of complications for HIV/HBV co-infected patients, we reviewed the literature on LT in HBV/HIV co-infected patients, revealing 1-year and 3-year cumulative survival rates of 85.9% and 77.3%, respectively. Moreover, due to the high recurrence rate of HBV viremia, lifelong prophylactic medication is recommended[21].

LIVER TRANSPLANTATION FOR HIV-POSITIVE PATIENTS IN MAINLAND CHINA

According to a cross-sectional study in China, the hepatitis B surface antigen infection rate among HIV-infected individuals can reach 14.5%, nearly three times higher than the general population[22]. In mainland China, HIV infection has long been considered an absolute contraindication for LT. The advent of HAART in 1996 improved the prognosis for HIV-infected individuals and encouraged some transplant centers in China to accept organ transplant candidates who were HIV positive. Until June 2004, mainland Chinese scholars performed LT on two HIV patients[23], but these cases were only followed up for 24 months and 22 months, respectively. Subsequently, there were no reported cases of LT in mainland China for patients with concomitant HIV infection until April 2019, when our transplant center performed LT for a patient with liver failure co-infected with HIV and HBV. This case is the first reported instance of ABO-incompatible LT for HIV/HBV co-infection[21]. As of the latest follow-up, the patient has survived healthily for over 4 years, with normal liver enzyme levels and no transplant rejection reactions. To date, our transplant center has conducted LT for eight ESLD patients co-infected with HIV, and all but one, who died two months postoperatively due to sepsis and progressive multi-organ failure, have survived. There were no statistically significant differences in acute rejection reactions, cytomegalovirus infection, bacteremia, pulmonary infections, acute kidney injury, new-onset cancers, and vascular or biliary complications compared to HBV-infected patients during the same period. The preoperative CD4(+) T cell count for the first ABO-incompatible patient in our preliminary report was only 42 cells/μL, while the preoperative CD4(+) T cell counts for the remaining patients were all below 200 cells/μL. With the exception of one case resulting in mortality, all other patients have maintained good health postoperatively.

CONCLUSION

Our study findings suggest that the criteria for preoperative CD4(+) T cell counts in LT recipients co-infected with HIV still require further exploration. Also, a comprehensive assessment beyond preoperative CD4(+) T cell counts is essential to ensure the safety of LT recipients in this category. Despite the relatively low number of cases of LT in HIV-infected individuals in mainland China, postoperative survival rates are comparable to those in Western countries. Given the limited number of cases included in the study, our next step will involve expanding the sample size and conducting more in-depth clinical research.

FOOTNOTES

Author contributions: Zhao D contributed to study conception and design, and administrative support; Zhao D and Tang JX contributed to provision of the study materials, and collection and assembly of the data; and all authors contributed to the writing and final approval of the manuscript.

Supported by the Shenzhen Science and Technology R&D Fund, No. JCYJ20220530163011026; and Shenzhen Third People's Hospital, No. G2022008 and No. G2021008.

Conflict-of-interest statement: No conflict-of-interest to disclose.

Country/Territory of origin: China

ORCID number: Jian-Xin Tang 0000-0003-4416-5336; Dong Zhao 0000-0003-3773-721X.

S-Editor: Chen YL
L-Editor: A
P-Editor: Yuan YY

REFERENCES

1 **Ostankova YV**, Shchemelev AN, Thu HHK, Davydenko VS, Reingardt DE, Serikova EN, Zueva EB, Totolian AA. HIV Drug Resistance Mutations and Subtype Profiles among Pregnant Women of Ho Chi Minh City, South Vietnam. *Viruses* 2023; **15** [PMID: 37896785 DOI: 10.3390/v15102008]

2 **Rowell-Cunsolo TL**, Hu G, Bellerose M, Liu J. Trends in Comorbidities Among Human Immunodeficiency Virus-Infected Hospital Admissions in New York City from 2006-2016. *Clin Infect Dis* 2021; **73**: e1957-e1963 [PMID: 33245318 DOI: 10.1093/cid/ciaa1760]

3 **Smith CJ**, Ryom L, Weber R, Morlat P, Pradier C, Reiss P, Kowalska JD, de Wit S, Law M, el Sadr W, Kirk O, Friis-Moller N, Monforte Ad, Phillips AN, Sabin CA, Lundgren JD; D:A:D Study Group. Trends in underlying causes of death in people with HIV from 1999 to 2011 (D:A:D): a multicohort collaboration. *Lancet* 2014; **384**: 241-248 [PMID: 25042234 DOI: 10.1016/S0140-6736(14)60604-8]

4 **Puri P**, Kumar S. Liver involvement in human immunodeficiency virus infection. *Indian J Gastroenterol* 2016; **35**: 260-273 [PMID: 27256434 DOI: 10.1007/s12664-016-0666-8]

5 **Abdi M**, Ahmadi A, Mokarizadeh A. Biomarkers for Assessment of Human Immunodeficiency Virus and its Co-Infection with Hepatitis B and Hepatitis C Viruses: A Comprehensive Review. *Iran J Pathol* 2023; **18**: 230-243 [PMID: 37942194 DOI: 10.30699/IJP.2023.1972384.3009]

6 **Stock P**, Roland M, Carlson L, Freise C, Hirose R, Terrault N, Frassetto L, Coates T, Roberts J, Ascher N. Solid organ transplantation in HIV-positive patients. *Transplant Proc* 2001; **33**: 3646-3648 [PMID: 11750549 DOI: 10.1016/s0041-1345(01)02569-6]

7 **Roland ME**, Stock PG. Liver transplantation in HIV-infected recipients. *Semin Liver Dis* 2006; **26**: 273-284 [PMID: 16850377 DOI: 10.1055/s-2006-947297]

8 **Mohsen AH**, Easterbrook P, Taylor CB, Norris S. Hepatitis C and HIV-1 coinfection. *Gut* 2002; **51**: 601-608 [PMID: 12235089 DOI: 10.1136/gut.51.4.601]

9 **Roland ME**, Barin B, Huprikar S, Murphy B, Hanto DW, Blumberg E, Olthoff K, Simon D, Hardy WD, Beatty G, Stock PG; HIVTR Study Team. Survival in HIV-positive transplant recipients compared with transplant candidates and with HIV-negative controls. *AIDS* 2016; **30**: 435-444 [PMID: 26765937 DOI: 10.1097/QAD.0000000000000934]

10 **Campos-Varela I**, Dodge JL, Berenguer M, Adam R, Samuel D, Di Benedetto F, Karam V, Belli LS, Duvoux C, Terrault NA. Temporal Trends and Outcomes in Liver Transplantation for Recipients With HIV Infection in Europe and United States. *Transplantation* 2020; **104**: 2078-2086 [PMID: 32969987 DOI: 10.1097/TP.0000000000003107]

11 **Coffin CS**, Stock PG, Dove LM, Berg CL, Nissen NN, Curry MP, Ragni M, Regenstein FG, Sherman KE, Roland ME, Terrault NA. Virologic and clinical outcomes of hepatitis B virus infection in HIV-HBV coinfected transplant recipients. *Am J Transplant* 2010; **10**: 1268-1275 [PMID: 20346065 DOI: 10.1111/j.1600-6143.2010.03070.x]

12 **Jacob JS**, Shaikh A, Goli K, Rich NE, Benhammou JN, Ahmed A, Kim D, Rana A, Goss JA, Naggie S, Lee TH, Kanwal F, Cholankeril G. Improved Survival After Liver Transplantation for Patients With Human Immunodeficiency Virus (HIV) and HIV/Hepatitis C Virus Coinfection in the Integrase Strand Transfer Inhibitor and Direct-Acting Antiviral Eras. *Clin Infect Dis* 2023; **76**: 592-599 [PMID: 36221143 DOI: 10.1093/cid/ciac821]

13 **Kardashian AA**, Price JC. Hepatitis C virus-HIV-coinfected patients and liver transplantation. *Curr Opin Organ Transplant* 2015; **20**: 276-285 [PMID: 25944240 DOI: 10.1097/MOT.0000000000000199]

14 **Manzardo C**, Londoño MC, Castells L, Testillano M, Luis Montero J, Peñafiel J, Subirana M, Moreno A, Aguilera V, Luisa González-Diéguez M, Calvo-Pulido J, Xiol X, Salcedo M, Cuervas-Mons V, Manuel Sousa J, Suarez F, Serrano T, Ignacio Herrero J, Jiménez M, Fernandez JR, Giménez C, Del Campo S, Esteban-Mur JI, Crespo G, de la Rosa G, Rimola A, Miro JM; FIPSE LT-HIV investigators. Direct-acting antivirals are effective and safe in HCV/HIV-coinfected liver transplant recipients who experience recurrence of hepatitis C: A prospective nationwide cohort study. *Am J Transplant* 2018; **18**: 2513-2522 [PMID: 29963780 DOI: 10.1111/ajt.14996]

15 **Duclos-Vallée JC**, Féray C, Sebagh M, Teicher E, Roque-Afonso AM, Roche B, Azoulay D, Adam R, Bismuth H, Castaing D, Vittecoq D, Samuel D; THEVIC Study Group. Survival and recurrence of hepatitis C after liver transplantation in patients coinfected with human immunodeficiency virus and hepatitis C virus. *Hepatology* 2008; **47**: 407-417 [PMID: 18098295 DOI: 10.1002/hep.21990]

16 **Miro JM**, Montejo M, Castells L, Rafecas A, Moreno S, Agüero F, Abradelo M, Miralles P, Torre-Cisneros J, Pedreira JD, Cordero E, de la Rosa G, Moyano B, Moreno A, Perez I, Rimola A; Spanish OLT in HIV-Infected Patients Working Group investigators. Outcome of HCV/HIV-coinfected liver transplant recipients: a prospective and multicenter cohort study. *Am J Transplant* 2012; **12**: 1866-1876 [PMID: 22471341 DOI: 10.1111/j.1600-6143.2012.04028.x]

17 **Locke JE**, Durand C, Reed RD, MacLennan PA, Mehta S, Massie A, Nellore A, DuBay D, Segev DL. Long-term Outcomes After Liver Transplantation Among Human Immunodeficiency Virus-Infected Recipients. *Transplantation* 2016; **100**: 141-146 [PMID: 26177090 DOI: 10.1097/TP.0000000000000829]

18 **Terrault NA**, Carter JT, Carlson L, Roland ME, Stock PG. Outcome of patients with hepatitis B virus and human immunodeficiency virus infections referred for liver transplantation. *Liver Transpl* 2006; **12**: 801-807 [PMID: 16628690 DOI: 10.1002/Lt.20776]

19 **Anadol E**, Beckebaum S, Radecke K, Paul A, Zoufaly A, Bickel M, Hitzenbichler F, Ganten T, Kittner J, Stoll M, Berg C, Manekeller S, Kalff JC, Sauerbruch T, Rockstroh JK, Spengler U. Orthotopic liver transplantation in human-immunodeficiency-virus-positive patients in Germany. *AIDS Res Treat* 2012; **2012**: 197501 [PMID: 22900154 DOI: 10.1155/2012/197501]

20 **Tateo M**, Roque-Afonso AM, Antonini TM, Medja F, Lombes A, Jardel C, Teicher E, Sebagh M, Roche B, Castaing D, Samuel D, Duclos-Vallee JC. Long-term follow-up of liver transplanted HIV/hepatitis B virus coinfected patients: perfect control of hepatitis B virus replication and absence of mitochondrial toxicity. *AIDS* 2009; **23**: 1069-1076 [PMID: 19417577 DOI: 10.1097/QAD.0b013e32832c2a37]

21 **Tang JX**, Zhang KJ, Fang TS, Weng RH, Liang ZM, Yan X, Jin X, Xie LJ, Zeng XC, Zhao D. Outcomes of ABO-incompatible liver transplantation in end-stage liver disease patients co-infected with hepatitis B and human immunodeficiency virus. *World J Gastroenterol* 2023; **29**: 1745-1756 [PMID: 37077518 DOI: 10.3748/wjg.v29.i11.1745]

22 **Xie J**, Han Y, Qiu Z, Li Y, Song X, Wang H, Thio CL, Li T. Prevalence of hepatitis B and C viruses in HIV-positive patients in China: a cross-sectional study. *J Int AIDS Soc* 2016; **19**: 20659 [PMID: 26979535 DOI: 10.7448/ias.19.1.20659]

23 **Shen ZY**, Zheng H, Deng YL, Zhu ZJ, Pan C. Two cases of liver transplantation in patients infected with human immunodeficiency virus. *Chin J Organ Transplant* 2007; **28**: 250 [DOI: 10.1097/mot.0b013e3282f1fbd9]

World Journal of Gastroenterology

Submit a Manuscript: https://www.f6publishing.com

World J Gastroenterol 2024 April 14; 30(14): 1963-1967

DOI: 10.3748/wjg.v30.i14.1963

ISSN 1007-9327 (print) ISSN 2219-2840 (online)

EDITORIAL

Bowel function and inflammation: Is motility the other side of the coin?

Alba Panarese

Specialty type: Gastroenterology and hepatology

Provenance and peer review: Invited article; Externally peer reviewed.

Peer-review model: Single blind

Peer-review report's scientific quality classification

Grade A (Excellent): A
Grade B (Very good): 0
Grade C (Good): 0
Grade D (Fair): D
Grade E (Poor): 0

P-Reviewer: Banerjee A, United States; Poddighe D, Kazakhstan

Received: December 31, 2023
Peer-review started: December 31, 2023
First decision: January 10, 2024
Revised: January 23, 2024
Accepted: March 21, 2024
Article in press: March 21, 2024
Published online: April 14, 2024

Alba Panarese, Division of Gastroenterology and Digestive Endoscopy, Department of Medical Sciences, Central Hospital - Azienda Ospedaliera, Taranto 74123, Italy

Corresponding author: Alba Panarese, MD, Director, Division of Gastroenterology and Digestive Endoscopy, Department of Medical Sciences, Central Hospital - Azienda Ospedaliera, Francesco Bruno Street, 1, Taranto 74123, Italy. albapanarese@libero.it

Abstract

Digestion and intestinal absorption allow the body to sustain itself and are the emblematic functions of the bowel. On the flip side, functions also arise from its role as an interface with the environment. Indeed, the gut houses microorganisms, collectively known as the gut microbiota, which interact with the host, and is the site of complex immune activities. Its role in human pathology is complex and scientific evidence is progressively elucidating the functions of the gut, especially regarding the pathogenesis of chronic intestinal diseases and inflammatory conditions affecting various organs and systems. This editorial aims to highlight and relate the factors involved in the pathogenesis of intestinal and systemic inflammation.

Key Words: Motility; Inflammation; Pathogenesis; Vitamin D; Microbiota; Gut; Chronic intestinal pseudo-obstruction

Core Tip: The pathophysiology and pathogenesis of inflammatory bowel diseases, functional bowel diseases and inflammatory diseases affecting other organs and systems is being defined. The gut is intended to be the site where inflammatory processes with systemic implications are triggered. A wide-ranging view is required to clarify these pathways with the aim of increasing differential diagnosis, early diagnosis, and treatment to improve prognosis of chronic bowel and systemic inflammation.

Citation: Panarese A. Bowel function and inflammation: Is motility the other side of the coin? *World J Gastroenterol* 2024; 30(14): 1963-1967
URL: https://www.wjgnet.com/1007-9327/full/v30/i14/1963.htm
DOI: https://dx.doi.org/10.3748/wjg.v30.i14.1963

INTRODUCTION

Bowel disease is a substantial and growing factor driving access to medical care, with notable economic and social impacts, especially in the context of chronic inflammatory diseases[1]. These diseases encompass not only inflammatory bowel disease (IBD), but also other intestinal inflammations, such as diverticulosis and functional disorders[2]. Additionally, chronic systemic and organ inflammation is also increasing, carrying both epidemiological and clinical implications[3]. Currently, the pathogenetic role of the gut in chronic systemic inflammation depends on the function of the gut barrier. This functionality is related to the composition of the gut microbiota and the activity of tight junctions, influenced by inflammatory factors, diet, hormones, and the enteric system[4]. The gut barrier disruption, the "leaky gut", contributes to the development and progression of metabolic, ischemic, neoplastic, neurodegenerative and autoimmune systemic diseases with a substantial epidemiological impact[5-8].

The established role of gut microbiota/microbiome and intercellular junctions prompts a comprehensive exploration of all the factors influencing them. The rapidly accumulating volume of publications serves to enrich our understanding of biological processes and review data[9]. If environmental factors act unconditionally on all individuals, with variations across geographical area[2,5,9-11], among host factors, the genome is the most important. It determines intestinal nutrient absorption and availability, intrinsic intestinal motility, expression of structural proteins (including those of intercellular junctions), interaction with the gut microbiota, and immune response[3,7,8,12-14]. Gut and systemic inflammation, resulting from impaired gut immune activity, are primarily determined by genome[10,12-15]. The potential of intestinal inflammation to induce systemic inflammation may be attributed to the number of exogenous factors. These factors act over a very large surface, involving multiple types of cells and tissues[8-11,13,16]. The well-being of the human body depends on the homeostasis of the intestinal balance, which is unique in many respects. In the presence of favorable genetic characteristics exogenous factors have the potential to shift the immune response towards an inflammatory/autoimmune direction, carrying systemic implications[2-5,9,14,15,17].

RELEVANCE OF THE GENOME

Genome is the main determinant of gut biological processes for several reasons. First, the host genomics has an impact on the gut microbiota/microbiome[15-17]. Second, the genome determines the gut barrier, a dynamic structure that serves as a defense mechanism by shielding the intestinal structures and processes from external aggression[12,13,18]. The microbiota, located in the intestinal lumen, at the interface with the intestinal epithelium, interacts with the gut barrier[16,19]. Third, intestinal immune activity, protected by the gut barrier, also has characteristics conferred by the genome[3,13,14,16,20]. Therefore, exogenous factors, as well as the microbiota, interact with a genetically set immune response[21,22]. The expression of structural, enzymatic and functional proteins, including those involved in the gut barrier, immune response, digestive function and absorption, and neuromuscular components, depends on genetic characteristics[23,24].

The fact that family history is relevant in the onset of intestinal and systemic/organ diseases (inflammation, malabsorption, allergies and neuromuscular diseases) confirms the relevance of the genome, for genetic syndromes such as idiopathic chronic intestinal pseudo-obstruction (mutation in ACTG2, ERBB2-3, *etc.*) and for diseases in which immune and oxidative stress is a determining factor[25]. Obviously, phenotypic expression is influenced by exogenous factors that interfere with the immune activities of the lamina propria by crossing the gut barrier, as well as the genome[2,5,9,26]. In the presence of these factors, including the microbiota and the intestinal barrier, stromal cells, fibroblasts, endothelial cells, and inflammatory and immune cells, alter their interactions[2,4,5,11,13,16,27].

CENTRALITY OF MICROBIOTA, MOTILITY AND NUTRIENTS

Among the factors that act on intestinal biological processes, a phenotypic manifestation of the genome, the microbiota play a crucial role in both physiological and pathological conditions[2,4,5,7]. Various factors modify the microbiota and intestinal activities (the intestinal barrier, immune response, neuromuscular activity). Ultimately, these modifications can amplify or inhibit the inflammatory cascade[2,5,9,28-30]. Among the factors, vitamin D plays an important protective role because vitamin D signaling strengthens the gut barrier by upregulating the tight junctions of intestinal epithelial cells, and increasing the production of mucin and antibacterial peptides; downregulates dendritic cells activity; induces the differentiation and function of tolerogenic rather than pro-inflammatory T cells [increases the production of anti-inflammatory cytokines interleukin (IL)-4/IL-10 and decreases IL-17/IL-6/IL-2/interferon γ/tumor necrosis factor α][30]. Vitamin D/vitamin D receptor (VDR), by influencing both innate and adaptive immunity, plays a role in regulating the intestinal inflammation switch[30,31].

Scientific literature affirms the association between leaky gut and T cell dysfunction with the onset of conditions such as diabetes, cancers, depression and cardiovascular disease. Additionally, factors such obesity, diet, psychosocial stress, and early life stress are implicated in these associations[6,19,20]. Moreover, vitamin D signaling is related to type 2 diabetes, nonalcoholic fatty liver disease, multiple sclerosis and others autoimmune diseases, neurodegenerative diseases, allergies, cancers, IBDs, and chronic intestinal constipation[29,31-33]. Vitamin D deficiency may lead to gut dysbiosis and endotoxemia, potentially leading to systemic inflammation[22,30,31]. Essentially, vitamin D/VDR is involved in the pathogenesis of intestinal inflammation, with repercussions on systemic inflammation[30,31]. However, at the root of the pathogenetic sequence leading to diseases "related" to vitamin D deficiency there may be a defect in intestinal motility. Chronically reduced, whether idiopathic or secondary, intestinal motility can result in decreased absorption of vitamin D

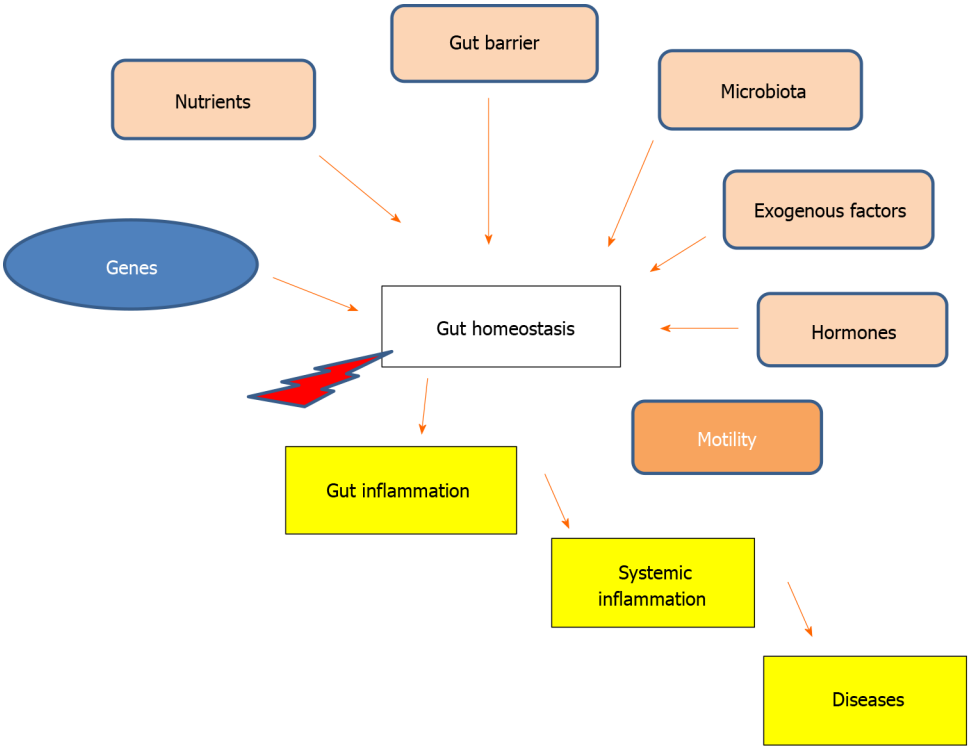

Figure 1 Simplified model of gut homeostasis. Gut homeostasis depends on the balance between the human genome, intestinal barrier, microbiota, nutrients, hormones, exogenous factors, which interact with each other. Intestinal, systemic and organ inflammation results from impaired homeostasis. Gut homeostasis also depends on gut motility, which is determined by genes and other factors.

and other nutrients due to dysbiosis. Under favorable conditions, this scenario may lead to chronic intestinal and systemic inflammation[32]. By considering these premises, we can aim to prevent or treat diseases by modifying factors that reduce intestinal motility[25,34-41] (Figure 1).

CONCLUSION

Gut homeostasis depends on the balance between phenotype characteristics and exogenous factors, which collectively foster the stability of the microbiota. Clinical trials are required to validate the pathogenetic role of intestinal motility in impairing gut homeostasis consequently leading to inflammation with systemic involvement.

FOOTNOTES

Author contributions: Panarese A wrote and revised the manuscript.

Conflict-of-interest statement: The author reported no relevant conflicts of interest for this article.

Country/Territory of origin: Italy

ORCID number: Alba Panarese 0000-0002-6931-2171.

S-Editor: Wang JJ
L-Editor: A
P-Editor: Yuan YY

REFERENCES

1 **Agrawal M**, Jess T. Implications of the changing epidemiology of inflammatory bowel disease in a changing world. *United European Gastroenterol J* 2022; **10**: 1113-1120 [PMID: 36251359 DOI: 10.1002/ueg2.12317]

2 **Sanmarco LM**, Chao CC, Wang YC, Kenison JE, Li Z, Rone JM, Rejano-Gordillo CM, Polonio CM, Gutierrez-Vazquez C, Piester G, Plasencia A, Li L, Giovannoni F, Lee HG, Faust Akl C, Wheeler MA, Mascanfroni I, Jaronen M, Alsuwailm M, Hewson P, Yeste A, Andersen BM, Franks DG, Huang CJ, Ekwudo M, Tjon EC, Rothhammer V, Takenaka M, de Lima KA, Linnerbauer M, Guo L, Covacu R, Queva H, Fonseca-Castro PH, Bladi MA, Cox LM, Hodgetts KJ, Hahn ME, Mildner A, Korzenik J, Hauser R, Snapper SB, Quintana FJ. Identification of environmental factors that promote intestinal inflammation. *Nature* 2022; **611**: 801-809 [PMID: 36266581 DOI: 10.1038/s41586-022-05308-6]

3 **Furman D**, Campisi J, Verdin E, Carrera-Bastos P, Targ S, Franceschi C, Ferrucci L, Gilroy DW, Fasano A, Miller GW, Miller AH, Mantovani A, Weyand CM, Barzilai N, Goronzy JJ, Rando TA, Effros RB, Lucia A, Kleinstreuer N, Slavich GM. Chronic inflammation in the etiology of disease across the life span. *Nat Med* 2019; **25**: 1822-1832 [PMID: 31806905 DOI: 10.1038/s41591-019-0675-0]

4 **Di Vincenzo F**, Del Gaudio A, Petito V, Lopetuso LR, Scaldaferri F. Gut microbiota, intestinal permeability, and systemic inflammation: a narrative review. *Intern Emerg Med* 2024; **19**: 275-293 [PMID: 37505311 DOI: 10.1007/s11739-023-03374-w]

5 **Malesza IJ**, Malesza M, Walkowiak J, Mussin N, Walkowiak D, Aringazina R, Bartkowiak-Wieczorek J, Mądry E. High-Fat, Western-Style Diet, Systemic Inflammation, and Gut Microbiota: A Narrative Review. *Cells* 2021; **10** [PMID: 34831387 DOI: 10.3390/cells10113164]

6 **Martel J**, Chang SH, Ko YF, Hwang TL, Young JD, Ojcius DM. Gut barrier disruption and chronic disease. *Trends Endocrinol Metab* 2022; **33**: 247-265 [PMID: 35151560 DOI: 10.1016/j.tem.2022.01.002]

7 **Mou Y**, Du Y, Zhou L, Yue J, Hu X, Liu Y, Chen S, Lin X, Zhang G, Xiao H, Dong B. Gut Microbiota Interact With the Brain Through Systemic Chronic Inflammation: Implications on Neuroinflammation, Neurodegeneration, and Aging. *Front Immunol* 2022; **13**: 796288 [PMID: 35464431 DOI: 10.3389/fimmu.2022.796288]

8 **Liu X**, Liu Y, Liu J, Zhang H, Shan C, Guo Y, Gong X, Cui M, Li X, Tang M. Correlation between the gut microbiome and neurodegenerative diseases: a review of metagenomics evidence. *Neural Regen Res* 2024; **19**: 833-845 [PMID: 37843219 DOI: 10.4103/1673-5374.382223]

9 **Usuda H**, Okamoto T, Wada K. Leaky Gut: Effect of Dietary Fiber and Fats on Microbiome and Intestinal Barrier. *Int J Mol Sci* 2021; **22** [PMID: 34299233 DOI: 10.3390/ijms22147613]

10 **Chang CS**, Kao CY. Current understanding of the gut microbiota shaping mechanisms. *J Biomed Sci* 2019; **26**: 59 [PMID: 31434568 DOI: 10.1186/s12929-019-0554-5]

11 **Andersen-Civil AIS**, Arora P, Williams AR. Regulation of Enteric Infection and Immunity by Dietary Proanthocyanidins. *Front Immunol* 2021; **12**: 637603 [PMID: 33717185 DOI: 10.3389/fimmu.2021.637603]

12 **Wibbe N**, Ebnet K. Cell Adhesion at the Tight Junctions: New Aspects and New Functions. *Cells* 2023; **12** [PMID: 38067129 DOI: 10.3390/cells12232701]

13 **Spalinger MR**, Sayoc-Becerra A, Santos AN, Shawki A, Canale V, Krishnan M, Niechcial A, Obialo N, Scharl M, Li J, Nair MG, McCole DF. PTPN2 Regulates Interactions Between Macrophages and Intestinal Epithelial Cells to Promote Intestinal Barrier Function. *Gastroenterology* 2020; **159**: 1763-1777.e14 [PMID: 32652144 DOI: 10.1053/j.gastro.2020.07.004]

14 **Kline EM**, Houser MC, Herrick MK, Seibler P, Klein C, West A, Tansey MG. Genetic and Environmental Factors in Parkinson's Disease Converge on Immune Function and Inflammation. *Mov Disord* 2021; **36**: 25-36 [PMID: 33314312 DOI: 10.1002/mds.28411]

15 **Qin Y**, Havulinna AS, Liu Y, Jousilahti P, Ritchie SC, Tokolyi A, Sanders JG, Valsta L, Brożyńska M, Zhu Q, Tripathi A, Vázquez-Baeza Y, Loomba R, Cheng S, Jain M, Niiranen T, Lahti L, Knight R, Salomaa V, Inouye M, Méric G. Combined effects of host genetics and diet on human gut microbiota and incident disease in a single population cohort. *Nat Genet* 2022; **54**: 134-142 [PMID: 35115689 DOI: 10.1038/s41588-021-00991-z]

16 **Kayama H**, Okumura R, Takeda K. Interaction Between the Microbiota, Epithelia, and Immune Cells in the Intestine. *Annu Rev Immunol* 2020; **38**: 23-48 [PMID: 32340570 DOI: 10.1146/annurev-immunol-070119-115104]

17 **Kolde R**, Franzosa EA, Rahnavard G, Hall AB, Vlamakis H, Stevens C, Daly MJ, Xavier RJ, Huttenhower C. Host genetic variation and its microbiome interactions within the Human Microbiome Project. *Genome Med* 2018; **10**: 6 [PMID: 29378630 DOI: 10.1186/s13073-018-0515-8]

18 **Yao Y**, Kim G, Shafer S, Chen Z, Kubo S, Ji Y, Luo J, Yang W, Perner SP, Kanellopoulou C, Park AY, Jiang P, Li J, Baris S, Aydiner EK, Ertem D, Mulder DJ, Warner N, Griffiths AM, Topf-Olivestone C, Kori M, Werner L, Ouahed J, Field M, Liu C, Schwarz B, Bosio CM, Ganesan S, Song J, Urlaub H, Oellerich T, Malaker SA, Zheng L, Bertozzi CR, Zhang Y, Matthews H, Montgomery W, Shih HY, Jiang J, Jones M, Baras A, Shuldiner A, Gonzaga-Jauregui C, Snapper SB, Muise AM, Shouval DS, Ozen A, Pan KT, Wu C, Lenardo MJ. Mucus sialylation determines intestinal host-commensal homeostasis. *Cell* 2022; **185**: 1172-1188.e28 [PMID: 35303419 DOI: 10.1016/j.cell.2022.02.013]

19 **Di Tommaso N**, Gasbarrini A, Ponziani FR. Intestinal Barrier in Human Health and Disease. *Int J Environ Res Public Health* 2021; **18** [PMID: 34886561 DOI: 10.3390/ijerph182312836]

20 **Montgomery TL**, Künstner A, Kennedy JJ, Fang Q, Asarian L, Culp-Hill R, D'Alessandro A, Teuscher C, Busch H, Krementsov DN. Interactions between host genetics and gut microbiota determine susceptibility to CNS autoimmunity. *Proc Natl Acad Sci U S A* 2020; **117**: 27516-27527 [PMID: 33077601 DOI: 10.1073/pnas.2002817117]

21 **Kopp EB**, Agaronyan K, Licona-Limón I, Nish SA, Medzhitov R. Modes of type 2 immune response initiation. *Immunity* 2023; **56**: 687-694 [PMID: 37044059 DOI: 10.1016/j.immuni.2023.03.015]

22 **Geuking MB**, Burkhard R. Microbial modulation of intestinal T helper cell responses and implications for disease and therapy. *Mucosal Immunol* 2020; **13**: 855-866 [PMID: 32792666 DOI: 10.1038/s41385-020-00335-w]

23 **Li X**, Li W, Zeng M, Zheng R, Li M. Network-based methods for predicting essential genes or proteins: a survey. *Brief Bioinform* 2020; **21**: 566-583 [PMID: 30776072 DOI: 10.1093/bib/bbz017]

24 **Poddighe D**, Capittini C. The Role of HLA in the Association between IgA Deficiency and Celiac Disease. *Dis Markers* 2021; **2021**: 8632861 [PMID: 35186163 DOI: 10.1155/2021/8632861]

25 **Stavely R**, Ott LC, Rashidi N, Sakkal S, Nurgali K. The Oxidative Stress and Nervous Distress Connection in Gastrointestinal Disorders. *Biomolecules* 2023; **13** [PMID: 38002268 DOI: 10.3390/biom13111586]

26 **Guo T**, Li X. Machine learning for predicting phenotype from genotype and environment. *Curr Opin Biotechnol* 2023; **79**: 102853 [PMID: 36463837 DOI: 10.1016/j.copbio.2022.102853]

27 **Nolan LS**, Rimer JM, Good M. The Role of Human Milk Oligosaccharides and Probiotics on the Neonatal Microbiome and Risk of Necrotizing Enterocolitis: A Narrative Review. *Nutrients* 2020; **12** [PMID: 33036184 DOI: 10.3390/nu12103052]

28 **Wang J**, Thingholm LB, Skiecevičienė J, Rausch P, Kummen M, Hov JR, Degenhardt F, Heinsen FA, Rühlemann MC, Szymczak S, Holm K, Esko T, Sun J, Pricop-Jeckstadt M, Al-Dury S, Bohov P, Bethune J, Sommer F, Ellinghaus D, Berge RK, Hübenthal M, Koch M, Schwarz K, Rimbach G, Hübbe P, Pan WH, Sheibani-Tezerji R, Häsler R, Rosenstiel P, D'Amato M, Cloppenborg-Schmidt K, Künzel S, Laudes M, Marschall HU, Lieb W, Nöthlings U, Karlsen TH, Baines JF, Franke A. Genome-wide association analysis identifies variation in vitamin D receptor and other host factors influencing the gut microbiota. *Nat Genet* 2016; **48**: 1396-1406 [PMID: 27723756 DOI: 10.1038/ng.3695]

29 **Vernia F**, Valvano M, Longo S, Cesaro N, Viscido A, Latella G. Vitamin D in Inflammatory Bowel Diseases. Mechanisms of Action and Therapeutic Implications. *Nutrients* 2022; **14** [PMID: 35057450 DOI: 10.3390/nu14020269]

30 **Sassi F**, Tamone C, D'Amelio P. Vitamin D: Nutrient, Hormone, and Immunomodulator. *Nutrients* 2018; **10** [PMID: 30400332 DOI: 10.3390/nu10111656]

31 **L Bishop E**, Ismailova A, Dimeloe S, Hewison M, White JH. Vitamin D and Immune Regulation: Antibacterial, Antiviral, Anti-Inflammatory. *JBMR Plus* 2021; **5**: e10405 [PMID: 32904944 DOI: 10.1002/jbm4.10405]

32 **Panarese A**, Pesce F, Porcelli P, Riezzo G, Iacovazzi PA, Leone CM, De Carne M, Rinaldi CM, Shahini E. Chronic functional constipation is strongly linked to vitamin D deficiency. *World J Gastroenterol* 2019; **25**: 1729-1740 [PMID: 31011257 DOI: 10.3748/wjg.v25.i14.1729]

33 **Khatoon S**, Kalam N, Rashid S, Bano G. Effects of gut microbiota on neurodegenerative diseases. *Front Aging Neurosci* 2023; **15**: 1145241 [PMID: 37323141 DOI: 10.3389/fnagi.2023.1145241]

34 **Giambra V**, Pagliari D, Rio P, Totti B, Di Nunzio C, Bosi A, Giaroni C, Gasbarrini A, Gambassi G, Cianci R. Gut Microbiota, Inflammatory Bowel Disease, and Cancer: The Role of Guardians of Innate Immunity. *Cells* 2023; **12** [PMID: 37998389 DOI: 10.3390/cells12222654]

35 **Katsirma Z**, Dimidi E, Rodriguez-Mateos A, Whelan K. Fruits and their impact on the gut microbiota, gut motility and constipation. *Food Funct* 2021; **12**: 8850-8866 [PMID: 34505614 DOI: 10.1039/d1fo01125a]

36 **Ding N**, Zhang X, Zhang XD, Jing J, Liu SS, Mu YP, Peng LL, Yan YJ, Xiao GM, Bi XY, Chen H, Li FH, Yao B, Zhao AZ. Impairment of spermatogenesis and sperm motility by the high-fat diet-induced dysbiosis of gut microbes. *Gut* 2020; **69**: 1608-1619 [PMID: 31900292 DOI: 10.1136/gutjnl-2019-319127]

37 **Fournier N**, Fabre A. Smooth muscle motility disorder phenotypes: A systematic review of cases associated with seven pathogenic genes (ACTG2, MYH11, FLNA, MYLK, RAD21, MYL9 and LMOD1). *Intractable Rare Dis Res* 2022; **11**: 113-119 [PMID: 36200034 DOI: 10.5582/irdr.2022.01060]

38 **Zhernakova DV**, Wang D, Liu L, Andreu-Sánchez S, Zhang Y, Ruiz-Moreno AJ, Peng H, Plomp N, Del Castillo-Izquierdo Á, Gacesa R, Lopera-Maya EA, Temba GS, Kullaya VI, van Leeuwen SS; Lifelines Cohort Study, Xavier RJ, de Mast Q, Joosten LAB, Riksen NP, Rutten JHW, Netea MG, Sanna S, Wijmenga C, Weersma RK, Zhernakova A, Harmsen HJM, Fu J. Host genetic regulation of human gut microbial structural variation. *Nature* 2024; **625**: 813-821 [PMID: 38172637 DOI: 10.1038/s41586-023-06893-w]

39 **Wang S**, Hou H, Tang Y, Zhang S, Wang G, Guo Z, Zhu L, Wu J. An overview on CV2/CRMP5 antibody-associated paraneoplastic neurological syndromes. *Neural Regen Res* 2023; **18**: 2357-2364 [PMID: 37282453 DOI: 10.4103/1673-5374.371400]

40 **Sarfo BO**, Kopdag H, Pott MC, Stiedenroth L, Nahrstedt U, Schäfer H, von Wichert G. Postinfectious T-lymphocytic enteral leiomyositis as a rare cause of chronic intestinal pseudoobstruction. *Z Gastroenterol* 2021; **59**: 326-330 [PMID: 33845499 DOI: 10.1055/a-1310-4500]

41 **Radocchia G**, Neroni B, Marazzato M, Capuzzo E, Zuccari S, Pantanella F, Zenzeri L, Evangelisti M, Vassallo F, Parisi P, Di Nardo G, Schippa S. Chronic Intestinal Pseudo-Obstruction: Is There a Connection with Gut Microbiota? *Microorganisms* 2021; **9** [PMID: 34946150 DOI: 10.3390/microorganisms9122549]

World Journal of Gastroenterology

Submit a Manuscript: https://www.f6publishing.com

World J Gastroenterol 2024 April 14; 30(14): 1968-1981

DOI: 10.3748/wjg.v30.i14.1968

ISSN 1007-9327 (print) ISSN 2219-2840 (online)

REVIEW

Necroptosis contributes to non-alcoholic fatty liver disease pathoetiology with promising diagnostic and therapeutic functions

Hong-Ju Sun, Bo Jiao, Yan Wang, Yue-Hua Zhang, Ge Chen, Zi-Xuan Wang, Hong Zhao, Qing Xie, Xiao-Hua Song

Specialty type: Gastroenterology and hepatology

Provenance and peer review: Unsolicited article; Externally peer reviewed.

Peer-review model: Single blind

Peer-review report's scientific quality classification

Grade A (Excellent): A
Grade B (Very good): 0
Grade C (Good): 0
Grade D (Fair): 0
Grade E (Poor): 0

P-Reviewer: Beenet L, United States

Received: January 6, 2024
Peer-review started: January 6, 2024
First decision: February 2, 2024
Revised: February 15, 2024
Accepted: March 25, 2024
Article in press: March 25, 2024
Published online: April 14, 2024

Hong-Ju Sun, Bo Jiao, Department of General Medicine, Qingdao Central Hospital, University of Health and Rehabilitation Sciences (Qingdao Central Medical Group), Qingdao 266042, Shandong Province, China

Yan Wang, Ge Chen, Zi-Xuan Wang, Hong Zhao, Xiao-Hua Song, Department of Gastroenterology, Qingdao Central Hospital, University of Health and Rehabilitation Sciences (Qingdao Central Medical Group), Qingdao 266042, Shandong Province, China

Yue-Hua Zhang, Department of Medical Administration, Qingdao Central Hospital, University of Health and Rehabilitation Sciences (Qingdao Central Medical Group), Qingdao 266042, Shandong Province, China

Ge Chen, Zi-Xuan Wang, Qingdao Medical College, Qingdao University, Qingdao 266042, Shandong Province, China

Qing Xie, Department of Infectious Diseases, Ruijin Hospital, Shanghai Jiao Tong University School of Medicine, Shanghai 200025, China

Corresponding author: Xiao-Hua Song, PhD, Professor, Department of Gastroenterology, Qingdao Central Hospital, University of Health and Rehabilitation Sciences (Qingdao Central Medical Group), No. 127 Siliu South Road, Qingdao 266042, Shandong Province, China. sxh72@sina.com

Abstract

Nonalcoholic fatty liver disease (NAFLD) is the most prevalent type of chronic liver disease. However, the disease is underappreciated as a remarkable chronic disorder as there are rare managing strategies. Several studies have focused on determining NAFLD-caused hepatocyte death to elucidate the disease pathoetiology and suggest functional therapeutic and diagnostic options. Pyroptosis, ferroptosis, and necroptosis are the main subtypes of non-apoptotic regulated cell deaths (RCDs), each of which represents particular characteristics. Considering the complexity of the findings, the present study aimed to review these types of RCDs and their contribution to NAFLD progression, and subsequently discuss in detail the role of necroptosis in the pathoetiology, diagnosis, and treatment of the disease. The study revealed that necroptosis is involved in the occurrence of NAFLD and its progression towards steatohepatitis and cancer, hence it has potential in diagnostic and therapeutic approaches. Nevertheless, further studies are necessary.

Key Words: Nonalcoholic fatty liver disease; Apoptosis; Necroptosis; Cell death; Diagnosis; Treatment

Core Tip: Hepatocyte death has been hypothesized as a major contributor to nonalcoholic fatty liver disease (NAFLD) progression, however, the role of regulated cell death (RCD) programs in NAFLD pathophysiology and their potential as diagnostic/therapeutic strategies has not been comprehensively discussed. The present study reviewed the participation of pyroptosis, ferroptosis, and necroptosis in the establishment of NAFLD and its progression toward steatohepatitis and cancer and discussed the potential RCDs in the diagnosis/treatment of the disease. Particularly, the present findings revealed that necroptosis significantly contributes to NAFLD occurrence and progress that may represent promising functions as diagnostic/therapeutic tools.

Citation: Sun HJ, Jiao B, Wang Y, Zhang YH, Chen G, Wang ZX, Zhao H, Xie Q, Song XH. Necroptosis contributes to non-alcoholic fatty liver disease pathoetiology with promising diagnostic and therapeutic functions. *World J Gastroenterol* 2024; 30(14): 1968-1981
URL: https://www.wjgnet.com/1007-9327/full/v30/i14/1968.htm
DOI: https://dx.doi.org/10.3748/wjg.v30.i14.1968

INTRODUCTION

Nonalcoholic fatty liver disease (NAFLD) is described as the most prevalent type of chronic liver disease worldwide[1]. NAFLD is considered a growing cause of end-stage hepatic disorders throughout the world and emerged as a pathoetiology of hepatocellular carcinoma (HCC) even when the underlying cirrhosis is absent[2,3]. In fact, the excessive accumulation of lipids in the hepatocytes (in the form of triglycerides, > 5% fat content in the liver; referred to as steatosis) of people consuming alcohol at low-risk amounts is the main characteristic of patients with NAFLD[4]. Clinically, the condition may be restricted to excessive liver fat, known as NAFL, or progress to necroinflammation and fibrosis, called non-alcoholic steatohepatitis (NASH), to NASH-cirrhosis, and eventually to HCC[5,6]. In Western countries, it is estimated that one-third of the general population is affected by NAFLD which is associated with excess body weight and diabetes mellitus. Moreover, the disease is highly prevalent in the Middle East and the rate of incidence is growing in the Asian subcontinent and the Far East nations[7-9]. Altogether, NAFLD has become the most common chronic liver disorder with a worldwide prevalence of around 25% of the adult population that is recognized to be closely and bidirectionally related to components of metabolic syndrome[9,10].

The most important challenge is the identification of people with NAFLD who are at the highest risk of developing liver-related complications. The burden of end-stage liver disease is estimated to increase two to three times globally by 2030[11]. Although NALFD is clinically accepted as the most rapidly increasing cause of liver-related mortality emerged as a significant cause of end-stage liver disease, HCC, and liver transplantation with a substantial health economic burden, NAFLD is underappreciated as a remarkable chronic disorder and there is a few numbers of managing strategies or policies[12,13]. In addition, even though a variety of ongoing studies have assumed several genetic/metabolic aberrations as the causes of NAFLD pathogenesis, the underlying mechanism by which the disease occurs and progresses remains unclear, making early laboratory diagnosis and effective treatment challenging[14-17].

Generally, a variety of unrecoverable intra- or extra-cellular perturbations capable of disrupting cellular survival affect cells by the activation of one of many signaling cascades, causing the death of cells and tissue damage[18-20]. The gross diversity in cell death programs has made these processes fall into two major categories including accidental cell death, and regulated cell death (RCD). Accidental cell death is described as a passive process in which uninspected necrosis is the main type, while RCD is an active process that includes a number of subtypes[18-21]. Specific molecular mechanisms are considered the initiating and propagating agents of RCD modalities with remarkable interactivity. In addition, each type of RCD, discussed later, represents distinct molecular, biochemical, functional, and morphological properties with particular pathophysiological consequences. Two main categories of RCDs consist of apoptotic and non-apoptotic cell death programs, which include apoptosis in the first subtype and necroptosis, pyroptosis, autophagy, and ferroptosis in the second one[18-20,22]. Fortunately, a large number of studies have recently focused on determining the process of hepatocyte cell death related to NAFLD in order to elucidate the etiology of the disease and suggest effective therapeutic and diagnostic options[23]. Considering the breadth and complexity of the findings, the present study has aimed to first provide an overview of the types of RCDs and the contribution of each one in the disease progression briefly, and then discuss in detail the role of necroptosis, a novel form of RCD, in the pathoetiology and treatment of the disease.

RCDs contribute to the progression of NAFLD

RCD is considered intrinsically associated with inflammatory disorders of hepatic tissue and is documented to be pivotal in governing the clinical consequences of liver disorder[24,25]. A plethora of evidence has revealed different forms of RCD pathways with increasingly identified correlations with NAFLD[23]. Significantly, the novel described forms of RCDs may co-exist simultaneously in diseases, and a number of them portion overlapping molecular processes that may

function as a backup dying approach to provide the survival of an organism when a cellular threshold induced by death is established[26-28]. In fact, hepatocellular death could be triggered by metabolic, viral, toxic, and/or autoimmune mediators accompanied by inflammation and compensatory proliferation which frequently represent a close association with the development of cirrhosis, fibrosis, and HCC[29].

Conventionally, apoptosis was described as a strictly controlled pathway, as opposed to the passive form of cell death known as necrosis which is an irregulated and accidental form of cellular death[30]. The external forces cause irreparably cell injury the passive form of cell death occurs which is characterized by oncosis, a rapid organelle, and cytoplasmic swelling[31]. Moreover, cell membrane permeabilization followed by leakage of damage-associated molecular patterns (DAMPs) occurs that initiates the immune response[32]. Recently, a plethora of research highlights a variety of forms of RCD modalities such as autophagy, ferroptosis, pyroptosis, and necroptosis that represent similar main morphological characteristics with necrosis[33,34], however, are regulated molecular pathways and have well-defined processes (Table 1).

Necroptosis represents several similar molecular components with apoptosis, particularly the extrinsic pathway, hence it may be the best-understood form of regulated necrosis. Also, necroptosis provides the progression of cellular death when apoptosis is pathologically inhibited, which in turn could be assumed as a disease state in the hepatic tissue[4]. Nonetheless, other mentioned forms of RCD probably be significant in the progression of NAFLD as a proper characterization of RCD in the disease can lead to promising diagnostic and therapeutic options. The novelty of the field has led to the rapid progress of research, and recent studies sought to describe the association between the non-apoptotic forms of RCD and the progression of NAFLD. Although the focus of the current study has been on elucidating the contribution of necroptosis in the pathogenesis of NAFLD, it is essential to first acquainted with other forms of non-apoptotic RCDs and briefly discuss the involvement of each one in the development of the disease.

An overview of pyroptosis

Zychlinsky *et al*[35] initially reported pyroptosis in the 1990s and described a lytic form of cell death in macrophages infected by *Shigella flexneri*. Nevertheless, the 'pyroptosis' term emerged in 2001 as scientists revealed that the death of macrophages induced by *Salmonella* was dependent on caspase (CASP)-1[36]. Subsequently, the number of pyroptosis-related CASPs that are opposed to apoptosis-related CASPs has significantly elevated and includes CASP-1, CASP-11, and the human orthologs CASP-4 and CASP-5[35,36]. Surprisingly the well-known apoptotic effector CASP-3 is considered a pyroptotic CASP under specific conditions[37,38]. Primarily, this type of RCD occurs after intracellular pathogens cause infection leading to the formation of cell membrane pores dependent on CASP activity, swelling, cell rupture, and release of pro-inflammatory interleukins[39] such as interleukin (IL)-1β and IL-18[40-42].

The pore-forming gasdermin D (GSDMD) was characterized in 2015 contributing as the executioner of pyroptosis[43,44]. 31-KDa N-terminal GSDMDNT fragment is produced when GSDMD is cleaved by the action of CASP-1 and CASP-11. GSDMDNT exhibits intrinsic pore-forming activity. Moreover, the cleavage of GSDMD produces a 22-kDa C-terminal GSDMDCT fragment. This fragment attaches to GSDMDNT in order to inhibit the protein[43,44]. The upregulation of GSDMDNT alone is followed by the induction of pyroptosis, however, GSDMDCT blocks GSDMDNT-induced pyroptosis[43,44]. Importantly, it is documented that GSDMD belongs to a larger family of proteins consisting of GSDMA to GSDME (also known as DFNA5), and DFNB59[45]. Recent investigations revealed that GSDME functions as another pyroptosis executioner, that is capable of switching CASP-3-mediated apoptosis to pyroptosis[46,47]. The majority of GSDMs have been linked to the incidence and development of a variety of diseases, however, the exact molecular and functional activation mechanisms remain mainly unknown[48].

Two signaling pathways including canonical and non-canonical signalings activate pyroptosis. These two signalings differ in the application of cytoplasmic multiprotein complexes known as inflammasomes[49,50]. Inflammasomes trigger the canonical pathway of pyroptosis. In this regard, inflammasomes can recognize different endogenous and exogenous danger signals such as pathogen-associated molecular patterns (PAMPs) and DAMPs. The canonical inflammasomes consist of a sensor protein that belongs to the nucleotide-binding domain (NBD), apoptosis-associated speck-like protein containing a CARD (ASC), AIM2-like receptor or NLR (leucine-rich-repeat-containing) or pyrin family, and pro-CASP-1 which is an inactive zymogen[51]. When the canonical inflammasome is formed, the activation of CASP-1 leads to the cleavage of pro-IL-1β and pro-IL-18 into their active forms. Next, these two ILs are released extracellularly subsequent to the action of GSDMDNT that causes spore formation in the cell membrane. Whereas, the non-canonical pathway is CASP-11-dependent without inflammasome priming cleaves GSDMD. In this type of pyroptosis, GSDMDNT signals back to canonical NLRP3 inflammasome leading to the activation of the CASP-1-dependent pathway[52].

Pyroptosis may contribute to NAFLD progression and transition to NASH

A variety of factors such as lipotoxicity, mitochondrial dysfunction, endoplasmic reticulum stress, hepatocyte death pathways, and innate immune response are able to initiate chronic inflammatory processes in the liver that may provide fuel for the transition from NAFL to NASH[53-55]. The infiltration of macrophages and activation of local Kupffer cells is considered a key characteristic of disease pathoetiology[56]. Tumor necrosis factor (TNF)-α is released by Kupffer cells [57] which feeds a vicious cycle of inflammatory responses and initiates fibrosis after activating apoptosis. Nonetheless, it has recently appeared that inflammatory CASPs such as human CASP-4/5, CASP-1, and murine CASP-11 contribute pivotally as inflammation mediators[44]. Thereby, it is assumed that pyroptosis is crucially involved in NAFL development and progression to NASH.

It is documented that the activation of inflammasome by typical factors such as uric acid, DAMPs, and fatty acids, which increase the expression of NLRP3 components, could trigger the activity of CASPs, promoting inflammation, and causing liver fibrosis[58]. The excessive function of inflammation-related CASPs is implicated directly in the NAFLD pathoetiology, where key effector molecules are considered to be pro-inflammatory cytokines released meanwhile[59,60].

Table 1 The unique morphological and biochemical hallmarks of regulated cell deaths

		Morphological characteristics	Biochemical hallmarks
Apoptotic RCD	Apoptosis	Cell and nucleus shrinkage, nuclear chromatin condensation, karyorrhexis, the formation of apoptotic bodies, and cell fragmentation	↑CASPs (8, 9, 3, and 7), ↑BAD and BAX, ↓BCL2
Non-apoptotic RCDs	Pyroptosis	Inflammasomes caused membrane rupture, cell swelling/cell lysis, DNA fragmentation, nuclear condensation, and nuclear pores	↑CASPs (1 and 7), ↑GSDMs (D, E, *etc.*), ↑IL-18, ↑IL-1β
	Ferroptosis	Cell swelling, mitochondria shrinkage, cristae disappearance, increased density of mitochondrial membrane, the rupture of the outer mitochondrial membrane	↑Fe^{2+}, ROS, lipid peroxidation, ↑ ACSL4 and PTGS2, ↓GPX4 and GSH
	Necroptosis	Organelles swelling, cell membrane rupture, cell lysis, loss of cell membrane integrity, nuclear chromatin deficiency	↑RIPK1, ↑RIPK3, ↑MLKL, ↓CASP-8

RIPK1: Receptor-interacting protein kinase 1; MLKL: Mixed lineage kinase domain-like pseudokinase; RCD: Regulated cell death; CASP: Caspase; ROS: Reactive oxygen species; GSDM: Gasdermin; IL: Interleukin; ACSL4: Acyl-CoA synthetase long-chain family member 4; GPX4: Glutathione peroxidase 4; GSH: Glutathione.

Moreover, the generic substrate for inflammatory CASPs, GSDMD, functions as a downstream mediator of the activation of non-canonical inflammasome by contributing to inflammatory CASP-mediated pyroptosis[61,62]. Importantly, the GSDMDNT domain representing intrinsic pyroptosis-inducing activity in patients with NASH was positively associated with the NAFLD activity score and fibrosis[63]. In fact, the lipogenic gene *Srebp1c* downregulation and upregulation of *Pparα*, a lipolytic gene, and its downstream targets, induced the protection of *Gsdmd*-/- animals from steatosis[63].

As mentioned earlier, DAMPs and PAMPs can cause pyroptosis-related hepatocyte death directly or indirectly causing hepatic damage. It is reported that animals with mutations in myeloid-specific *Nlrp3* do not reveal detectable pyroptotic-mediated hepatocyte death and represent less severe hematopoietic stem cell activation[64]. Hence, one can conclude that in addition to immune cells, pyroptosis in hepatocytes caused by the activation of intrinsic inflammasome can exacerbate inflammation and fibrosis in the liver, determining that both immune cell- and liver-specific NLRP3 inflammasome activation as essential contributors to liver injury[64,65]. However, it is required to investigate hepatocyte-specific *NLRP3* mutant animals to provide convincing evidence of the correlation between hepatocytes and pyroptosis in the onset and progression of liver injury in NAFLD.

An overview of ferroptosis

Ferroptosis was initially reported early 20th century by a cell-permeable compound called erastin, a compound which was lethal to cancer cells of humans with an oncogenic *RAS* mutation[66]. A decade later the term ferroptosis was established to describe an erastin-caused RCD mediated by the accumulation of lipid peroxides dependent on iron[67]. Ferroptosis exerts tumor-suppressor activities, increased mitochondrial membrane density, and cell shrinkage without any typical necrotic or apoptotic manifestations[67]. Similar to pyroptosis, two different signalings including canonical and noncanonical pathways are described as ferroptosis inducers. In the canonical pathway, the glutathione (GSH) peroxidase 4 (GPX4) enzyme is inactivated eighter directly or indirectly which induces ferroptosis, whereas, in a noncanonical manner, the labile iron pool is increased[67].

The direct interaction of erastin with the transporter solute carrier family 7 member 5 (SLC7A5) and subsequent disruption of amino acids transport into the cell by the Xc- system occurs in the canonical pathway of ferroptosis[67]. The regulatory SLC3A2 and a catalytic subunit SLC7A11 are components of the Xc- system that are responsible for the exchange of cystine with glutamate by elevated promotion of cystine cellular uptake[68]. Cystine is the plasma precursor of cysteine that is essential for the synthesis of GSH, a major redox regulatory system[69]. Therefore, the blockage of cystine by inhibitors (*e.g.*, erastin, L-glutamate, *etc.*) is followed by the inhibition of GSH synthesis, suppression of GPX4, and accumulation of phospholipid hydroperoxides (PL-OOH), considered the main mediator of lipoxygenases (LOXs) chain reactions[70].

In the state of intracellular free iron overload, it interacts with reactive oxygen species[71] which ultimately leads to the production of hydroxyl radical that is highly reactive to macromolecules such as polyunsaturated fatty acids (PUFAs)[72]. The oxidation of PUFAs *via* a pathway involving lysophosphatidylcholine acyltransferase 3, acyl-CoA synthetase long-chain family member 4, and LOXs is required for ferroptosis caused lipotoxicity[73-75]. GPX4 is considered the only member capable of reducing membrane phospholipid hydroperoxides determining its significant contribution to confronting permeabilization of plasma membrane, peroxidation of lipids, and ultimately release of DAMPs[76]. In the non-canonical pathway, oxidative damage and ferroptosis are promoted by elevated uptake of iron by transferrin receptor and reduced export of iron by ferroportin[77,78].

Scarce information on the ferroptosis involvement in NAFLD progression

Unfortunately, there is scarce evidence demonstrating the contribution of ferroptosis in NAFLD pathogenesis. However, malondialdehyde and 4-hydroxynonenal[71], as secondary lipid peroxidation products, are suggested as stress markers in patients with NASH[79]. In this regard, well-known antioxidants capable of suppressing lipid peroxidation such as vitamin E and quercetin[80,81] potentially could reduce the levels of alanine transferase in patients with NASH[82,83]. In addition, the accumulation of iron due to metabolic dysfunction is followed by the aggravation of NASH as liver cirrhosis

was reported[39]. Similarly, the exacerbation of primary hemochromatosis is observed in patients with NASH and iron overload[84], while the removal of iron was accompanied by the amelioration of hepatic damage and alanine transferase levels[85]. Furthermore, evidence suggesting the role of ferroptosis in liver steatosis has been discussed[86,87]. Nevertheless, documented information regarding the role of ferroptosis in NAFLD deserves further investigation in appropriate patient models with the disorder, particularly since currently no exact therapeutic strategies are available.

The modification of ferroptosis is considered a novel therapeutic option to confront malignancies[88]. Tyrosine kinase inhibitors (TKIs) are described as the first approved systemic treatments for advanced HCC, however, the systemic treatment of HCC has been further developed with the immune checkpoint inhibitor[89]. Recent evidence suggests the treatment with atezolizumab plus bevacizumab over sorafenib. Fortunately, the latest findings have suggested novel therapeutic strategies based on RCD modifications to confront HCC[89,90]. Lenvatinib, a well-known TKI, could suppress HCC progression *via* the induction of ferroptosis through the inhibition of fibroblast growth factor receptor-4[91]. Metronomic capecitabine, as another example, has been suggested as a second-line therapy in HCC patients after sorafenib failure[92] or discontinuation[93]. Similarly, the study conducted by Wang *et al*[94] indicated the ability of metronomic capecitabine to induce ferroptosis in CD4+ T cells, which is probably attributed to autophagy-related GPX4 degradation in these immune cells, caused the amelioration of liver transplantation rejection[94]. Concordantly, artesunate is considered a well-tolerated and appropriate combination therapy that synergizes with sorafenib to promote ferroptosis in HCC cells[95]. Moreover, GSH S-transferase zeta 1, an enzyme involved in the catabolism of phenylalanine, can inhibit the NRF2/GPX4 axis leading to sensitizes HCC cells to sorafenib-induced ferroptosis[96]. Similarly, tiliroside induces ferroptosis *via* targeting TANK-binding kinase 1 leading to the death of sorafenib-resistant HCC cells[97]. Therefore, it appears necessary for further studies to address the effects of ferroptosis modulators on the death of HCC cells treated with chemotherapeutics.

An overview of necroptosis

Ray and Pickup[98] provided the first evidence of necroptosis in 1996 when they observed a lytic mode of pig kidney cell death infected with the cowpox virus governed by the expression of a CASP inhibitor known as the viral cytokine response modifier A. Four years later, Holler *et al*[71] revealed that the classical death receptors including FAS, TRAIL, and TNF receptors triggered cell death by two alternative pathways. One of these pathways relied on CASP-8, the classical extrinsic pathway of apoptosis, while the one that was dependent on the receptor-interacting protein kinase 1 (RIPK1), the necroptosis. Nevertheless, it was in 2005 when this mode of cell death was named as Degterev *et al*[99] demonstrated that a compound that inhibits the kinase activity of RIPK1, known as necrostatin-1, could inhibit the death of TNF-treated cell lines. Subsequently, the two downstream core components of the necroptotic machinery have been identified that are RIPK3 and mixed lineage kinase domain-like pseudokinase (MLKL)[100-102]. Necroptosis is primarily initiated after infections and stressors such as chemotherapy or radiation and morphologically exhibits the characteristics of necrosis, for example in response to extreme external factors with loss of membrane integrity, elevated cell volume, swelling of organelles, and cellular collapse. In addition, necroptosis is followed by the release of DAMPs such as IL-1α, high-mobility group box 1, and IL-33[103,104]. Specific DAMPs related to necroptosis have not been documented so far, however, the release of DAMPs during necroptosis provokes a severe inflammatory response associated with the development of several diseases[103,104].

The activation of death receptors (DRs) (*e.g.*, TRAIL-R, CD95, TNFR1) and the inactivation, inhibition, or absence of apoptosis signaling components are the two main preconditions for the initiation of necroptosis. In fact, the formation of the RIPK1/RIPK3 platform known as necrosome occurs upon the activation of DRs[20]. In the necrosome, RIPK1 and RIPK3 interact with critical RIP homotypic interaction motifs to adopt a hetero-amyloid structure[105]. Next, RIPK3 phosphorylates MLKL leading to the oligomerization and finally translocation of MLKL to the cell membrane[20]. Along with RIPK1, it is suggested that family proteins of casein kinase 1 as necrosome ingredients directly phosphorylate human RIPK3 to induce necroptosis[106]. Ultimately, pore formation in the cell membrane occurs upon MLKL translocation accompanied by the increment of permeability through activation of Ca^{2+} influx, metalloproteinase and A disintegrin, and phosphatidylserine externalization[107-109]. It is widely accepted that remarkable crosstalk regulations exist between necroptosis and apoptosis in DR-dependent cell death pathways[110], hence one cannot be activated without inhibiting the other. Concordantly, CASP-8 cleaves and inactivates RIPK3 and RIPK1 revealing that apoptosis initiation suppresses necroptosis[111], whereas the activity of RIPK3 determines whether cells die by necroptosis or apoptosis[111,112].

In addition to DRs, a variety of pathways such as nucleic acid sensors (*e.g.*, Z-DNA-binding protein 1, also known as DAI)[113], toll-like receptors (TLRs) such as TLR4 and TLR3[114], retinoic acid-inducible gene 1 protein[115], TNF[116], and adhesion receptors[117] could initiate necroptosis. However, these signaling pathways are frequently RIPK1-independent, although phosphorylation and activation of RIPK3 and MLKL are required[20]. It should be noted that a membrane remodeling and scission machinery known as the endosomal sorting complexes required for transport-III complexes can promote membrane repair and thereby limit MLKL-mediated necroptosis[118]. The contribution of MLKL to the regulation of endosomal trafficking and extracellular vesicle generation reveals a delicate balance between membrane injury and repair determining the ultimate cell fate in necroptosis[119].

Necroptosis exerts a pivotal role in NAFLD

A plethora of evidence has considered an increased level of necroptosis in human cells as one of the main events in the progression of different pathological states including NAFLD, which is generally accompanied by an increase in the infiltration of immune cells and the induction of inflammation[120-122]. Therefore, necroptosis can be assumed as a potential therapeutic target. In addition, the detection of patients with NAFLD and distinguishing it from pathological states with similarities in clinical manifestations and laboratory findings may be another merit of examining necroptosis in patients.

In the following, the current study first discusses the participation of necroptosis in the pathoetiology of the disease and then critically reviews the possible application of necroptosis as a novel diagnostic and therapeutic strategy.

Necroptosis contributes to the progression of the disease

Shreds of evidence during the last two decades have suggested that necroptosis is involved in the occurrence of the disease and actively participates in the progression of NAFLD towards NASH and HCC. The occurrence of cell death in hepatocytes is assumed to be necessary for the occurrence and progression of NAFLD[123,124]. Accordingly, it has been documented that NAFLD coincides with the induction of inflammation, disruption of lipid homeostasis, and characteristics of metabolic syndrome[125], meanwhile, necroptosis is involved with inflammatory responses and intracellular bioenergetic regulation[126,127]. In this regard, the involvement of the RIPK3 in the mitochondrial bioenergetics of hepatocytes[128], the necroptotic death of white adipocytes in NAFLD patients[129], and the induction of necroptosis caused by oleic/palmitic acid imbalance in hepatocytes isolated from patients[130] with NAFLD could be assumed valid markers of the contribution of necroptosis to the lipid metabolism-dependent occurrence of NAFLD. In addition, the induction of necroptosis caused by inflammatory mediators such as TNF[131,132], TLR4[133], and IL-6[134] is considered another event involved in the occurrence of NAFLD.

In addition to inflammatory and metabolic mediators, other signaling pathways may initiate necroptosis and cause NAFLD occurrence. For instance, it has been demonstrated that polarity protein AF6 can directly interact with the intermediate domain of RIPK1 and regulate its ubiquitination mediated by the deubiquitylase enzyme USP21 leading to the promotion of necroptosis in hepatocytes[135]. In this regard, the overexpression of AF6 results in the TNFα-induced necroptosis-mediated mortality of liver cells while hepatocyte-specific deletion of AF6 suppressed necroptosis and the subsequent inflammation in different non-alcoholic liver diseases[135]. The prevention of NAFLD *via* restriction of MLKL-dependent necroptosis by epigenetic silencing of RIPK3 reveals that the initiation of necroptotic-mediated liver cell death contributes to the NAFLD occurrence[136]. In addition to necroptosis-related death, MLKL signaling is involved in NAFLD pathogenesis by regulating other cell death programs such as autophagic flux[137]. Forkhead box protein O1 (FOXO1) is another effective factor in inducing necroptosis and NAFLD where two distinct studies have covered this issue with a different approach. The first study by Qian *et al*[133] showed that Serpina3c deficiency induced necroptosis and NAFLD by FOXO1 overexpression, while the other assumed that FOXO1 induces necroptosis and endoplasmic reticulum stress, and as a result, is involved in the pathogenesis of the disease[138]. Similarly, it has been documented that necroptosis induced by oxidative stress plays a key role in the pathogenesis of NAFLD and subsequent liver fibrosis[139,140].

Disease progression towards NASH and HCC is one of the undesired consequences of necroptosis induction in NAFLD patients. Several studies have assumed that cross-talk between RCDs is involved in the promotion of inflammation and the establishment of NASH following NAFLD[87,137,141,142]. It has been repeatedly shown that the induction of inflammation (for example, through TNF and TLR) and the resulting necroptosis actively cause NAFLD-to-NASH transition[143,144]. Importantly, necroptosis has been described as a pathological event in the liver that facilitates the appearance of steatohepatitis, as it has been reported that RIPK1 and RIPK3 cause hepatocyte death and exacerbation of NASH by inducing inflammation within macrophages and interacting with the JNK pathway[145-147]. In addition, diet is one of the factors that may contribute to NAFLD progression and steatosis by modulating RIPK3, inflammation, and necroptosis[148,149]. Although rare evidence of necroptosis involvement in the NAFLD-to-HCC transition has been reported, two recent studies have clarified that RIPK3 as a regulator of lipid metabolism participates in liver carcinogenesis, and RIPK3/MLKL absence reduces the risk of carcinogenesis[150,151].

The active involvement of necroptosis in the occurrence and progression of the disease continues with its effect in determining the severity of hepatic tissue injury. For example, the exacerbation of liver injury due to myeloid deficiency of CCN3 is mediated through the activation of necroptosis[152]. Also, the crosstalk between necroptosis and inflammatory mediators promoted both necroptosis and inflammation in liver fatty cells and as a result, aggravated liver damage in NAFLD models[134,153,154]. SPARC overexpression is another pathological event that leads to severe liver damage in patients with NAFLD by increasing the level of RIPK1/RIPK3 and promoting necroptosis[155]. Importantly, the involvement of necroptosis in the pathogenesis of the disease as well as the aggravation of pathological consequences can promise it as a potential biomarker for NAFLD early detection, grading, and prediction of progression. Moreover, targeting upstream effectors that promote necroptosis is an interesting novel strategy that may be effective in disease management. Therefore, in the next two sections, the findings related to the diagnostic and therapeutic efficacy of necroptosis in patients with NAFLD have been reviewed (Table 2).

The diagnostic value of necroptosis

Although the involvement of necroptosis in the occurrence of NAFLD and its progression to NASH and HCC has been appropriately elucidated, rare reports of the diagnostic value of necroptosis in the early detection and grading of the disease have been presented. Considering the coincidence of necroptosis and inflammation and the strengthening effect they have on each other, the main markers presented have been related to inflammatory responses. For example, the evidence presented on the changed levels of TNF-α, IL-10, and IL-1α in MAFLD patients can be considered a potential diagnostic marker[134,156,157]. In addition, it has been demonstrated that the high level of TNF-α along with the low level of serum IL-10 can be an indicator of the severity of NAFLD in the morbidity of obese men[156], and these two markers have provided promising efficacy in the follow-up of patients with NAFLD[158]. Similarly, it has been suggested that polymorphisms in the gene encoding TNF-α may be a marker of NAFLD progression and risk of coronary artery disease[159]. Accordingly, a 4-year follow-up study has revealed that TNF-α can function as a predictor of NAFLD development[131]. Although TNF-α is one of the triggering factors of the necroptotic cell death pathway and its diagnostic ability can be assumed to be related to necroptosis, further studies to find innate markers of necroptosis appear

Table 2 Participation of necroptosis in the occurrence and progression of the disease and its effectiveness as a diagnostic marker and therapeutic target

Function	Advantages/limitations
Pathoetiology	The upregulation of RIPK1, RIPK3, and MLKL leads to the necroptosis of hepatocytes in the fatty liver, which along with inflammatory responses contributes to the induction of NAFLD. In addition, the intensification of necroptotic death of hepatocytes is followed by the aggravation of the disease and its progress toward NASH and HCC
Diagnosis	Most of the presented biomarkers are related to the upstream inflammatory inducers of necroptosis such as TNF and ILs. Although the aforementioned markers have provided diagnostic and prognostic properties, changes in inflammatory markers occur in a variety of disorders. In addition, the uncertainty of the sensitivity and specificity of the few suggested markers complicates the evaluation of their diagnostic value. Therefore, more studies that evaluate specific necroptotic biomarkers in NAFLD patients are encouraged
Therapy	Direct inhibitors of necroptosis (RIPK1 inhibitors for example) and a variety of herbal antioxidants with anti-necroptotic, anti-inflammatory, and regulating lipid metabolism properties have been proposed in experimental and human studies. However, no clinical trial has been registered in this direction, which reveals the necessity of designing further studies

NAFLD: Nonalcoholic fatty liver disease; NASH: Non-alcoholic steatohepatitis; HCC: Hepatocellular carcinoma; TNF: Tumor necrosis factor; IL: Interleukin; RIPK1: Receptor-interacting protein kinase 1; MLKL: Mixed lineage kinase domain-like pseudokinase.

necessary. Moreover, inflammatory markers are mainly expressed in a wide range of disorders, and the lack of reporting of the sensitivity and specificity of the proposed markers complicates the determination of their diagnostic value.

Pathological alterations in the expression of MLKL, RIPK1, and RIPK3 can be suggested as the most potential markers related to necroptosis in diagnosing NAFLD and predicting its progress[136,150,160,161]. A recent study has determined that metabolomic and lipidomic screening has identified the participation of RCDs, particularly necroptosis, in the progression of NAFLD toward cancer[162], which may be of possible clinical importance in the follow-up of patients and determining the risk of disease progression. Nevertheless, the available evidence is rare, therefore further studies on this content represent a crucial necessity.

Necroptosis as a potential therapeutic target

It was previously discussed that the induction of necroptosis in hepatocytes is related to the occurrence and progression of NAFLD, therefore this pathway of cell death displays the characteristics of a therapeutic target. Several studies have investigated the efficiency of such properties, which can be reviewed in two categories, one contains the direct inhibitors of the mediators of the necroptosis pathway, and the other includes the herbals/chemicals that have revealed therapeutic properties through modulation of necroptosis.

It has been demonstrated that a highly specific inhibitor of RIPK1 known as RIPA-56 was able to ameliorate an animal model of NAFLD *via* down-regulation of MLKL, reduction of hepatic damage, inflammation, fibrosis, characteristic of NASH, as well as of steatosis[163]. In addition, the inhibition of MLKL resulted in a reduction of fat *de novo* synthesis and chemokine ligand expression in patients with NAFLD[164]. Similarly, chemical compounds that inhibited necroptosis along with apoptosis in hepatocytes were able to alleviate NAFLD-related characteristics[165-168]. Due to the cross-talk between RCDs, it is clinically important to note that the process of necroptosis inhibition should not activate other cell death pathways, as the absence of RIPK3 increased inflammation and hepatocyte apoptosis as well as early fibrotic responses leading to exacerbation of the disease[169].

Interestingly, a variety of herbal compounds such as epigallocatechin gallate, pentoxifylline, kaempferol, quercetin, metformin, *etc.* demonstrated anti-necroptotic properties that benefited the alleviation of NAFLD[170-174]. Regulating lipid metabolism, suppressing destructive inflammatory responses, maintaining cellular homeostasis, and also the rarity of adverse effects are attractive properties that antioxidant compounds provide in the treatment of NAFLD, in addition to inhibiting necroptosis. However, no clinical trials have been registered on the clinicaltrials.gov website, which indicates insufficient current information to confirm treatment strategies based on inhibition of necroptosis. Therefore, the conduct of further studies on this content is pivotally encouraged.

CONCLUSION

The findings of the current review revealed that the induction of necroptosis along with inflammatory responses pivotally contributes to the occurrence of NAFLD. Moreover, the continuation of the necroptotic death of hepatocytes can cause the disease to progress to NASH and HCC. Nevertheless, the diagnostic value of necroptosis-based markers has been rarely evaluated and disease management strategies based on necroptosis necessarily require further investigations in this direction.

FOOTNOTES

Co-corresponding authors: Qing Xie and Xiao-Hua Song.

Author contributions: Sun HJ, Jiao B, Xie Q, and Song XH designed the research and supervised the study; Wang Y, Zhang YH, Chen G, Wang ZX, and Zhao H performed the source searching and determined included material; Jiao B, Wang Y, Wang ZX, and Zhao H contributed interpretation of included material; Sun HJ, Jiao B, Zhang YH, Chen G, Xie Q, and Song XH prepared the primary draft of the manuscript; and all authors read and approved the final version of the article. Due to the identical collaboration of Xie Q and Song XH, both authors were considered as co-corresponding authors. Song XH was determined as the responsible author for submission of the manuscript and submission of peer review and publication processes.

Conflict-of-interest statement: All the authors report no relevant conflicts of interest for this article.

Country/Territory of origin: China

ORCID number: Qing Xie 0000-0002-2582-8803; Xiao-Hua Song 0009-0005-2174-1232.

S-Editor: Wang JJ
L-Editor: A
P-Editor: Zheng XM

REFERENCES

1 **Younossi ZM**, Golabi P, Paik JM, Henry A, Van Dongen C, Henry L. The global epidemiology of nonalcoholic fatty liver disease (NAFLD) and nonalcoholic steatohepatitis (NASH): a systematic review. *Hepatology* 2023; **77**: 1335-1347 [PMID: 36626630 DOI: 10.1097/HEP.0000000000000004]
2 **Estes C**, Razavi H, Loomba R, Younossi Z, Sanyal AJ. Modeling the epidemic of nonalcoholic fatty liver disease demonstrates an exponential increase in burden of disease. *Hepatology* 2018; **67**: 123-133 [PMID: 28802062 DOI: 10.1002/hep.29466]
3 **Mosavat SH**. Efficacy of traditional Persian medicine-based diet on non-alcoholic fatty liver disease: a randomized, controlled, clinical trial. *Galen Med J* 2017; **6**: 208-216 [DOI: 10.22086/gmj.v6i3.813]
4 **Ludwig J**, Viggiano TR, McGill DB, Oh BJ. Nonalcoholic steatohepatitis: Mayo Clinic experiences with a hitherto unnamed disease. *Mayo Clin Proc* 1980; **55**: 434-438 [PMID: 7382552]
5 **Geh D**, Anstee QM, Reeves HL. NAFLD-Associated HCC: Progress and Opportunities. *J Hepatocell Carcinoma* 2021; **8**: 223-239 [PMID: 33854987 DOI: 10.2147/JHC.S272213]
6 **Michelotti GA**, Machado MV, Diehl AM. NAFLD, NASH and liver cancer. *Nat Rev Gastroenterol Hepatol* 2013; **10**: 656-665 [PMID: 24080776 DOI: 10.1038/nrgastro.2013.183]
7 **Farrell GC**, Wong VW, Chitturi S. NAFLD in Asia--as common and important as in the West. *Nat Rev Gastroenterol Hepatol* 2013; **10**: 307-318 [PMID: 23458891 DOI: 10.1038/nrgastro.2013.34]
8 **Younossi ZM**, Blissett D, Blissett R, Henry L, Stepanova M, Younossi Y, Racila A, Hunt S, Beckerman R. The economic and clinical burden of nonalcoholic fatty liver disease in the United States and Europe. *Hepatology* 2016; **64**: 1577-1586 [PMID: 27543837 DOI: 10.1002/hep.28785]
9 **Younossi ZM**, Koenig AB, Abdelatif D, Fazel Y, Henry L, Wymer M. Global epidemiology of nonalcoholic fatty liver disease-Meta-analytic assessment of prevalence, incidence, and outcomes. *Hepatology* 2016; **64**: 73-84 [PMID: 26707365 DOI: 10.1002/hep.28431]
10 **Younossi Z**, Anstee QM, Marietti M, Hardy T, Henry L, Eslam M, George J, Bugianesi E. Global burden of NAFLD and NASH: trends, predictions, risk factors and prevention. *Nat Rev Gastroenterol Hepatol* 2018; **15**: 11-20 [PMID: 28930295 DOI: 10.1038/nrgastro.2017.109]
11 **Estes C**, Anstee QM, Arias-Loste MT, Bantel H, Bellentani S, Caballeria J, Colombo M, Craxi A, Crespo J, Day CP, Eguchi Y, Geier A, Kondili LA, Kroy DC, Lazarus JV, Loomba R, Manns MP, Marchesini G, Nakajima A, Negro F, Petta S, Ratziu V, Romero-Gomez M, Sanyal A, Schattenberg JM, Tacke F, Tanaka J, Trautwein C, Wei L, Zeuzem S, Razavi H. Modeling NAFLD disease burden in China, France, Germany, Italy, Japan, Spain, United Kingdom, and United States for the period 2016-2030. *J Hepatol* 2018; **69**: 896-904 [PMID: 29886156 DOI: 10.1016/j.jhep.2018.05.036]
12 **Alexander M**, Loomis AK, Fairburn-Beech J, van der Lei J, Duarte-Salles T, Prieto-Alhambra D, Ansell D, Pasqua A, Lapi F, Rijnbeek P, Mosseveld M, Avillach P, Egger P, Kendrick S, Waterworth DM, Sattar N, Alazawi W. Real-world data reveal a diagnostic gap in non-alcoholic fatty liver disease. *BMC Med* 2018; **16**: 130 [PMID: 30099968 DOI: 10.1186/s12916-018-1103-x]
13 **Wong RJ**, Cheung R, Ahmed A. Nonalcoholic steatohepatitis is the most rapidly growing indication for liver transplantation in patients with hepatocellular carcinoma in the U.S. *Hepatology* 2014; **59**: 2188-2195 [PMID: 24375711 DOI: 10.1002/hep.26986]
14 **Cleveland E**, Bandy A, VanWagner LB. Diagnostic challenges of nonalcoholic fatty liver disease/nonalcoholic steatohepatitis. *Clin Liver Dis (Hoboken)* 2018; **11**: 98-104 [PMID: 30147867 DOI: 10.1002/cld.716]
15 **Roeb E**. Diagnostic and Therapy of Nonalcoholic Fatty Liver Disease: A Narrative Review. *Visc Med* 2022; **38**: 126-132 [PMID: 35614896 DOI: 10.1159/000519611]
16 **Wong VWS**, Zelber-Sagi S, Cusi K, Carrieri P, Wright E, Crespo J, Lazarus JV. Management of NAFLD in primary care settings. *Liver Int* 2022; **42**: 2377-2389 [PMID: 35986897 DOI: 10.1111/liv.15404]
17 **Zou YG**, Wang H, Li WW, Dai DL. Challenges in pediatric inherited/metabolic liver disease: Focus on the disease spectrum, diagnosis and management of relatively common disorders. *World J Gastroenterol* 2023; **29**: 2114-2126 [PMID: 37122598 DOI: 10.3748/wjg.v29.i14.2114]
18 **Ashkenazi A**, Salvesen G. Regulated cell death: signaling and mechanisms. *Annu Rev Cell Dev Biol* 2014; **30**: 337-356 [PMID: 25150011 DOI: 10.1146/annurev-cellbio-100913-013226]
19 **Christgen S**, Tweedell RE, Kanneganti TD. Programming inflammatory cell death for therapy. *Pharmacol Ther* 2022; **232**: 108010 [PMID:

34619283 DOI: 10.1016/j.pharmthera.2021.108010]
20 **Tang D**, Kang R, Berghe TV, Vandenabeele P, Kroemer G. The molecular machinery of regulated cell death. *Cell Res* 2019; **29**: 347-364 [PMID: 30948788 DOI: 10.1038/s41422-019-0164-5]
21 **Jaeschke H**, Ramachandran A. Acetaminophen-induced apoptosis: Facts versus fiction. *J Clin Transl Res* 2020; **6**: 36-47 [PMID: 33426354]
22 **Samare-Najaf M**, Neisy A, Samareh A, Moghadam D, Jamali N, Zarei R, Zal F. The constructive and destructive impact of autophagy on both genders' reproducibility, a comprehensive review. *Autophagy* 2023; **19**: 3033-3061 [PMID: 37505071 DOI: 10.1080/15548627.2023.2238577]
23 **Xiao Z**, Liu M, Yang F, Liu G, Liu J, Zhao W, Ma S, Duan Z. Programmed cell death and lipid metabolism of macrophages in NAFLD. *Front Immunol* 2023; **14**: 1118449 [PMID: 36742318 DOI: 10.3389/fimmu.2023.1118449]
24 **Gautheron J**, Gores GJ, Rodrigues CMP. Lytic cell death in metabolic liver disease. *J Hepatol* 2020; **73**: 394-408 [PMID: 32298766 DOI: 10.1016/j.jhep.2020.04.001]
25 **Clarke JI**, Brillanf N, Antoine DJ. Novel circulating- and imaging-based biomarkers to enhance the mechanistic understanding of human drug-induced liver injury. *J Clin Transl Res* 2017; **3**: 199-211 [PMID: 30873474]
26 **Ajoolabady A**, Tang D, Kroemer G, Ren J. Ferroptosis in hepatocellular carcinoma: mechanisms and targeted therapy. *Br J Cancer* 2023; **128**: 190-205 [PMID: 36229582 DOI: 10.1038/s41416-022-01998-x]
27 **Gibellini L**, Moro L. Programmed Cell Death in Health and Disease. *Cells* 2021; **10** [PMID: 34359935 DOI: 10.3390/cells10071765]
28 **Schwabe RF**, Luedde T. Apoptosis and necroptosis in the liver: a matter of life and death. *Nat Rev Gastroenterol Hepatol* 2018; **15**: 738-752 [PMID: 30250076 DOI: 10.1038/s41575-018-0065-y]
29 **Wang K**. Molecular mechanisms of hepatic apoptosis. *Cell Death Dis* 2014; **5**: e996 [PMID: 24434519 DOI: 10.1038/cddis.2013.499]
30 **Kim-Campbell N**, Gomez H, Bayir H. Cell death pathways: apoptosis and regulated necrosis. In: Critical care nephrology (Third Edition). Amsterdam: Elsevier, 2019: 113-121.e112
31 **Zhang Q**, Jia M, Wang Y, Wang Q, Wu J. Cell Death Mechanisms in Cerebral Ischemia-Reperfusion Injury. *Neurochem Res* 2022; **47**: 3525-3542 [PMID: 35976487 DOI: 10.1007/s11064-022-03697-8]
32 **Lukenaite B**, Griciune E, Leber B, Strupas K, Stiegler P, Schemmer P. Necroptosis in Solid Organ Transplantation: A Literature Overview. *Int J Mol Sci* 2022; **23** [PMID: 35409037 DOI: 10.3390/ijms23073677]
33 **Galluzzi L**, Myint M. Cell death and senescence. *J Transl Med* 2023; **21**: 425 [PMID: 37386590 DOI: 10.1186/s12967-023-04297-y]
34 **Shen J**, San W, Zheng Y, Zhang S, Cao D, Chen Y, Meng G. Different types of cell death in diabetic endothelial dysfunction. *Biomed Pharmacother* 2023; **168**: 115802 [PMID: 37918258 DOI: 10.1016/j.biopha.2023.115802]
35 **Zychlinsky A**, Prevost MC, Sansonetti PJ. Shigella flexneri induces apoptosis in infected macrophages. *Nature* 1992; **358**: 167-169 [PMID: 1614548 DOI: 10.1038/358167a0]
36 **Cookson BT**, Brennan MA. Pro-inflammatory programmed cell death. *Trends Microbiol* 2001; **9**: 113-114 [PMID: 11303500 DOI: 10.1016/s0966-842X(00)01936-3]
37 **Ma Y**, Zhao R, Guo H, Tong Q, Langdon WY, Liu W, Zhang J. Cytosolic LPS-induced caspase-11 oligomerization and activation is regulated by extended synaptotagmin 1. *Cell Rep* 2023; **42**: 112726 [PMID: 37393619 DOI: 10.1016/j.celrep.2023.112726]
38 **Song H**, Yang B, Li Y, Qian A, Kang Y, Shan X. Focus on the Mechanisms and Functions of Pyroptosis, Inflammasomes, and Inflammatory Caspases in Infectious Diseases. *Oxid Med Cell Longev* 2022; **2022**: 2501279 [PMID: 35132346 DOI: 10.1155/2022/2501279]
39 **Nelson JE**, Wilson L, Brunt EM, Yeh MM, Kleiner DE, Unalp-Arida A, Kowdley KV; Nonalcoholic Steatohepatitis Clinical Research Network. Relationship between the pattern of hepatic iron deposition and histological severity in nonalcoholic fatty liver disease. *Hepatology* 2011; **53**: 448-457 [PMID: 21274866 DOI: 10.1002/hep.24038]
40 **Hachim MY**, Khalil BA, Elemam NM, Maghazachi AA. Pyroptosis: The missing puzzle among innate and adaptive immunity crosstalk. *J Leukoc Biol* 2020; **108**: 323-338 [PMID: 32083338 DOI: 10.1002/JLB.3MIR0120-625R]
41 **Huang X**, Feng Y, Xiong G, Whyte S, Duan J, Yang Y, Wang K, Yang S, Geng Y, Ou Y, Chen D. Caspase-11, a specific sensor for intracellular lipopolysaccharide recognition, mediates the non-canonical inflammatory pathway of pyroptosis. *Cell Biosci* 2019; **9**: 31 [PMID: 30962873 DOI: 10.1186/s13578-019-0292-0]
42 **Shariati A**, Raberi VS, Masumi M, Tarbiat A, Rastgoo E, Faramarzzadeh R. The Regulation of Pyroptosis and Ferroptosis by MicroRNAs in Cardiovascular Diseases. *Galen Med J* 2023; **12**: e2933 [DOI: 10.31661/gmj.v12i.2933]
43 **Kayagaki N**, Stowe IB, Lee BL, O'Rourke K, Anderson K, Warming S, Cuellar T, Haley B, Roose-Girma M, Phung QT, Liu PS, Lill JR, Li H, Wu J, Kummerfeld S, Zhang J, Lee WP, Snipas SJ, Salvesen GS, Morris LX, Fitzgerald L, Zhang Y, Bertram EM, Goodnow CC, Dixit VM. Caspase-11 cleaves gasdermin D for non-canonical inflammasome signalling. *Nature* 2015; **526**: 666-671 [PMID: 26375259 DOI: 10.1038/nature15541]
44 **Shi J**, Zhao Y, Wang K, Shi X, Wang Y, Huang H, Zhuang Y, Cai T, Wang F, Shao F. Cleavage of GSDMD by inflammatory caspases determines pyroptotic cell death. *Nature* 2015; **526**: 660-665 [PMID: 26375003 DOI: 10.1038/nature15514]
45 **Orning P**, Lien E, Fitzgerald KA. Gasdermins and their role in immunity and inflammation. *J Exp Med* 2019; **216**: 2453-2465 [PMID: 31548300 DOI: 10.1084/jem.20190545]
46 **Jiang M**, Qi L, Li L, Li Y. The caspase-3/GSDME signal pathway as a switch between apoptosis and pyroptosis in cancer. *Cell Death Discov* 2020; **6**: 112 [PMID: 33133646 DOI: 10.1038/s41420-020-00349-0]
47 **Shen X**, Wang H, Weng C, Jiang H, Chen J. Caspase 3/GSDME-dependent pyroptosis contributes to chemotherapy drug-induced nephrotoxicity. *Cell Death Dis* 2021; **12**: 186 [PMID: 33589596 DOI: 10.1038/s41419-021-03458-5]
48 **Broz P**, Pelegrín P, Shao F. The gasdermins, a protein family executing cell death and inflammation. *Nat Rev Immunol* 2020; **20**: 143-157 [PMID: 31690840 DOI: 10.1038/s41577-019-0228-2]
49 **Gan C**, Cai Q, Tang C, Gao J. Inflammasomes and Pyroptosis of Liver Cells in Liver Fibrosis. *Front Immunol* 2022; **13**: 896473 [PMID: 35707547 DOI: 10.3389/fimmu.2022.896473]
50 **Sun P**, Zhong J, Liao H, Loughran P, Mulla J, Fu G, Tang D, Fan J, Billiar TR, Gao W, Scott MJ. Hepatocytes Are Resistant to Cell Death From Canonical and Non-Canonical Inflammasome-Activated Pyroptosis. *Cell Mol Gastroenterol Hepatol* 2022; **13**: 739-757 [PMID: 34890842 DOI: 10.1016/j.jcmgh.2021.11.009]
51 **Vanaja SK**, Rathinam VA, Fitzgerald KA. Mechanisms of inflammasome activation: recent advances and novel insights. *Trends Cell Biol* 2015; **25**: 308-315 [PMID: 25639489 DOI: 10.1016/j.tcb.2014.12.009]
52 **Wright SS**, Vasudevan SO, Rathinam VA. Mechanisms and Consequences of Noncanonical Inflammasome-Mediated Pyroptosis. *J Mol Biol* 2022; **434**: 167245 [PMID: 34537239 DOI: 10.1016/j.jmb.2021.167245]

53 **Armandi A**, Bugianesi E. Natural history of NASH. *Liver Int* 2021; **41** Suppl 1: 78-82 [PMID: 34155792 DOI: 10.1111/liv.14910]

54 **Dong J**, Viswanathan S, Adami E, Singh BK, Chothani SP, Ng B, Lim WW, Zhou J, Tripathi M, Ko NSJ, Shekeran SG, Tan J, Lim SY, Wang M, Lio PM, Yen PM, Schafer S, Cook SA, Widjaja AA. Hepatocyte-specific IL11 cis-signaling drives lipotoxicity and underlies the transition from NAFLD to NASH. *Nat Commun* 2021; **12**: 66 [PMID: 33397952 DOI: 10.1038/s41467-020-20303-z]

55 **Velliou RI**, Legaki AI, Nikolakopoulou P, Vlachogiannis NI, Chatzigeorgiou A. Liver endothelial cells in NAFLD and transition to NASH and HCC. *Cell Mol Life Sci* 2023; **80**: 314 [PMID: 37798474 DOI: 10.1007/s00018-023-04966-7]

56 **Baffy G**. Kupffer cells in non-alcoholic fatty liver disease: the emerging view. *J Hepatol* 2009; **51**: 212-223 [PMID: 19447517 DOI: 10.1016/j.jhep.2009.03.008]

57 **Tosello-Trampont AC**, Landes SG, Nguyen V, Novobrantseva TI, Hahn YS. Kuppfer cells trigger nonalcoholic steatohepatitis development in diet-induced mouse model through tumor necrosis factor-α production. *J Biol Chem* 2012; **287**: 40161-40172 [PMID: 23066023 DOI: 10.1074/jbc.M112.417014]

58 **Szabo G**, Petrasek J. Inflammasome activation and function in liver disease. *Nat Rev Gastroenterol Hepatol* 2015; **12**: 387-400 [PMID: 26055245 DOI: 10.1038/nrgastro.2015.94]

59 **Beier JI**, Banales JM. Pyroptosis: An inflammatory link between NAFLD and NASH with potential therapeutic implications. *J Hepatol* 2018; **68**: 643-645 [PMID: 29408544 DOI: 10.1016/j.jhep.2018.01.017]

60 **Bessone F**, Razori MV, Roma MG. Molecular pathways of nonalcoholic fatty liver disease development and progression. *Cell Mol Life Sci* 2019; **76**: 99-128 [PMID: 30343320 DOI: 10.1007/s00018-018-2947-0]

61 **Kamajaya LJ**, Boucher D. Gasdermin D Cleavage Assay Following Inflammasome Activation. *Methods Mol Biol* 2022; **2459**: 39-49 [PMID: 35212952 DOI: 10.1007/978-1-0716-2144-8_4]

62 **Yang R**. Interaction between caspases and their substrates in the inflammasome signaling pathway. [cited 15 November 2023]. Available from: https://etd.ohiolink.edu/acprod/odb_etd/etd/r/1501/10?clear=10&p10_accession_num=case1559917811566556

63 **Xu B**, Jiang M, Chu Y, Wang W, Chen D, Li X, Zhang Z, Zhang D, Fan D, Nie Y, Shao F, Wu K, Liang J. Gasdermin D plays a key role as a pyroptosis executor of non-alcoholic steatohepatitis in humans and mice. *J Hepatol* 2018; **68**: 773-782 [PMID: 29273476 DOI: 10.1016/j.jhep.2017.11.040]

64 **Wree A**, Eguchi A, McGeough MD, Pena CA, Johnson CD, Canbay A, Hoffman HM, Feldstein AE. NLRP3 inflammasome activation results in hepatocyte pyroptosis, liver inflammation, and fibrosis in mice. *Hepatology* 2014; **59**: 898-910 [PMID: 23813842 DOI: 10.1002/hep.26592]

65 **Wree A**, McGeough MD, Inzaugarat ME, Eguchi A, Schuster S, Johnson CD, Peña CA, Geisler LJ, Papouchado BG, Hoffman HM, Feldstein AE. NLRP3 inflammasome driven liver injury and fibrosis: Roles of IL-17 and TNF in mice. *Hepatology* 2018; **67**: 736-749 [PMID: 28902427 DOI: 10.1002/hep.29523]

66 **Dolma S**, Lessnick SL, Hahn WC, Stockwell BR. Identification of genotype-selective antitumor agents using synthetic lethal chemical screening in engineered human tumor cells. *Cancer Cell* 2003; **3**: 285-296 [PMID: 12676586 DOI: 10.1016/s1535-6108(03)00050-3]

67 **Dixon SJ**, Lemberg KM, Lamprecht MR, Skouta R, Zaitsev EM, Gleason CE, Patel DN, Bauer AJ, Cantley AM, Yang WS, Morrison B 3rd, Stockwell BR. Ferroptosis: an iron-dependent form of nonapoptotic cell death. *Cell* 2012; **149**: 1060-1072 [PMID: 22632970 DOI: 10.1016/j.cell.2012.03.042]

68 **Lo M**, Wang YZ, Gout PW. The x(c)- cystine/glutamate antiporter: a potential target for therapy of cancer and other diseases. *J Cell Physiol* 2008; **215**: 593-602 [PMID: 18181196 DOI: 10.1002/jcp.21366]

69 **Lu SC**. Glutathione synthesis. *Biochim Biophys Acta* 2013; **1830**: 3143-3153 [PMID: 22995213 DOI: 10.1016/j.bbagen.2012.09.008]

70 **Yang WS**, SriRamaratnam R, Welsch ME, Shimada K, Skouta R, Viswanathan VS, Cheah JH, Clemons PA, Shamji AF, Clish CB, Brown LM, Girotti AW, Cornish VW, Schreiber SL, Stockwell BR. Regulation of ferroptotic cancer cell death by GPX4. *Cell* 2014; **156**: 317-331 [PMID: 24439385 DOI: 10.1016/j.cell.2013.12.010]

71 **Holler N**, Zaru R, Micheau O, Thome M, Attinger A, Valitutti S, Bodmer JL, Schneider P, Seed B, Tschopp J. Fas triggers an alternative, caspase-8-independent cell death pathway using the kinase RIP as effector molecule. *Nat Immunol* 2000; **1**: 489-495 [PMID: 11101870 DOI: 10.1038/82732]

72 **Feng H**, Stockwell BR. Unsolved mysteries: How does lipid peroxidation cause ferroptosis? *PLoS Biol* 2018; **16**: e2006203 [PMID: 29795546 DOI: 10.1371/journal.pbio.2006203]

73 **Doll S**, Proneth B, Tyurina YY, Panzilius E, Kobayashi S, Ingold I, Irmler M, Beckers J, Aichler M, Walch A, Prokisch H, Trümbach D, Mao G, Qu F, Bayir H, Füllekrug J, Scheel CH, Wurst W, Schick JA, Kagan VE, Angeli JP, Conrad M. ACSL4 dictates ferroptosis sensitivity by shaping cellular lipid composition. *Nat Chem Biol* 2017; **13**: 91-98 [PMID: 27842070 DOI: 10.1038/nchembio.2239]

74 **Kagan VE**, Mao G, Qu F, Angeli JP, Doll S, Croix CS, Dar HH, Liu B, Tyurin VA, Ritov VB, Kapralov AA, Amoscato AA, Jiang J, Anthonymuthu T, Mohammadyani D, Yang Q, Proneth B, Klein-Seetharaman J, Watkins S, Bahar I, Greenberger J, Mallampalli RK, Stockwell BR, Tyurina YY, Conrad M, Bayır H. Oxidized arachidonic and adrenic PEs navigate cells to ferroptosis. *Nat Chem Biol* 2017; **13**: 81-90 [PMID: 27842066 DOI: 10.1038/nchembio.2238]

75 **Yang WS**, Kim KJ, Gaschler MM, Patel M, Shchepinov MS, Stockwell BR. Peroxidation of polyunsaturated fatty acids by lipoxygenases drives ferroptosis. *Proc Natl Acad Sci U S A* 2016; **113**: E4966-E4975 [PMID: 27506793 DOI: 10.1073/pnas.1603244113]

76 **Xie Y**, Kang R, Klionsky DJ, Tang D. GPX4 in cell death, autophagy, and disease. *Autophagy* 2023; **19**: 2621-2638 [PMID: 37272058 DOI: 10.1080/15548627.2023.2218764]

77 **Kang YP**, Mockabee-Macias A, Jiang C, Falzone A, Prieto-Farigua N, Stone E, Harris IS, DeNicola GM. Non-canonical Glutamate-Cysteine Ligase Activity Protects against Ferroptosis. *Cell Metab* 2021; **33**: 174-189.e7 [PMID: 33357455 DOI: 10.1016/j.cmet.2020.12.007]

78 **Wang X**, Wang Y, Li Z, Qin J, Wang P. Regulation of Ferroptosis Pathway by Ubiquitination. *Front Cell Dev Biol* 2021; **9**: 699304 [PMID: 34485285 DOI: 10.3389/fcell.2021.699304]

79 **Loguercio C**, De Girolamo V, de Sio I, Tuccillo C, Ascione A, Baldi F, Budillon G, Cimino L, Di Carlo A, Di Marino MP, Morisco F, Picciotto F, Terracciano L, Vecchione R, Verde V, Del Vecchio Blanco C. Non-alcoholic fatty liver disease in an area of southern Italy: main clinical, histological, and pathophysiological aspects. *J Hepatol* 2001; **35**: 568-574 [PMID: 11690701 DOI: 10.1016/S0168-8278(01)00192-1]

80 **Jafari Khorchani M**, Samare-Najaf M, Abbasi A, Vakili S, Zal F. Effects of quercetin, vitamin E, and estrogen on Metabolic-Related factors in uterus and serum of ovariectomized rat models. *Gynecol Endocrinol* 2021; **37**: 764-768 [PMID: 33525940 DOI: 10.1080/09513590.2021.1879784]

81 **Samare-Najaf M**, Zal F, Jamali N, Vakili S, Khodabandeh Z. Do Quercetin and Vitamin E Properties Preclude Doxorubicin-induced Stress and Inflammation in Reproductive Tissues? *Curr Cancer Ther Rev* 2022; **18** [DOI: 10.2174/1573394718666220726105843]

82 **Gnoni A**, Di Chiara Stanca B, Giannotti L, Gnoni GV, Siculella L, Damiano F. Quercetin Reduces Lipid Accumulation in a Cell Model of NAFLD by Inhibiting De Novo Fatty Acid Synthesis through the Acetyl-CoA Carboxylase 1/AMPK/PP2A Axis. *Int J Mol Sci* 2022; **23** [PMID: 35162967 DOI: 10.3390/ijms23031044]

83 **Sanyal AJ**, Chalasani N, Kowdley KV, McCullough A, Diehl AM, Bass NM, Neuschwander-Tetri BA, Lavine JE, Tonascia J, Unalp A, Van Natta M, Clark J, Brunt EM, Kleiner DE, Hoofnagle JH, Robuck PR; NASH CRN. Pioglitazone, vitamin E, or placebo for nonalcoholic steatohepatitis. *N Engl J Med* 2010; **362**: 1675-1685 [PMID: 20427778 DOI: 10.1056/NEJMoa0907929]

84 **Bonkovsky HL**, Jawaid Q, Tortorelli K, LeClair P, Cobb J, Lambrecht RW, Banner BF. Non-alcoholic steatohepatitis and iron: increased prevalence of mutations of the HFE gene in non-alcoholic steatohepatitis. *J Hepatol* 1999; **31**: 421-429 [PMID: 10488699 DOI: 10.1016/s0168-8278(99)80032-4]

85 **Valenti L**, Moscatiello S, Vanni E, Fracanzani AL, Bugianesi E, Fargion S, Marchesini G. Venesection for non-alcoholic fatty liver disease unresponsive to lifestyle counselling--a propensity score-adjusted observational study. *QJM* 2011; **104**: 141-149 [PMID: 20851820 DOI: 10.1093/qjmed/hcq170]

86 **Hernández-Alvarez MI**, Sebastián D, Vives S, Ivanova S, Bartoccioni P, Kakimoto P, Plana N, Veiga SR, Hernández V, Vasconcelos N, Peddinti G, Adrover A, Jové M, Pamplona R, Gordaliza-Alaguero I, Calvo E, Cabré N, Castro R, Kuzmanic A, Boutant M, Sala D, Hyotylainen T, Orešič M, Fort J, Errasti-Murugarren E, Rodrígues CMP, Orozco M, Joven J, Cantó C, Palacin M, Fernández-Veledo S, Vendrell J, Zorzano A. Deficient Endoplasmic Reticulum-Mitochondrial Phosphatidylserine Transfer Causes Liver Disease. *Cell* 2019; **177**: 881-895.e17 [PMID: 31051106 DOI: 10.1016/j.cell.2019.04.010]

87 **Tsurusaki S**, Tsuchiya Y, Koumura T, Nakasone M, Sakamoto T, Matsuoka M, Imai H, Yuet-Yin Kok C, Okochi H, Nakano H, Miyajima A, Tanaka M. Hepatic ferroptosis plays an important role as the trigger for initiating inflammation in nonalcoholic steatohepatitis. *Cell Death Dis* 2019; **10**: 449 [PMID: 31209199 DOI: 10.1038/s41419-019-1678-y]

88 **Samare-Najaf M**, Samareh A, Savardashtaki A, Khajehyar N, Tajbakhsh A, Vakili S, Moghadam D, Rastegar S, Mohsenizadeh M, Jahromi BN, Vafadar A, Zarei R. Non-apoptotic cell death programs in cervical cancer with an emphasis on ferroptosis. *Crit Rev Oncol Hematol* 2024; **194**: 104249 [PMID: 38145831 DOI: 10.1016/j.critrevonc.2023.104249]

89 **Stefanini B**, Ielasi L, Chen R, Abbati C, Tonnini M, Tovoli F, Granito A. TKIs in combination with immunotherapy for hepatocellular carcinoma. *Expert Rev Anticancer Ther* 2023; **23**: 279-291 [PMID: 36794716 DOI: 10.1080/14737140.2023.2181162]

90 **Nie J**, Lin B, Zhou M, Wu L, Zheng T. Role of ferroptosis in hepatocellular carcinoma. *J Cancer Res Clin Oncol* 2018; **144**: 2329-2337 [PMID: 30167889 DOI: 10.1007/s00432-018-2740-3]

91 **Iseda N**, Itoh S, Toshida K, Tomiyama T, Morinaga A, Shimokawa M, Shimagaki T, Wang H, Kurihara T, Toshima T, Nagao Y, Harada N, Yoshizumi T, Mori M. Ferroptosis is induced by lenvatinib through fibroblast growth factor receptor-4 inhibition in hepatocellular carcinoma. *Cancer Sci* 2022; **113**: 2272-2287 [PMID: 35466502 DOI: 10.1111/cas.15378]

92 **Granito A**, Marinelli S, Terzi E, Piscaglia F, Renzulli M, Venerandi L, Benevento F, Bolondi L. Metronomic capecitabine as second-line treatment in hepatocellular carcinoma after sorafenib failure. *Dig Liver Dis* 2015; **47**: 518-522 [PMID: 25861840 DOI: 10.1016/j.dld.2015.03.010]

93 **Trevisani F**, Brandi G, Garuti F, Barbera MA, Tortora R, Casadei Gardini A, Granito A, Tovoli F, De Lorenzo S, Inghilesi AL, Foschi FG, Bernardi M, Marra F, Sacco R, Di Costanzo GG. Metronomic capecitabine as second-line treatment for hepatocellular carcinoma after sorafenib discontinuation. *J Cancer Res Clin Oncol* 2018; **144**: 403-414 [PMID: 29249005 DOI: 10.1007/s00432-017-2556-6]

94 **Wang H**, Yang R, Wang Z, Cao L, Kong D, Sun Q, Yoshida S, Ren J, Chen T, Duan J, Lu J, Shen Z, Zheng H. Metronomic capecitabine with rapamycin exerts an immunosuppressive effect by inducing ferroptosis of CD4(+) T cells after liver transplantation in rat. *Int Immunopharmacol* 2023; **124**: 110810 [PMID: 37625370 DOI: 10.1016/j.intimp.2023.110810]

95 **Li ZJ**, Dai HQ, Huang XW, Feng J, Deng JH, Wang ZX, Yang XM, Liu YJ, Wu Y, Chen PH, Shi H, Wang JG, Zhou J, Lu GD. Artesunate synergizes with sorafenib to induce ferroptosis in hepatocellular carcinoma. *Acta Pharmacol Sin* 2021; **42**: 301-310 [PMID: 32699265 DOI: 10.1038/s41401-020-0478-3]

96 **Wang Q**, Bin C, Xue Q, Gao Q, Huang A, Wang K, Tang N. GSTZ1 sensitizes hepatocellular carcinoma cells to sorafenib-induced ferroptosis *via* inhibition of NRF2/GPX4 axis. *Cell Death Dis* 2021; **12**: 426 [PMID: 33931597 DOI: 10.1038/s41419-021-03718-4]

97 **Yang C**, Lu T, Liu M, Yuan X, Li D, Zhang J, Zhou L, Xu M. Tiliroside targets TBK1 to induce ferroptosis and sensitize hepatocellular carcinoma to sorafenib. *Phytomedicine* 2023; **111**: 154668 [PMID: 36657316 DOI: 10.1016/j.phymed.2023.154668]

98 **Ray CA**, Pickup DJ. The mode of death of pig kidney cells infected with cowpox virus is governed by the expression of the crmA gene. *Virology* 1996; **217**: 384-391 [PMID: 8599227 DOI: 10.1006/viro.1996.0128]

99 **Degterev A**, Huang Z, Boyce M, Li Y, Jagtap P, Mizushima N, Cuny GD, Mitchison TJ, Moskowitz MA, Yuan J. Chemical inhibitor of nonapoptotic cell death with therapeutic potential for ischemic brain injury. *Nat Chem Biol* 2005; **1**: 112-119 [PMID: 16408008 DOI: 10.1038/nchembio711]

100 **He S**, Wang L, Miao L, Wang T, Du F, Zhao L, Wang X. Receptor interacting protein kinase-3 determines cellular necrotic response to TNF-alpha. *Cell* 2009; **137**: 1100-1111 [PMID: 19524512 DOI: 10.1016/j.cell.2009.05.021]

101 **Zhang DW**, Shao J, Lin J, Zhang N, Lu BJ, Lin SC, Dong MQ, Han J. RIP3, an energy metabolism regulator that switches TNF-induced cell death from apoptosis to necrosis. *Science* 2009; **325**: 332-336 [PMID: 19498109 DOI: 10.1126/science.1172308]

102 **Zhao J**, Jitkaew S, Cai Z, Choksi S, Li Q, Luo J, Liu ZG. Mixed lineage kinase domain-like is a key receptor interacting protein 3 downstream component of TNF-induced necrosis. *Proc Natl Acad Sci U S A* 2012; **109**: 5322-5327 [PMID: 22421439 DOI: 10.1073/pnas.1200012109]

103 **Frank D**, Vince JE. Pyroptosis versus necroptosis: similarities, differences, and crosstalk. *Cell Death Differ* 2019; **26**: 99-114 [PMID: 30341423 DOI: 10.1038/s41418-018-0212-6]

104 **Weinlich R**, Oberst A, Beere HM, Green DR. Necroptosis in development, inflammation and disease. *Nat Rev Mol Cell Biol* 2017; **18**: 127-136 [PMID: 27999438 DOI: 10.1038/nrm.2016.149]

105 **Mompeán M**, Li W, Li J, Laage S, Siemer AB, Bozkurt G, Wu H, McDermott AE. The Structure of the Necrosome RIPK1-RIPK3 Core, a Human Hetero-Amyloid Signaling Complex. *Cell* 2018; **173**: 1244-1253.e10 [PMID: 29681455 DOI: 10.1016/j.cell.2018.03.032]

106 **Hanna-Addams S**, Liu S, Liu H, Chen S, Wang Z. CK1α, CK1δ, and CK1ε are necrosome components which phosphorylate serine 227 of human RIPK3 to activate necroptosis. *Proc Natl Acad Sci U S A* 2020; **117**: 1962-1970 [PMID: 31932442 DOI: 10.1073/pnas.1917112117]

107 **Cai Z**, Jitkaew S, Zhao J, Chiang HC, Choksi S, Liu J, Ward Y, Wu LG, Liu ZG. Plasma membrane translocation of trimerized MLKL protein is required for TNF-induced necroptosis. *Nat Cell Biol* 2014; **16**: 55-65 [PMID: 24316671 DOI: 10.1038/ncb2883]

108 **Cai Z**, Zhang A, Choksi S, Li W, Li T, Zhang XM, Liu ZG. Activation of cell-surface proteases promotes necroptosis, inflammation and cell migration. *Cell Res* 2016; **26**: 886-900 [PMID: 27444869 DOI: 10.1038/cr.2016.87]

109 **Furuta Y**, Zhou Z. How do necrotic cells expose phosphatidylserine to attract their predators-What's unique and what's in common with apoptotic cells. *Front Cell Dev Biol* 2023; **11**: 1170551 [PMID: 37091984 DOI: 10.3389/fcell.2023.1170551]

110 **Gullett JM**, Tweedell RE, Kanneganti TD. It's All in the PAN: Crosstalk, Plasticity, Redundancies, Switches, and Interconnectedness Encompassed by PANoptosis Underlying the Totality of Cell Death-Associated Biological Effects. *Cells* 2022; **11** [PMID: 35563804 DOI: 10.3390/cells11091495]

111 **Li X**, Li F, Zhang X, Zhang H, Zhao Q, Li M, Wu X, Wang L, Liu J, Ou Y, Xing M, Zhang Y, Deng J, Wang X, Luo Y, Li J, Zhao Y. Caspase-8 auto-cleavage regulates programmed cell death and collaborates with RIPK3/MLKL to prevent lymphopenia. *Cell Death Differ* 2022; **29**: 1500-1512 [PMID: 35064213 DOI: 10.1038/s41418-022-00938-9]

112 **Contreras CJ**, Mukherjee N, Branco RCS, Lin L, Hogan MF, Cai EP, Oberst AA, Kahn SE, Templin AT. RIPK1 and RIPK3 regulate TNFα-induced β-cell death in concert with caspase activity. *Mol Metab* 2022; **65**: 101582 [PMID: 36030035 DOI: 10.1016/j.molmet.2022.101582]

113 **Chen XY**, Dai YH, Wan XX, Hu XM, Zhao WJ, Ban XX, Wan H, Huang K, Zhang Q, Xiong K. ZBP1-Mediated Necroptosis: Mechanisms and Therapeutic Implications. *Molecules* 2022; **28** [PMID: 36615244 DOI: 10.3390/molecules28010052]

114 **Nakano H**, Murai S, Moriwaki K. Regulation of the release of damage-associated molecular patterns from necroptotic cells. *Biochem J* 2022; **479**: 677-685 [PMID: 35293986 DOI: 10.1042/BCJ20210604]

115 **Schock SN**, Chandra NV, Sun Y, Irie T, Kitagawa Y, Gotoh B, Coscoy L, Winoto A. Induction of necroptotic cell death by viral activation of the RIG-I or STING pathway. *Cell Death Differ* 2017; **24**: 615-625 [PMID: 28060376 DOI: 10.1038/cdd.2016.153]

116 **Ye K**, Chen Z, Xu Y. The double-edged functions of necroptosis. *Cell Death Dis* 2023; **14**: 163 [PMID: 36849530 DOI: 10.1038/s41419-023-05691-6]

117 **Wang X**, He Z, Liu H, Yousefi S, Simon HU. Neutrophil Necroptosis Is Triggered by Ligation of Adhesion Molecules following GM-CSF Priming. *J Immunol* 2016; **197**: 4090-4100 [PMID: 27815445 DOI: 10.4049/jimmunol.1600051]

118 **Gong YN**, Guy C, Olauson H, Becker JU, Yang M, Fitzgerald P, Linkermann A, Green DR. ESCRT-III Acts Downstream of MLKL to Regulate Necroptotic Cell Death and Its Consequences. *Cell* 2017; **169**: 286-300.e16 [PMID: 28388412 DOI: 10.1016/j.cell.2017.03.020]

119 **Park SY**, Park HH, Park SY, Hong SM, Yoon S, Morgan MJ, Kim YS. Reduction in MLKL-mediated endosomal trafficking enhances the TRAIL-DR4/5 signal to increase cancer cell death. *Cell Death Dis* 2020; **11**: 744 [PMID: 32917855 DOI: 10.1038/s41419-020-02941-9]

120 **Chavoshinezhad S**, Beirami E, Izadpanah E, Feligioni M, Hassanzadeh K. Molecular mechanism and potential therapeutic targets of necroptosis and ferroptosis in Alzheimer's disease. *Biomed Pharmacother* 2023; **168**: 115656 [PMID: 37844354 DOI: 10.1016/j.biopha.2023.115656]

121 **Kolbrink B**, von Samson-Himmelstjerna FA, Murphy JM, Krautwald S. Role of necroptosis in kidney health and disease. *Nat Rev Nephrol* 2023; **19**: 300-314 [PMID: 36596919 DOI: 10.1038/s41581-022-00658-w]

122 **Yan J**, Wan P, Choksi S, Liu ZG. Necroptosis and tumor progression. *Trends Cancer* 2022; **8**: 21-27 [PMID: 34627742 DOI: 10.1016/j.trecan.2021.09.003]

123 **Aravinthan A**, Scarpini C, Tachtatzis P, Verma S, Penrhyn-Lowe S, Harvey R, Davies SE, Allison M, Coleman N, Alexander G. Hepatocyte senescence predicts progression in non-alcohol-related fatty liver disease. *J Hepatol* 2013; **58**: 549-556 [PMID: 23142622 DOI: 10.1016/j.jhep.2012.10.031]

124 **Carranza-Trejo AM**, Vetvicka V, Vistejnova L, Kralickova M, Montufar EB. Hepatocyte and immune cell crosstalk in non-alcoholic fatty liver disease. *Expert Rev Gastroenterol Hepatol* 2021; **15**: 783-796 [PMID: 33557653 DOI: 10.1080/17474124.2021.1887730]

125 **Vanni E**, Bugianesi E, Kotronen A, De Minicis S, Yki-Järvinen H, Svegliati-Baroni G. From the metabolic syndrome to NAFLD or vice versa? *Dig Liver Dis* 2010; **42**: 320-330 [PMID: 20207596 DOI: 10.1016/j.dld.2010.01.016]

126 **Agmon E**, Stockwell BR. Lipid homeostasis and regulated cell death. *Curr Opin Chem Biol* 2017; **39**: 83-89 [PMID: 28645028 DOI: 10.1016/j.cbpa.2017.06.002]

127 **Newton K**, Manning G. Necroptosis and Inflammation. *Annu Rev Biochem* 2016; **85**: 743-763 [PMID: 26865533 DOI: 10.1146/annurev-biochem-060815-014830]

128 **Islam T**, Afonso MB, Rodrigues CMP. The role of RIPK3 in liver mitochondria bioenergetics and function. *Eur J Clin Invest* 2022; **52**: e13648 [PMID: 34219227 DOI: 10.1111/eci.13648]

129 **Leven AS**, Gieseler RK, Schlattjan M, Schreiter T, Niedergethmann M, Baars T, Baba HA, Özçürümez MK, Sowa JP, Canbay A. Association of cell death mechanisms and fibrosis in visceral white adipose tissue with pathological alterations in the liver of morbidly obese patients with NAFLD. *Adipocyte* 2021; **10**: 558-573 [PMID: 34743657 DOI: 10.1080/21623945.2021.1982164]

130 **Scavo MP**, Negro R, Arrè V, Depalo N, Carrieri L, Rizzi F, Mastrogiacomo R, Serino G, Notarnicola M, De Nunzio V, Lippolis T, Pesole PL, Coletta S, Armentano R, Curri ML, Giannelli G. The oleic/palmitic acid imbalance in exosomes isolated from NAFLD patients induces necroptosis of liver cells *via* the elongase-6/RIP-1 pathway. *Cell Death Dis* 2023; **14**: 635 [PMID: 37752143 DOI: 10.1038/s41419-023-06161-9]

131 **Seo YY**, Cho YK, Bae JC, Seo MH, Park SE, Rhee EJ, Park CY, Oh KW, Park SW, Lee WY. Tumor Necrosis Factor-α as a Predictor for the Development of Nonalcoholic Fatty Liver Disease: A 4-Year Follow-Up Study. *Endocrinol Metab (Seoul)* 2013; **28**: 41-45 [PMID: 24396649 DOI: 10.3803/EnM.2013.28.1.41]

132 **Zhang W**, Kudo H, Kawai K, Fujisaka S, Usui I, Sugiyama T, Tsukada K, Chen N, Takahara T. Tumor necrosis factor-alpha accelerates apoptosis of steatotic hepatocytes from a murine model of non-alcoholic fatty liver disease. *Biochem Biophys Res Commun* 2010; **391**: 1731-1736 [PMID: 20043871 DOI: 10.1016/j.bbrc.2009.12.144]

133 **Qian LL**, Ji JJ, Jiang Y, Guo JQ, Wu Y, Yang Z, Ma GS, Yao YY. Serpina3c deficiency induced necroptosis promotes non-alcoholic fatty liver disease through β-catenin/Foxo1/TLR4 signaling. *FASEB J* 2022; **36**: e22316 [PMID: 35429042 DOI: 10.1096/fj.202101345RRR]

134 **Coulon S**, Francque S, Colle I, Verrijken A, Blomme B, Heindryckx F, De Munter S, Prawitt J, Caron S, Staels B, Van Vlierberghe H, Van Gaal L, Geerts A. Evaluation of inflammatory and angiogenic factors in patients with non-alcoholic fatty liver disease. *Cytokine* 2012; **59**: 442-449 [PMID: 22658783 DOI: 10.1016/j.cyto.2012.05.001]

135 **Xinyu W**, Qian W, Yanjun W, Jingwen K, Keying X, Jiazheng J, Haibing Z, Kai W, Xiao X, Lixing Z. Polarity protein AF6 functions as a modulator of necroptosis by regulating ubiquitination of RIPK1 in liver diseases. *Cell Death Dis* 2023; **14**: 673 [PMID: 37828052 DOI: 10.1038/s41419-023-06170-8]

136 **Preston SP**, Stutz MD, Allison CC, Nachbur U, Gouil Q, Tran BM, Duvivier V, Arandjelovic P, Cooney JP, Mackiewicz L, Meng Y, Schaefer J, Bader SM, Peng H, Valaydon Z, Rajasekaran P, Jennison C, Lopaticki S, Farrell A, Ryan M, Howell J, Croagh C, Karunakaran D, Schuster-Klein C, Murphy JM, Fifis T, Christophi C, Vincan E, Blewitt ME, Thompson A, Boddey JA, Doerflinger M, Pellegrini M. Epigenetic Silencing of RIPK3 in Hepatocytes Prevents MLKL-mediated Necroptosis From Contributing to Liver Pathologies. *Gastroenterology* 2022;

163: 1643-1657.e14 [PMID: 36037995 DOI: 10.1053/j.gastro.2022.08.040]

137 **Wu X**, Poulsen KL, Sanz-Garcia C, Huang E, McMullen MR, Roychowdhury S, Dasarathy S, Nagy LE. MLKL-dependent signaling regulates autophagic flux in a murine model of non-alcohol-associated fatty liver and steatohepatitis. *J Hepatol* 2020; **73**: 616-627 [PMID: 32220583 DOI: 10.1016/j.jhep.2020.03.023]

138 **Ding HR**, Tang ZT, Tang N, Zhu ZY, Liu HY, Pan CY, Hu AY, Lin YZ, Gou P, Yuan XW, Cai JH, Dong CL, Wang JL, Ren HZ. Protective Properties of FOXO1 Inhibition in a Murine Model of Non-alcoholic Fatty Liver Disease Are Associated With Attenuation of ER Stress and Necroptosis. *Front Physiol* 2020; **11**: 177 [PMID: 32218743 DOI: 10.3389/fphys.2020.00177]

139 **Mohammed S**, Nicklas EH, Thadathil N, Selvarani R, Royce GH, Kinter M, Richardson A, Deepa SS. Role of necroptosis in chronic hepatic inflammation and fibrosis in a mouse model of increased oxidative stress. *Free Radic Biol Med* 2021; **164**: 315-328 [PMID: 33429022 DOI: 10.1016/j.freeradbiomed.2020.12.449]

140 **Oh JH**, Saeed WK, Kim HY, Lee SM, Lee AH, Park GR, Yoon EL, Jun DW. Hepatic stellate cells activate and avoid death under necroptosis stimuli: Hepatic fibrosis during necroptosis. *J Gastroenterol Hepatol* 2023; **38**: 2206-2214 [PMID: 37811601 DOI: 10.1111/jgh.16368]

141 **Inaba Y**, Hashiuchi E, Watanabe H, Kimura K, Oshima Y, Tsuchiya K, Murai S, Takahashi C, Matsumoto M, Kitajima S, Yamamoto Y, Honda M, Asahara SI, Ravnskjaer K, Horike SI, Kaneko S, Kasuga M, Nakano H, Harada K, Inoue H. The transcription factor ATF3 switches cell death from apoptosis to necroptosis in hepatic steatosis in male mice. *Nat Commun* 2023; **14**: 167 [PMID: 36690638 DOI: 10.1038/s41467-023-35804-w]

142 **Zhang NP**, Liu XJ, Xie L, Shen XZ, Wu J. Impaired mitophagy triggers NLRP3 inflammasome activation during the progression from nonalcoholic fatty liver to nonalcoholic steatohepatitis. *Lab Invest* 2019; **99**: 749-763 [PMID: 30700851 DOI: 10.1038/s41374-018-0177-6]

143 **Mridha AR**, Haczeyni F, Yeh MM, Haigh WG, Ioannou GN, Barn V, Ajamieh H, Adams L, Hamdorf JM, Teoh NC, Farrell GC. TLR9 is up-regulated in human and murine NASH: pivotal role in inflammatory recruitment and cell survival. *Clin Sci (Lond)* 2017; **131**: 2145-2159 [PMID: 28687713 DOI: 10.1042/CS20160838]

144 **Tomita K**, Tamiya G, Ando S, Ohsumi K, Chiyo T, Mizutani A, Kitamura N, Toda K, Kaneko T, Horie Y, Han JY, Kato S, Shimoda M, Oike Y, Tomizawa M, Makino S, Ohkura T, Saito H, Kumagai N, Nagata H, Ishii H, Hibi T. Tumour necrosis factor alpha signalling through activation of Kupffer cells plays an essential role in liver fibrosis of non-alcoholic steatohepatitis in mice. *Gut* 2006; **55**: 415-424 [PMID: 16174657 DOI: 10.1136/gut.2005.071118]

145 **Afonso MB**, Rodrigues PM, Carvalho T, Caridade M, Borralho P, Cortez-Pinto H, Castro RE, Rodrigues CM. Necroptosis is a key pathogenic event in human and experimental murine models of non-alcoholic steatohepatitis. *Clin Sci (Lond)* 2015; **129**: 721-739 [PMID: 26201023 DOI: 10.1042/CS20140732]

146 **Gautheron J**, Vucur M, Reisinger F, Cardenas DV, Roderburg C, Koppe C, Kreggenwinkel K, Schneider AT, Bartneck M, Neumann UP, Canbay A, Reeves HL, Luedde M, Tacke F, Trautwein C, Heikenwalder M, Luedde T. A positive feedback loop between RIP3 and JNK controls non-alcoholic steatohepatitis. *EMBO Mol Med* 2014; **6**: 1062-1074 [PMID: 24963148 DOI: 10.15252/emmm.201403856]

147 **Tao L**, Yi Y, Chen Y, Zhang H, Orning P, Lien E, Jie J, Zhang W, Xu Q, Li Y, Ding Z, Wu C, Ding Q, Wang J, Zhang J, Weng D. RIP1 kinase activity promotes steatohepatitis through mediating cell death and inflammation in macrophages. *Cell Death Differ* 2021; **28**: 1418-1433 [PMID: 33208891 DOI: 10.1038/s41418-020-00668-w]

148 **Liu XJ**, Duan NN, Liu C, Niu C, Liu XP, Wu J. Characterization of a murine nonalcoholic steatohepatitis model induced by high fat high calorie diet plus fructose and glucose in drinking water. *Lab Invest* 2018; **98**: 1184-1199 [PMID: 29959418 DOI: 10.1038/s41374-018-0074-z]

149 **Saeed WK**, Jun DW, Jang K, Ahn SB, Oh JH, Chae YJ, Lee JS, Kang HT. Mismatched effects of receptor interacting protein kinase-3 on hepatic steatosis and inflammation in non-alcoholic fatty liver disease. *World J Gastroenterol* 2018; **24**: 5477-5490 [PMID: 30622377 DOI: 10.3748/wjg.v24.i48.5477]

150 **Afonso MB**, Rodrigues PM, Mateus-Pinheiro M, Simão AL, Gaspar MM, Majdi A, Arretxe E, Alonso C, Santos-Laso A, Jimenez-Agüero R, Eizaguirre E, Bujanda L, Pareja MJ, Banales JM, Ratziu V, Gautheron J, Castro RE, Rodrigues CMP. RIPK3 acts as a lipid metabolism regulator contributing to inflammation and carcinogenesis in non-alcoholic fatty liver disease. *Gut* 2021; **70**: 2359-2372 [PMID: 33361348 DOI: 10.1136/gutjnl-2020-321767]

151 **Mohammed S**, Thadathil N, Ohene-Marfo P, Tran AL, Van Der Veldt M, Georgescu C, Oh S, Nicklas EH, Wang D, Haritha NH, Luo W, Janknecht R, Miller BF, Wren JD, Freeman WM, Deepa SS. Absence of Either Ripk3 or Mlkl Reduces Incidence of Hepatocellular Carcinoma Independent of Liver Fibrosis. *Mol Cancer Res* 2023; **21**: 933-946 [PMID: 37204757 DOI: 10.1158/1541-7786.MCR-22-0820]

152 **Wu W**, Hu X, Zhou X, Klenotic PA, Zhou Q, Lin Z. Myeloid deficiency of CCN3 exacerbates liver injury in a mouse model of nonalcoholic fatty liver disease. *J Cell Commun Signal* 2018; **12**: 389-399 [PMID: 29214510 DOI: 10.1007/s12079-017-0432-4]

153 **Chen H**, McKeen T, Chao X, Chen A, Deng F, Jaeschke H, Ding WX, Ni HM. The role of MLKL in Hepatic Ischemia-Reperfusion Injury of Alcoholic Steatotic Livers. *Int J Biol Sci* 2022; **18**: 1096-1106 [PMID: 35173541 DOI: 10.7150/ijbs.67533]

154 **Yang F**, Shang L, Wang S, Liu Y, Ren H, Zhu W, Shi X. TNFα-Mediated Necroptosis Aggravates Ischemia-Reperfusion Injury in the Fatty Liver by Regulating the Inflammatory Response. *Oxid Med Cell Longev* 2019; **2019**: 2301903 [PMID: 31214277 DOI: 10.1155/2019/2301903]

155 **Mazzolini G**, Atorrasagasti C, Onorato A, Peixoto E, Schlattjan M, Sowa JP, Sydor S, Gerken G, Canbay A. SPARC expression is associated with hepatic injury in rodents and humans with non-alcoholic fatty liver disease. *Sci Rep* 2018; **8**: 725 [PMID: 29335425 DOI: 10.1038/s41598-017-18981-9]

156 **Paredes-Turrubiarte G**, González-Chávez A, Pérez-Tamayo R, Salazar-Vázquez BY, Hernández VS, Garibay-Nieto N, Fragoso JM, Escobedo G. Severity of non-alcoholic fatty liver disease is associated with high systemic levels of tumor necrosis factor alpha and low serum interleukin 10 in morbidly obese patients. *Clin Exp Med* 2016; **16**: 193-202 [PMID: 25894568 DOI: 10.1007/s10238-015-0347-4]

157 **Poniachik J**, Csendes A, Díaz JC, Rojas J, Burdiles P, Maluenda F, Smok G, Rodrigo R, Videla LA. Increased production of IL-1alpha and TNF-alpha in lipopolysaccharide-stimulated blood from obese patients with non-alcoholic fatty liver disease. *Cytokine* 2006; **33**: 252-257 [PMID: 16564703 DOI: 10.1016/j.cyto.2006.02.006]

158 **Zahran WE**, Salah El-Dien KA, Kamel PG, El-Sawaby AS. Efficacy of Tumor Necrosis Factor and Interleukin-10 Analysis in the Follow-up of Nonalcoholic Fatty Liver Disease Progression. *Indian J Clin Biochem* 2013; **28**: 141-146 [PMID: 24426199 DOI: 10.1007/s12291-012-0236-5]

159 **Cheng Y**, An B, Jiang M, Xin Y, Xuan S. Association of Tumor Necrosis Factor-alpha Polymorphisms and Risk of Coronary Artery Disease in Patients With Non-alcoholic Fatty Liver Disease. *Hepat Mon* 2015; **15**: e26818 [PMID: 25825591 DOI: 10.5812/hepatmon.26818]

160 **Miyata T**, Wu X, Fan X, Huang E, Sanz-Garcia C, Ross CKC, Roychowdhury S, Bellar A, McMullen MR, Dasarathy J, Allende DS, Caballeria J, Sancho-Bru P, McClain CJ, Mitchell M, McCullough AJ, Radaeva S, Barton B, Szabo G, Dasarathy S, Nagy LE. Differential role of MLKL in alcohol-associated and non-alcohol-associated fatty liver diseases in mice and humans. *JCI Insight* 2021; **6** [PMID: 33616081

DOI: 10.1172/jci.insight.140180]

161 **Kondo T**, Macdonald S, Engelmann C, Habtesion A, Macnaughtan J, Mehta G, Mookerjee RP, Davies N, Pavesi M, Moreau R, Angeli P, Arroyo V, Andreola F, Jalan R. The role of RIPK1 mediated cell death in acute on chronic liver failure. *Cell Death Dis* 2021; **13**: 5 [PMID: 34921136 DOI: 10.1038/s41419-021-04442-9]

162 **Ahmed EA**, El-Derany MO, Anwar AM, Saied EM, Magdeldin S. Metabolomics and Lipidomics Screening Reveal Reprogrammed Signaling Pathways toward Cancer Development in Non-Alcoholic Steatohepatitis. *Int J Mol Sci* 2022; **24** [PMID: 36613653 DOI: 10.3390/ijms24010210]

163 **Majdi A**, Aoudjehane L, Ratziu V, Islam T, Afonso MB, Conti F, Mestiri T, Lagouge M, Foufelle F, Ballenghien F, Ledent T, Moldes M, Cadoret A, Fouassier L, Delaunay JL, Aït-Slimane T, Courtois G, Fève B, Scatton O, Prip-Buus C, Rodrigues CMP, Housset C, Gautheron J. Inhibition of receptor-interacting protein kinase 1 improves experimental non-alcoholic fatty liver disease. *J Hepatol* 2020; **72**: 627-635 [PMID: 31760070 DOI: 10.1016/j.jhep.2019.11.008]

164 **Saeed WK**, Jun DW, Jang K, Oh JH, Chae YJ, Lee JS, Koh DH, Kang HT. Decrease in fat de novo synthesis and chemokine ligand expression in non-alcoholic fatty liver disease caused by inhibition of mixed lineage kinase domain-like pseudokinase. *J Gastroenterol Hepatol* 2019; **34**: 2206-2218 [PMID: 31132314 DOI: 10.1111/jgh.14740]

165 **Briand F**, Heymes C, Bonada L, Angles T, Charpentier J, Branchereau M, Brousseau E, Quinsat M, Fazilleau N, Burcelin R, Sulpice T. A 3-week nonalcoholic steatohepatitis mouse model shows elafibranor benefits on hepatic inflammation and cell death. *Clin Transl Sci* 2020; **13**: 529-538 [PMID: 31981449 DOI: 10.1111/cts.12735]

166 **Hua X**, Sun DY, Zhang WJ, Fu JT, Tong J, Sun SJ, Zeng FY, Ouyang SX, Zhang GY, Wang SN, Li DJ, Miao CY, Wang P. P7C3-A20 alleviates fatty liver by shaping gut microbiota and inducing FGF21/FGF1, *via* the AMP-activated protein kinase/CREB regulated transcription coactivator 2 pathway. *Br J Pharmacol* 2021; **178**: 2111-2130 [PMID: 32037512 DOI: 10.1111/bph.15008]

167 **Malaguarnera L**, Di Rosa M, Zambito AM, dell'Ombra N, Nicoletti F, Malaguarnera M. Chitotriosidase gene expression in Kupffer cells from patients with non-alcoholic fatty liver disease. *Gut* 2006; **55**: 1313-1320 [PMID: 16825325 DOI: 10.1136/gut.2005.075697]

168 **Shao Y**, Wang X, Zhou Y, Jiang Y, Wu R, Lu C. Pterostilbene attenuates RIPK3-dependent hepatocyte necroptosis in alcoholic liver disease *via* SIRT2-mediated NFATc4 deacetylation. *Toxicology* 2021; **461**: 152923 [PMID: 34474091 DOI: 10.1016/j.tox.2021.152923]

169 **Roychowdhury S**, McCullough RL, Sanz-Garcia C, Saikia P, Alkhouri N, Matloob A, Pollard KA, McMullen MR, Croniger CM, Nagy LE. Receptor interacting protein 3 protects mice from high-fat diet-induced liver injury. *Hepatology* 2016; **64**: 1518-1533 [PMID: 27301788 DOI: 10.1002/hep.28676]

170 **Abdel-Hamed AR**, Hamouda AO, Abo-elmatty DM, Khedr NF, Ghattas MH. Role of Kaempferol Combined with Pioglitazone in the Alleviation of Inflammation and Modulation of Necroptosis and Apoptosis Pathways in NASH-induced Mice. *J Med Chem Sci* 2023; **6**: 250-268 [DOI: 10.26655/JMCHEMSCI.2023.2.8]

171 **Fawzy MA**, Nasr G, Ali FEM, Fathy M. Quercetin potentiates the hepatoprotective effect of sildenafil and/or pentoxifylline against intrahepatic cholestasis: Role of Nrf2/ARE, TLR4/NF-κB, and NLRP3/IL-1β signaling pathways. *Life Sci* 2023; **314**: 121343 [PMID: 36592787 DOI: 10.1016/j.lfs.2022.121343]

172 **Hamouda AO**, Abdel-Hamed AR, Abo-Elmatty DM, Khedr NF, Ghattas MH. Pentoxifylline and its association with kaempferol improve NASH-associated manifestation in mice through anti-apoptotic, anti-necroptotic, antioxidant, and anti-inflammatory mechanisms. *Eur Rev Med Pharmacol Sci* 2022; **26**: 8644-8659 [PMID: 36524484 DOI: 10.26355/eurrev_202212_30535]

173 **Park J**, Rah SY, An HS, Lee JY, Roh GS, Ryter SW, Park JW, Yang CH, Surh YJ, Kim UH, Chung HT, Joe Y. Metformin-induced TTP mediates communication between Kupffer cells and hepatocytes to alleviate hepatic steatosis by regulating lipophagy and necroptosis. *Metabolism* 2023; **141**: 155516 [PMID: 36773805 DOI: 10.1016/j.metabol.2023.155516]

174 **Xiao J**, Ho CT, Liong EC, Nanji AA, Leung TM, Lau TY, Fung ML, Tipoe GL. Epigallocatechin gallate attenuates fibrosis, oxidative stress, and inflammation in non-alcoholic fatty liver disease rat model through TGF/SMAD, PI3 K/Akt/FoxO1, and NF-kappa B pathways. *Eur J Nutr* 2014; **53**: 187-199 [PMID: 23515587 DOI: 10.1007/s00394-013-0516-8]

World Journal of Gastroenterology

Submit a Manuscript: https://www.f6publishing.com

World J Gastroenterol 2024 April 14; 30(14): 1982-1989

DOI: 10.3748/wjg.v30.i14.1982

ISSN 1007-9327 (print) ISSN 2219-2840 (online)

MINIREVIEWS

Omics-based biomarkers as useful tools in metabolic dysfunction-associated steatotic liver disease clinical practice: How far are we?

Julieta Trinks, María F Mascardi, Adrián Gadano, Sebastián Marciano

Specialty type: Gastroenterology and hepatology

Provenance and peer review: Invited article; Externally peer reviewed.

Peer-review model: Single blind

Peer-review report's scientific quality classification

Grade A (Excellent): 0
Grade B (Very good): B
Grade C (Good): C
Grade D (Fair): 0
Grade E (Poor): 0

P-Reviewer: de la Monte SM, United States; Lee YM, Singapore

Received: December 27, 2023
Peer-review started: December 27, 2023
First decision: January 27, 2024
Revised: February 19, 2024
Accepted: March 25, 2024
Article in press: March 25, 2024
Published online: April 14, 2024

Julieta Trinks, María F Mascardi, Sebastián Marciano, Instituto de Medicina Traslacional e Ingeniería Biomédica - Consejo Nacional de Investigaciones Científicas y Técnicas - Instituto Universitario del Hospital Italiano - Hospital Italiano de Buenos Aires, Ciudad Autónoma de Buenos Aires C1199ACL, Argentina

Julieta Trinks, María F Mascardi, Sebastián Marciano, Consejo Nacional de Investigaciones Científicas y Técnicas, Ciudad Autónoma de Buenos Aires C1425FQB, Argentina

Adrián Gadano, Sebastián Marciano, Liver Unit, Hospital Italiano de Buenos Aires, Ciudad Autónoma de Buenos Aires C1199DF, Argentina

Adrián Gadano, Sebastián Marciano, Department of Research, Hospital Italiano de Buenos Aires, Ciudad Autónoma de Buenos Aires C1199DF, Argentina

Corresponding author: Julieta Trinks, MD, PhD, Professor, Instituto de Medicina Traslacional e Ingeniería Biomédica - Consejo Nacional de Investigaciones Científicas y Técnicas - Instituto Universitario del Hospital Italiano - Hospital Italiano de Buenos Aires, Potosí 4240, Ciudad Autónoma de Buenos Aires C1199ACL, Argentina. julieta.trinks@hospitalitaliano.org.ar

Abstract

Unmet needs exist in metabolic dysfunction-associated steatotic liver disease (MASLD) risk stratification. Our ability to identify patients with MASLD with advanced fibrosis and at higher risk for adverse outcomes is still limited. Incorporating novel biomarkers could represent a meaningful improvement to current risk predictors. With this aim, omics technologies have revolutionized the process of MASLD biomarker discovery over the past decades. While the research in this field is thriving, much of the publication has been haphazard, often using single-omics data and specimen sets of convenience, with many identified candidate biomarkers but lacking clinical validation and utility. If we incorporate these biomarkers to direct patients' management, it should be considered that the roadmap for translating a newly discovered omics-based signature to an actual, analytically valid test useful in MASLD clinical practice is rigorous and, therefore, not easily accomplished. This article presents an overview of this area's current state, the conceivable opportunities and challenges of omics-based laboratory diagnostics, and a roadmap for improving MASLD biomarker research.

Key Words: Metabolic dysfunction-associated steatotic liver disease; Non-alcoholic steatohepatitis; Biomarker; Risk stratification; Omics

Core Tip: Identifying patients with metabolic dysfunction-associated steatotic liver disease (MASLD) at higher risk for adverse outcomes is still a crucial clinical challenge. Novel and non-invasive screening, monitoring, and risk stratification methods are urgently needed. With this aim, omics technologies have revolutionized the process of MASLD biomarker discovery. Although many omics-based biomarkers were identified over the past decades, their translation into clinically useful tests that can guide management decisions has proven more difficult than expected. This review presents an overview of this area's current state, the conceivable opportunities and challenges of omics-based laboratory diagnostics, and a roadmap for improving MASLD biomarker research.

Citation: Trinks J, Mascardi MF, Gadano A, Marciano S. Omics-based biomarkers as useful tools in metabolic dysfunction-associated steatotic liver disease clinical practice: How far are we? *World J Gastroenterol* 2024; 30(14): 1982-1989
URL: https://www.wjgnet.com/1007-9327/full/v30/i14/1982.htm
DOI: https://dx.doi.org/10.3748/wjg.v30.i14.1982

INTRODUCTION

The exponential global increase in obesity and type 2 diabetes is to blame for the rising epidemic of metabolic dysfunction-associated steatotic liver disease (MASLD) in the last two decades. Globally, nearly a quarter of the world's population is estimated to be affected by MASLD, with even higher rates in the Middle East, Northern Africa, and Central and South America. Without clear risk stratification and therapeutic options, MASLD has soon become the leading cause of chronic liver disease and liver-related morbidity and mortality worldwide[1].

Unfortunately, over half the adult population is expected to have MASLD by 2040, mainly affecting women, smokers, and those without metabolic syndrome[2]. This scenario will expand the number of patients with advanced liver fibrosis and end-stage liver disease, increasing the rates of liver transplantation and multiplying healthcare costs.

Current measures to overcome this situation are centered on the identification of people at the highest risk of progression to advanced liver disease so they can be offered interventions and appropriate care before they develop liver-related complications[3]. However, this represents a crucial and tough challenge in the clinical management of MASLD[4-6]. First, not all patients with MASLD will ever develop non-alcoholic steatohepatitis (NASH) with clinically significant fibrosis, and advanced liver fibrosis has the highest risk of adverse liver-related outcomes[7]. Second, liver biopsy is the best available method to evaluate liver fibrosis. Still, it is a costly and invasive technique, prone to sampling bias and intra-observer and inter-observer variability, and not recommended to screen liver disease progression[8,9].

These limitations have driven the need for non-invasive MASLD screening, monitoring, and risk stratification methods. In this regard, imaging methods such as ultrasound, computed tomography, and magnetic resonance are valuable for detecting lipid accumulation in MAFLD patients. Still, they are useless for evaluating inflammation and degrees of fibrosis less than cirrhosis[10,11].

On the contrary, low-tech methods such as the anthropometric clinical indicators of visceral obesity have been promising for the primary prevention and screening of MASLD. These non-invasive indicators, such as body mass index, abdomen, waist and chest circumferences, and trunk fat, can be easily determined to screen the presence or absence of MASLD using affordable equipment, which makes them ideal for their use in remote areas or in primary clinical practice [12,13]. Although these indicators show suboptimal accuracy (57%) in detecting fibrosis[13], the identification of their specific cutoff points, taking into consideration the anthropometric differences in each ethnic and racial group[12], may be useful in the early diagnosis of MASLD, and especially NASH, offering a new therapeutic and preventive method to this population. Therefore, the epicenter of all research efforts around MASLD is currently focused on identifying and validating new non-invasive and cost-effective biological markers (or biomarkers) for risk stratification[4].

Since the Human Genome Project, the development of new technologies called "omics" has made it possible to measure a vast number of biological molecules within a tissue or cell in a high-throughput way. Many areas of research can be classified as omics, and the terms used to define them depend on the type of biological molecules globally analyzed by these techniques; for example, genes (genomics), methylated DNA, or modified histone proteins in chromosomes (epigenomics), RNA (transcriptomics), proteins (proteomics), metabolites (metabolomics), lipids (lipidomics)[14]. These techniques require next-generation sequencing (NGS) or mass spectrometry (MS). While sequencing-based approaches are applied to study the genome, transcriptome, and epitomes, an MS is necessary to explore the proteome, metabolome, and lipidome[14].

In MASLD research, new innovative omics technologies are extensively used in both preclinical (*in vitro* and *in vivo*) models and retrospective studies with archived samples, as they offer the possibility of in-depth screening for novel biomarkers and a better understanding of MASLD pathological processes[15]. However, translating their results into clinically useful tests that can guide management decisions has proven more difficult than expected. This article presents an overview of this area's current state, the conceivable opportunities and challenges of omics-based laboratory diagnostics, and a roadmap for improving MASLD biomarker research.

CURRENT STATE OF OMICS-DERIVED BIOMARKER DEVELOPMENT IN MASLD

We used PubMed (National Library of Medicine) and *Reference Citation Analysis* (*RCA*) databases to search and retrieve scientific articles to describe the current state of omics-derived biomarker development in MASLD. The "OR" and "AND" connectors were used to combine the descriptors: ("non-alcoholic fatty liver disease" or "non-alcoholic steatohepatitis", "fatty liver" or "NAFLD" or "NASH" or "metabolic-associated fatty liver disease" or "MAFLD" "metabolic dysfunction–associated steatotic liver disease" or "MASLD") and ("human") and ("biomarker") and ("omics" or "multi-omics" or "microbiome" or "genomics" or "proteomics" or "metabolomics" or "metagenomics" or "transcriptomics").

Inclusion criteria were the availability of the full-text publication written in English up to December 2023. Review studies, publications present in more than one database, and out-of-scope studies were excluded. After reading the titles and abstracts of the studies, 24 of 163 studies found in the databases were excluded: 2 duplicate studies, 5 Chinese studies, 11 *in vitro* studies, and six evaluated individuals with other chronic liver diseases. The remaining studies were fully read according to the eligibility criteria. Thus, 139 articles were included in the analysis. The complete list of articles included in the analysis and their primary information (authorship and year of publication, type of sample, and omic technique/s used in the study) are shown in Supplementary Table 1.

Primarily, omic papers on MASLD biomarker research were scarce 20 years ago. Since then, the number of omic articles has increased exponentially (Figure 1A). This systematic literature review showed that the recent and scanty publication of multi-omic studies focuses on three levels of omics data including transcripts, genes, and proteins. This is followed by other omics areas, comprising metabolites, epigenetic changes, and combinations thereof (Figure 1B).

Of the types of samples analyzed for MASLD biomarker research, the rise in the number of omic studies was followed by a boost of papers aimed at discovering MASLD biomarkers on a diverse array of biological samples (Figure 1C). However, liver tissue samples were the most frequently featured. Stool, plasma, and serum samples have dominated over the last few years (Figure 1C). These results indicate a current interest in the search for non-invasive biomarkers, primarily focusing on gut microbiota studies and its well-described relationship to MASLD development and progression.

The 139 studies were also analyzed according to a previously published set of criteria that evaluate the internal validity of individual studies[16,17]. The most common limitations observed in these studies were a small sample size (16.5%), followed by the presence of bias in the selection and stratification of patients due to the lack of histological diagnosis of MASLD using liver biopsies (12.2%). Moreover, disregard for potential confounding variables (such as age, gender, ethnicity, body mass index, or presence of comorbidities) and their appropriate adjustments in the data analysis was observed in 13 studies (9.35%).

The validity of a study can also be evaluated by its reproducibility. In the case of omics research, depositing raw data, complete protocols, and bioinformatics codes and workflows in a public repository is considered a first step to replicating a study's findings[17]. Although many leading journals now demand to make data and protocols publicly available as a prerequisite for publication[18], this practice remains inconsistent across journals and omics studies. In fact, seven (5%) of the studies included in our literature search did not offer public access to their data nor indicate how others may obtain it in case specific legal or ethical restrictions prohibit public sharing of the data set.

However, these flaws aren't recurrently detected in some fields of omics research. In the case of genomics, genome-wide association studies require high degree of certainty in the results (P values $< 5 \times 10^{-8}$), develop large, multi-centric replication studies, and have good compliance with data availability policies[19], as was observed in the two studies of this type (1.4%) analyzed in the literature search carried out in this review.

ADDRESSING THE LACK OF CLINICALLY USEFUL OMICS-BASED BIOMARKERS IN MASLD: WHAT ARE THE CHALLENGES?

Despite this progress, the omics-derived biomarker research in MASLD has resulted in several candidate biomarkers that lack clinical validation and utility; that is, it is yet unknown if the identified biomarkers are accurate, reproducible, or reliable in terms of the analytical and clinical/biological validation, or even if there is enough evidence to consistently demonstrate that the use of the omics-based predictor results in a better outcome for patient care (utility).

There are many reasons for this disappointing output. First, the advent of omics-based biomarker studies has led to an excess of highly confounded reports by a superlative number of variables applied to a small sample size. Conditions for sample collection, transport, and storage can significantly affect the quantity and quality of the molecules (nucleic acid, proteins, metabolites) to be analyzed in the biological sample[20]. Moreover, using different NGS platforms or reagents with dissimilar lot numbers can be a source of technical bias that can alter results[21].

Second, the analysis of an outstanding number of data can be challenging. This is especially true if no consensus exists on the data processing pipeline or the software and packages to be used[22,23]. In the case of those omics studies focused on the search for MASLD biomarkers in the human microbiome, the need for complete and curated databases for the human microbiota's less-studied viral and fungal components poses an obstacle to thorough data analysis[24].

Finally, the shift from a single-omic to a multi-omic approach to biomarker research is critical for increasing the chances of identifying an accurate biomarker for MASLD risk stratification. The number of multi-omics studies on MASLD biomarker research is still scarce but on the rise, as shown by the systematic literature review results. Multi-omic applications provide novel insights and a more holistic understanding of biological processes. Thus, this type of omic study could advance our ability to understand and treat the complex underlying biology of MASLD[25]. Unfortunately, the need for a rigorous study design, accurate sample size and statistical power calculation, and problematic data

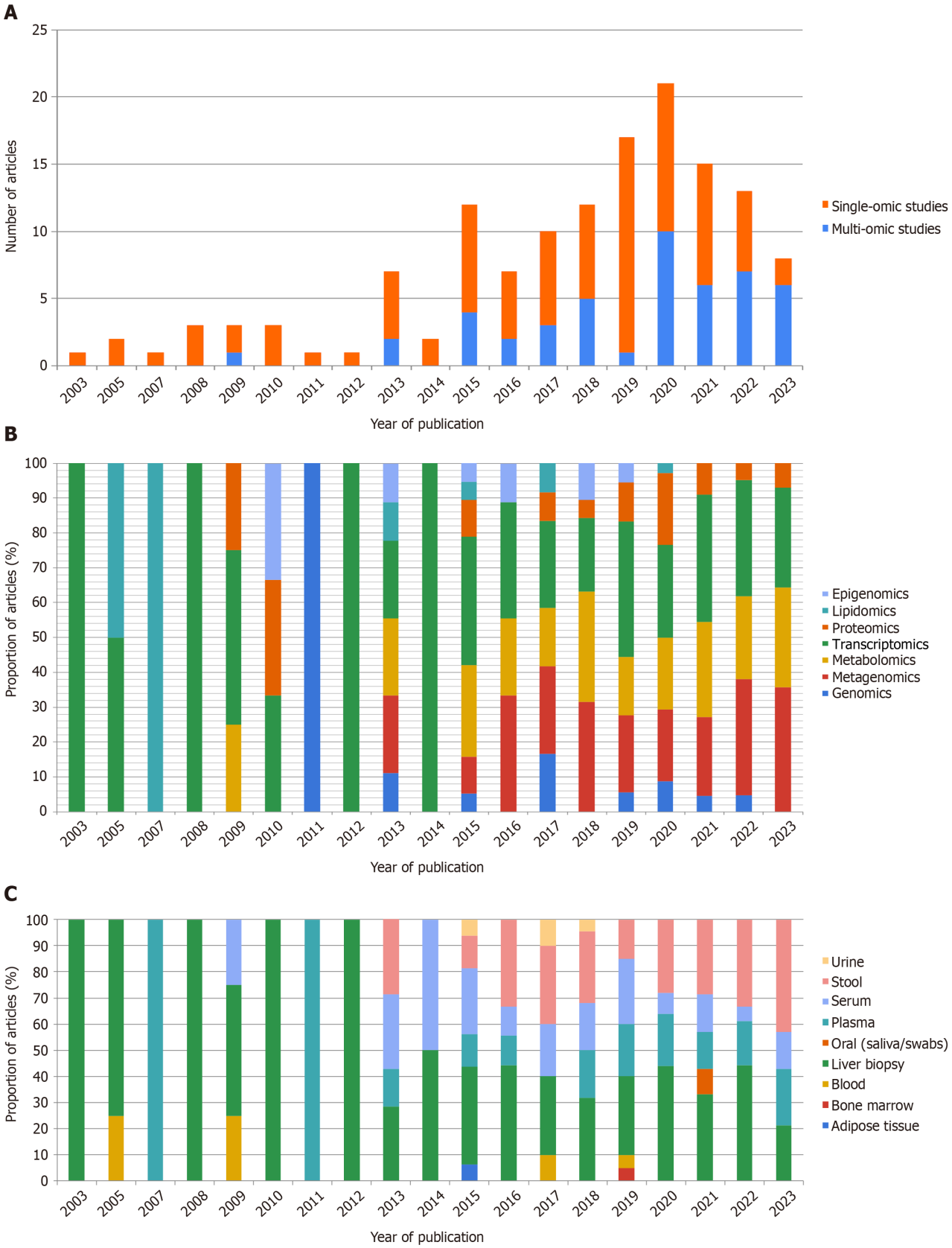

Figure 1 Characterization of omics literature based on a systematic screen of PubMed indexed research articles on metabolic dysfunction-associated steatotic liver disease biomarker (up to December 2023). A: Plot representing the rapidly increasing number of omics articles indexed in PubMed indicating the use of single-omic (red) or multi-omic technologies (blue); the dip in 2023 can be attributed to indexing delay which was not accounted for in the current plot; B: Proportion of omics and combinations of omics (grouped by the characterized entities) commonly used in the analyzed articles; C: Distribution of sample types used in the analyzed articles. The details of articles included in the analysis are listed in Supplementary Table 1.

integration interfere with the expansion of these studies[26].

A ROADMAP FOR THE IMPROVEMENT OF BIOMARKER RESEARCH IN MASLD

A lesson can be learned from cancer research. As a consequence of the premature use of omics-based tests developed to predict sensitivity to chemotherapeutic agents in lung and breast cancer clinical trials at Duke University, a committee of the Institute of Medicine generated a series of recommendations that are considered a roadmap of the best scientific practices for the development, validation and clinical translation of omics-based biomarkers and tests[27]. In 2013, the United States National Cancer Institute proposed a practical guideline[28,29] that lists 30 criteria for the development path of omics-based predictors from high-throughput technology to clinical trials (Figure 2). In brief, researchers should take into account: (1) Clinical specimen issues: Collection, processing, storage conditions, availability, quality, amount (mass or volume), and composition of appropriate clinical specimens; (2) Assay issues: Standardization of technical protocols, reagents, and scoring and reporting methods required for the analytical performance of the omics assay in the clinical setting; (3) Model development and evaluation: Avoidance of errors, inconsistencies, or bias in approachs for omics data pre-processing, preparation of the mathematical predictor model, and evaluation of its performance (validation); (4) Clinical trial design: Adherence to accepted standards for good clinical practice, including the development of a formal protocol, an informatics workflow for the analysis of clinical and omics data, a pre-defined study plan and statistical analysis strategy, and the pre-registration of the study and analysis plan in a public registry. The three possible study designs to evaluate the clinical utility are: Prospective-retrospective studies using stored samples; prospective clinical studies, where the biomarker is not involved in patient management decisions; or prospective clinical studies, where the biomarker guides patient management decisions; and (5) Ethical, legal, and regulatory issues: Commitment to protecting human subjects involved in the research, performance of certified laboratory tests if the results have significant clinical value and need to be communicated to the patient or the patient's physician, documentation of intellectual property rights.

Although there are subtle differences in how this checklist is applied to a particular omics test and clinical setting, it is recognized that any field of omics-based biomarker research should take notice of the abovementioned criteria to determine when there is sufficient and reliable evidence to justify the clinical use of an omics-based biomarker, or even that it is ready for evaluation in a clinical trial.

After demonstrating its clinical usefulness, the new biomarker must prove its cost-effectiveness or cost-utility, mainly as its use will be widespread (up to 30% of the general population in some geographical regions). The benefit the application of the biomarker produces, measured by healthy life years' indicator, must exceed the cost of the intervention. The application of the biomarker is considered cost-effective if it produces at least USD 50000 per quality-adjusted life year gained[30].

WILL SERUM BIOMARKERS WIN THE RACE FOR CLINICAL USEFULNESS?

Regarding MASLD biomarker research, a significant step forward was recently taken by the non-invasive biomarkers for metabolic liver disease (NIMBLE) and liver investigation: testing marker utility in steatohepatitis (LITMUS) projects, as multiple circulating biomarkers made the first step in the biomarker qualification path[31,32].

The LITMUS project[32] evaluated the diagnostic accuracy of 5 single biomarkers (CK-18 M30, CK-18 M65, PRO-C3, PRO-C4, and PRO-C6), 9 multimarker scores (FIB-4, MACK-3, a scoring system proposed by Cao *et al*[33] in 2013, ADAPT, FIBC3, ABC3D, NFS, ELF, and SomaSignal), as well as liver stiffness measurement (LSM) and controlled attenuation parameter vibration-controlled transient elastography (VCTE) in detecting at-risk NASH and fibrosis severity in a European cohort of 966 biopsy-proven participants with MASLD (of which 335 patients had at-risk NASH and 271 advanced fibrosis).

None of the single markers or multimarker scores achieved the predefined acceptable area under the curve (AUC) of 0.8 to be considered a diagnostic marker of acceptable accuracy and for replacing biopsy in detecting people with both NASH and clinically significant fibrosis. However, the SomaSignal test, the ADAPT score, and the LSM VCTE could be used as prescreening methods in clinical trials. The SomaSignal test showed the best results, with AUC values higher for diagnosing advanced fibrosis than for detecting NASH and clinically significant fibrosis[32].

On the other hand, the NIMBLE project tested the performance metrics of 5 biomarker panels (NIS4, OWLiver, PROC3, ELF, and FibroMeter VCTE) for the diagnosis of NASH, at-risk NASH or fibrosis severity in an American cohort of 1073 biopsy-proven individuals with the full spectrum of MASLD[31].

In this case, panels with an area under the receiver operating characteristic of 0.7 or higher were considered a diagnostic marker of acceptable accuracy. In contrast, primacy over alanine aminotransferase (ALT) and fibrosis-4 (FIB-4) for disease activity and fibrosis severity were considered, respectively, as a pragmatic initial step to move to final qualification. The results demonstrate that the NIS4 score excedeed the prespecified performance metric for diagnosis of at-risk NASH. Also, in diagnosing clinically significant fibrosis, advanced fibrosis, and cirrhosis in individuals with MASLD, the ELF test and FibroMeter VCTE outperformed FIB-4[31].

However, despite several limitations (data not applicable to all ethnicities, the use of a curated patient population, limited quantity of sample material, lack of evaluation of omics-based biomarkers, *etc*.) added to the known inter-observer variability in the histology scoring of the reference method, these groundbreaking studies represent an advance towards having regulatory approved biomarkers for MASLD risk stratification[5,6]. Moreover, as many tested biomar-

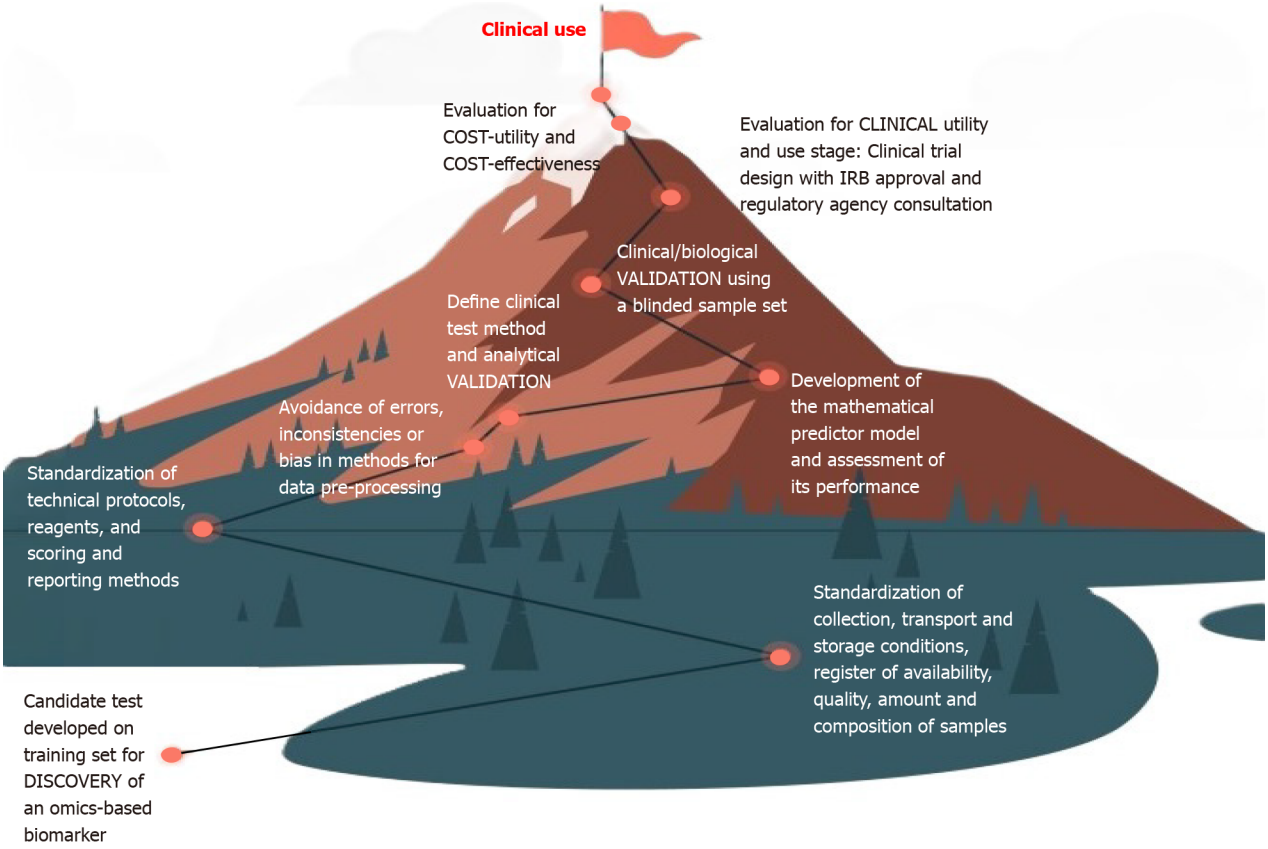

Figure 2 A roadmap for the improvement of biomarker research in metabolic dysfunction-associated steatotic liver disease: Discovery of a biologically, and perhaps clinically, interesting omics-based biomarker; analytical, biological/clinical validation of the discovered biomarker; and finally, the evaluation for its clinical utility and use, and the evaluation for its economic benefits (cost-effectiveness or cost-utility studies). A summary of the criteria for the development path of omics-based predictors proposed by the United States National Cancer Institute are also included in the roadmap. Modified from freepik.com.

kers outperformed laboratory tools routinely used in the clinical practice, such as ALT and FIB-4, they could be applied in a pre-screening strategy in clinical trial recruitment[5,6].

CONCLUSION

The expectation of omics technologies is that in the future, patients might be diagnosed and treated according to their personalized MASLD molecular signatures. However, we have a long and arduous path to reach our goal. A consensus regarding best practices on sampling conditions, technical issues, and data processing on discovery studies is mandatory before omics-based biomarkers for MASLD can be validated and their clinical utility tested.

The increasing burden of MASLD emphasizes the pressing need for a novel biomarker that can surpass the "imperfect" liver histology. Moreover, it should be simple, cheap, and easy to adapt to different situations (population screening or stratification in clinical trials). Due to the complex multisystemic pathophysiology of MASLD, it seems unlikely that a single biomarker featuring all these attributes will be identified in the near future. On the contrary, different algorithms integrating clinical data with an arrangement of previously reported omics-based, circulating, anthropometric, and/or imaging-based markers could be considered strong candidates for clinical evaluation.

FOOTNOTES

Author contributions: Trinks J, Mascardi MF, and Marciano S wrote the paper; Trinks J and Mascardi MF performed the literature search and data analysis; Gadano A contributed to the review and editing of the manuscript; and all authors have read and approved the final manuscript.

Supported by PIP-CONICET 2021-2023 grant, No. 11220200100875CO; PICT-2020-Serie, No. A-00788; and "Florencio Fiorini Foundation" grants.

Conflict-of-interest statement: Authors declare no conflict of interests for this article.

Country/Territory of origin: Argentina

ORCID number: Julieta Trinks 0000-0003-4781-8005; Adrián Gadano 0000-0002-3590-2472; Sebastián Marciano 0000-0002-7983-1450.

S-Editor: Wang JJ
L-Editor: A
P-Editor: Zhao YQ

REFERENCES

1 **Rinella ME**, Lazarus JV, Ratziu V, Francque SM, Sanyal AJ, Kanwal F, Romero D, Abdelmalek MF, Anstee QM, Arab JP, Arrese M, Bataller R, Beuers U, Boursier J, Bugianesi E, Byrne CD, Castro Narro GE, Chowdhury A, Cortez-Pinto H, Cryer DR, Cusi K, El-Kassas M, Klein S, Eskridge W, Fan J, Gawrieh S, Guy CD, Harrison SA, Kim SU, Koot BG, Korenjak M, Kowdley KV, Lacaille F, Loomba R, Mitchell-Thain R, Morgan TR, Powell EE, Roden M, Romero-Gómez M, Silva M, Singh SP, Sookoian SC, Spearman CW, Tiniakos D, Valenti L, Vos MB, Wong VW, Xanthakos S, Yilmaz Y, Younossi Z, Hobbs A, Villota-Rivas M, Newsome PN; NAFLD Nomenclature consensus group. A multisociety Delphi consensus statement on new fatty liver disease nomenclature. *Hepatology* 2023; **78**: 1966-1986 [PMID: 37363821 DOI: 10.1097/HEP.0000000000000520]

2 **Le MH**, Yeo YH, Zou B, Barnet S, Henry L, Cheung R, Nguyen MH. Forecasted 2040 global prevalence of nonalcoholic fatty liver disease using hierarchical bayesian approach. *Clin Mol Hepatol* 2022; **28**: 841-850 [PMID: 36117442 DOI: 10.3350/cmh.2022.0239]

3 **Valery PC**, Powell EE. Predicting clinical outcomes in people with NAFLD: no need for a crystal ball? *Lancet Gastroenterol Hepatol* 2023; **8**: 684-685 [PMID: 37290470 DOI: 10.1016/S2468-1253(23)00149-8]

4 **Sanyal AJ**, Castera L, Wong VW. Noninvasive Assessment of Liver Fibrosis in NAFLD. *Clin Gastroenterol Hepatol* 2023; **21**: 2026-2039 [PMID: 37062495 DOI: 10.1016/j.cgh.2023.03.042]

5 **Sebastiani G**. The quest for the ideal NASH biomarker. *Lancet Gastroenterol Hepatol* 2023; **8**: 685-687 [PMID: 36958368 DOI: 10.1016/S2468-1253(23)00063-8]

6 **Krag A**, Rinella ME. Pioneering the path to NASH biomarker approval. *Nat Med* 2023; **29**: 2416-2417 [PMID: 37679432 DOI: 10.1038/s41591-023-02527-w]

7 **Taylor RS**, Taylor RJ, Bayliss S, Hagström H, Nasr P, Schattenberg JM, Ishigami M, Toyoda H, Wai-Sun Wong V, Peleg N, Shlomai A, Sebastiani G, Seko Y, Bhala N, Younossi ZM, Anstee QM, McPherson S, Newsome PN. Association Between Fibrosis Stage and Outcomes of Patients With Nonalcoholic Fatty Liver Disease: A Systematic Review and Meta-Analysis. *Gastroenterology* 2020; **158**: 1611-1625.e12 [PMID: 32027911 DOI: 10.1053/j.gastro.2020.01.043]

8 **Davison BA**, Harrison SA, Cotter G, Alkhouri N, Sanyal A, Edwards C, Colca JR, Iwashita J, Koch GG, Dittrich HC. Suboptimal reliability of liver biopsy evaluation has implications for randomized clinical trials. *J Hepatol* 2020; **73**: 1322-1332 [PMID: 32610115 DOI: 10.1016/j.jhep.2020.06.025]

9 **Siddiqui MS**, Yamada G, Vuppalanchi R, Van Natta M, Loomba R, Guy C, Brandman D, Tonascia J, Chalasani N, Neuschwander-Tetri B, Sanyal AJ; NASH Clinical Research Network. Diagnostic Accuracy of Noninvasive Fibrosis Models to Detect Change in Fibrosis Stage. *Clin Gastroenterol Hepatol* 2019; **17**: 1877-1885.e5 [PMID: 30616027 DOI: 10.1016/j.cgh.2018.12.031]

10 **Zhou JH**, Cai JJ, She ZG, Li HL. Noninvasive evaluation of nonalcoholic fatty liver disease: Current evidence and practice. *World J Gastroenterol* 2019; **25**: 1307-1326 [PMID: 30918425 DOI: 10.3748/wjg.v25.i11.1307]

11 **Miele L**, Zocco MA, Pizzolante F, De Matthaeis N, Ainora ME, Liguori A, Gasbarrini A, Grieco A, Rapaccini G. Use of imaging techniques for non-invasive assessment in the diagnosis and staging of non-alcoholic fatty liver disease. *Metabolism* 2020; **112**: 154355 [PMID: 32916154 DOI: 10.1016/j.metabol.2020.154355]

12 **Almeida NS**, Rocha R, Cotrim HP, Daltro C. Anthropometric indicators of visceral adiposity as predictors of non-alcoholic fatty liver disease: A review. *World J Hepatol* 2018; **10**: 695-701 [PMID: 30386462 DOI: 10.4254/wjh.v10.i10.695]

13 **Razmpour F**, Daryabeygi-Khotbehsara R, Soleimani D, Asgharnezhad H, Shamsi A, Bajestani GS, Nematy M, Pour MR, Maddison R, Islam SMS. Application of machine learning in predicting non-alcoholic fatty liver disease using anthropometric and body composition indices. *Sci Rep* 2023; **13**: 4942 [PMID: 36973382 DOI: 10.1038/s41598-023-32129-y]

14 **Dai X**, Shen L. Advances and Trends in Omics Technology Development. *Front Med (Lausanne)* 2022; **9**: 911861 [PMID: 35860739 DOI: 10.3389/fmed.2022.911861]

15 **Martinou E**, Pericleous M, Stefanova I, Kaur V, Angelidi AM. Diagnostic Modalities of Non-Alcoholic Fatty Liver Disease: From Biochemical Biomarkers to Multi-Omics Non-Invasive Approaches. *Diagnostics (Basel)* 2022; **12** [PMID: 35204498 DOI: 10.3390/diagnostics12020407]

16 **Ioannidis JP**, Khoury MJ. Improving validation practices in "omics" research. *Science* 2011; **334**: 1230-1232 [PMID: 22144616 DOI: 10.1126/science.1211811]

17 **Perng W**, Aslibekyan S. Find the Needle in the Haystack, Then Find It Again: Replication and Validation in the 'Omics Era. *Metabolites* 2020; **10** [PMID: 32664690 DOI: 10.3390/metabo10070286]

18 **Hamilton DG**, Hong K, Fraser H, Rowhani-Farid A, Fidler F, Page MJ. Prevalence and predictors of data and code sharing in the medical and health sciences: systematic review with meta-analysis of individual participant data. *BMJ* 2023; **382**: e075767 [PMID: 37433624 DOI: 10.1136/bmj-2023-075767]

19 **Lin X**. Learning Lessons on Reproducibility and Replicability in Large Scale Genome-Wide Association Studies. *Harv Data Sci Rev* 2020; **2** [PMID: 38362534 DOI: 10.1162/99608f92.33703976]

20 **Wu WK**, Chen CC, Panyod S, Chen RA, Wu MS, Sheen LY, Chang SC. Optimization of fecal sample processing for microbiome study - The journey from bathroom to bench. *J Formos Med Assoc* 2019; **118**: 545-555 [PMID: 29490879 DOI: 10.1016/j.jfma.2018.02.005]

21 **Zheng Y**. Study Design Considerations for Cancer Biomarker Discoveries. *J Appl Lab Med* 2018; **3**: 282-289 [PMID: 30828695 DOI: 10.1373/jalm.2017.025809]

22 **Yamada R**, Okada D, Wang J, Basak T, Koyama S. Interpretation of omics data analyses. *J Hum Genet* 2021; **66**: 93-102 [PMID: 32385339 DOI: 10.1038/s10038-020-0763-5]

23 **Hu B**, Canon S, Eloe-Fadrosh EA, Anubhav, Babinski M, Corilo Y, Davenport K, Duncan WD, Fagnan K, Flynn M, Foster B, Hays D, Huntemann M, Jackson EKP, Kelliher J, Li PE, Lo CC, Mans D, McCue LA, Mouncey N, Mungall CJ, Piehowski PD, Purvine SO, Smith M, Varghese NJ, Winston D, Xu Y, Chain PSG. Challenges in Bioinformatics Workflows for Processing Microbiome Omics Data at Scale. *Front Bioinform* 2021; **1**: 826370 [PMID: 36303775 DOI: 10.3389/fbinf.2021.826370]

24 **Cobbin JC**, Charon J, Harvey E, Holmes EC, Mahar JE. Current challenges to virus discovery by meta-transcriptomics. *Curr Opin Virol* 2021; **51**: 48-55 [PMID: 34592710 DOI: 10.1016/j.coviro.2021.09.007]

25 **Santiago-Rodriguez TM**, Hollister EB. Multi 'omic data integration: A review of concepts, considerations, and approaches. *Semin Perinatol* 2021; **45**: 151456 [PMID: 34256961 DOI: 10.1016/j.semperi.2021.151456]

26 **Krassowski M**, Das V, Sahu SK, Misra BB. State of the Field in Multi-Omics Research: From Computational Needs to Data Mining and Sharing. *Front Genet* 2020; **11**: 610798 [PMID: 33362867 DOI: 10.3389/fgene.2020.610798]

27 Evolution of Translational Omics: Lessons Learned and the Path Forward. Washington (DC): National Academies Press (US); 2012-Mar-23 [PMID: 24872966]

28 **McShane LM**, Cavenagh MM, Lively TG, Eberhard DA, Bigbee WL, Williams PM, Mesirov JP, Polley MY, Kim KY, Tricoli JV, Taylor JM, Shuman DJ, Simon RM, Doroshow JH, Conley BA. Criteria for the use of omics-based predictors in clinical trials: explanation and elaboration. *BMC Med* 2013; **11**: 220 [PMID: 24228635 DOI: 10.1186/1741-7015-11-220]

29 **McShane LM**, Cavenagh MM, Lively TG, Eberhard DA, Bigbee WL, Williams PM, Mesirov JP, Polley MY, Kim KY, Tricoli JV, Taylor JM, Shuman DJ, Simon RM, Doroshow JH, Conley BA. Criteria for the use of omics-based predictors in clinical trials. *Nature* 2013; **502**: 317-320 [PMID: 24132288 DOI: 10.1038/nature12564]

30 **Scott MG**. When do new biomarkers make economic sense? *Scand J Clin Lab Invest Suppl* 2010; **242**: 90-95 [PMID: 20515285 DOI: 10.3109/00365513.2010.493411]

31 **Sanyal AJ**, Shankar SS, Yates KP, Bolognese J, Daly E, Dehn CA, Neuschwander-Tetri B, Kowdley K, Vuppalanchi R, Behling C, Tonascia J, Samir A, Sirlin C, Sherlock SP, Fowler K, Heymann H, Kamphaus TN, Loomba R, Calle RA. Diagnostic performance of circulating biomarkers for non-alcoholic steatohepatitis. *Nat Med* 2023; **29**: 2656-2664 [PMID: 37679433 DOI: 10.1038/s41591-023-02539-6]

32 **Vali Y**, Lee J, Boursier J, Petta S, Wonders K, Tiniakos D, Bedossa P, Geier A, Francque S, Allison M, Papatheodoridis G, Cortez-Pinto H, Pais R, Dufour JF, Leeming DJ, Harrison SA, Chen Y, Cobbold JF, Pavlides M, Holleboom AG, Yki-Jarvinen H, Crespo J, Karsdal M, Ostroff R, Zafarmand MH, Torstenson R, Duffin K, Yunis C, Brass C, Ekstedt M, Aithal GP, Schattenberg JM, Bugianesi E, Romero-Gomez M, Ratziu V, Anstee QM, Bossuyt PM; Liver Investigation: Testing Marker Utility in Steatohepatitis (LITMUS) consortium investigators. Biomarkers for staging fibrosis and non-alcoholic steatohepatitis in non-alcoholic fatty liver disease (the LITMUS project): a comparative diagnostic accuracy study. *Lancet Gastroenterol Hepatol* 2023; **8**: 714-725 [PMID: 36958367 DOI: 10.1016/S2468-1253(23)00017-1]

33 **Cao W**, Zhao C, Shen C, Wang Y. Cytokeratin 18, alanine aminotransferase, platelets and triglycerides predict the presence of nonalcoholic steatohepatitis. *PLoS One* 2013; **8**: e82092 [PMID: 24324749 DOI: 10.1371/journal.pone.0082092]

World Journal of Gastroenterology

Submit a Manuscript: https://www.f6publishing.com

World J Gastroenterol 2024 April 14; 30(14): 1990-2005

DOI: 10.3748/wjg.v30.i14.1990

ISSN 1007-9327 (print) ISSN 2219-2840 (online)

ORIGINAL ARTICLE

Retrospective Study

Characteristics of early gastric tumors with different differentiation and predictors of long-term outcomes after endoscopic submucosal dissection

Hong-Yi Zhu, Jie Wu, Yuan-Miao Zhang, Fang-Lan Li, Jin Yang, Bin Qin, Jiong Jiang, Ning Zhu, Meng-Yao Chen, Bai-Cang Zou

Specialty type: Gastroenterology and hepatology

Provenance and peer review: Unsolicited article; Externally peer reviewed.

Peer-review model: Single blind

Peer-review report's scientific quality classification

Grade A (Excellent): 0
Grade B (Very good): B
Grade C (Good): 0
Grade D (Fair): 0
Grade E (Poor): 0

P-Reviewer: Cesaretti M, Italy

Received: December 21, 2023
Peer-review started: December 21, 2023
First decision: January 30, 2024
Revised: February 12, 2024
Accepted: March 19, 2024
Article in press: March 19, 2024
Published online: April 14, 2024

Hong-Yi Zhu, Yuan-Miao Zhang, Bin Qin, Jiong Jiang, Ning Zhu, Meng-Yao Chen, Bai-Cang Zou, Department of Gastroenterology, The Second Affiliated Hospital of Xi'an Jiaotong University, Xi'an 710004, Shaanxi Province, China

Jie Wu, Department of Pathology, The Second Affiliated Hospital of Xi'an Jiaotong University, Xi'an 710004, Shaanxi Province, China

Fang-Lan Li, Department of Gastroenterology, Xianyang Hospital of Yan'an University, Xianyang 712000, Shaanxi Province, China

Jin Yang, Department of Gastroenterology, The First Hospital of Xi'an, Xi'an 710000, Shaanxi Province, China

Corresponding author: Bai-Cang Zou, PhD, Chief Physician, Department of Gastroenterology, The Second Affiliated Hospital of Xi'an Jiaotong University, No. 157 West Fifth Road, Xi'an 710004, Shaanxi Province, China. zoubaicang2@163.com

Abstract

BACKGROUND

Gastric cancer is a common malignant tumor of the digestive tract, and endoscopic submucosal dissection (ESD) is the preferred treatment for early-stage gastric cancer. The analysis of the epidemiological characteristics of gastric mucosal tumors with different differentiation degrees and the influencing factors of long-term ESD efficacy may have certain significance for revealing the development of gastric cancer and ESD.

AIM

To analyze the features of gastric mucosal tumors at different differentiation levels, and to explore the prognostic factors of ESD.

METHODS

We retrospectively studied 301 lesions in 285 patients at The Second Affiliated Hospital of Xi'an Jiaotong University from 2014 to 2021, according to the latest Japanese guidelines (sixth edition), and divided them into low-grade intraepithelial neoplasia (LGIN), high-grade intraepithelial neoplasia (HGIN), and

differentiated and undifferentiated early carcinoma. They are followed up by endoscopy, chest and abdominal computed tomography at 3, 6 and 12 months after ESD. We compared clinicopathologic characteristics, ESD efficacy, and complications with different degrees of differentiation, and analyzed the related factors associated with ESD.

RESULTS

HGIN and differentiated carcinoma patients were significantly older compared with LGIN patients ($P < 0.001$) and accounted for more 0-IIc ($P < 0.001$), atrophic gastritis was common ($P < 0.001$), and irregular microvascular patterns (IMVPs) and demarcation lines (DLs) were more obvious ($P < 0.001$). There was more infiltration in the undifferentiated carcinoma tissue ($P < 0.001$), more abnormal folds and poorer mucosal peristalsis ($P < 0.001$), and more obvious IMVPs, irregular microsurface patterns and DLs ($P < 0.05$) than in the LGIN and HGIN tissues. The disease-free survival rates at 2, 5, and 8 years after ESD were 95.0%, 90.1%, and 86.9%, respectively. Undifferentiated lesions (HR 5.066), white moss (HR 7.187), incomplete resection (HR 3.658), and multiple primary cancers (HR 2.462) were significantly associated with poor prognosis.

CONCLUSION

Differentiations of gastric mucosal tumors have different epidemiological and endoscopic characteristics, which are closely related to the safety and efficacy of ESD.

Key Words: Gastric mucosal epithelial neoplasia; Differentiated early gastric cancer; Undifferentiated early gastric cancer; Endoscopic submucosal dissection; Long-term outcomes

Core Tip: Endoscopic diagnosis and treatment of early gastric cancer is a hot topic in gastroenterology. By analyzing gastric mucosal tumors treated with endoscopic submucosal dissection (ESD) at a high-volume center in Northwest China, this study investigated the differences in characteristics of gastric mucosal tumors with different degrees of differentiation and the predictors of ESD efficacy and safety, providing data support for the further development of endoscopic technology.

Citation: Zhu HY, Wu J, Zhang YM, Li FL, Yang J, Qin B, Jiang J, Zhu N, Chen MY, Zou BC. Characteristics of early gastric tumors with different differentiation and predictors of long-term outcomes after endoscopic submucosal dissection. *World J Gastroenterol* 2024; 30(14): 1990-2005

URL: https://www.wjgnet.com/1007-9327/full/v30/i14/1990.htm

DOI: https://dx.doi.org/10.3748/wjg.v30.i14.1990

INTRODUCTION

Gastric cancer is a malignant tumor of the gastrointestinal tract with high morbidity and mortality. The annual incidence and death rate of gastric cancer in China account for nearly half of the global incidence. The early symptoms of gastric cancer are relatively difficult to identify, and they are usually found in the advanced stage. Surgery and drug treatment are less effective than other methods, so early diagnosis and treatment are crucial measures for improving the survival rate of gastric cancer patients. Early intervention can lead to a 5-year survival rate exceeding 90%[1-3].

Gastric epithelial neoplasia can be divided into nonneoplastic lesions, uncertain neoplastic lesions, low-grade intraepithelial neoplasia (LGIN), high-grade intraepithelial neoplasia (HGIN), early gastric cancer (EGC), and advanced cancer based on the Vienna classification. EGC is a superficial cancer confined to the mucosa and submucosa, with or without lymph node metastasis[4]. Japanese scholars have classified gastric cancer into differentiated and undifferentiated types based on the tissue source. The differentiated types included tubular and papillary adenocarcinomas, while the undifferentiated types included poorly differentiated adenocarcinomas, mucinous adenocarcinomas, and signet ring cell carcinomas[5]. It is widely accepted that intraepithelial neoplasia is a precancerous lesion of gastric cancer that progresses through a process known as the Correa cascade reaction. However, this concept requires further research, and the occurrence and development of gastric cancer and its influencing factors are still unclear[6].

Endoscopic submucosal dissection (ESD) is a minimally invasive technique that originated in Japan for the treatment of EGC. The high safety and short-term efficacy of ESD have led to its use worldwide. Despite the great success of ESD, the endoscopic treatment of gastric cancer is still progressing, and the indications are constantly being updated. According to the latest guidelines in Japan, previous expanded indications are included in absolute indications: Differentiated intramucosal cancer, without ulcers, of any size; differentiated intramucosal cancer, with ulcers, ≤ 3 cm; and undifferentiated intramucosal cancer, without ulcers, ≤ 2 cm. Reports of curative resection rates for ESD vary widely. Lee *et al*[7] reported an uncurative resection rate of 6.6%-28.4% after ESD. The long-term efficacy of ESD is still under observation and summarized, with discrepancies in different reports[8,9], and the risk factors affecting the efficacy and prognosis of ESD still need to be clarified.

Analysis of the epidemiological characteristics of gastric mucosal tumors with different degrees of differentiation may be important for revealing the developmental pattern and influencing factors of gastric cancer. The outcomes of endoscopic resection are closely related to the degree of differentiation, so accurate preoperative judgment of differentiation type is highly important for successful treatment[10]. This study incorporates epidemiological, pathological, and endoscopic features to compare the differences among intraepithelial neoplasia and differentiated and undifferentiated early cancers, and can help to explore the features and risk factors for gastric mucosal tumors of different differentiation types, which is beneficial for early and accurate diagnosis and prognosis.

MATERIALS AND METHODS

Patient selection

This study included EGC patients who underwent ESD at our center from March 2014 to December 2021. We collected patient information through the hospital HIS system. The inclusion criteria for patients were as follows: (1) Patients diagnosed with early gastric tumors based on gastroscopy and biopsy; (2) the relevant imaging examination had no contraindications, such as lymph node or distant metastasis, the patient met the indications for ESD, and informed consent was signed before surgery; and (3) the study protocol was approved by the Medical Ethics Committee (approval number: 2023530). The exclusion criteria for patients were as follows: (1) Patients had gastric mucosal tumors and did not undergo ESD; (2) patients had incomplete follow-up data; and (3) patients had serious cardiovascular, hematologic, neuropsychiatric disease and severe liver and kidney dysfunction.

ESD process

Preoperative preparation: Endoscopic examinations, such as white light, magnified endoscopy with narrow-band imaging (ME + NBI), and chemical staining (indigo carmine and acetic acid staining), were performed to determine the extent and depth of the lesion, and endoscopic ultrasonography was used to clarify the depth of tumor infiltration. The diet was restricted before surgery, antiplatelet drugs were stopped for 1 wk, and intravenous general anesthesia was initiated.

Procedure: The lesion boundary was determined 0.3-0.5 cm from the edge of the lesion, and multiple submucosal injections of 1 mL of 0.3% indigo carmine, 1 mL of epinephrine, and 100 mL of saline mixture were administered until the lesion was raised. The mucosa was cut along the marked point with a needle knife, the submucosal layer was peeled, and the bleeding was properly stopped. The specimen was sent to the pathology department to clarify the pathological nature and whether the margin was involved (Figure 1).

Postoperative management: Included fasting for 1-2 d after the operation; the use of antibiotics, gastric mucosal protectors, and acid suppressants; and the observation of wound healing and hospitalization for 2-3 d after the operation. Endoscopy, computed tomography (CT) or magnetic resonance imaging, and serum tumor marker data were regularly reviewed at 3, 6, and 12 months and annually after discharge to monitor for recurrence or metastasis.

Tumor pathological characteristics

According to the Paris classification, gastric mucosal tumors can be subgrouped into the following six types: Polypoid/protruded (type 0-I), superficial elevated (type 0-IIa), flat (type 0-IIb), superficial depressed (type 0-IIc), superficial depressed area in an elevated lesion (type 0-IIa+IIc) and excavated (type 0-III). The depth of tumor invasion was measured under a microscope: (1) M1, tumor limited to the mucosal epithelium; (2) M2, tumor limited to the lamina propria without involvement of the muscularis mucosa; (3) M3, tumor involving the muscularis mucosa; (4) SM1, tumor infiltrated into the superficial submucosa (from the muscularis mucosa to the submucosa < 500 μm); and (5) SM2, tumor involved the deep submucosa (≥ 500 μm in submucosa). In this study, tumors were rarely located in the lamina propria of the mucosa, so M1 and M2 were divided into one group.

Safety and efficacy of ESD

The main complications after ESD were bleeding, perforation, and stenosis. Early delayed bleeding was defined as bleeding that was endoscopically visible within 48 h after ESD. Patients with clinical manifestations of melena, hematemesis, or a significant decrease in hemoglobin levels need emergency endoscopy or surgical hemostasis. Bleeding events treated with hemostatic forceps during ESD were excluded. Delayed bleeding was defined as bleeding detected more than 48 h after ESD. Perforation was defined as the absence of the gastric wall under endoscopy, yellow adipose tissue could be observed directly, or free gas could be found on the abdominal X-ray. Stenosis was diagnosed when the endoscope could not easily reach the cardia through the lower esophagus.

En bloc resection was defined as complete endoscopic removal of the lesion. Complete resection meant that the lesion was removed in its entirety and there was no histopathological evidence of tumor involvement in the lateral or vertical margins. Curative resection was defined as meeting eCuraA and eCuraB, and the evaluation system includes: eCuraA: The tumor was En bloc resection, negative horizontal and vertical margins, without lymphatic and vascular invasion and meets one of the following criteria: (1) Postoperative pathology showed that the tumor was pT1a with predominantly differentiated carcinoma without ulceration; (2) postoperative pathology showed that the tumor was pT1a with predominantly undifferentiated carcinoma without ulceration and a long diameter ≤ 2 cm; and (3) postoperative pathology showed that the tumor was pT1a with predominantly differentiated carcinoma with ulceration and a long diameter ≤ 3

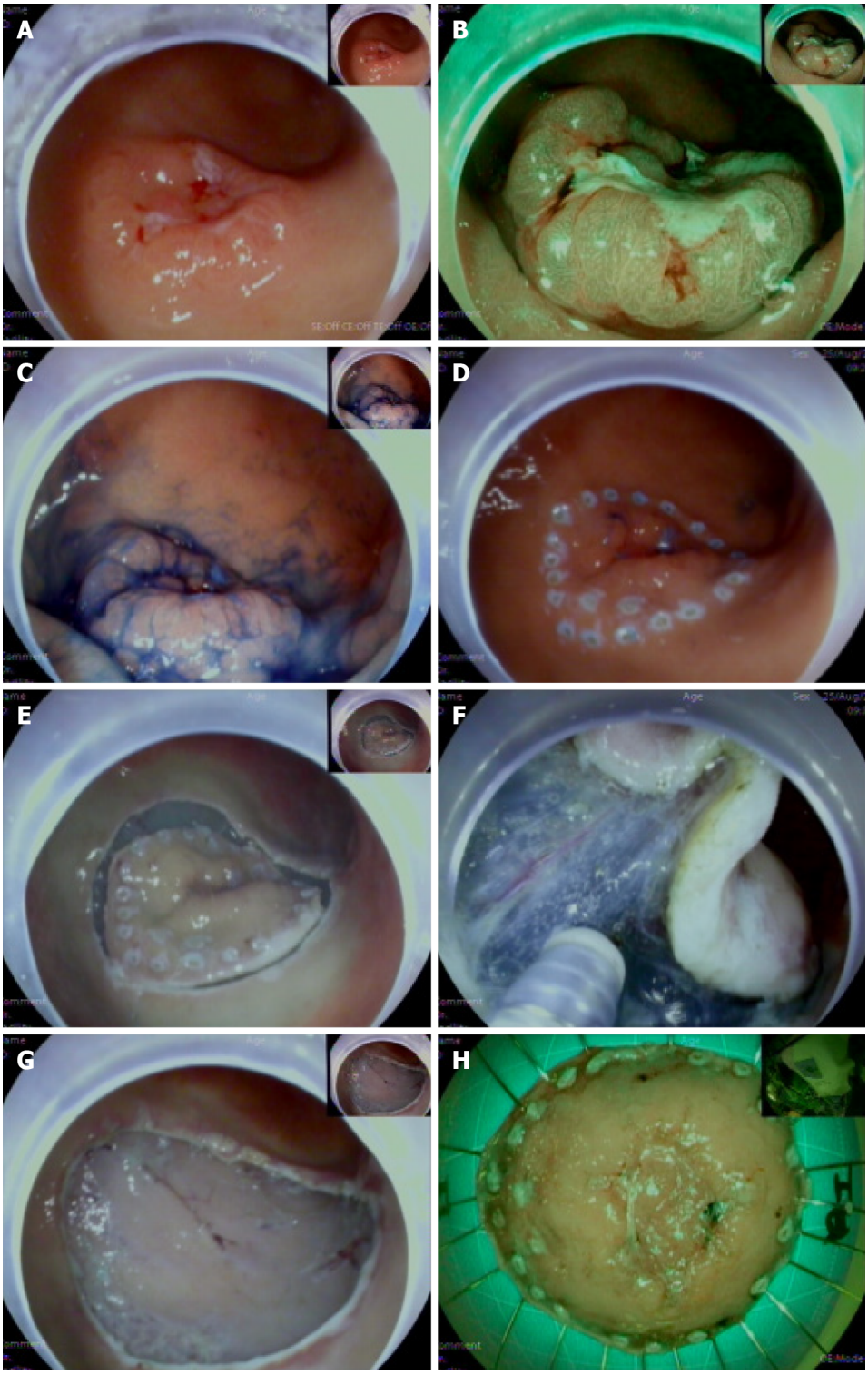

Figure 1 Endoscopic submucosal dissection process. A: 0-IIa + 0-IIc lesion in the greater curvature of the antrum (white light), the lesion flattened after inflation; B: NBI + ME: DL (+), the lesion elevation was evident after inspiration; C: Indigo carmine staining; D: Peripherally marked lesion; E: The surrounding mucosa was incised; F: Submucosal dissection; G: The resected wound; H: Fixed specimen.

cm. eCuraB: The tumor was resected en bloc. Postoperative pathology revealed that the tumor was pT1b but infiltrated < 500 μm, with predominantly differentiated carcinoma, a long diameter ≤ 3 cm, negative horizontal and vertical margins, and no lymphatic or vascular invasion. eCuraC: Includes eCuraC1 and eCuraC2. eCuraC1 refers to differentiated cancers that satisfied some of the conditions of eCuraA or eCuraB but were not treated with en bloc resection or had positive margins; eCuraC2 refers to those that did not satisfy the conditions of eCuraA, eCuraB, or eCuraC1.

Follow-up

For eCuraA and eCuraB, Japanese guidelines recommend endoscopy once or twice a year (eCuraB resection patients should also undergo abdominal ultrasound or CT to determine metastasis); in principle, eCuraC1 resection patients could

undergo ESD or gastrectomy, while eCuraC2 resection patients were required to undergo additional gastrectomy with lymphadenectomy. If patients refused additional resection, they were advised to follow up with endoscopy and CT after 3-6 months. Tumors found at the same site within 1 year after ESD were local recurrence, tumors found at other sites were simultaneous tumors, and more than one year later, the tumors found at other sites were metachronous tumors. Disease-free survival (DFS) was defined as the survival rate without recurrence, metastasis, or death from any cause.

Statistical analysis

SPSS 26.0 was used for statistical analysis, and GraphPad Prism 9.0 was used for plotting the data. Measurement data were compared by ANOVA if they were normally distributed and had a chi-square test. Comparisons between two groups were performed using the LSD test, and the Kruskal-Wallis rank sum test was used if the data were not normally distributed. Outcome unordered categorical data were compared using the chi-square test or Fisher exact test, and outcome ordered categorical data were compared using the Kruskal-Wallis rank sum test. The missing data among the measurement data were analyzed *via* the SPSS multiple interpolation method, and the missing data among the categorical data were analyzed *via* the virtual variable method, where the missing data were reassigned to a new classification. Logistic regression was used in multifactor analysis, the forward or backward method was selected for single-factor analysis with more variables, and the input method was selected for fewer variables. The overall survival rate and DFS rate were estimated by the Kaplan-Meier method and log-rank test, and survival-related multifactorial analysis was performed by Cox regression. A P value of < 0.05 was considered to indicate statistical significance.

RESULTS

This study included the clinical data of 285 patients with 301 Lesions treated with ESD at our hospital from March 2014 to December 2021.

Clinical characteristics

Compared with LGIN patients, HGIN patients were significantly older (average age: 57 years *vs* average age: 63 years, $P < 0.001$), had more smoking habits (27.1% *vs* 49.0%, $P = 0.004$), and had more atrophic gastritis (75.0% *vs* 93.0%, $P < 0.001$). A higher proportion of patients with differentiated early cancer were male (63.5% *vs* 82.0%, $P = 0.013$), were older (average age: 57 years *vs* average age: 63 years, $P < 0.001$), had more smoking habits (27.1% *vs* 50.6%, $P = 0.004$), and had more atrophic gastritis (75.0% *vs* 94.4%, $P < 0.001$) than LGIN patients (Table 1).

Pathological characteristics

Compared with LGIN patients, HGIN patients had fewer lesions located in the antrum area (69.8% *vs* 48.0%, $P = 0.006$), fewer type 0-I lesions (25.0% *vs* 3.0%, $P < 0.001$), and more type 0-IIc lesions (20.8% *vs* 39.0%, $P < 0.001$). Differentiated early cancer patients had fewer lesions located in the antrum area (69.8% *vs* 48.3%, $P = 0.006$), a larger volume ($Z = -40.767$, $P = 0.006$), a greater invasion depth ($Z = -76.983$, $P < 0.001$), fewer type 0-I lesions (25.0% *vs* 3.4%, $P < 0.001$), and more type 0-IIc lesions than LGIN lesions (20.8% *vs* 43.8%, $P < 0.001$). Compared with LGIN, undifferentiated early cancer was larger ($Z = -59.771$, $P = 0.049$) and resulted in deeper invasion ($Z = -107.937$, $P < 0.001$). The depth of invasion was greater in differentiated and undifferentiated early cancers than in HGIN ($Z = -76.983$, $P < 0.001$; $Z = -107.937$, $P < 0.001$) (Table 2).

White light endoscopic features

Spontaneous bleeding was more frequent in differentiated early cancers than in LGIN lesions (3.1% *vs* 20.2%, $P < 0.001$). Patients with undifferentiated early cancer had significantly more abnormal folds and mucosal peristalsis (elevation and extension of the lesion mucosa during suction and insufflation in the gastric cavity) than patients with LGIN or HGIN (3.1% *vs* 25.0%, 2.1% *vs* 18.8%, $P < 0.001$; 1.0% *vs* 25.0%, 1.0% *vs* 18.8%, $P < 0.001$). Compared with that of HGIN patients, the mucosal peristalsis of differentiated early cancer patients was more abnormal according to white light endoscopy (1.0% *vs* 10.1%, $P < 0.001$) (Table 3).

ME + NBI endoscopic features

Compared with those in LGIN patients, the irregular microvascular patterns, and demarcation lines (DLs) in patients with HGIN and differentiated early cancer were more obvious (38.5% *vs* 66.2%, 63.0% *vs* 86.3%, $P < 0.001$; 38.5% *vs* 77.8%, 63.0% *vs* 90.6%, $P < 0.001$). Patients with undifferentiated early cancer had more irregular microvascular and microsurface patterns and DLs than patients with LGIN (38.5% *vs* 100.0%, 49.2% *vs* 90.9%, and 63.0% *vs* 91.7%, $P < 0.05$) (Table 4).

ESD outcomes and complications

Undifferentiated early cancers exceeded ESD indications more often than LGIN (5.2% *vs* 87.5%, $P < 0.001$), with a higher percentage of noncurative resections (13.5% *vs* 87.5%, $P < 0.001$), and a higher incidence of postoperative complications (stenosis) (5.2% *vs* 25.0%, $P = 0.007$). More differentiated, undifferentiated early cancer exceeded ESD indications compared to HGIN (3.0% *vs* 13.5%, $P < 0.001$; 3.0% *vs* 87.5%, $P < 0.001$). Undifferentiated early cancer patients, compared with HGIN patients, had a higher percentage of noncurative resections (13.0% *vs* 87.5%, $P < 0.001$) and a greater risk of postoperative hemorrhage (1.0% *vs* 18.8%, $P = 0.002$) and stenosis (0.0% *vs* 6.3%, $P < 0.001$). Compared with differentiated early cancers, undifferentiated early cancers were more likely to beyond the ESD indications (13.5% *vs* 87.5%, $P < 0.001$),

Table 1 Clinical characteristics of gastric mucosal tumors with different degrees of differentiation, *n* (%)

	LGIN (*n* = 96)	HGIN (*n* = 100)	Differentiated-type (*n* = 89)	Undifferentiated-type (*n* = 16)	*P* value
Gender					0.013
Male	61 (63.5)[a]	76 (76.0)[a,b]	73 (82.0)[b]	9 (56.3)[a,b]	
Female	35 (36.5)[a]	24 (24.0)[a,b]	16 (18.0)[b]	7 (43.8)[a,b]	
Age (yr) (range)	57 (55-59)[a]	63 (61-65)[b]	63 (61-65)[b]	64 (59-68)[a,b]	< 0.001
Comorbidity					
Diabetes	6 (6.3)	15 (15.0)	9 (10.1)	0 (0.0)	0.108
Hypertension	17 (17.7)	31 (31.0)	19 (21.3)	4 (25.0)	0.161
Cardiovascular disease	5 (5.2)	8 (8.0)	9 (10.1)	2 (12.5)	0.572
Liver cirrhosis	5 (5.2)	1 (1.0)	2 (2.2)	0 (0.0)	0.265
Chronic pulmonary disease	2 (2.1)	6 (6.0)	1 (1.1)	0 (0.0)	0.175
Reflux esophagitis	15 (15.6)	12 (12.0)	11 (12.4)	3 (18.8)	0.794
Barrett's esophagus	4 (4.2)	2 (2.0)	1 (1.1)	0 (0.0)	0.489
Atrophic gastritis	72 (75.0)[a]	93 (93.0)[b]	84 (94.4)[b]	13 (81.3)[a,b]	< 0.001
Previous gastric cancer	1 (1.0)	0 (0.0)	2 (2.2)	0 (0.0)	0.461
Smoking history	26 (27.1)[a]	49 (49.0)[b]	45 (50.6)[b]	6 (37.5)[a,b]	0.004
Drinking history	24 (25.0)	31 (31.0)	24 (27.0)	3 (18.8)	0.673
Family history	15 (15.6)	11 (11.0)	19 (21.3)	0 (0.0)	0.074

[a]$P < 0.05$.
[b]$P < 0.05$.
Data in the same row are superscripted with the same letter or have no superscript to indicate a non-significant difference ($P > 0.05$). Different letters to indicate a significant difference ($P < 0.05$). LGIN: Low-grade intraepithelial neoplasia; HGIN: High-grade intraepithelial neoplasia.

with a greater risk of postoperative hemorrhage (2.2% *vs* 18.8%, $P = 0.002$) and stenosis (0.0% *vs* 6.3%, $P < 0.001$), and a higher percentage of ESD noncurative resections (21.3% *vs* 87.5%, $P < 0.001$) (Table 5).

Follow-up

The median follow-up period was 49 months (range 0.6-112.5 months), with overall survival rates of 99.0%, 97.7%, and 95.7% at 2, 5, and 8 years, respectively, and DFS rates of 95.0%, 90.1% and 86.9%, respectively (Figure 1). Patients with differentiated and undifferentiated early cancers had a lower body mass index (BMI) than those with LGIN (average: 23.87 *vs* 22.37, $P = 0.003$; average: 23.87 *vs* 21.44, $P = 0.003$). Compared with patients with LGIN, HGIN and differentiated early cancer, the percentage of undifferentiated early cancer with poor long-term outcome (recurrence, metastasis or death) was higher (8.3% *vs* 37.5%, $P < 0.001$; 6.0% *vs* 37.5%, $P < 0.001$; 7.9% *vs* 37.5%, $P < 0.001$), and undifferentiated early cancer was more likely to metastasize than HGIN and differentiated early cancer (0.0% *vs* 18.8%, $P < 0.001$; 2.2% *vs* 18.8%, $P < 0.001$) (Table 6).

Analysis of factors affecting diagnosis and treatment efficacy

Barrett esophagus (OR 7.805) and lesion location (lower third of the stomach) (OR 2.399) were independent risk factors for high preoperative pathological diagnosis, and BMI (OR 0.906) was an independent risk factor for postoperative pathological upgrading. The depth of lesion invasion (M1M2 OR 11.200, M3 OR 7.600) was significantly associated with complete resection. Based on the eCura system, lesion size, degree of differentiation, depth of invasion, ulceration, and complete resection were considered influencing factors for curative resection. Our study revealed that poor mucosal peristalsis (OR 0.185), ulcers (OR 0.073), and irregular microsurface patterns (IMSPs) (OR 0.410) were significantly associated with curative resection. Pathology (signet ring cell carcinoma OR 32.627, mucinous adenocarcinoma OR 49.855) and the Paris classification (III OR 30.406) were significantly associated with complications. Undifferentiated lesions (HR 5.066), white moss (HR 7.187), incomplete resection (HR 3.658), and multiple primary cancers (HR 2.462) were significantly associated with poor prognosis (Figure 2, Tables 7-12).

DISCUSSION

Currently, Japanese scholars believe that the development of differentiated gastric cancer involves multiple stages and

Table 2 Pathological characteristics of gastric mucosal tumors with different degrees of differentiation, *n* (%)

	LGIN (*n* = 96)	HGIN (*n* = 100)	Differentiated-type (*n* = 89)	Undifferentiated-type (*n* = 16)	*P* value
Size (cm) (range)	2.7 (2.2-3.7)[a]	3.2 (2.4-3.7)[a,b]	3.7 (2.7-4.2)[b]	3.5 (2.8-4.6)[b]	0.001
Location					0.006
Top 1/3	19 (19.8)	30 (30.0)	33 (37.1)	2 (12.5)	
Medium 1/3	10 (10.4)	22 (22.0)	13 (14.6)	5 (31.3)	
Lower 1/3	67 (69.8)[a]	48 (48.0)[b]	43 (48.3)[b]	9 (56.3)[a,b]	
Paris classification					< 0.001
0-I	24 (25.0)[a]	3 (3.0)[b]	3 (3.4)[b]	2 (12.5)[a,b]	
0-IIa	19 (19.8)	14 (14.0)	11 (12.4)	0 (0.0)	
0-IIb	9 (9.4)	11 (11.0)	9 (10.1)	0 (0.0)	
0-IIc	20 (20.8)[a]	39 (39.0)[b]	39 (43.8)[b]	8 (50.0)[a,b]	
0-III	1 (1.0)	1 (1.0)	1 (1.1)	0 (0.0)	
0-IIa+ IIc	23 (24.0)	32 (32.0)	26 (29.2)	6 (37.5)	
Invasion depth					< 0.001
M1M2	96 (100.0)[a]	100 (100.0)[a]	43 (48.3)[b]	5 (31.3)[b]	
M3	0 (0.0)[a]	0 (0.0)[a]	37 (41.6)[b]	6 (37.5)[b]	
SM1	0 (0.0)[a,b]	0 (0.0)[b]	6 (6.7)[a,c]	2 (12.5)[c]	
SM2	0 (0.0)[a]	0 (0.0)[a]	3 (3.4)[a,b]	3 (18.8)[b]	
Presence of *H. pylori*	37 (48.7)	38 (52.8)	32 (56.1)	4 (40.0)	0.727
Presence of ulceration	6 (6.3)	6 (6.0)	7 (7.9)	4 (25.0)	0.058

[a]$P < 0.05$.
[b]$P < 0.05$.
[c]$P < 0.05$.
Data in the same row are superscripted with the same letter or have no superscript to indicate a non-significant difference ($P > 0.05$). Different letters to indicate a significant difference ($P < 0.05$). LGIN: Low-grade intraepithelial neoplasia; HGIN: High-grade intraepithelial neoplasia.

Table 3 The white light endoscopic manifestations of gastric mucosal tumors with different degrees of differentiation, *n* (%)

	LGIN (*n* = 96)	HGIN (*n* = 100)	Differentiated-type (*n* = 89)	Undifferentiated-type (*n* = 16)	*P* value
Nodularity	65 (67.7)	65 (65.0)	60 (67.4)	11 (68.8)	0.974
Redness	51 (53.1)	50 (50.0)	60 (67.4)	7 (43.8)	0.059
Whiteness	7 (7.3)	5 (5.0)	2 (2.2)	0 (0.0)	0.324
White moss	10 (10.4)	14 (14.0)	15 (16.9)	2 (12.5)	0.646
Spontaneous bleeding	3 (3.1)[a]	11 (11.0)[a,b]	18 (20.2)[b]	0 (0.0)[a,b]	0.001
Abnormal fold	3 (3.1)[a]	1 (1.0)[a]	6 (6.7)[a,b]	4 (25.0)[b]	< 0.001
Poor peristalsis	2 (2.1)[a,b]	1 (1.0)[b]	9 (10.1)[a,c]	3 (18.8)[c]	< 0.001

[a]$P < 0.05$.
[b]$P < 0.05$.
[c]$P < 0.05$.
Data in the same row are superscripted with the same letter or have no superscript to indicate a non-significant difference ($P > 0.05$). Different letters to indicate a significant difference ($P < 0.05$). LGIN: Low-grade intraepithelial neoplasia; HGIN: High-grade intraepithelial neoplasia.

Table 4 Magnified endoscopy with narrow-band imaging manifestations of gastric mucosal tumors with different degrees of differentiation, *n* (%)

	LGIN (*n* = 96)	HGIN (*n* = 100)	Differentiated-type (*n* = 89)	Undifferentiated-type (*n* = 16)	*P* value
IMVP	25 (38.5)[a]	51 (66.2)[b]	49 (77.8)[b]	11 (100.0)[b]	< 0.001
IMSP	32 (49.2)[a]	46 (59.7)[a,b]	44 (69.8)[a,b]	10 (90.9)[b]	0.018
DL	46 (63.0)[a]	69 (86.3)[b]	58 (90.6)[b]	11 (91.7)[b]	< 0.001

[a]$P < 0.05$.
[b]$P < 0.05$.
Data in the same row are superscripted with the same letter or have no superscript to indicate a non-significant difference ($P > 0.05$). Different letters to indicate a significant difference ($P < 0.05$). LGIN: Low-grade intraepithelial neoplasia; HGIN: High-grade intraepithelial neoplasia; IMVP: Irregular microvascular pattern; IMSP: Irregular microsurface pattern; DL: Demarcation line.

Table 5 Endoscopic submucosal dissection efficacy and safety of gastric mucosal tumors with different degrees of differentiation, *n* (%)

	LGIN (*n* = 96)	HGIN (*n* = 100)	Differentiated-type (*n* = 89)	Undifferentiated-type (*n* = 16)	*P* value
Absolute indication	91 (94.8)[a,b]	97 (97.0)[b]	77 (86.5)[a]	2 (12.5)[c]	< 0.001
En bloc resection	93 (96.9)	98 (98.0)	88 (98.9)	16 (100.0)	0.729
Complete resection	88 (91.7)	90 (90.0)	79 (88.8)	13 (81.3)	0.630
Curative resection	83 (86.5)[a]	87 (87.0)[a]	70 (78.7)[a]	2 (12.5)[b]	< 0.001
Complication	5 (5.2)[a]	5 (5.0)[a]	3 (3.4)[a]	4 (25.0)[b]	0.007
Bleeding	3 (3.1)[a,b]	1 (1.0)[b]	2 (2.2)[b]	3 (18.8)[a]	0.002
Perforation	2 (2.1)	4 (4.0)	2 (2.2)	1 (6.3)	0.710
Stenosis	0 (0.0)[a]	0 (0.0)[a]	0 (0.0)[a]	1 (6.3)[b]	< 0.001

[a]$P < 0.05$.
[b]$P < 0.05$.
[c]$P < 0.05$.
Data in the same row are superscripted with the same letter or have no superscript to indicate a non-significant difference ($P > 0.05$). Different letters to indicate a significant difference ($P < 0.05$). LGIN: Low-grade intraepithelial neoplasia; HGIN: High-grade intraepithelial neoplasia.

Table 6 Follow-up results of gastric mucosal tumors with different degrees of differentiation, *n* (%)

	LGIN (*n* = 96)	HGIN (*n* = 100)	Differentiated-type (*n* = 89)	Undifferentiated-type (*n* = 16)	*P* value
BMI (range)	23.87 (23.19-24.54)[a]	23.09 (22.41-23.77)[a,b]	22.37 (21.71-23.02)[b]	21.44 (20.08-22.79)[b]	0.003
Adverse outcome	8 (8.3)[a]	6 (6.0)[a]	7 (7.9)[a]	6 (37.5)[b]	< 0.001
Recurrence	5 (5.2)	6 (6.0)	6 (6.7)	2 (12.5)	0.734
Metastasis	3 (3.1)[a,b]	0 (0.0)[b]	2 (2.2)[b]	3 (18.8)[a]	< 0.001
Multiple primary cancer	24 (25.0)	15 (15.0)	15 (16.9)	4 (25.0)	0.276

[a]$P < 0.05$.
[b]$P < 0.05$.
Data in the same row are superscripted with the same letter or have no superscript to indicate a non-significant difference ($P > 0.05$). Different letters to indicate a significant difference ($P < 0.05$). LGIN: Low-grade intraepithelial neoplasia; HGIN: High-grade intraepithelial neoplasia; BMI: Body mass index.

gradual progression (Correa cascade), usually due to long-term chronic inflammation stimulating the differentiation of gastric mucosal glandular neck stem cells to the intestinal epithelium, intestinal metaplasia and dysplasia, which ultimately induces gastric cancer occurrence. However, undifferentiated gastric cancer cells do not undergo this process and directly form diffuse cancer cells. Scientists have shown that this change is related to the destruction of intercellular connections caused by a lack of E-cadherin expression[11]. Since some people will not continue to progress even if they develop intestinal metaplasia or intraepithelial neoplasia, some scholars believe that different differentiation types of

Table 7 Multivariate analysis of time-related factors of adverse outcomes such as recurrence, metastasis and death

Variable	Category	*P* value	Hazard ratio	95%CI
Differentiation degree	Undifferentiated-type	0.004	5.066	1.688-15.200
	LGIN		1	
White moss	Yes	< 0.001	7.187	3.122-16.546
	No		1	
Complete resection	No	0.012	3.658	1.337-10.010
	Yes		1	
Multiple primary cancer	Yes	0.030	2.462	1.090-5.562
	No		1	

LGIN: Low-grade intraepithelial neoplasia.

Table 8 Multivariate analysis of factors associated with incomplete resection

Variable	Category	*P* value	Odds ratio	95%CI
Invasion depth	M1M2	0.004	11.200	2.120-59.163
	M3	0.032	7.600	1.192-48.437
	SM2	-	1	-

Table 9 Multivariate analysis of factors associated with noncurative resection

Variable	Category	*P* value	Odds ratio	95%CI
Peristaltic condition	Poor	0.009	0.185	0.052-0.653
	Normal		1	
Microsurface pattern	Irregular	0.043	0.410	0.173-0.972
	Regular		1	
Ulceration	Yes	< 0.001	0.073	0.026-0.207
	No		1	

Table 10 Multivariate analysis of complications related factors

Variable	Categor	*P* value	Odds ratio	95%CI
Histologic type	Signet ring cell (sig)	0.032	32.627	1.357-784.415
	Mucinous (muc)	0.006	49.855	3.051-814.724
	LGIN	-	1	-
Paris classification	0-III	0.020	30.406	1.695-545.565
	0-I		1	

LGIN: Low-grade intraepithelial neoplasia.

gastric mucosal tumors might have primary genetic causes, interact with the environment, and ultimately determine the development direction of gastric cancer[6,12]. In this study, we retrospectively analyzed the cases of patients who underwent ESD at a high-volume center in Northwest China within 8 years and compared the differences in the characteristics of LGIN, HGIN, and differentiated and undifferentiated cancers, to provide ideas for further exploration of the mechanism of gastric cancer and analysis of the efficacy and related influencing factors of ESD treatment in Northwest China.

Table 11 Multivariate analysis of factors related to postoperative pathological degradation

Variable	Category	*P* value	Odds ratio	95%CI
Location	Lower 1/3	0.037	2.399	1.055-5.455
	Top 1/3		1	
Barrett's esophagus	Yes	0.026	7.805	1.277-47.689
	No		1	

Table 12 Multivariate analysis of factors related to postoperative pathological upgrading

Variable	*P* value	Odds ratio	95%CI
BMI	0.022	0.906	0.833-0.986

BMI: Body mass index.

From this study, it was clear that the greater the differentiation degree of the lesion was, the more likely it was to develop into depression, the greater the depth of invasion, and the more obvious the NBI + ME abnormality. Among them, patients with differentiated tumors were older than those with intraepithelial neoplasia; most were male patients and had a longer history of smoking. Most of these patients had a history of atrophic gastritis, which is in line with the classical evolution of gastric cancer. However, there was no significant difference in age or smoking history between patients with undifferentiated tumors and those with intraepithelial neoplasia, and the number of lesions that developed from nonatrophic gastritis increased, suggesting that age, smoking history, and atrophic gastritis may not be necessary factors. Patients with undifferentiated tumors were more likely to have poor mucosal peristalsis and abnormal folds under white light endoscopy, which might be related to their deep invasion and large extent. The efficacy, safety, and long-term follow-up outcomes of ESD were worse than those of other types of tumors.

Our results suggested that ESD was a safe and effective treatment. The en bloc resection rate, complete resection rate, and curative resection rate were 98%, 90%, and 80.4%, respectively. There were 59 cases of noncurative resection, among which 31 patients underwent noncomplete resection, 11 patients underwent immediate additional gastrectomy, 4 patients had no obvious residual cancer tissue after surgery, and 2 patients died of liver metastasis; the remaining 48 patients did not receive additional treatments, partly because they did not satisfy the conditions of curative resection of the eCura but pathology suggested complete resection, and partly because of poor quality of life after surgery, advanced age, comorbidities and other reasons. During the follow-up of patients without additional treatment, 5 patients experienced recurrence, 4 patients died, and 3 patients experienced tumor metastasis. Combined with the findings of previous studies, the survival outcome of patients who underwent noncurative resection or additional surgery was better than that of patients who did not undergo additional surgery, but there was no difference between the two in this study because there were fewer patients who underwent noncurative resection or additional surgery, including 1 patient with recurrence and 2 patients with metastasis that resulted in death. Choi *et al*[13] reported no significant difference in overall survival or DFS between patients treated with additional surgery and those followed up after ESD alone, which is consistent with the findings of our study. However, additional studies have suggested that noncurative resection *via* ESD, especially in patients with lymphovascular invasion or positive vertical margins with submucosal invasion, should include further surgical treatment, which is safe and effective, and that results in better survival outcomes[14-17].

The incidences of bleeding, perforation, and stenosis after ESD treatment were 3%, 3%, and 0.3%, respectively, and the only patient with postoperative stenosis had a lesion located at the cardia, which was considered to be related to postoperative scar contracture. There were 19 patients (6.3%) with recurrence, including 3 patients with simultaneous tumors who underwent complete resection by ESD or endoscopic mucosal resection; 6 patients with metachronous tumors; 2 patients who underwent major gastrectomy; 2 patients who underwent ESD treatment again; and 2 patients who underwent regular gastroscopy to assess the lesions. Another 10 patients had local recurrence; 3 of these patients underwent ESD surgery again; 3 patients were transferred to the surgery department for gastrectomy; and another 4 patients underwent regular gastroscopy. The pathologic result for all untreated patients after recurrence was LGIN, which was temporarily treated with oral medication according to the patient's wishes and condition, with regular follow-up gastroscopy and additional surgery if necessary. There were 8 metastases (2.7%), including 5 liver metastases, 1 retroperitoneal metastasis, 1 lung metastasis, and 1 lymph node metastasis. The overall survival rates at 2, 5, and 8 years were 99.0%, 97.7%, and 95.7%, respectively, and the DFS rates were 95.0%, 90.1%, and 86.9%, respectively.

Choi *et al*[18] assessed 522 EGC lesions treated with ESD, the en bloc resection rate was 97.1%, and the local recurrence rate was 1.8% (median follow-up was 24 months) for lesions with absolute indications; the en bloc resection rate was 96.1%, and the local recurrence rate was 7.0% for lesions with expanded indications. No metastasis was observed at any of the follow-ups. Kosaka *et al*[19] followed up EGC patients treated with ESD for 5-9 years and reported that the en bloc resection rate, curative resection rate, and local recurrence rate of lesions meeting the absolute indications were 98.0%, 96.0%, and 0.3%, respectively; and the en bloc resection rate, curative resection rate, and local recurrence rate of expanded indication lesions were 89.7%, 72.0%, and 3.7%, respectively; and there were no deaths. Nakamura *et al*[20] studied 1332

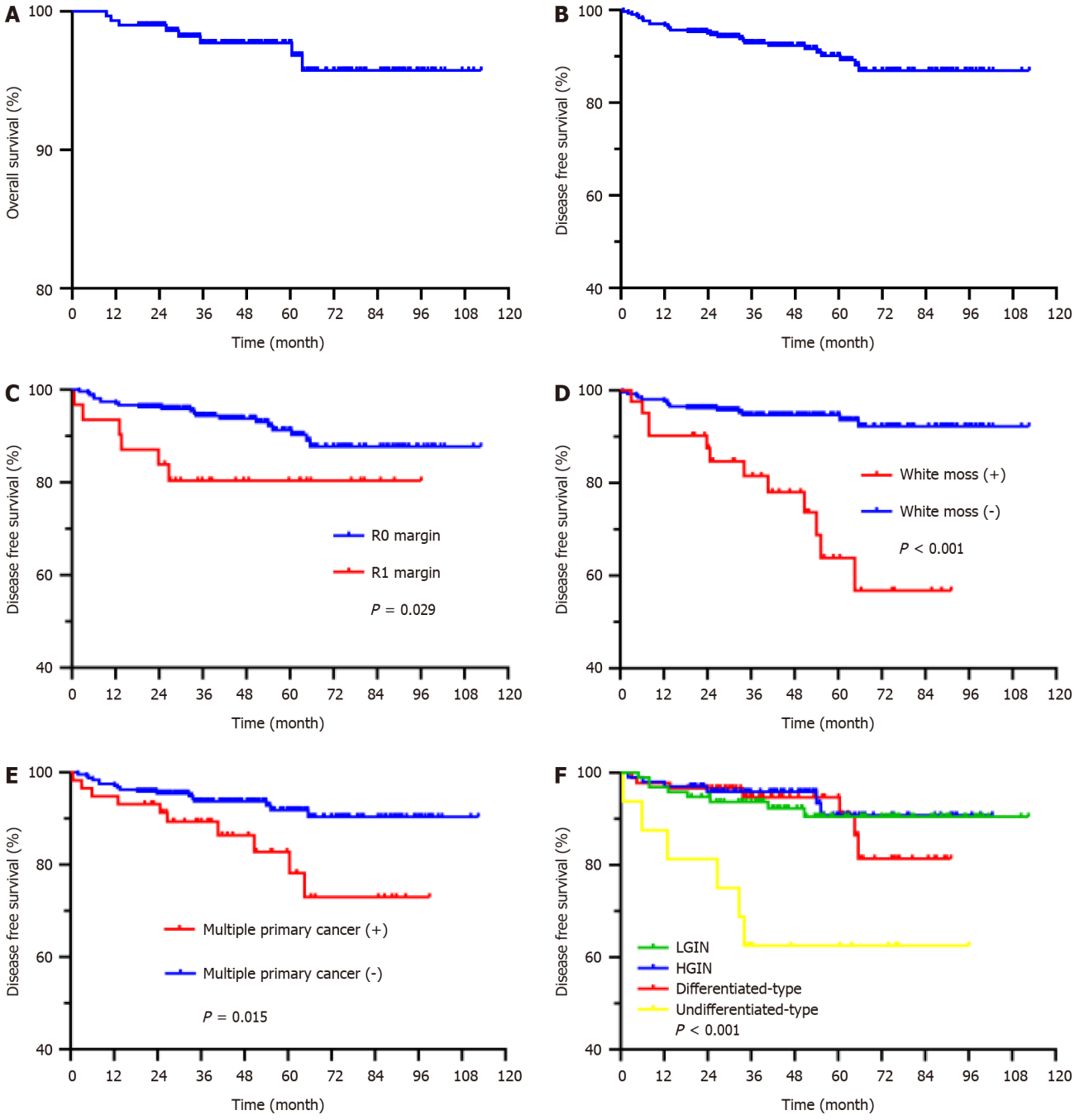

Figure 2 Kaplan-Meier curves showed overall survival and disease-free survival during the follow-up period. A: Overall survival; B: Disease-free survival (DFS); C: DFS based on complete resection; D: DFS based on white moss; E: DFS based on multiple primary cancer; F: DFS based on lesion differentiation. LGIN: Low-grade intraepithelial neoplasia; HGIN: High-grade intraepithelial neoplasia.

lesions treated with ESD; the en bloc resection rate was 99.0%, the curative resection rate was 96.4%, and the local recurrence rate was 0.2% (median follow-up was 29.5 months) for lesions of absolute indication; the en bloc resection rate, curative resection rate, and local recurrence rate of expanded indication lesions were 97.4%, 93.4%, and 0.9%, respectively; and there was 1 case of liver metastasis (0.2%). This study used the latest Japanese guidelines, which categorized previous expanded indications as absolute indications; thus, the results were consistent, indicating that the ESD level in our hospital had reached the standard, which provided a strong guarantee for the treatment of gastric cancer in Northwest China. Bhandari *et al*[21], in Western countries, reported that the 2-year recurrence-free survival rate after ESD for EGCs was 94%, but this rate decreased to 83% at 5 years. A total of 722 EGCs in 697 patients treated with ESD in Kim's study showed a 5-year follow-up overall survival rate of 96.6%, a DFS rate of 90.6%, a local recurrence rate of 0.9%, a metachronous tumor incidence of 7.8%, and a distant metastasis incidence of 0.5%[22]. The long-term follow-up results of the above study were consistent with our study, but the recurrence and metastasis rates were low. These findings were related to the 34 patients in this study who did not meet the absolute indications for ESD, possibly because of the patients' wishes. These findings also indicated that ESD technology was gradually improving and that doctors were gradually challenging and exploring the best indications. We should disseminate knowledge of the high recurrence risk after ESD

for EGC patients so that patients have a positive attitude toward completing postoperative monitoring on time, which will further improve the diagnosis and treatment of gastric cancer in China[23]. Na *et al*[24] showed that postoperative bleeding occurred in 325 (5.8%) of 5629 ESD-treated EGC patients. Oda *et al*[25] reported that there were 11 cases (3.6%) of perforation in 303 EGC patients treated with ESD, which was roughly equal to the probability of occurrence in this study. Most cases of stenosis that occur during ESD are located in the cardia. According to the study by Cao *et al*[26], stenosis occurred in 22 patients (1.9%) of 1133 Lesions, 18 of whom had cardia cancer; these findings suggest that ESD of cardia tumors, similar to esophageal tumors, should be used to prevent stenosis and dilation if necessary.

Our data revealed a significant discrepancy between the preoperative biopsy pathology and postoperative specimen pathology results, with a concordance rate of only 46.8%; 16.6% of the patients were diagnosed with high pathological grade (postoperative pathological downgrade) and 36.5% were diagnosed with low diagnostic grade (postoperative pathological escalation). Multivariate analysis revealed that, compared with the consistent pathology of patients before and after ESD, Barrett's esophagus and lesion location were found to be independent risk factors for preoperative pathological hypertension, and BMI was found to be an independent risk factor for postoperative pathological upgrading. The high judgment may be due to the biopsy revealing the most obvious structural abnormality with the naked eye, that is, the traditional definition of "one point cancer", and the biopsy completes the treatment process. Barrett's esophagus is a gastroesophageal reflux-induced lesion that manifests as the degeneration of esophageal squamous epithelium into columnar epithelium and is considered to be a risk factor for the development of the adenocarcinoma of the esophagogastric conjunction. Therefore, when patients have Barrett's esophagus, the mucosa located in the cardia should be observed carefully to prevent missed diagnoses, but the diagnosis and treatment should not be overly rigorous. Lesions located in the antral and pyloric regions of the stomach are susceptible to high pathological grade, probably because this area is a high incidence area for gastric cancer, and inflammation in the stomach caused by *Helicobacter pylori* bacteria most often occurs here, with varied manifestations, which can easily arouse physician's suspicion. A lower BMI was associated with postoperative pathological escalation, and relevant studies have shown that a low BMI was associated with more aggressive gastric cancer. Our study showed that, compared with those of LGIN patients, the malignancy of undifferentiated early cancer was greater, differentiated early cancer patients were older and had a longer medical history; additionally, most of these patients had atrophic gastritis, which affected the patients' eating and nutrient absorption, resulting in a relatively low BMI. Therefore, when there is more weight loss, we should reasonably suspect that the malignancy of the lesions is greater.

Among the 1541 patients studied by Ryu *et al*[27], the concordance rate of pathological diagnosis before and after ESD was 31.1%, the postoperative pathological upgrading rate was 23.8%, and the degradation rate was 7.3%. The factors related to postoperative pathological upgrading of LGIN lesions were central depression (OR 2.959), surface nodule (OR 6.581), and surface redness (OR 6.399). The factors related to postoperative pathological escalation of HGIN lesions were central depression (OR 1.999), surface nodules (OR 1.733), surface redness (OR 2.283), lesions located in the upper 1/3 of the stomach (OR 3.989), and lesion sizes ≥ 10 mm (OR 2.200). Ryu *et al*[28] reported a pathological concordance rate of 76.3%, a diagnostic upgrade rate of 66.5%, and a downgrade rate of 9.8% in 427 patients with HGIN who underwent ESD. Central depression (OR 4.151), surface nodules (OR 5.582), surface redness (OR 2.926), lesion sites in the upper 1/3 of the stomach (OR 3.894), and tumor sizes ≥ 10 mm (OR 2.287) were associated with postoperative pathology upgrading to EGC. Surface nodules (OR 2.746), submucosal fibrosis (OR 3.958), lesion sites in the upper 1/3 of the stomach (OR 6.652), and tumor sizes ≥ 10 mm (OR 4.935) were significantly associated with invasive submucosal cancers. There were some differences between the results of this study and those of the above studies, which might be related to the small sample size and the lack of stratified analysis; therefore, the sample size needs to be expanded for further research. Most doctors rely on preoperative biopsy pathology when making treatment decisions, but current research has suggested that additional inconsistencies occur; therefore, experts need to determine the optimal treatment plan by combining white light, NBI + ME, ultrasound endoscopy, and patient conditions.

Cox regression showed that the factors affecting DFS (no outcomes such as tumor recurrence, metastasis, or death) were the degree of differentiation, white moss, multiple primary cancers, and complete resection. Undifferentiated cancers grow diffusely and are prone to have undetectable margin remnants. White moss more often combined with ulcers, suggesting deeper infiltration, and according to the eCura system, ESD treatment requires the lesion to be differentiated into intramucosal carcinoma and ≤ 3 cm in length. This study introduced the concept of multiple primary cancers, also known as duplicated cancers, which refer to the simultaneous or successive occurrence of two or more primary malignant tumors in a single or multiple organs of the same host. When intraepithelial neoplasia or carcinoma also existed in other parts of the body, postoperative recurrence, metastasis, or death were more likely to occur, which deserved our attention, and indicated that if patients had a history of tumors in other parts of the body, close monitoring was more necessary, and we should not ignore the chest and abdominal CT and tumor marker screening, in addition to gastroscopy. Patients who underwent incomplete resection *via* ESD were more likely to have adverse outcomes, which was consistent with the findings of other studies, and required good preoperative evaluation and intraoperative rigor.

This study suggested that the depth of lesion invasion was an independent risk factor for complete resection of early EGCs. Doctors should accurately determine the edge of the lesion before ESD surgery, with the help of NBI + ME endoscopy, ultrasound endoscopy, staining, and other technologies, and not be too close to avoid residual margins.

In this study, poor gastric mucosal peristalsis under white light endoscopy, ulcers, and IMSP were found to be independent risk factors for curative resection. Poor gastric mucosal peristalsis under white light indicates a poor degree of lesion differentiation and invasive growth of cancer cells, such as "leather stomach", which is a typical manifestation of signet ring cell carcinoma. The presence of ulcers indicated deep infiltration. The Japanese scholar Kishino *et al*[29] proposed that microvasculature and microsurfaces should be taken into account but focused more on whether the structures were regular or had disappeared during the endoscopic identification of EGC. The microsurface was divided into the pit structure (pit) of the gastric fundus and the villus structure (villi) of the gastric antrum, and it was believed

that the glandular duct was the culprit and that the blood vessel was the accomplice in the development of gastric cancer. The results of this study suggested that lesions with IMSP were more likely to undergo noncurative resection, which confirmed Kishino's theory that IMSP might indicate a longer development time and a greater degree of malignancy in gastric cancer patients. Therefore, when poor gastric mucosal peristalsis, ulcers, or IMSP occur, the biological behavior of the tumor should be vigilant, and whether the patient meets the indications for curative resection *via* ESD should be strictly assessed.

The pathological classification and Paris classification of lesions were found to be independent risk factors for complications after ESD. Patients with signet ring cell carcinoma and mucinous adenocarcinoma were more prone to complications such as bleeding, perforation, and stenosis. In this study, 1 out of 2 patients with signet ring cell carcinoma had hemorrhages, 1 out of 3 patients with mucinous adenocarcinoma had perforations, and 1 out of 3 patients with mucinous adenocarcinoma had hemorrhages and stenoses. These findings may be related to the small number of lesions, and it is necessary to expand the sample size for further exploration. Perforation occurred in 2 of the 3 Paris type 0-III, because these lesions had deeper infiltration and were often associated with ulceration, which increased the difficulty of submucosal dissection.

This study used the latest Japanese guidelines (sixth edition). According to the old guidelines, some of our lesions were extended or beyond the scope of indications. After the guidelines were updated, 34 lesions that still extended or exceeded the indications were not curatively resected, but some lesions were stable during follow-up, such as differentiated carcinoma with ulcers > 3 cm, differentiated carcinoma with invasion depth of SM1 > 3 cm, and undifferentiated intramucosal carcinoma > 2 cm. These types of lesions suggested a higher probability of lymph node metastasis in the available studies; however, a larger number of patients were still doing well during subsequent follow-up, and with the improvement of the skills of endoscopists, the indications for ESD might further expand, requiring further studies.

This study has several limitations: (1) In this study, bleeding, perforation, and stenosis occurred in 9, 9, and 1 patients, respectively. The number of patients was small when analyzing the risk factors for each complication individually, so a combined analysis was performed, which might lack the precision of analyzing the factors affecting the occurrence of each complication; (2) the lack of complete endoscopic follow-up data for all study subjects was a major limitation of most published studies on gastric ESD. Our study was no exception, and to overcome this limitation, we conducted a rigorous DFS analysis, including the time factor of the occurrence event, which could effectively reduce the impact of lost follow-up data; and (3) this was a single-center study, which might lack representativeness of ESD efficacy across Northwest China; therefore, a joint multicenter study might be more useful.

CONCLUSION

Despite these limitations, we could draw the following conclusions after carefully analyzing the relevant data. Gastric mucosal tumors with different degrees of differentiation had different characteristics that were closely related to ESD indications and need to be further explored to provide a clinical basis for the pathogenesis, diagnosis and treatment of gastric mucosal tumors. The findings of this study suggested a high rate of curative resection and few adverse events associated with early gastric tumors after ESD. After noncurative resection, additional surgical resection and lymph node dissection should be considered according to the patient's condition to potentially improve long-term survival. All patients should closely monitored after ESD to detect recurrence and metastasis promptly.

ARTICLE HIGHLIGHTS

Research background

Timely intervention in early gastric cancer can improve the 5-year survival rate to more than 90%. Endoscopic submucosal dissection (ESD) is a safe and mature endoscopic treatment method, but its indications, postoperative management strategies and related influencing factors are still under exploration.

Research motivation

The aim of this study was to explore the underlying factors affecting the development of gastric mucosal tumors, the efficacy of ESD and the underlying scientific prevention and treatment strategies after surgery.

Research objectives

The epidemiological, clinical, and endoscopic features and ESD efficacy of gastric mucosal tumors with different degrees of differentiation were analyzed by stratification, and the related risk factors affecting preoperative diagnosis, ESD efficacy and long-term disease-free survival (DFS) were explored.

Research methods

According to the latest Japanese guidelines (sixth edition), 301 patients with gastric mucosal tumors treated with ESD at our center from 2014 to 2021 were enrolled, and followed up by endoscopy and chest and abdominal computed tomography at 3, 6 and 12 months after surgery for monitoring, and the data were retrospectively analyzed.

Research results

The greater the degree of differentiation of the lesion is, the more likely the lesion is to develop into depression, the deeper the infiltration depth, the more obvious the magnified endoscopy with narrow-band imaging (ME + NBI) abnormality, and the more postoperative complications and adverse outcomes there are. The overall survival rates at 2, 5 and 8 years were 99.0%, 97.7% and 95.7%, respectively, and the DFS rates were 95.0%, 90.1% and 86.9%, respectively. Undifferentiated lesions (HR 5.066), coating with white moss (HR 7.187), incomplete resection (HR 3.658), and multiple primary cancers (HR 2.462) were risk factors for poor prognosis.

Research conclusions

Before ESD, it is necessary to strictly screen lesions that meet the indications and be aware of the risk factors that affect the efficacy of ESD. Patients with high-risk factors should be followed up more closely after surgery to identify any recurrence and metastasis in a timely manner. After noncurative resection, additional surgical resection and lymph node dissection should be performed according to the patient's condition.

Research perspectives

A large-scale, multicenter retrospective study in Northwest China is needed to increase the sample size and the number of positive outcomes, and further exploration of treatment options for patients with noncurative resections is necessary.

FOOTNOTES

Author contributions: Zhu HY wrote the article and collected the data; Wu J offered help with pathology; Zhang YM, Li FL, Yang J, Jiang J, Qin B, Zhu N, Chen MY analysis and interpretation; Zou BC designed the study, revised the paper critically for important intellectual content; all the authors approved the final version of the article to be published.

Supported by Development Program of Shaanxi Province, No. 2021SF-221.

Institutional review board statement: This study was reviewed and approved by the Ethics Committee of The Second Affiliated Hospital of Xi'an Jiaotong university.

Informed consent statement: All study participants or their legal guardian provided informed written consent about personal and medical data collection prior to study enrolment.

Conflict-of-interest statement: The authors declare that there is no conflict of interest.

Data sharing statement: The data that support the findings of this study are available from the corresponding author upon reasonable request.

Country/Territory of origin: China

ORCID number: Hong-Yi Zhu 0009-0008-1477-1478; Jie Wu 0000-0002-5821-9705; Yuan-Miao Zhang 0009-0001-9283-4373; Fang-Lan Li 0009-0003-5458-0530; Jiong Jiang 0000-0003-0386-4640; Ning Zhu 0009-0005-4237-4646; Meng-Yao Chen 0009-0001-6489-9946; Bai-Cang Zou 0000-0002-1648-4965.

S-Editor: Qu XL
L-Editor: A
P-Editor: Yuan YY

REFERENCES

1 **Isobe Y**, Nashimoto A, Akazawa K, Oda I, Hayashi K, Miyashiro I, Katai H, Tsujitani S, Kodera Y, Seto Y, Kaminishi M. Gastric cancer treatment in Japan: 2008 annual report of the JGCA nationwide registry. *Gastric Cancer* 2011; **14**: 301-316 [PMID: 21894577 DOI: 10.1007/s10120-011-0085-6]

2 **Ajani JA**, Bentrem DJ, Besh S, D'Amico TA, Das P, Denlinger C, Fakih MG, Fuchs CS, Gerdes H, Glasgow RE, Hayman JA, Hofstetter WL, Ilson DH, Keswani RN, Kleinberg LR, Korn WM, Lockhart AC, Meredith K, Mulcahy MF, Orringer MB, Posey JA, Sasson AR, Scott WJ, Strong VE, Varghese TK Jr, Warren G, Washington MK, Willett C, Wright CD, McMillian NR, Sundar H; National Comprehensive Cancer Network. Gastric cancer, version 2.2013: featured updates to the NCCN Guidelines. *J Natl Compr Canc Netw* 2013; **11**: 531-546 [PMID: 23667204 DOI: 10.6004/jnccn.2013.0070]

3 **Ishii N**, Shiratori Y, Ishikane M, Omata F. Population effectiveness of endoscopy screening for mortality reduction in gastric cancer. *DEN Open* 2024; **4**: e296 [PMID: 37731836 DOI: 10.1002/deo2.296]

4 **Japanese Gastric Cancer Association**. Japanese Gastric Cancer Treatment Guidelines 2021 (6th edition). *Gastric Cancer* 2023; **26**: 1-25 [PMID: 36342574 DOI: 10.1007/s10120-022-01331-8]

5 **Nagtegaal ID**, Odze RD, Klimstra D, Paradis V, Rugge M, Schirmacher P, Washington KM, Carneiro F, Cree IA; WHO Classification of Tumours Editorial Board. The 2019 WHO classification of tumours of the digestive system. *Histopathology* 2020; **76**: 182-188 [PMID: 31433515 DOI: 10.1111/his.13975]

6 **Yeoh KG**, Tan P. Mapping the genomic diaspora of gastric cancer. *Nat Rev Cancer* 2022; **22**: 71-84 [PMID: 34702982 DOI: 10.1038/s41568-021-00412-7]

7 **Lee H**, Lee HH, Song KY, Park CH, Lee J. Negative Impact of Endoscopic Submucosal Dissection on Short-Term Surgical Outcomes of Subsequent Laparoscopic Distal Gastrectomy for Gastric Cancer. *Ann Surg Oncol* 2020; **27**: 313-320 [PMID: 31641951 DOI: 10.1245/s10434-019-07962-z]

8 **Tanabe S**, Ishido K, Matsumoto T, Kosaka T, Oda I, Suzuki H, Fujisaki J, Ono H, Kawata N, Oyama T, Takahashi A, Doyama H, Kobayashi M, Uedo N, Hamada K, Toyonaga T, Kawara F, Tanaka S, Yoshifuku Y. Long-term outcomes of endoscopic submucosal dissection for early gastric cancer: a multicenter collaborative study. *Gastric Cancer* 2017; **20**: 45-52 [PMID: 27807641 DOI: 10.1007/s10120-016-0664-7]

9 **Nishizawa T**, Yahagi N. Long-Term Outcomes of Using Endoscopic Submucosal Dissection to Treat Early Gastric Cancer. *Gut Liver* 2018; **12**: 119-124 [PMID: 28673068 DOI: 10.5009/gnl17095]

10 **Okada K**, Fujisaki J, Yoshida T, Ishikawa H, Suganuma T, Kasuga A, Omae M, Kubota M, Ishiyama A, Hirasawa T, Chino A, Inamori M, Yamamoto Y, Yamamoto N, Tsuchida T, Tamegai Y, Nakajima A, Hoshino E, Igarashi M. Long-term outcomes of endoscopic submucosal dissection for undifferentiated-type early gastric cancer. *Endoscopy* 2012; **44**: 122-127 [PMID: 22271022 DOI: 10.1055/s-0031-1291486]

11 **Wang Q**, Qi C, Min P, Wang Y, Ye F, Xia T, Zhang Y, Du J. MICAL2 contributes to gastric cancer cell migration *via* Cdc42-dependent activation of E-cadherin/β-catenin signaling pathway. *Cell Commun Signal* 2022; **20**: 136 [PMID: 36064550 DOI: 10.1186/s12964-022-00952-x]

12 **Sugano K**, Moss SF, Kuipers EJ. Gastric Intestinal Metaplasia: Real Culprit or Innocent Bystander as a Precancerous Condition for Gastric Cancer? *Gastroenterology* 2023; **165**: 1352-1366.e1 [PMID: 37652306 DOI: 10.1053/j.gastro.2023.08.028]

13 **Choi JY**, Jeon SW, Cho KB, Park KS, Kim ES, Park CK, Chung YJ, Kwon JG, Jung JT, Kim EY, Kim KO, Jang BI, Lee SH, Park JB, Yang CH. Non-curative endoscopic resection does not always lead to grave outcomes in submucosal invasive early gastric cancer. *Surg Endosc* 2015; **29**: 1842-1849 [PMID: 25294549 DOI: 10.1007/s00464-014-3874-2]

14 **Hu ZH**, Wang JT, Li RX, Wang GJ, Gao BL. Short-term efficacy of additional laparoscopic-assisted radical gastrectomy after non-curative endoscopic submucosal dissection for early gastric cancer. *Langenbecks Arch Surg* 2023; **408**: 354 [PMID: 37697006 DOI: 10.1007/s00423-023-03085-y]

15 **Kim ER**, Lee H, Min BH, Lee JH, Rhee PL, Kim JJ, Kim KM, Kim S. Effect of rescue surgery after non-curative endoscopic resection of early gastric cancer. *Br J Surg* 2015; **102**: 1394-1401 [PMID: 26313295 DOI: 10.1002/bjs.9873]

16 **Suzuki S**, Gotoda T, Hatta W, Oyama T, Kawata N, Takahashi A, Yoshifuku Y, Hoteya S, Nakagawa M, Hirano M, Esaki M, Matsuda M, Ohnita K, Yamanouchi K, Yoshida M, Dohi O, Takada J, Tanaka K, Yamada S, Tsuji T, Ito H, Hayashi Y, Shimosegawa T. Survival Benefit of Additional Surgery After Non-curative Endoscopic Submucosal Dissection for Early Gastric Cancer: A Propensity Score Matching Analysis. *Ann Surg Oncol* 2017; **24**: 3353-3360 [PMID: 28795364 DOI: 10.1245/s10434-017-6039-4]

17 **Suzuki H**, Oda I, Abe S, Sekiguchi M, Nonaka S, Yoshinaga S, Saito Y, Fukagawa T, Katai H. Clinical outcomes of early gastric cancer patients after noncurative endoscopic submucosal dissection in a large consecutive patient series. *Gastric Cancer* 2017; **20**: 679-689 [PMID: 27722825 DOI: 10.1007/s10120-016-0651-z]

18 **Choi MK**, Kim GH, Park DY, Song GA, Kim DU, Ryu DY, Lee BE, Cheong JH, Cho M. Long-term outcomes of endoscopic submucosal dissection for early gastric cancer: a single-center experience. *Surg Endosc* 2013; **27**: 4250-4258 [PMID: 23765426 DOI: 10.1007/s00464-013-3030-4]

19 **Kosaka T**, Endo M, Toya Y, Abiko Y, Kudara N, Inomata M, Chiba T, Takikawa Y, Suzuki K, Sugai T. Long-term outcomes of endoscopic submucosal dissection for early gastric cancer: a single-center retrospective study. *Dig Endosc* 2014; **26**: 183-191 [PMID: 23560494 DOI: 10.1111/den.12099]

20 **Nakamura K**, Honda K, Akahoshi K, Ihara E, Matsuzaka H, Sumida Y, Yoshimura D, Akiho H, Motomura Y, Iwasa T, Komori K, Chijiiwa Y, Harada N, Ochiai T, Oya M, Oda Y, Takayanagi R. Suitability of the expanded indication criteria for the treatment of early gastric cancer by endoscopic submucosal dissection: Japanese multicenter large-scale retrospective analysis of short- and long-term outcomes. *Scand J Gastroenterol* 2015; **50**: 413-422 [PMID: 25635364 DOI: 10.3109/00365521.2014.940377]

21 **Bhandari P**, Abdelrahim M, Alkandari AA, Galtieri PA, Spadaccini M, Groth S, Pilonis ND, Subhramaniam S, Kandiah K, Hossain E, Arndtz S, Bassett P, Siggens K, Htet H, Maselli R, Kaminski MF, Seewald S, Repici A. Predictors of long-term outcomes of endoscopic submucosal dissection of early gastric neoplasia in the West: a multicenter study. *Endoscopy* 2023; **55**: 898-906 [PMID: 37230471 DOI: 10.1055/a-2100-2258]

22 **Kim SG**, Park CM, Lee NR, Kim J, Lyu DH, Park SH, Choi IJ, Lee WS, Park SJ, Kim JJ, Kim JH, Lim CH, Cho JY, Kim GH, Lee YC, Jung HY, Lee JH, Chun HJ, Seol SY. Long-Term Clinical Outcomes of Endoscopic Submucosal Dissection in Patients with Early Gastric Cancer: A Prospective Multicenter Cohort Study. *Gut Liver* 2018; **12**: 402-410 [PMID: 29588436 DOI: 10.5009/gnl17414]

23 **Yang XY**, Wang C, Hong YP, Zhu TT, Qian LJ, Hu YB, Teng LH, Ding J. Knowledge, attitude, and practice of monitoring early gastric cancer after endoscopic submucosal dissection. *World J Gastrointest Surg* 2023; **15**: 1751-1760 [PMID: 37701694 DOI: 10.4240/wjgs.v15.i8.1751]

24 **Na JE**, Lee YC, Kim TJ, Lee H, Won HH, Min YW, Min BH, Lee JH, Rhee PL, Kim JJ. Utility of a deep learning model and a clinical model for predicting bleeding after endoscopic submucosal dissection in patients with early gastric cancer. *World J Gastroenterol* 2022; **28**: 2721-2732 [PMID: 35979158 DOI: 10.3748/wjg.v28.i24.2721]

25 **Oda I**, Saito D, Tada M, Iishi H, Tanabe S, Oyama T, Doi T, Otani Y, Fujisaki J, Ajioka Y, Hamada T, Inoue H, Gotoda T, Yoshida S. A multicenter retrospective study of endoscopic resection for early gastric cancer. *Gastric Cancer* 2006; **9**: 262-270 [PMID: 17235627 DOI: 10.1007/s10120-006-0389-0]

26 **Cao S**, Zou T, Sun Q, Liu T, Fan T, Yin Q, Fan X, Jiang J, Raymond D, Wang Y, Zhang B, Lv Y, Zhang X, Ling T, Zhuge Y, Wang L, Zou X, Xu G, Huang Q. Safety and long-term outcomes of early gastric cardiac cancer treated with endoscopic submucosal dissection in 499 Chinese patients. *Therap Adv Gastroenterol* 2020; **13**: 1756284820966929 [PMID: 33193812 DOI: 10.1177/1756284820966929]

27 **Ryu DG**, Choi CW, Kang DH, Kim HW, Park SB, Kim SJ, Nam HS. Pathologic outcomes of endoscopic submucosal dissection for gastric epithelial neoplasia. *Medicine (Baltimore)* 2018; **97**: e11802 [PMID: 30113468 DOI: 10.1097/MD.0000000000011802]

28 **Ryu DG**, Choi CW, Kang DH, Kim HW, Park SB, Kim SJ, Nam HS. Clinical outcomes of endoscopic submucosa dissection for high-grade dysplasia from endoscopic forceps biopsy. *Gastric Cancer* 2017; **20**: 671-678 [PMID: 27822683 DOI: 10.1007/s10120-016-0665-6]

29 **Kishino T**, Oyama T, Funakawa K, Ishii E, Yamazato T, Shibagaki K, Miike T, Tanuma T, Kuwayama Y, Takeuchi M, Kitamura Y. Multicenter prospective study on the histological diagnosis of gastric cancer by narrow band imaging-magnified endoscopy with and without acetic acid. *Endosc Int Open* 2019; **7**: E155-E163 [PMID: 30705947 DOI: 10.1055/a-0806-7275]

World Journal of Gastroenterology

Submit a Manuscript: https://www.f6publishing.com

World J Gastroenterol 2024 April 14; 30(14): 2006-2017

DOI: 10.3748/wjg.v30.i14.2006

ISSN 1007-9327 (print) ISSN 2219-2840 (online)

ORIGINAL ARTICLE

Observational Study

Preoperative albumin-bilirubin score and liver resection percentage determine postoperative liver regeneration after partial hepatectomy

Kazuhiro Takahashi, Masahiko Gosho, Yoshihiro Miyazaki, Hiromitsu Nakahashi, Osamu Shimomura, Kinji Furuya, Manami Doi, Yohei Owada, Koichi Ogawa, Yusuke Ohara, Yoshimasa Akashi, Tsuyoshi Enomoto, Shinji Hashimoto, Tatsuya Oda

Specialty type: Gastroenterology and hepatology

Provenance and peer review: Invited article; Externally peer reviewed.

Peer-review model: Single blind

Peer-review report's scientific quality classification

Grade A (Excellent): 0
Grade B (Very good): B
Grade C (Good): C
Grade D (Fair): 0
Grade E (Poor): 0

P-Reviewer: Elchaninov AV, Russia; Massimi M, Italy

Received: December 7, 2023
Peer-review started: December 7, 2023
First decision: January 24, 2024
Revised: February 5, 2024
Accepted: March 25, 2024
Article in press: March 25, 2024
Published online: April 14, 2024

Kazuhiro Takahashi, Yoshihiro Miyazaki, Hiromitsu Nakahashi, Osamu Shimomura, Kinji Furuya, Manami Doi, Yohei Owada, Koichi Ogawa, Yusuke Ohara, Yoshimasa Akashi, Tsuyoshi Enomoto, Shinji Hashimoto, Tatsuya Oda, Department of Gastrointestinal and Hepatobiliary-Pancreatic Surgery, University of Tsukuba, Tsukuba 3058-575, Ibaraki, Japan

Masahiko Gosho, Department of Biostatistics, University of Tsukuba, Tsukuba 3058-575, Ibaraki, Japan

Corresponding author: Kazuhiro Takahashi, FACS, MD, PhD, Assistant Professor, Surgeon, Department of Gastrointestinal and Hepatobiliary-Pancreatic Surgery, University of Tsukuba, Tennodai 1-1-1, Tsukuba 3058-575, Ibaraki, Japan. kazu1123@md.tsukuba.ac.jp

Abstract

BACKGROUND

The success of liver resection relies on the ability of the remnant liver to regenerate. Most of the knowledge regarding the pathophysiological basis of liver regeneration comes from rodent studies, and data on humans are scarce. Additionally, there is limited knowledge about the preoperative factors that influence postoperative regeneration.

AIM

To quantify postoperative remnant liver volume by the latest volumetric software and investigate perioperative factors that affect posthepatectomy liver regeneration.

METHODS

A total of 268 patients who received partial hepatectomy were enrolled. Patients were grouped into right hepatectomy/trisegmentectomy (RH/Tri), left hepatectomy (LH), segmentectomy (Seg), and subsegmentectomy/nonanatomical hepatectomy (Sub/Non) groups. The regeneration index (RI) and late regeneration rate were defined as (postoperative liver volume)/[total functional liver volume (TFLV)] × 100 and (RI at 6-months - RI at 3-months)/RI at 6-months, respectively. The lower 25th percentile of RI and the higher 25th percentile of late regeneration rate in each group were defined as "low regeneration" and "delayed regeneration". "Restoration to the original size" was defined as regeneration of

the liver volume by more than 90% of the TFLV at 12 months postsurgery.

RESULTS

The numbers of patients in the RH/Tri, LH, Seg, and Sub/Non groups were 41, 53, 99 and 75, respectively. The RI plateaued at 3 months in the LH, Seg, and Sub/Non groups, whereas the RI increased until 12 months in the RH/Tri group. According to our multivariate analysis, the preoperative albumin-bilirubin (ALBI) score was an independent factor for low regeneration at 3 months [odds ratio (OR) 95%CI = 2.80 (1.17-6.69), P = 0.02; per 1.0 up] and 12 months [OR = 2.27 (1.01-5.09), P = 0.04; per 1.0 up]. Multivariate analysis revealed that only liver resection percentage [OR = 1.03 (1.00-1.05), P = 0.04] was associated with delayed regeneration. Furthermore, multivariate analysis demonstrated that the preoperative ALBI score [OR = 2.63 (1.00-1.05), P = 0.02; per 1.0 up] and liver resection percentage [OR = 1.02 (1.00-1.05), P = 0.04; per 1.0 up] were found to be independent risk factors associated with volume restoration failure.

CONCLUSION

Liver regeneration posthepatectomy was determined by the resection percentage and preoperative ALBI score. This knowledge helps surgeons decide the timing and type of rehepatectomy for recurrent cases.

Key Words: Liver regeneration; Albumin-bilirubin score; Liver resection percentage; Partial hepatectomy; Human; Regeneration index

Core Tip: Insights into posthepatectomy liver regeneration in humans are limited. We quantified liver volumes using the latest volumetric software and investigated perioperative factors that affect posthepatectomy liver regeneration. It was revealed that liver regeneration continues after 3 months of hepatectomy with more than one-fourth of the liver resection and decline in preoperative liver function, reflected by the albumin-bilirubin (ALBI) score, is associated with decreased regeneration. Furthermore, restoring to the original volume depended on the combination of the preoperative ALBI score and liver resection percentage. With this knowledge, surgeons can select an appropriate hepatectomy type with rehepatectomy in mind after intrahepatic recurrence.

Citation: Takahashi K, Gosho M, Miyazaki Y, Nakahashi H, Shimomura O, Furuya K, Doi M, Owada Y, Ogawa K, Ohara Y, Akashi Y, Enomoto T, Hashimoto S, Oda T. Preoperative albumin-bilirubin score and liver resection percentage determine postoperative liver regeneration after partial hepatectomy. *World J Gastroenterol* 2024; 30(14): 2006-2017
URL: https://www.wjgnet.com/1007-9327/full/v30/i14/2006.htm
DOI: https://dx.doi.org/10.3748/wjg.v30.i14.2006

INTRODUCTION

Liver regeneration after partial hepatectomy proceeds through the action of several cells that compose the liver, including hepatocytes, bile duct epithelial cells, hepatic sinusoidal endothelial cells, Kupffer cells, and hepatic stellate cells[1]. Hepatocytes are normally dormant but undergo one or two rounds of cell division after hepatectomy. The onset of hepatocyte cell division varies among animal species, with that of rats beginning 24 h after hepatectomy and that of humans and mice beginning 48 h after hepatectomy. Growth factors and cytokines such as hepatocyte growth factor (HGF), tumor necrosis factor-α (TNF-α), interleukin-6 (IL-6), transforming growth factor-α, and epidermal growth factor are involved in this process[1]. Both of these growth factors and cytokines activate downstream growth signaling pathways, ultimately leading to the transition from quiescent cells in G0 phase to G1/S phase and initiation of the cell cycle. In rodents, the remnant liver after 70% partial hepatectomy returns to a size of 100% in 7 to 10 d, and in humans, the liver mass is believed to be completely restored in 3 to 6 months[1-3]. Even small resections with a resection percentage of 10% or less are followed by eventual restoration of the liver to its full size[3].

Liver regeneration is an important topic not only for basic science but also for clinicians because liver regeneration failure could cause serious complications that could lead to patient mortality. Although this topic has been well described, most related studies have been conducted in animal models, and there are limited data on this topic in humans [1]. Furthermore, most of those previous reports focused on liver regeneration only after major hepatectomy[4,5]; few reports provided insights into liver regeneration after minor hepatectomy, and few studies have compared regeneration between hepatectomy types. Moreover, the volumetric assessments in most of the previous studies were performed before the development of computer-based volumetry or used prototype volumetry before the early 2000s. In this study, we quantified postoperative remnant liver volumes using the latest volumetric software in patients who underwent partial hepatectomy and had various backgrounds. We observed postoperative parenchymal regeneration according to hepatectomy type and identified perioperative factors that affect postoperative liver regeneration.

MATERIALS AND METHODS

Study population and data collection

Between January 2006 and October 2022, 762 patients with hepatocellular carcinoma (HCC), cholangiocellular carcinoma (CCC), combined HCC and CCC (CHC), colorectal metastasis, or other diseases underwent partial hepatectomy at the University of Tsukuba Hospital (Tsukuba, Japan). Patient records were identified by an administrative database. Patients who (1) were less than 14 years old; (2) underwent partial hepatectomy with concomitant gastrointestinal surgical procedures, biliary reconstruction, or splenectomy; (3) underwent partial hepatectomy with a liver resection percentage of less than 10%; (4) had macroscopic evidence of noncurative resection; (5) had incomplete records, including postoperative computed tomography (CT) data; and (6) had recurrence were excluded. All the data for the current study were collected in accordance with the University of Tsukuba Hospital Institutional Review Board.

Definition of major hepatectomy and minor hepatectomy, posthepatectomy liver failure, and liver fibrosis

Major hepatectomy was defined as right trisegmentectomy, left trisegmentectomy, right hepatectomy or left hepatectomy (LH), while minor hepatectomy was defined as segmentectomy (Seg), subsegmentectomy, or nonanatomical hepatectomy, according to the Tokyo 2020 terminology of the liver[6]. Posthepatectomy liver failure (PHLF) was defined according to the International Study Group of Liver Surgery criteria and was based on an increased international normalized ratio and concomitant hyperbilirubinemia on or after postoperative Day 5[7]. Liver fibrosis was stratified into stages 0 to 4 using the METAVIR scoring system (F0: No fibrosis, F1: Portal fibrosis, F2: Periportal fibrosis, F3: Bridging fibrosis, F4: Cirrhosis).

Liver volumetry was used to calculate the liver resection percentage, regeneration index, remnant liver growth rate and late regeneration rate

In 2006, an IDT-16 multidetector row CT scanner (Philips, Netherlands) was used to obtain images with a slice thickness of 5 mm. From 2007 to 2013, a Brilliance 64 multidetector row CT scanner (Philips, Netherlands) was used to obtain images with slice thicknesses of 2-5 mm. From 2014 to the present, an iCT 128 multidetector row CT scanner (Philips, Netherlands) was used to obtain 1-2 mm image slices. Medical image analysis software was used for volumetry (Synapse Vincent® version 6.7; Fujifilm Global, Tokyo, Japan). Volumetric values were obtained by the inherent software volume rendering algorithm. Accurate simulation of liver resection was performed postoperatively by manually tracing the resected border on CT images based on intraoperative images of the resected liver plane, resected specimen, and medical records. The total liver volume (TLV), resected liver volume (RLV), tumor volume (Tuv), and postoperative liver volume were automatically measured. Postoperative liver volume was measured at 3 months (Supplementary Figure 1), 6 months, and 12 months after surgery. The total functional liver volume (TFLV) was calculated by subtracting Tuv from the TLV, and the RLV was calculated by subtracting Tuv from the postoperative reconstructed resected specimen volume. The liver resection percentage (%), regeneration index (RI) (%), remnant liver growth rate (fold) and late regeneration rate (fold) were calculated according to the following formulas.

Liver resection percentage (%) = [postoperative reconstructed resected specimen volume (mL)-Tuv (mL)]/[TFLV (mL)] × 100.

RI (%) = [postoperative liver volume (mL)]/[TFLV (mL)] × 100.

Remnant liver growth rate (fold) = [postoperative remnant liver volume (mL)]/[TFLV (mL) - RLV (mL)].

Late regeneration rate (fold) = [RI at 6 months (%) - RI at 3 months (%)]/[RI at 6 months (%)].

Definitions of "low regeneration", "delayed regeneration" and "restoration to the original volume"

The patients were classified into the "low regeneration" group based on the RI at 3 months and 12 months, which was < the 25th percentile. "Delayed liver regeneration" was defined as a late regeneration rate ≥ the 25th percentile. "Restoration to the original volume" was defined as regeneration of the remnant liver to more than 90% of the TFLV.

Statistical analysis

Categorical variables were compared using the chi-square test or Fisher's exact test. Continuous variables are expressed as the median, minimum, or maximum. Pearson's correlation coefficients were calculated, and unpaired *t* tests were used to compare two groups. Comparisons among more than three groups were performed using one-way analysis of variance. Significant differences were examined using the Bonferroni-Dunn multiple comparison post hoc test. Low regeneration, delayed regeneration and volume restoration failure were analyzed using univariate and multivariate logistic regression models. Receiver operating characteristic (ROC) analysis was also conducted using the constructed multivariate logistic model. Independent predictors in the multivariate model were selected based on the results of the univariate analysis ($P < 0.10$). $P < 0.05$ was considered to indicate statistical significance. All the statistical analyses were performed using SPSS 29.0 (SPSS, Inc., Chicago, IL, United States).

RESULTS

Demographics

A total of 268 patients who underwent partial hepatectomy were included. Patients were classified according to the hepatectomy type: Right hepatectomy and trisegmentectomy (RH/Tri) group, LH group, Seg group, and subseg-

mentectomy and nonanatomical hepatectomy (Sub/Non) group. The numbers of patients in the RH/Tri, LH, Seg, and Sub/Non groups were 41, 53, 99 and 75, respectively (Table 1). All patients demonstrated similar baseline characteristics except for body mass index (BMI) (kg/m^2), background disease, hepatitis C virus positivity, liver resection percentage (%), heavy alcohol history and preoperative platelet count (μL) (Table 1).

Regarding postoperative outcomes, there were significant differences in operation time (min), total Pringle maneuver time (min), and PHLF grade B/C occurrence rate (%) among the groups. In particular, the incidence rate of PHLF was significantly greater in the RH/Tri group (Table 1).

Comparison of the RI, remnant liver growth rate and postoperative ALBI score at 3, 6 and 12 months among the RH/Tri, LH, Seg, and Sub/Non groups

The RI plateaued at 3 months in the LH, Seg and Sub/Non groups, whereas the RI continued to increase until 12 months in the RH/Tri group (Figure 1A). A comparison of the RIs among these four groups at 3 months showed that the RIs were significantly lower in the RH/Tri group than in the other groups (77% *vs* 85% *vs* 90% *vs* 92%, Figure 1B). However, there was no difference in the RI between the RH/Tri group and the LH group (85% and 87%, $P = 0.12$) at 12 months; both of these values are below the criterion for restoring the original volume. On the other hand, the RIs in the RH/Tri group were significantly lower than those in the Seg group and the Sub/Non group (92% and 93%, Figure 1B), both of which met the criterion of restoring the original volume.

The remnant liver growth rate plateaued at 3 months in the LH, Seg and Sub/Non groups, whereas the remnant liver growth rate continued to increase until 12 months in the RH/Tri group (Figure 2).

Although the postoperative ALBI scores in the Seg group tended to increase during the early period postsurgery, the postoperative ALBI scores in general were not significantly different at any time point in either group at 3, 6 or 12 months posthepatectomy (Supplementary Figure 2A). There was no difference in the postoperative ALBI score among the four groups at 3 or 12 months (Supplementary Figure 2B).

Univariate and multivariate analyses to identify risk factors for low regeneration at 3 months and 12 months

Univariate analysis revealed that a background disease of CCC or CHC (compared with that of HCC), a preoperative ALBI score (per 1.0 up), rehepatectomy and a postoperative complication according to the Clavien-Dindo (CD) classification of grade 3 or higher were associated with low regeneration at 3 months (Table 2). Multivariate analysis demonstrated that the preoperative ALBI score [per 1.0 up, odds ratio (OR) 95%CI = 2.80 (1.17-6.69), $P = 0.02$] and a postoperative complication CD classification of grade 3 or higher [OR = 0.29 (0.10-0.82), $P = 0.02$] were found to be independent risk factors for low regeneration at 3 months. ROC analysis demonstrated an area under the ROC curve (AUROC) of 0.60 for the ALBI score, which was the highest among the representative liver function parameters, Child-Pugh score, model for end-stage liver disease (MELD) score, MELD-Na score, and indocyanine green 15-min rate (0.53, 0.56, 0.58, 0.55, respectively), and its cutoff value was -2.69.

Univariate analysis revealed that a preoperative platelet count < 100 × 10^3/μL and a preoperative ALBI score (per 1.0 up) were associated with low regeneration at 12 months (Table 2). Multivariate analysis demonstrated that both a preoperative platelet count < 100 × 10^3/μL [OR = 5.01 (1.14-21.95), $P = 0.03$} and a preoperative ALBI score [per 1.0 up, OR = 2.27 (1.01-5.09), $P = 0.04$] were found to be independent risk factors for low regeneration at 12 months. ROC analysis demonstrated an AUROC of 0.57 for the ALBI score, and its cutoff value was -2.73.

Changes in the RI with/without severe liver fibrosis

Pathologically, F3 and F4 were classified into the severe fibrosis group. In the RH/Tri and LH groups, patients in the severe fibrosis group tended to have delayed liver regeneration, but the final liver volume at 12 months was not different. On the other hand, in the Seg and Sub/Non groups, the RI did not significantly differ between the severe fibrosis group and the nonsevere liver fibrosis group at any time point (Supplementary Figure 3). The preoperative ALBI score and F stage were not correlated ($r = 0.08$, $P = 0.22$).

Univariate and multivariate analyses were used to identify risk factors for delayed regeneration and failure of the restoration to the original volume

Univariate analysis revealed that only the liver resection percentage [OR = 1.03 (1.00-1.05), $P = 0.04$] was associated with delayed regeneration (Table 3). ROC analysis demonstrated an AUROC of 0.61 for the liver resection percentage, and its cutoff value was 26%.

Univariate analysis revealed that other background diseases (compared with HCC), the presence of diabetes mellitus, a preoperative platelet count < 100 × 10^3/μL, a preoperative ALBI score (per 1.0 up), liver resection percentage, and postoperative complication CD classification of grade 3 or higher were associated with volume restoration failure. The multivariate analysis demonstrated that the preoperative ALBI score [per 1.0 up, OR = 2.63 (1.15-6.04), $P = 0.02$] and the liver resection percentage [OR = 1.02 (1.00-1.05), $P = 0.04$] were found to be independent risk factors associated with volume restoration failure.

Prediction of volume restoration failure by the combination of the preoperative ALBI score and liver resection percentage

A heatmap for predicting the probability of volume restoration failure was constructed by combining the preoperative ALBI score and liver resection percentage (Figure 3). The gradient shows the risk level: Blue indicates a low risk of volume restoration failure (less than 10%), whereas red indicates a high risk of volume restoration failure (higher than

Table 1 Demographics, *n* (%)

	RH/Tri group (*n* = 41)	LH group (*n* = 53)	Seg group (*n* = 99)	Sub/Non group (*n* = 75)	*P* value
Baseline characteristics					
Age	68 (16-80)	69 (14-86)	68 (46-83)	70 (52-90)	0.06
Sex, male, yes	29 (71)	33 (62)	73 (74)	58 (77)	0.29
BMI (kg/m^2)	21.8 (15.4-31.3)	22.3 (15.2-29.4)	230 (15.5-32.8)	23.4 (17.8-35.5)	0.009
Background disease					
HCC	21 (51)	14 (26)	63 (64)	56 (75)	< 0.001
CCC & CHC	4 (10)	19 (36)	9 (9)	8 (11)	-
Colorectal liver metastasis	10 (24)	6 (11)	16 (16)	11 (15)	-
Others	6 (15)	14 (26)	11 (11)	0 (0)	-
HCV, yes	6 (15)	9 (17)	26 (26)	29 (39)	0.01
Liver resection percentage	52 (21-71)	32 (13-49)	27 (10-56)	15 (10-32)	< 0.001
Diabetes mellitus, yes	13 (32)	16 (30)	34 (34)	33 (44)	0.36
Renal complication	3 (7)	3 (6)	6 (6)	6 (8)	0.94
Heavy alcoholic[1]	15 (37)	9 (17)	39 (39)	32 ()	0.03
ICG 15 min	10.7 (0.1-81.1)	9.0 (1.4-66.4)	10.1 (1.3-80.0)	11.5 (2.8-33.4)	0.65
Preoperative ALBI score	-2.56 (-3.46 to -1.40)	-2.73 (-3.50 to -0.69)	-2.85 (-3.75 to -1.51)	-2.78 (-3.38 to -1.82)	0.07
Preoperative platelet count (/uL)	205 (95-562)	198 (78-504)	186 (61-542)	182 (91-396)	0.02
Liver cirrhosis (F4), yes	4 (10)	2 (4)	18 (18)	9 (12)	0.08
Laparoscopic hepatectomy	3 (7)	2 (38)	13 (13)	7 (9)	0.28
Re-hepatectomy	3 (7)	4 (8)	5 (5)	7 (9)	0.74
Preoperative Chemotherapy	10 (24)	9 (17)	15 (15)	5 (7)	0.06
Postoperative outcomes					
Operation time (min)	383 (218-644)	354 (183-629)	388 (151-742)	341 (153-584)	0.008
Intraoperative blood loss (mL)	680 (110-13360)	378 (68-3660)	525 (0-32150)	470 (0-1894)	0.25
RBC transfusion	6 (15)	3 (6)	8 (8)	3 (4)	0.19
Total Pringle time (min)	56 (0-179)	45 (0-131)	75 (0-202)	78 (0-167)	< 0.001
Posthepatectomy liver failure grade B/C	10 (24)	3 (6)	7 (7)	3 (4)	0.001
Complication CD grade ≥ 3	9 (22)	10 (19)	22 (22)	12 (16)	0.75
Length of Hospital stay (d)	16 (7-41)	11 (5-54)	11 (6-40)	11 (6-167)	0.46

[1]Daily alcohol consumption 30 g/d or higher.

RH/Tri: Right hepatectomy/Trisegmentectomy; LH: Left hepatectomy; Seg: Segmentectomy; Sub/Non: Subsegmentectomy and nonanatomical hepatectomy; BMI: Body mass index; HCC: Hepatocellular carcinoma; CCC: Cholangiocellular carcinoma; CHC: Combined hepatocellular carcinoma and cholangiocellular carcinoma; HCV: Hepatitis C virus; ALBI: Albumin-bilirubin; ICG: Indocyanine green; RBC: Red blood cell; CD: Clavien-Dindo.

90%). As the ALBI score and liver resection percentage increased, the risk of volume restoration failure increased.

DISCUSSION

The novelty of this study is that liver regeneration after partial hepatectomy was determined by the preoperative liver function reserve reflected by the ALBI score, and prolonged regenerative activity was dependent on the liver resection percentage. It was also acknowledged that although the remnant liver volume after minor hepatectomy could return to its initial size, the residual liver volume after major resection does not necessarily return to its original volume. Furthermore,

Table 2 Risk factors for low regeneration at 3-months and 12-months posthepatectomy

	3-months (*n* = 187)				12-months (*n* = 192)			
	Univariate OR (95%CI)	*P* value	Multivariate OR (95%CI)	*P* value	Univariate OR (95%CI)	*P* value	Multivariate OR (95%CI)	*P* value
Age > 75, yes	0.69 (0.30-1.56)	0.37	-	-	0.48 (0.19-1.24)	0.13	-	-
Sex, male, yes	1.40 (0.66-32.94)	0.38	-	-	0.79 (0.39-1.62)	0.79	-	-
BMI >28 kg/m^2, yes	0.19 (0.02-1.44)	0.11	-	-	0.42 (0.09-1.94)	0.42	-	-
Background, HCC	-	Ref.			-	Ref.		
CCC & CHC	0.30 (0.09-1.08)	0.07	0.31 (0.08-1.17)	0.08	0.81 (0.31-2.07)	0.65	-	-
Colorectal liver metastasis	0.98 (0.41-2.38)	0.96	0.88 (0.35-2.21)	0.79	0.88 (0.34-2.27)	0.79	-	-
Others	0.76 (0.31-2.37)	0.76	0.93 (0.30-2.88)	0.90	0.97 (0.35-2.71)	0.96	-	-
HCV positive, yes	0.63 (0.29-1.38)	0.25	-	-	1.18 (0.58-2.39)	0.65		
Diabetes mellitus, yes	0.93 (0.47-1.83)	0.84	-	-	0.77 (0.39-1.52)	0.45	-	-
Renal complication, yes	2.50 (0.73-8.60)	0.15	-	-	0.51 (0.11-2.37)	0.39	-	-
Heavy alcoholic, yes	1.10 (0.56-2.18)	0.77	-	-	0.86 (0.44-1.69)	0.66	-	-
Preoperative platelet count < 100 × 10^3/L, yes	2.19 (0.47-10.13)	0.32			5.30 (1.22-23.09)	0.03	5.01 (1.14-21.95)	0.03
Preoperative ALBI score (per 1.0 up)	2.85 (1.21-6.71)	0.02	2.80 (1.17-6.69)	0.02	2.33 (1.05-5.18)	0.04	2.27 (1.01-5.09)	0.04
ICG 15 minutes rate (per 1.0 up)	0.97 (0.93-1.01)	0.15	-	-	1.00 (0.97-1.04)	0.92	-	-
Liver cirrhosis (F4), yes	1.22 (0.47-23.14)	0.69	-	-	1.42 (0.51-3.97)	0.51	-	-
Preoperative chemotherapy, yes	0.66 (0.25-1.73)	0.40	-	-	0.84 (0.32-2.24)	0.73	-	-
Re-hepatectomy, yes	2.65 (0.84-8.33)	0.09	2.81 (0.84-9.47)	0.09	0.28 (0.04-2.25)	0.23	-	-
Liver resection percentage (per 1.0% up)	1.01 (0.99-1.04)	0.22	-	-	1.01 (0.99-1.04)	0.24	-	-
Intraoperative blood loss > 1000mL, yes	1.73 (0.83-3.62)	0.14	-	-	1.04 (0.47-2.34)	0.92	-	-
RBC transfusion, yes	0.75 (0.20-2.82)	0.67	-	-	0.81 (0.22-3.02)	0.75	-	-
Pringle time > 90 min, yes	1.07 (0.49-2.34)	0.86	-	-	1.09 (0.51-2.31)	0.83	-	-
Posthepatectomy liver failure grade B/C, yes	0.58 (0.16-2.10)	0.41	-	-	0.72 (0.21-2.93)	0.72	-	-
Postoperative complication CD grade ≥ 3, yes	0.31 (0.11-0.84)	0.02	0.29 (0.10-0.82)	0.02	1.79 (0.83-3.87)	0.14	-	-

OR: Odds ratio; BMI: Body mass index; HCC: Hepatocellular carcinoma; CCC: Cholangiocellular carcinoma; CHC: Combined hepatocellular carcinoma and cholangiocellular carcinoma; HCV: Hepatitis C virus; ALBI: Albumin-bilirubin; ICG: Indocyanine green; RBC: Red blood cell; CD: Clavien-Dindo.

the degree to which the original volume was restored after hepatectomy was determined by the preoperative ALBI score and the liver resection percentage. This knowledge, along with our heatmap, can aid surgeons in deciding the timing and type of hepatectomy after intrahepatic recurrence.

Liver resection success relies on the ability of the remnant liver to regenerate. Most of the knowledge regarding the pathophysiological basis of liver regeneration comes from rodent studies, and data on humans are scarce. Among the limited reports on humans, early studies in the 1970s and 1980s revealed that mitotic activity occurred 3 d after partial hepatectomy, and cellular proliferation continued for several weeks[8]. The liver remnant returned to its original size in approximately 3 to 6 months. At that time, the liver volume was calculated by multiplying the liver area measured by hand using tracing paper and a CT width greater than 1 cm[8]. This could cause significant mismatches in the extraction results, depending on the examiners. On the other hand, studies from the 1990s to the early 2000s reported different results based on the experience in donor hepatectomy. Using prototype CT-volumetric software, they reported that the volume of the normal liver after major hepatectomy increased up to 70%-80% in 6 months and up to 85%-90% in 12 months; however, the liver did not reach its initial volume[9-11]. In our study, we used the latest CT-volumetric software,

Table 3 Risk factors for delayed regeneration and failure for restoration of the original volume

	Delayed regeneration (total *n* = 153)				Volume restoration failure (total *n* = 191)			
	Univariate OR (95%CI)	*P* value	Multivariate OR (95%CI)	*P* value	Univariate OR (95%CI)	*P* value	Multivariate OR (95%CI)	*P* value
Age > 75, yes	0.67 (0.27-1.68)	0.45	-	-	0.94 (0.46-1.94)	0.88	-	-
Gender, male, yes	1.14 (0.48-2.67)	0.77	-	-	0.76 (0.40-1.45)	0.41	-	-
BMI > 28 kg/m^2, yes	0.22 (0.03-1.74)	0.15	-	-	0.44 (0.14-1.46)	0.18	-	-
Background, HCC	-	Ref.			-	Ref.		
CCC & CHC	0.49 (0.13-1.82)	0.29	-	-	1.64 (0.73-3.65)	0.23	0.40 (0.15-1.11)	0.08
Colorectal liver metastasis	1.83 (0.73-4.56)	0.19	-	-	0.88 (0.34-1.90)	0.81	0.71 (0.22-2.26)	0.56
Others	1.10 (0.27-4.42)	0.90	-	-	2.39 (0.95-6.00)	0.07	0.28 (0.08-0.97)	0.44
HCV positive, yes	0.61 (0.26-1.47)	0.27	-	-	0.70 (0.37-1.34)	0.28	-	-
Diabetes mellitus, yes	0.64 (0.30-1.39)	0.26	-	-	0.55 (0.30-1.00)	0.05	0.69 (0.36-1.35)	0.28
Renal complication, yes	0.89 (0.18-4.48)	0.88	-	-	1.15 (0.37-3.56)	0.81	-	-
Heavy alcoholic, yes	0.86 (0.39-1.88)	0.71	-	-	0.84 (0.46-1.53)	0.56	-	-
Preoperative platelet count < 100 × 10^3/uL, yes	1.60 (0.28-9.11)	0.60	-	-	4.17 (0.82-21.21)	0.09	4.34 (0.81-23.40)	0.09
Preoperative ALBI score (per 1.0 up)	1.13 (0.46-2.81)	0.79	-	-	2.76 (1.27-5.97)	0.01	2.63 (1.15-6.04)	0.02
ICG 15 min rate (per 1.0 up)	1.00 (0.97-1.04)	0.99	-	-	1.00 (0.98-1.04)	0.58	-	-
Liver cirrhosis (F4), yes	1.94 (0.70-5.38)	0.20	-	-	1.22 (0.47-3.15)	0.69	-	-
Preoperative chemotherapy, yes	2.01 (0.80-5.03)	0.14	-	-	0.80 (0.34-1.87)	0.60	-	-
Re-hepatectomy, yes	1.67 (0.40-7.03)	0.49	-	-	0.74 (0.21-2.62)	0.64	-	-
Liver resection percentage (per 1.0% up)	1.03 (1.00-1.05)	0.04	1.03 (1.00-1.05)	0.04	1.03 (1.01-1.05)	0.008	1.02 (1.00-1.05)	0.04
Intraoperative blood loss > 1000 mL, yes	1.35 (0.58-3.15)	0.49	-	-	1.41 (0.69-2.86)	0.34	-	-
RBC transfusion, yes	0.55 (0.12-2.58)	0.58	-	-	1.04 (0.35-3.12)	0.95	-	-
Pringle time > 90 min, yes	1.82 (0.80-4.14)	0.16	-	-	0.91 (0.46-1.81)	0.78	-	-
Posthepatectomy liver failure grade B/C, yes	0.95 (0.24-3.60)	0.92	-	-	1.83 (0.61-5.50)	0.28	-	-
Postoperative complication CD grade ≥ 3, yes	0.54 (0.19-1.53)	0.24	-	-	1.97 (0.95-4.07)	0.07	1.80 (0.83-3.91)	0.14

OR: Odds ratio; BMI: Body mass index; HCC: Hepatocellular carcinoma; CCC: Cholangiocellular carcinoma; CHC: Combined hepatocellular carcinoma and cholangiocellular carcinoma; HCV: Hepatitis C virus; ALBI: Albumin-bilirubin; ICG: Indocyanine green; RBC: Red blood cell; CD: Clavien-Dindo.

Synapse Vincent version 6.7, to measure postoperative remnant liver volume. This software calculates liver volume based on a high-speed and precise image-processing algorithm that uses an image processing method[12]. Using two different regeneration parameters (the RI and remnant liver growth rate), the remnant liver continued to regenerate until 12 months after right hepatectomy/trisegmentectomy. On the other hand, regeneration stopped less than 3 months after LH and minor hepatectomy. The remnant liver volume 12 months after RH/Tri increased but was not significantly different from that after LH and did not return to the original volume, while the liver volume after minor hepatectomy returned to almost the initial size. Regardless of the type of hepatectomy, postoperative liver function at 3, 6, and 12 months did not differ from preoperative liver function. In addition, a prolonged regenerative response was related to the amount of liver removed, especially for patients who underwent more than one-fourth resection. The difference in these regenerative reactions depends on the hepatectomy type, and it has been reported that the regenerative response of hepatocytes is altered by different resection rates[13,14]. In animal studies, hepatocytes removed *via* 1/3 hepatectomy were less proliferatively active and quieter and had a slower response than hepatocytes removed *via* 2/3 hepatectomy, and the regenerative response was very minimal when the liver resection rate was less than 10%[14,15]. It has also been reported that the number of hepatocytes involved in regeneration and DNA replication decreases as the resection rate decreases[16].

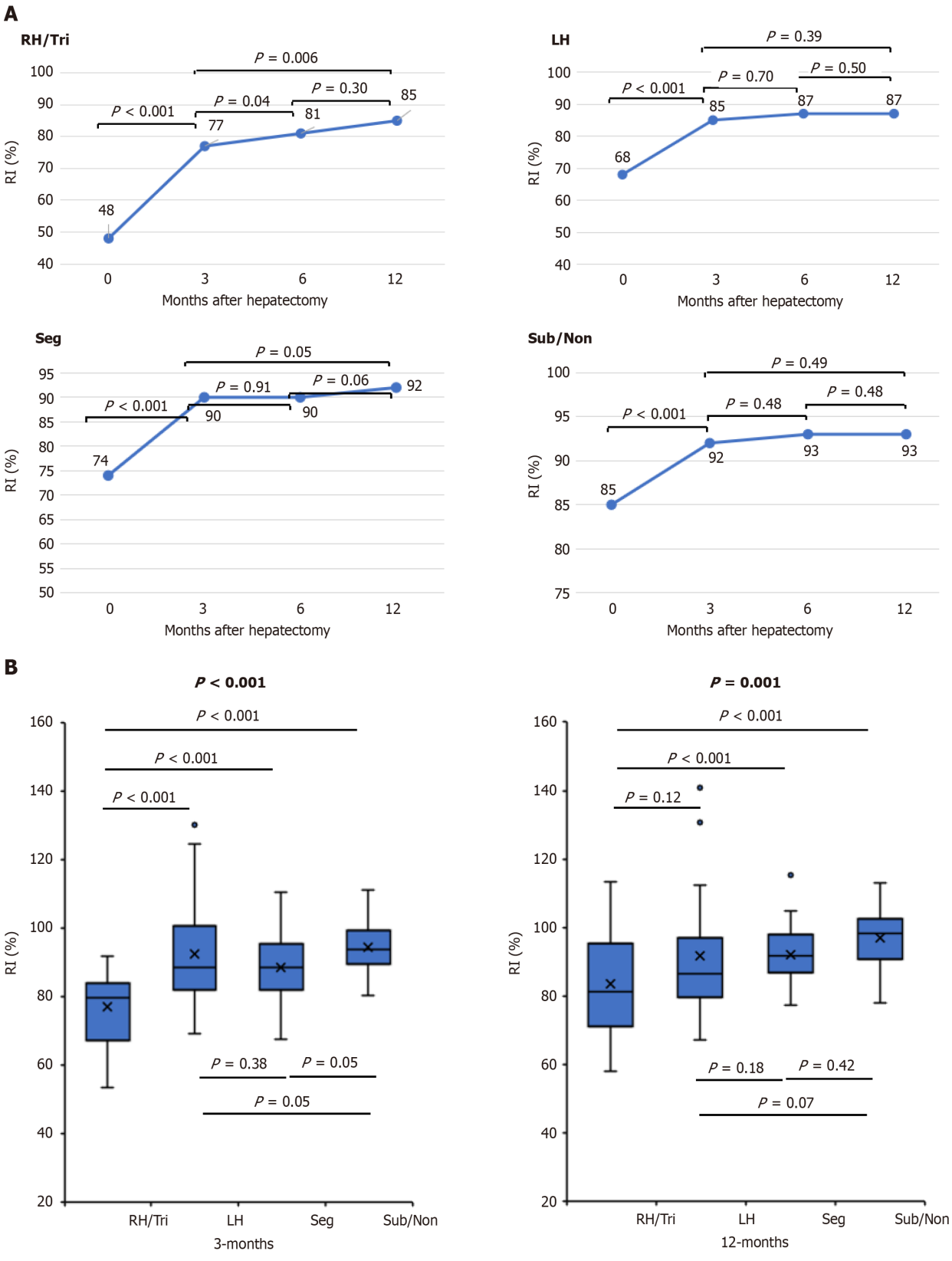

Figure 1 Comparison of the regeneration indices at 3, 6 and 12 months among the right hepatectomy and trisegmentectomy, left hepatectomy, segmentectomy, and subsegmentectomy and nonanatomical hepatectomy groups. A: Chronological changes in the regeneration index (RI) at 3, 6 and 12 months posthepatectomy, classified by hepatectomy type; B: Comparison of the RIs between patients who underwent hepatectomy at 3 months and 12 months. RH/Tri: Right hepatectomy and trisegmentectomy; LH: Left hepatectomy; Seg: Segmentectomy; Sub/Non: Subsegmentectomy and nonanatomical hepatectomy.

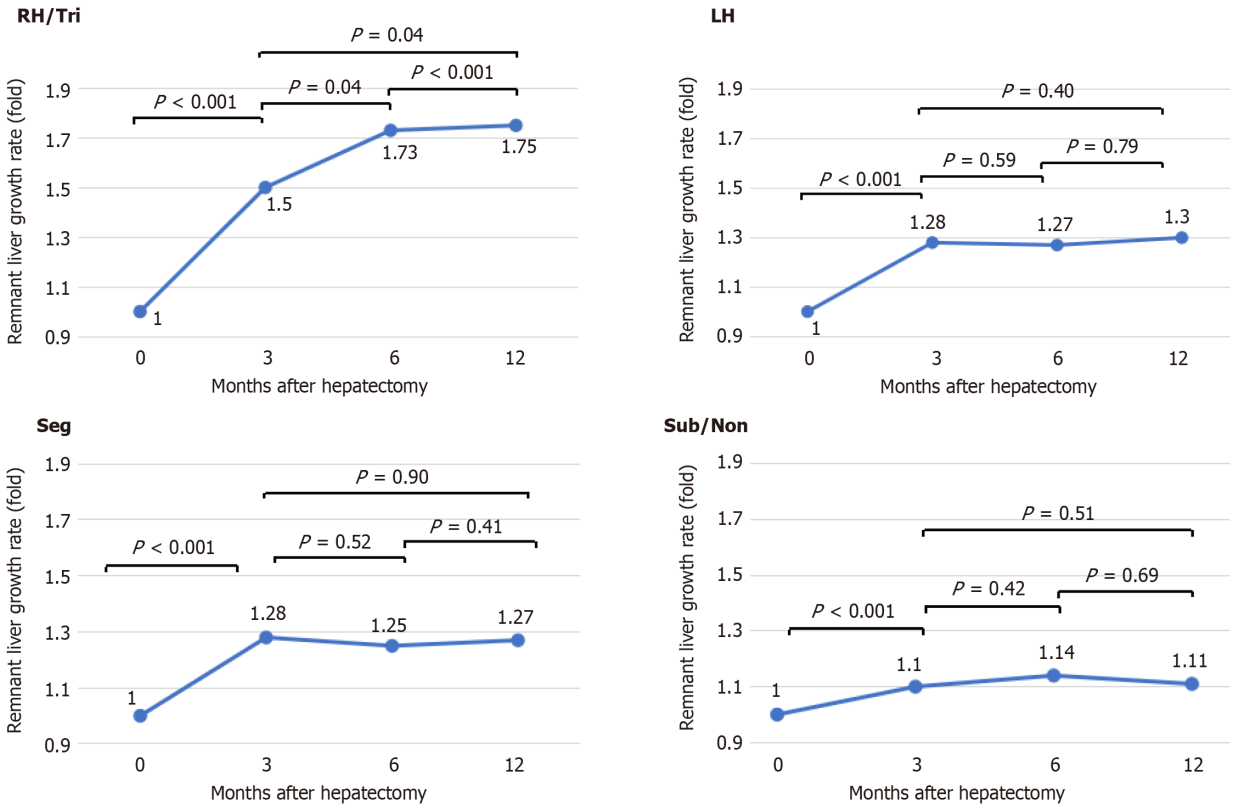

Figure 2 Comparison of the remnant liver growth rate at 3, 6 and 12 months among the right hepatectomy and trisegmentectomy, left hepatectomy, segmentectomy, and subsegmentectomy and nonanatomical hepatectomy groups. The remnant liver growth rate plateaued at 3 months in the left hepatectomy, segmentectomy, and subsegmentectomy and nonanatomical hepatectomy groups, whereas it continued to increase until 12 months in the right hepatectomy and trisegmentectomy group. RH/Tri: Right hepatectomy and trisegmentectomy; LH: Left hepatectomy; Seg: Segmentectomy; Sub/Non: Subsegmentectomy and nonanatomical hepatectomy.

Mitchell *et al*[14] reported that the G1/S transition in hepatocytes was disrupted by low expression of heparin-binding epidermal growth factor-like growth factor in rats with reduced liver resection, which was supported by human studies [14,17]. Recent human reports using volumetry have indicated an increase in the rate of regeneration and prolongation of the regeneration period as the liver resection rate increases[18]. The authors cite the relationship between resection rate and the number of portal processing vessels, explaining that the relative increase in portal blood flow to the remaining liver parenchyma caused hepatocytes to become more active and took a longer time to regenerate sufficient parenchyma to maintain hemostasis. On the other hand, similar to our results, these authors reported that the liver regeneration rate at 12 months decreased with increasing resection rate, but the reason for this was not clear. We further established a heatmap to predict volume restoration failure by combining the preoperative ALBI score and liver resection percentage. With this knowledge and the heatmap, it is possible to plan for liver resection with recurrence in mind at the initial liver resection stage for cancers with a high recurrence rate, such as HCC and metastatic liver cancers requiring repeat hepatectomy.

Liver regeneration after hepatectomy is modified by various factors, such as age, sex, BMI, degree of liver fibrosis, native liver disease, chemotherapy, preoperative portal pressure, and steatosis[4,19-21]. In animal models, platelets promoted liver regeneration by enhancing the production of TNF-α and IL-6 and accelerating hepatocyte mitosis in the acute phase after hepatectomy[22]. It has previously been shown that hepatic fibrosis has a negative impact on liver regeneration; *i.e.*, the liver regeneration in cirrhotic livers is significantly slower and less complete than that in noncirrhotic livers[20,23]. This was explained by the hypothesis that the regeneration-promoting factors TNF-α, IL-6 and HGF were significantly lower in cirrhotic livers than in normal livers[24]. However, some cirrhotic livers display a fair degree of regenerative capacity[19,25]. In fact, in our study, the severely fibrotic liver eventually regenerated to a point that was comparable to that of a normal liver. Interestingly, the progression of liver fibrosis did not directly affect postoperative low regeneration or delayed regeneration; rather, the preoperative ALBI score was more influential. Considering cutoff values of -2.69 and -2.73 at 3 months and 12 months, posthepatectomy liver regeneration could be attenuated in patients with preoperative liver function and an ALBI grade 2a or higher. This was because the progression of liver fibrosis does not always correlate with liver function, and liver function usually decreases after cirrhosis has progressed to advanced stages. Moreover, the attenuation of liver regeneration in patients with a low preoperative liver function reserve could be attributed to the disturbance of the intrahepatic microcirculation of materials such as oxygen, proteins, and growth factors in hepatocytes[26]. This condition is called "sinusoidal capillarization", which results in the defenestration of hepatic sinusoidal endothelial cells and the formation of a continuous basement membrane, compromising the bidirectional exchange of materials between sinusoids and hepatocytes and resulting in hepatocellular dysfunction. Sinusoidal

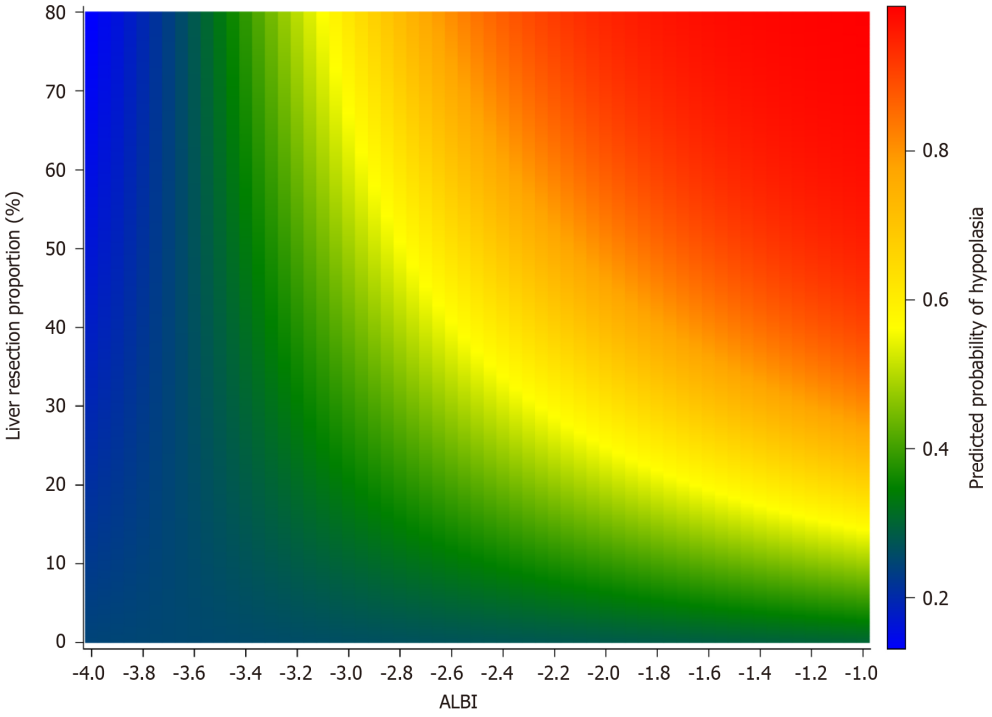

Figure 3 A heatmap for predicting the probability of volume restoration failure. The gradient shows the risk level: Blue indicates a low risk of volume restoration failure (less than 10%), whereas red indicates a high risk of volume restoration failure (higher than 90%). ALBI: Albumin-bilirubin.

capillarization is a reversible condition that is usually recognized in chronic liver diseases, such as alcoholic liver disease, nonalcoholic fatty liver disease, and chronic hepatitis viral disease. However, sinusoidal capillarization does not necessarily correlate with the fibrotic stage[25], which might explain why the preoperative ALBI score correlated more with low regeneration than with severe fibrosis. Another interesting finding of this study was that postoperative complication CD classifications of grade 3 or higher were related to greater regeneration at 3 months postsurgery. This might be because proinflammatory cytokines such as IL-6 and TNF-α released from Kupffer cells or liver sinusoidal endothelial cells also promote cytokines conducive to liver regeneration[1].

Parenchymal sparing hepatectomy has been proposed for its ability to prevent PHLF and its oncological efficacy against postoperative recurrence[27]. Owing to the improved accuracy of preoperative and intraoperative imaging modalities that are not limited to open hepatectomies, "parenchymal sparing hepatectomy" is widely applied in minimally invasive surgeries such as laparoscopic and robot-assisted hepatectomies. However, its effectiveness in performing hepatectomies adjacent to major large vessels and for accessing posterior superior segments (S7 and S8) has still not been established[28]. In accordance with "parenchymal sparing hepatectomy", surgeons will try to resect livers with the smallest volume possible. However, when the tumor is located close to a major blood vessel or deep inside the liver, it is often difficult to decide whether to choose major hepatectomy or Seg, which are technically simpler, but the resection volumes are larger, or subsegmentectomy or nonanatomical hepatectomy, which are sometimes technically more complicated, but the resection volumes are smaller. In our study, although the remnant liver volume after minor hepatectomy returned to the initial size, the residual liver volume after major hepatectomy did not return to its original volume. Based on these results, from the perspective of liver regeneration, it may be preferable to avoid major hepatectomies and instead choose minor hepatectomies when the minor hepatectomy can completely remove the tumor. However, since the liver regenerates to the original volume after minor hepatectomy, there is no need to forcibly choose more complicated minor hepatectomy procedures, such as subsegmentectomy or nonanatomical resection, as long as the preoperative liver function is sufficient to avoid severe PHLF, which can be assessed by preoperative surgical planning [29]. Instead, Seg, which is usually performed with a simpler resection procedure, might be preferable. This might be especially true in cases of minimally invasive surgeries that require the creation of complicated resection planes in a limited surgical view. This approach not only prolongs the operation time but can also cause intraoperative and postoperative complications such as bleeding and bile leakage. Specifically, robot-assisted hepatectomy requires the use of an inflexible scope, which obscures the surgical view in hepatectomies in the subphrenic area, such as in S7, S8, and S4a. Therefore, the usefulness of "parenchymal sparing hepatectomy" can vary depending on the patient and modality.

This study has several limitations. First, the data were retrospective in nature and were collected from a single center with a small sample size. Second, although we have evaluated different percentages of partial hepatectomy patients overall, the question remains as to whether this potentially different mode of regeneration can be assessed in the same way. In addition to the difference in the number of hepatocytes involved in regeneration depending on the resection rate, it was also reported that the remnant liver following 30% partial hepatectomy regenerated solely by hypertrophy without cell division; hypertrophy and subsequent proliferation equally contributed to regeneration after 70% partial hepatectomy[30]. As our comprehension of liver regeneration deepens, there may be a need to reconsider the approach to evaluating regeneration based on resection rates. Third, although patients were classified according to the type of

hepatectomy, patients with different backgrounds were analyzed together to provide a more intuitive understanding of clinical practice. This limitation may be overcome in the future by conducting a multicenter study and analyzing it in a larger population after sorting out background factors. Fourth, partial hepatectomies with a liver resection percentage of less than 10% were omitted from our data because of the potential for large errors in postoperative liver regeneration when assessed by CT volumetry**.** Despite these limitations, given the limited data on liver regeneration after partial hepatectomy in humans, this study offers unique implications for planning partial hepatectomy.

CONCLUSION

Liver regeneration after partial hepatectomy was determined by the liver resection percentage and the preoperative liver function reserve reflected by the ALBI score. With this knowledge and our heatmap, surgeons can choose the appropriate hepatectomy type on a case- and modality-specific basis, with rehepatectomy in mind after intrahepatic recurrence.

FOOTNOTES

Author contributions: Takahashi K designed and conducted the study and wrote the paper; Gosho M contributed to the analysis; Miyazaki Y, Nakahashi H, Shimomura O, Furuya K, Doi M, Owada Y, Ogawa K, Ohara Y, and Akashi Y provided clinical advice; and Enomoto T, Hashimoto S, and Oda T supervised the study.

Institutional review board statement: This study was reviewed and approved by the Ethics Committee of Tsukuba University Hospital.

Informed consent statement: Patients were not required to give informed consent to the study because the analysis used anonymous clinical data that were obtained after each patient agreed to treatment by written consent. We applied the Opt-out method to obtain consent for this study by using a poster. The poster was approved by the Institutional Review Board.

Conflict-of-interest statement: All the authors report no relevant conflicts of interest for this article.

Data sharing statement: Technical appendix, statistical code, and dataset available from the corresponding author at kazu1123@md.tsukuba.ac.jp.

STROBE statement: The authors have read the STROBE Statement—checklist of items—and the manuscript was prepared and revised according to the STROBE Statement—checklist of items.

Country/Territory of origin: Japan

ORCID number: Kazuhiro Takahashi 0000-0003-1089-0644; Masahiko Gosho 0000-0002-5973-9163; Yoshihiro Miyazaki 0000-0002-1851-964X; Hiromitsu Nakahashi 0000-0004-6419-0744; Osamu Shimomura 0000-0002-1735-5057; Kinji Furuya 0000-0002-2630-3072; Manami Doi 0000-0002-8731-3733; Yohei Owada 0000-0003-4979-7236; Koichi Ogawa 0000-0002-5710-4324; Yusuke Ohara 0000-0001-6807-6261; Yoshimasa Akashi 0000-0003-0589-3816; Tsuyoshi Enomoto 0000-0003-0540-2239; Shinji Hashimoto 0000-0003-3323-4594; Tatsuya Oda 0000-0001-6115-0158.

Corresponding Author's Membership in Professional Societies: The Japanese Society of Gastroenterology, G0323676.

S-Editor: Li L
L-Editor: A
P-Editor: Zhao YQ

REFERENCES

1 **Michalopoulos GK**, DeFrances MC. Liver regeneration. *Science* 1997; **276**: 60-66 [PMID: 9082986 DOI: 10.1126/science.276.5309.60]
2 **Yagi S**, Hirata M, Miyachi Y, Uemoto S. Liver Regeneration after Hepatectomy and Partial Liver Transplantation. *Int J Mol Sci* 2020; **21** [PMID: 33182515 DOI: 10.3390/ijms21218414]
3 **Michalopoulos GK**, Bhushan B. Liver regeneration: biological and pathological mechanisms and implications. *Nat Rev Gastroenterol Hepatol* 2021; **18**: 40-55 [PMID: 32764740 DOI: 10.1038/s41575-020-0342-4]
4 **Shimada M**, Matsumata T, Maeda T, Itasaka H, Suehiro T, Sugimachi K. Hepatic regeneration following right lobectomy: estimation of regenerative capacity. *Surg Today* 1994; **24**: 44-48 [PMID: 8054774 DOI: 10.1007/BF01676884]
5 **Akamatsu N**, Sugawara Y, Kaneko J, Sano K, Imamura H, Kokudo N, Makuuchi M. Effects of middle hepatic vein reconstruction on right liver graft regeneration. *Transplantation* 2003; **76**: 832-837 [PMID: 14501863 DOI: 10.1097/01.TP.0000085080.37235.81]

6 **Wakabayashi G**, Cherqui D, Geller DA, Abu Hilal M, Berardi G, Ciria R, Abe Y, Aoki T, Asbun HJ, Chan ACY, Chanwat R, Chen KH, Chen Y, Cheung TT, Fuks D, Gotohda N, Han HS, Hasegawa K, Hatano E, Honda G, Itano O, Iwashita Y, Kaneko H, Kato Y, Kim JH, Liu R, López-Ben S, Morimoto M, Monden K, Rotellar F, Sakamoto Y, Sugioka A, Yoshiizumi T, Akahoshi K, Alconchel F, Ariizumi S, Benedetti Cacciaguerra A, Durán M, Garcia Vazquez A, Golse N, Miyasaka Y, Mori Y, Ogiso S, Shirata C, Tomassini F, Urade T, Wakabayashi T, Nishino H, Hibi T, Kokudo N, Ohtsuka M, Ban D, Nagakawa Y, Ohtsuka T, Tanabe M, Nakamura M, Tsuchida A, Yamamoto M. The Tokyo 2020 terminology of liver anatomy and resections: Updates of the Brisbane 2000 system. *J Hepatobiliary Pancreat Sci* 2022; **29**: 6-15 [PMID: 34866349 DOI: 10.1002/jhbp.1091]

7 **Rahbari NN**, Garden OJ, Padbury R, Brooke-Smith M, Crawford M, Adam R, Koch M, Makuuchi M, Dematteo RP, Christophi C, Banting S, Usatoff V, Nagino M, Maddern G, Hugh TJ, Vauthey JN, Greig P, Rees M, Yokoyama Y, Fan ST, Nimura Y, Figueras J, Capussotti L, Büchler MW, Weitz J. Posthepatectomy liver failure: a definition and grading by the International Study Group of Liver Surgery (ISGLS). *Surgery* 2011; **149**: 713-724 [PMID: 21236455 DOI: 10.1016/j.surg.2010.10.001]

8 **Nagasue N**, Yukaya H, Ogawa Y, Kohno H, Nakamura T. Human liver regeneration after major hepatic resection. A study of normal liver and livers with chronic hepatitis and cirrhosis. *Ann Surg* 1987; **206**: 30-39 [PMID: 3038039 DOI: 10.1097/00000658-198707000-00005]

9 **Haga J**, Shimazu M, Wakabayashi G, Tanabe M, Kawachi S, Fuchimoto Y, Hoshino K, Morikawa Y, Kitajima M, Kitagawa Y. Liver regeneration in donors and adult recipients after living donor liver transplantation. *Liver Transpl* 2008; **14**: 1718-1724 [PMID: 19025926 DOI: 10.1002/lt.21622]

10 **Pomfret EA**, Pomposelli JJ, Gordon FD, Erbay N, Lyn Price L, Lewis WD, Jenkins RL. Liver regeneration and surgical outcome in donors of right-lobe liver grafts. *Transplantation* 2003; **76**: 5-10 [PMID: 12865779 DOI: 10.1097/01.TP.0000079064.08263.8E]

11 **Pascher A**, Sauer IM, Walter M, Lopez-Haeninnen E, Theruvath T, Spinelli A, Neuhaus R, Settmacher U, Mueller AR, Steinmueller T, Neuhaus P. Donor evaluation, donor risks, donor outcome, and donor quality of life in adult-to-adult living donor liver transplantation. *Liver Transpl* 2002; **8**: 829-837 [PMID: 12200786 DOI: 10.1053/jlts.2002.34896]

12 **Ohshima S**. Volume analyzer synapse Vincent for liver analysis. *J Hepatobiliary Pancreat Sci* 2014; **21**: 235-238 [PMID: 24520049 DOI: 10.1002/jhbp.81]

13 **Meier M**, Andersen KJ, Knudsen AR, Nyengaard JR, Hamilton-Dutoit S, Mortensen FV. Liver regeneration is dependent on the extent of hepatectomy. *J Surg Res* 2016; **205**: 76-84 [PMID: 27621002 DOI: 10.1016/j.jss.2016.06.020]

14 **Mitchell C**, Nivison M, Jackson LF, Fox R, Lee DC, Campbell JS, Fausto N. Heparin-binding epidermal growth factor-like growth factor links hepatocyte priming with cell cycle progression during liver regeneration. *J Biol Chem* 2005; **280**: 2562-2568 [PMID: 15536070 DOI: 10.1074/jbc.M412372200]

15 **Al-Ghamdi TH**, Atta IS, El-Refaei M. Role of interleukin 6 in liver cell regeneration after hemi-hepatectomy, correlation with liver enzymes and flow cytometric study. *Clin Exp Hepatol* 2020; **6**: 42-48 [PMID: 32166123 DOI: 10.5114/ceh.2020.93055]

16 **Bucher NL**, Swaffield MN. The rate of incorporation of labeled thymidine into the deoxyribonucleic acid of regenerating rat liver in relation to the amount of liver excised. *Cancer Res* 1964; **24**: 1611-1625 [PMID: 14234005]

17 **Yamada A**, Kawata S, Tamura S, Kiso S, Higashiyama S, Umeshita K, Sakon M, Taniguchi N, Monden M, Matsuzawa Y. Plasma heparin-binding EGF-like growth factor levels in patients after partial hepatectomy as determined with an enzyme-linked immunosorbent assay. *Biochem Biophys Res Commun* 1998; **246**: 783-787 [PMID: 9618289 DOI: 10.1006/bbrc.1998.8703]

18 **Inoue Y**, Fujii K, Ishii M, Kagota S, Tomioka A, Hamamoto H, Osumi W, Tsuchimoto Y, Masubuchi S, Yamamoto M, Asai A, Komeda K, Shimizu T, Asakuma M, Fukunishi S, Hirokawa F, Narumi Y, Higuchi K, Uchiyama K. Volumetric and Functional Regeneration of Remnant Liver after Hepatectomy. *J Gastrointest Surg* 2019; **23**: 914-921 [PMID: 30264387 DOI: 10.1007/s11605-018-3985-5]

19 **Shirabe K**, Motomura T, Takeishi K, Morita K, Kayashima H, Taketomi A, Ikegami T, Soejima Y, Yoshizumi T, Maehara Y. Human early liver regeneration after hepatectomy in patients with hepatocellular carcinoma: special reference to age. *Scand J Surg* 2013; **102**: 101-105 [PMID: 23820685 DOI: 10.1177/1457496913482250]

20 **Aierken Y**, Kong LX, Li B, Liu XJ, Lu S, Yang JY. Liver fibrosis is a major risk factor for liver regeneration: A comparison between healthy and fibrotic liver. *Medicine (Baltimore)* 2020; **99**: e20003 [PMID: 32481371 DOI: 10.1097/MD.0000000000020003]

21 **Gupta A**, Patil NS, Mohapatra N, Benjamin J, Thapar S, Kumar A, Rastogi A, Pamecha V. Lifestyle Optimization Leads to Superior Liver Regeneration in Live Liver Donors and Decreases Early Allograft Dysfunction in Recipients: A Randomized Control Trial. *Ann Surg* 2023; **278**: e430-e439 [PMID: 36912445 DOI: 10.1097/SLA.0000000000005836]

22 **Matsuo R**, Nakano Y, Ohkohchi N. Platelet administration *via* the portal vein promotes liver regeneration in rats after 70% hepatectomy. *Ann Surg* 2011; **253**: 759-763 [PMID: 21475016 DOI: 10.1097/SLA.0b013e318211caf8]

23 **Chen MF**, Hwang TL, Hung CF. Human liver regeneration after major hepatectomy. A study of liver volume by computed tomography. *Ann Surg* 1991; **213**: 227-229 [PMID: 1998403 DOI: 10.1097/00000658-199103000-00008]

24 **Shan YS**, Hsieh YH, Sy ED, Chiu NT, Lin PW. The influence of spleen size on liver regeneration after major hepatectomy in normal and early cirrhotic liver. *Liver Int* 2005; **25**: 96-100 [PMID: 15698405 DOI: 10.1111/j.1478-3231.2005.01037.x]

25 **Ogata T**, Okuda K, Ueno T, Saito N, Aoyagi S. Serum hyaluronan as a predictor of hepatic regeneration after hepatectomy in humans. *Eur J Clin Invest* 1999; **29**: 780-785 [PMID: 10469166 DOI: 10.1046/j.1365-2362.1999.00513.x]

26 **Mak KM**, Kee D, Shin DW. Alcohol-associated capillarization of sinusoids: A critique since the discovery by Schaffner and Popper in 1963. *Anat Rec (Hoboken)* 2022; **305**: 1592-1610 [PMID: 34766732 DOI: 10.1002/ar.24829]

27 **Torzilli G**, McCormack L, Pawlik T. Parenchyma-sparing liver resections. *Int J Surg* 2020; **82S**: 192-197 [PMID: 32335245 DOI: 10.1016/j.ijsu.2020.04.047]

28 **Katagiri H**, Nitta H, Kanno S, Umemura A, Takeda D, Ando T, Amano S, Sasaki A. Safety and Feasibility of Laparoscopic Parenchymal-Sparing Hepatectomy for Lesions with Proximity to Major Vessels in Posterosuperior Liver Segments 7 and 8. *Cancers (Basel)* 2023; **15** [PMID: 37046738 DOI: 10.3390/cancers15072078]

29 **Takahashi K**, Gosho M, Kim J, Shimomura O, Miyazaki Y, Furuya K, Akashi Y, Enomoto T, Hashimoto S, Oda T. Prediction of Posthepatectomy Liver Failure with a Combination of Albumin-Bilirubin Score and Liver Resection Percentage. *J Am Coll Surg* 2022; **234**: 155-165 [PMID: 35213436 DOI: 10.1097/XCS.0000000000000027]

30 **Miyaoka Y**, Ebato K, Kato H, Arakawa S, Shimizu S, Miyajima A. Hypertrophy and unconventional cell division of hepatocytes underlie liver regeneration. *Curr Biol* 2012; **22**: 1166-1175 [PMID: 22658593 DOI: 10.1016/j.cub.2012.05.016]

World Journal of Gastroenterology

Submit a Manuscript: https://www.f6publishing.com

World J Gastroenterol 2024 April 14; 30(14): 2018-2037

DOI: 10.3748/wjg.v30.i14.2018

ISSN 1007-9327 (print) ISSN 2219-2840 (online)

ORIGINAL ARTICLE

Basic Study

Fusobacterium nucleatum-induced imbalance in microbiome-derived butyric acid levels promotes the occurrence and development of colorectal cancer

Qi-Long Wu, Xiao-Ting Fang, Xin-Xin Wan, Qing-Yong Ding, Yan-Jun Zhang, Ling Ji, Yong-Liang Lou, Xiang Li

Specialty type: Gastroenterology and hepatology

Provenance and peer review: Unsolicited article; Externally peer reviewed.

Peer-review model: Single blind

Peer-review report's scientific quality classification

Grade A (Excellent): 0
Grade B (Very good): B, B
Grade C (Good): 0
Grade D (Fair): 0
Grade E (Poor): 0

P-Reviewer: Jordan P, Portugal

Received: October 31, 2023
Peer-review started: October 31, 2023
First decision: December 15, 2023
Revised: January 11, 2024
Accepted: February 29, 2024
Article in press: February 29, 2024
Published online: April 14, 2024

Qi-Long Wu, School of Laboratory Medicine and Life Sciences, Wenzhou Medical University, Key Laboratory of Laboratory Medicine, Ministry of Education, Wenzhou 325035, Zhejiang Province, China

Xiao-Ting Fang, Department of Health Inspection and Quarantine, School of Laboratory Medicine and Life Sciences, Wenzhou 325035, Zhejiang Province, China

Xin-Xin Wan, Qing-Yong Ding, Yan-Jun Zhang, School of Laboratory Medicine and Life Sciences, Wenzhou Medical University, Zhejiang Provincial Key Laboratory of Medical Genetics, Ministry of Education, Wenzhou 325035, Zhejiang Province, China

Ling Ji, Department of General Surgery, The First Affiliated Hospital of Wenzhou Medical University, Wenzhou 325035, Zhejiang Province, China

Yong-Liang Lou, School of Laboratory Medicine and Life Sciences, Institute of One Health, Wenzhou Medical University, Zhejiang Provincial Key Laboratory of Medical Genetics, Ministry of Education, Wenzhou 325035, Zhejiang Province, China

Xiang Li, Department of Health Inspection and Quarantine, School of Laboratory Medicine and Life Sciences, Institute of One Health, Wenzhou Medical University, Zhejiang Provincial Key Laboratory of Medical Genetics, Ministry of Education, Wenzhou 325035, Zhejiang Province, China

Corresponding author: Xiang Li, PhD, Associate Professor, Deputy Director, Postdoc, Department of Health Inspection and Quarantine, School of Laboratory Medicine and Life Sciences, Institute of One Health, Wenzhou Medical University, Zhejiang Provincial Key Laboratory of Medical Genetics, Ministry of Education, No. 1 Qiuzhen Road, Wenzhou 325035, Zhejiang Province, China. yhx2008@163.com

Abstract

BACKGROUND

Colorectal cancer (CRC) ranks among the most prevalent malignant tumors globally. Recent reports suggest that *Fusobacterium nucleatum* (*F. nucleatum*) contributes to the initiation, progression, and prognosis of CRC. Butyrate, a short-chain fatty acid derived from the bacterial fermentation of soluble dietary fiber, is

known to inhibit various cancers. This study is designed to explore whether *F. nucleatum* influences the onset and progression of CRC by impacting the intestinal metabolite butyric acid.

AIM

To investigate the mechanism by which *F. nucleatum* affects CRC occurrence and development.

METHODS

Alterations in the gut microbiota of BALB/c mice were observed following the oral administration of *F. nucleatum*. Additionally, DLD-1 and HCT116 cell lines were exposed to sodium butyrate (NaB) and *F. nucleatum in vitro* to examine the effects on proliferative proteins and mitochondrial function.

RESULTS

Our research indicates that the prevalence of *F. nucleatum* in fecal samples from CRC patients is significantly greater than in healthy counterparts, while the prevalence of butyrate-producing bacteria is notably lower. In mice colonized with *F. nucleatum*, the population of butyrate-producing bacteria decreased, resulting in altered levels of butyric acid, a key intestinal metabolite of butyrate. Exposure to NaB can impair mitochondrial morphology and diminish mitochondrial membrane potential in DLD-1 and HCT116 CRC cells. Consequently, this leads to modulated production of adenosine triphosphate and reactive oxygen species, thereby inhibiting cancer cell proliferation. Additionally, NaB triggers the adenosine monophosphate-activated protein kinase (AMPK) signaling pathway, blocks the cell cycle in HCT116 and DLD-1 cells, and curtails the proliferation of CRC cells. The combined presence of *F. nucleatum* and NaB attenuated the effects of the latter. By employing small interfering RNA to suppress AMPK, it was demonstrated that AMPK is essential for NaB's inhibition of CRC cell proliferation.

CONCLUSION

F. nucleatum can promote cancer progression through its inhibitory effect on butyric acid, *via* the AMPK signaling pathway.

Key Words: Colorectal cancer; *Fusobacterium nucleatum*; Butyric acid; Gut microbiota; Adenosine monophosphate-activated protein kinase signal pathway

Core Tip: In this study, we unravel the mechanism of *Fusobacterium nucleatum* (*F. nucleatum*) in the progression of colorectal cancer (CRC), focusing on the interplay between intestinal flora and metabolism. Our results reveal that *F. nucleatum* suppresses the production of the short-chain fatty acid butyric acid. We discovered that sodium butyrate impairs mitochondrial function and impedes the cell cycle in CRC cells. Furthermore, the study highlights that both sodium butyrate and *F. nucleatum* orchestrate CRC cell proliferation *via* the adenosine monophosphate-activated protein kinase signaling pathway. These insights may enhance our understanding of CRC pathogenesis and aid in the development of more effective treatment strategies.

Citation: Wu QL, Fang XT, Wan XX, Ding QY, Zhang YJ, Ji L, Lou YL, Li X. *Fusobacterium nucleatum*-induced imbalance in microbiome-derived butyric acid levels promotes the occurrence and development of colorectal cancer. *World J Gastroenterol* 2024; 30(14): 2018-2037

URL: https://www.wjgnet.com/1007-9327/full/v30/i14/2018.htm

DOI: https://dx.doi.org/10.3748/wjg.v30.i14.2018

INTRODUCTION

Colorectal cancer (CRC) is one of the most common malignant tumors in the world and is the second and third most common cancer in women and men, respectively[1]. In recent years, CRC has ranked fifth in malignant tumor mortality in China, and the incidence rate is increasing at an annual rate of 4%[2]. At present, it is one of the deadliest cancers globally. The occurrence of CRC is influenced by multiple factors, including genetics, dietary habits, and environmental influences[3,4], and its pathogenesis is complex and not yet fully understood.

The intestinal microenvironment contains a complex microbial ecosystem. In recent years, the interaction between gut microbiota and the occurrence and development of CRC has been a hot research topic[5]. Research has found that the gut microbiota balance in patients with CRC is disrupted, with significant differences in composition and proportion of intestinal microbes compared to normal, healthy individuals[6,7]. As early as 1997, Dove *et al*[8] found that in $Apc^{min/+}$ mice who spontaneously develop multiple intestinal tumors and numerous intestinal polyps, the number of small intestinal tumors was significantly reduced under germ-free conditions compared to $Apc^{min/+}$ mice in a regular environment, establishing an early association between the gut microbiota and CRC occurrence and development.

Preclinical and clinical evidence has also emphasized the role of gut microbiota in altering the therapeutic response of CRC patients to chemotherapy and immunotherapy[7].

In recent years, several studies have reported the association between various microorganisms and CRC development, including *Fusobacterium nucleatum* (*F. nucleatum*), *Peptostreptococcus anaerobius*, *Parvimonas micra*, *Enterotoxigenic Bacteroides fragilis*, *Peptostreptococcus stomatis*, and *Escherichia coli*[9-11]. Additionally, there have been studies applying high-abundance pathogenic bacteria and low-abundance probiotics to colorectal tumor diagnostic models[12]. Many studies have indicated that microbial imbalance and infection are major factors in CRC occurrence and development[13,14].

F. nucleatum has been reported to play a role in the occurrence, development, and prognosis of CRC. Castellarin *et al* [15] compared 99 cases of CRC patient tissues with corresponding normal mucosal tissues and found that the average abundance of *F. nucleatum* in cancerous tissues was 415 times higher than in normal specimens. The relative abundance of *F. nucleatum* increases from intramucosal carcinoma to advanced stages of CRC and with increasing tumor malignancy [16]. The abundance of *F. nucleatum* in tumor tissues and fecal samples of CRC patients is significantly higher than in the normal control group[17,18]. However, the exact mechanism by which *F. nucleatum* plays a role in the intestinal micro-ecology and its specific molecular mechanisms have not been fully clarified.

The gut microbiota can produce short-chain fatty acids (SCFAs), such as acetate, propionate, and butyrate, through the fermentation of dietary fiber[19]. Among the SCFA family, butyrate plays an extremely important role. It exerts anti-inflammatory and anti-tumor effects on the mucosa by regulating cell metabolism, maintaining microbial homeostasis, inhibiting cell proliferation, immunomodulation, and effecting genetic/epigenetic regulation. It also provides a good energy source for colonic cells[20]. Although butyrate acts through several signaling pathways, one of key interest is the adenosine monophosphate-activated protein kinase (AMPK) pathway, as butyrate can inhibit cell proliferation and promote autophagy through this pathway, two actions that are important in cancer progression.

AMPK is a serine/threonine kinase and serves as a major energy sensor in cells, playing a critical role in maintaining energy homeostasis[21]. Once activated, AMPK promotes catabolic processes to generate adenosine triphosphate (ATP), assisting cells in escaping death and leading to drug resistance and metastasis. On the other hand, AMPK has also been reported to be positively correlated with tumor suppressor genes such as p53 and LKB1. Therefore, AMPK activation results in cell cycle arrest and tumor growth inhibition, playing a key role in cancer prevention[22].

In this study, we elucidate the role of *F. nucleatum* in CRC development from the perspective of the intestinal flora and intestinal metabolites and investigate the role of the intestinal flora in CRC occurrence and development.

MATERIALS AND METHODS

Cell culture

HCT116 and DLD-1 cell lines were purchased from American Type Culture Collection [(ATCC) Manassas, VA, United States]. The HCT116 and DLD-1 cells were cultured in Dulbecco's modified Eagle medium in an incubator with 5% CO_2 at 37° C. Penicillin G (100 U/mL), streptomycin (100 mg/mL) (Beyotime, Nanjing, China), and 10% foetal bovine serum (Invitrogen, Waltham, MA, United States) were added to the culture medium. Two colonic cell lines were used to demonstrate reproducibility.

Bacteria strains

F. nucleatum strain ATCC 25586 was purchased from the ATCC. *F. nucleatum* was cultured in Fastidious Anaerobe Broth under anaerobic conditions.

Animal studies

Adult 6-8 wk-old male BALB/c mice and a weight of 18-22 g (Beijing Vital River Laboratory Animal Technology Co., Ltd., Beijing, China) were housed at the experimental animal center of Wenzhou Medical University and maintained under specific pathogen-free conditions (12-h light/dark cycle, 21° C ± 2° C, humidity 50% ± 10%). All animal studies were conducted in compliance with the animal experiment guidelines of Wenzhou Medical University. Study protocols were approved by the Animal Experimental Ethics Committee (wydw2022-0217).

All mice have free access to standard feed and water. After mice were habituated to their surroundings for a week, they were randomly divided into two groups of 12 mice per group. A suspension of *F. nucleatum* bacteria (1×10^8) was administered by gavage once a day for 5 d to mice in the treatment group. The control group was gavaged with physiological saline. Intervention was ceased for 1 wk, during which time, normal drinking water and diet were consumed, after which mice were gavaged with *F. nucleatum* again for 5 d. After repeating three cycles, the mice were euthanized using 1% pentobarbital sodium (administered by intraperitoneal injection). Feces were collected for subsequent experiments.

Fluorescence in situ hybridization

Fluorescence *in situ* hybridization (FISH) was conducted to examine the abundance of *F. nucleatum* using a specific probe. Briefly, sections of formalin-fixed, paraffin-embedded colonic tissue were cut into 5 μm sections and hybridized in accordance with the manufacturer's instructions (FOCOFISH, Guangzhou, China). The following universal bacterial probe (EUB338; Cy3-labeled) was used: 5'-GCTGCCTCCCGTAGGAGT-3'. The following probe specific to *F. nucleatum* (FUS664; FITC-labeled) was used: 5'-CTTGTAGTTCCGC(C/T)TACCTC-3'. The resulting slides were visualized and examined under a fluorescent microscope (BX53F; Olympus, Tokyo, Japan). Five random fields per sample (200 ×

magnification) were examined, and the average number of bacteria per field was calculated. A blinded reviewer examined five random fields per sample (200 × magnification), and the average number of bacteria per field was calculated. Demographics of patient tissues can be found in our previous study[23].

Cell cycle analysis

Cell cycle analysis was performed by flow cytometry using propidium iodide (PI). CRC cells were cultured on a six-well plate (2 × 10^5 cells per well) and incubated at 37° C and 5% CO_2 overnight. Cells were treated with *F. nucleatum* culture supernatants and sodium butyrate (NaB) for 24 h, after which cells were collected and incubated in the dark for 30 min with 1 mL DNA staining solution and 10 μL permeabilization solution treatment. Flow cytometry and CytExpert were used for cell cycle analysis, including G0/G1, S, and G2/M phases, and the proportion of cells in each phase was calculated.

Assessment of reactive oxygen species levels

Cells were cultured as described above. After 24 h of treatment with NaB or *F. nucleatum* culture supernatants, cells were centrifuged and resuspended in DCFH-DA staining solution (10 μmol/L) for 20 min at 37° C. Every 3-5 min, cell suspensions were mixed by inversion to ensure full contact with the probe. Cells were washed three times with serum-free cell culture medium to remove the DCFH-DA that did not enter the cell. Flow cytometry was used to measure fluorescence intensity.

Mitochondrial membrane potentials assay

Cellular mitochondrial depolarization was measured using a JC-1 dye, according to the manufacturer's instructions. Briefly, after 24 h of treatment with NaB or *F. nucleatum* culture supernatants, cells were collected, suspended in 0.5 mL of culture media, and thoroughly mixed with 0.5 mL of the JC-1 staining working solution and incubated for 20 min at 37° C. Supernatants were removed after incubation and cells were rinsed three times with JC-1 staining buffer. Cells were resuspended with the appropriate volume of JC-1 staining buffer, followed by flow cytometric analysis.

ATP assay

An ATP assay kit was used to measure ATP concentrations according to the manufacturer's instructions (Beyotime, Shanghai, China). Briefly, after 24 h of treatment with NaB or *F. nucleatum* culture supernatants, cells were lysed with ATP lysis buffer and centrifuged at 12000 rpm for 5 min at 4°C. Supernatants were collected and stored on ice. In 1.5 mL EP tubes, 100 μL ATP working solution (ATP test solution: ATP test dilution = 1:9) was added before the ATP test, and the tubes were incubated for 3-5 min at room temperature. Next, 20 μL of the sample or standard were added to the tube, mixed with a pipette, and the RLU values were measured with an enzyme marker after at least two seconds. The luminescence values were normalized against sample protein concentration. The data and images were processed by GraphPad Prism 6 statistical software (La Jolla, CA, United States).

Preparation and ultrastructural observation of electron microscope samples

After treatments, supernatant was removed and cells were fixed overnight at 4° C using 1-2 mL of 2.5% glutaraldehyde. The following day, a cell scraper was used to remove the cell layer and collected into a 1.5 mL EP tube. Cells were rinsed three times for 10 min with phosphate buffered saline, after which 1% osmic acid was added and cells were fixed in the dark at room temperature for 1 h. Cells were rinsed 3 times for 10 min with double distilled water, then stained at room temperature for 1 h with 1-2 drops of uranium acetate solution. Samples were placed in successive volumes of 50%, 70%, 80%, 90%, 100%, and 100% acetone solutions for 10 min for progressive dehydration, after which a 1:1 volume ratio of acetone to epoxy resin embedding agent was added for penetration treatment. After incubation for 60 min at 37° C, a 1:4 volume ratio mixture of acetone and embedding agent were added, and samples were incubated overnight at 37 °C. The pure embedding solution was added the following day, and samples were allowed to dry for 1 h in a 37° C oven. Pure embedding solution was added and polymerized at 45° C for 3 h and 65° C for 48 h. Semi-thin slices were then cut, followed by ultra-thin sections, which were then stained and dried for observation with transmission electron microscopy.

Transfection with small interfering RNA

Small interfering RNAs (siRNAs) specific for AMPKα were purchased from Tsingke Biotechnology Co., Ltd. (Beijing, China). Transfection of siRNA was performed using Lipo3000™ transfection reagent according to the manufacturer's protocol. The specific siRNA sequences are as follows: AMPKα siRNA - 1 sense: 5′-GCAGAAGUAUGUAGAGC-AAUCTT-3′, antisense: 5′-GAUUGCUCUACAUACUUCUGCTT-3′; AMPKα siRNA - 2 sense: 5′-GCUUGAUGCACACA-UGAAUTT-3′, antisense: 5′-AUUCAUGUGUGCAUCAAGCTT-3′. The control siRNA sequences were as follows: Sense: UUCUCCGAACGUGUCACGUTT; antisense: ACGUGACACGUUCGGAGAATT.

Western blot

Total protein concentrations were examined using the Bicinchoninic Acid Protein Assay. Samples were separated using sodium dodecyl sulfate polyacrylamide gel electrophoresis and transferred to polyvinylidene difluoride membranes. Skim milk was used for incubation with specific primary antibodies (1:1000 dilution) at 4° C overnight. The antibodies included phosphorylated AMPK (p-AMPK) (Cell Signaling Technology, Danvers, MA, United States), cyclin B1 (Diagbio, Hangzhou, China), Cdk1 (Abways, Beijing, China), p21 (Diagbio), C-myc (Diagbio), and GAPDH (Abways). The samples were incubated with secondary antibodies (1:2000 dilution) (Biosharp, Harjumaa, Estonia) at room temperature for 1 h.

Protein bands were visualized using a hypersensitive enhanced chemiluminescence kit (Beyotime). The Bio-Rad gel imaging system was used to photograph gels, and ImageJ software was used for analysis.

16S rDNA sequencing

Total genomic DNA of mice was obtained from their cecal contents. 16S/18S rRNA genes were amplified using specific primers. All polymerase chain reaction (PCR) steps were conducted in the reaction media (30 μL) containing 15 μL of High-Fidelity PCR Master Mix (New England Biolabs, Ipswich, MA, United States). The following thermocycling conditions were used: Predegeneration at 98° C for 1 min, denaturation at 98° C for 10 s, annealing at 50° C for 30 s, and extension at 7° C for 30 s (30 cycles); the final elongation step was carried out at 72° C for 5 min. PCR products were mixed and purified for quantification and identification. Sequencing libraries were generated by a TIANSeq Fast DNA Library Prep Kit (Illumina; Tiangen Biotech, Beijing, China). The library quality was evaluated using the Qubit@ 2.0 Fluorometer (Thermo Scientific, Waltham, MA, United States) and Agilent Bioanalyzer 2100 system (Santa Clara, CA, United States). Finally, the sequencing of the constructed library was performed on the Illumina platform using the 2 × 250 bp paired-end protocol and data analysis was conducted.

Statistical analysis

The above experiments were performed at least thrice. GraphPad Prism 6.0 software was used for graphing and statistical analysis. The BD FACS Aria II flow cytometer was used to measure the mitochondrial membrane potential and detect reactive oxygen species (ROS), and Treestar Flowjo 10.0 software (Eugene, OR, United States) was used to analyze the results. Cell cycle detection and data analysis were conducted by a CytExpert 2.3 flow cytometer (Beckman Coulter, Brea, CA, United States). All variables were presented as mean ± standard deviation. Other statistics were analyzed using Student's *t*-test. $P < 0.05$ was considered statistically significant.

RESULTS

Abundance of F. nucleatum is significantly high in CRC tissues

To study the difference in the flora in CRC tissues, 39 fresh clinical tissue samples (including 24 CRC samples, 10 normal tissue samples, and 5 paracancerous tissue samples) were collected for 16S rDNA sequencing. The results showed that there were significant differences between normal and CRC tissues at the family level ($P < 0.05$, Figure 1A). *Fusobacterium* was found at a higher abundance in CRC tissues, but in lower abundance in normal and adjacent tissues. *Clostridium* butyrate-producing bacteria were also found to drop in abundance as CRC spread, mostly because their abundance was substantially higher in normal tissue samples than in CRC and adjacent tissues.

Ten tissue samples were chosen from the aforementioned samples, including both normal and CRC tissue. FISH was used to determine the quantity of *F. nucleatum* in colorectal tissue. As shown in Figure 1B, the abundance of *F. nucleatum* in CRC tissue is significantly higher than in normal colorectal tissue, indicating that *F. nucleatum* is strongly associated with CRC occurrence and progression.

Abundance of butyrate-producing bacteria in fecal samples from CRC patients is lower compared to healthy individuals

To further study the effect of intestinal flora on CRC development, we sequenced 16S rDNA from 105 stool samples, including 44 CRC patients and 61 healthy people. The results of LefSe analysis showed that there are significant differences in bacteria between CRC and normal/adjacent tissues (Figure 2A and B). Compared to CRC patients, the abundance of *Lac_Lachnospira*, *Lac_Roseburia* and *Rum_Faecalibacterium* significantly increased in healthy fecal samples ($P < 0.05$), which is the characteristic bacteria in fecal samples of healthy people (Figure 2C). The abundance of *Trichospira* and *Rochella* is much higher in fecal samples from healthy people compared to patients with stage I-IV CRC. There was no significant difference between CRC stages. The abundance of *Rum_Faecalibacterium* in healthy people and patients with stage I CRC fecal samples were the same (Figure 2D), demonstrating that although there is a significant difference in the abundance of butyrate-producing bacteria between CRC patients and healthy people, its role in CRC development needs to be further explored.

Abundance of butyrate-producing bacteria decreased in mice treated with F. nucleatum

To further clarify the role and relationship between *F. nucleatum* and butyric acid bacteria in CRC occurrence and development, BALB/c mice were gavaged with an *F. nucleatum* suspension (1×10^8 CFU/d). 16S rDNA sequencing was used to detect changes in bacterial abundance in fecal samples. As shown in Figure 3A and B, intragastric administration of *F. nucleatum* resulted in significantly fewer butyric acid-producing bacteria in fecal samples compared to the control group.

F. nucleatum inhibits formation of the short chain fatty acid butyric acid

Fecal samples from mice treated with *F. nucleatum* were collected, and GC-MS targeted metabolomics were used to discover and evaluate the quantities of short chain fatty acids (SCFAs). The GC-MS data shown in Figure 4A and B shows a significant difference in the PC1 direction between the *F. nucleatum*-treated group and the control group, indicating a significant divergence in metabolic pathways between the two groups. According to targeted SCFA detection, the amount of SCFAs in the *F. nucleatum*-treated group was much lower than in the untreated group (Figure 4C). Butyric acid/

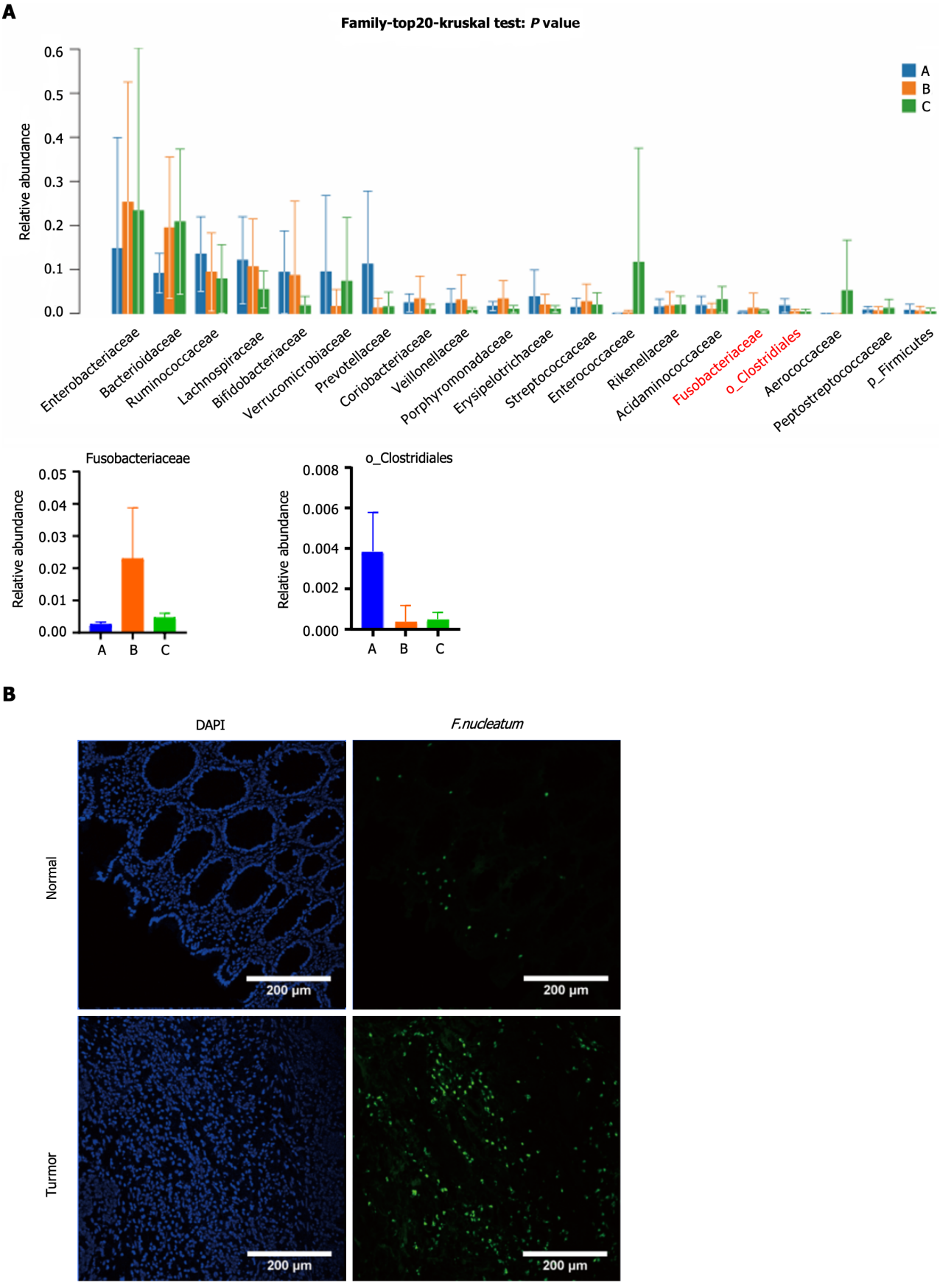

Figure 1 Abundance of *Fusobacterium nucleatum* is significantly increased in colorectal cancer tissues. A: 16S rDNA sequencing results of clinical tissue samples (A: Normal tissue; B: Colorectal cancer tissue; C: Paracancerous tissue); B: Fluorescence *in situ* hybridization results showed that the abundance of *Fusobacterium nucleium* in colorectal cancer tissue was significantly higher than that in normal colorectal tissue.

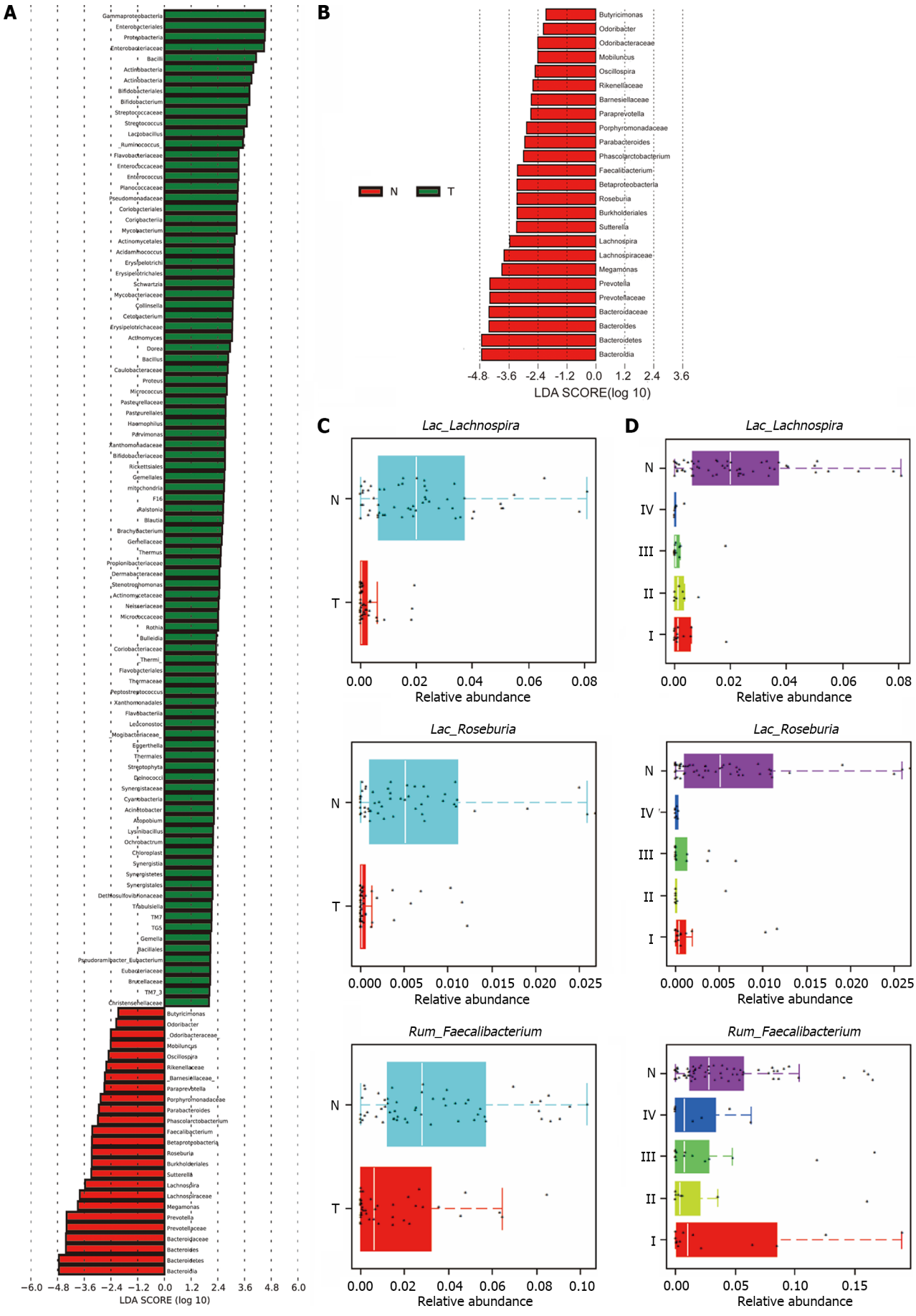

Figure 2 Abundance of butyrate-producing bacteria in fecal samples from colorectal cancer patients is lower compared to that of healthy

individuals. A: There were significant differences in bacterial composition between colorectal cancer and normal/adjacent tissues; B: *Butyricimonas*, *Roseburia*, *Faecalibacterium* and other butyric acid producing bacteria are enriched in the feces of healthy individuals; C: The abundance of *Lac_Lachnospira*, *Lac_Roseburia*, and *Rum_Faecalibacterium* in fecal samples of healthy people was significantly higher than that of colorectal cancer patients; D: The abundance of *Trichospira* and *Rochella* in the fecal samples of healthy people is significantly higher than that of patients with stage I-IV colorectal cancer, and the abundance of *Fecal bacilli* in the fecal samples of healthy people and patients with stage I colorectal cancer is higher.

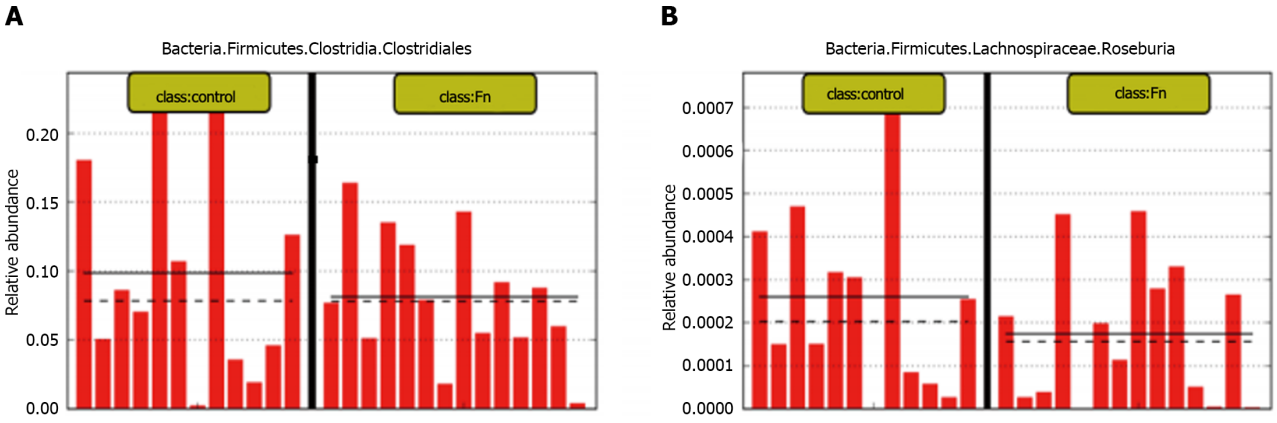

Figure 3 Abundance of butyrate-producing bacteria is decreased in mice treated with *Fusobacterium nucleatum*. A and B: The 16S rDNA sequencing results showed that the abundance of fecal butyric acid-producing bacteria (*Lac_Rosebaria* and *Clostridium*) was lower than those of the control group in mice treated with *Fusobacterium nucleatum* by gavage (n = 12 for each group). Each bar represents the content of *Clostridium* (A) or *Lactobacillus* (B) in the feces of mice in the treatment group.

isobutyric acid levels in fecal samples significantly decreased following *F. nucleatum* treatment ($P < 0.05$) (Figure 4D-F), which is one of the most prominent components of SCFAs. This suggests that in mice, *F. nucleatum* treatment changes intestinal metabolic patterns, due to a significant decrease in the proportion of butyric acid-producing bacteria. As a result, *F. nucleatum* may affect the gut microbiota in addition to influencing metabolites and metabolic rate.

NaB blocks the cell cycle in HCT116 and DLD-1 cells

We treated human CRC cells DLD-1 and HCT116 cells with 2 mmol/L NaB and used flow cytometry to examine the effects on the cell cycle of HCT116 and DLD-1 cells. The proportion of G2/M phase cells dramatically increased after 24 h of NaB administration, as shown in Figure 5A and B. This suggests that NaB can prevent HCT116 and DLD-1 cells from entering the G1 phase. There were no discernible alterations in the cell cycle when we exposed cells to *F. nucleatum* supernatant (FAB). However, these effects were reduced when cells were treated with NaB and *F. nucleatum* supernatant, showing that *F. nucleatum* can suppress the efficacy of NaB.

NaB reduces mitochondrial membrane potential and increases ROS content in CRC cells

An aberrant drop in mitochondrial membrane potential and a rise in ROS levels indicate mitochondrial malfunction. According to research, NaB can cause mitochondrial damage as part of its anti-tumor effect. We employed the JC-1 dye to measure mitochondrial membrane potential. HCT116 and DLD-1 cells were treated with 2 mmol/L NaB for 24 h and found that the mitochondrial membrane potential significantly decreased in both cell lines, whereas treatment with *F. nucleatum* supernatant increased the membrane potential of DLD-1 cells ($P < 0.001$) but did not significantly alter the mitochondrial membrane potential of HCT116 cells. The effect of NaB on mitochondrial membrane potential is eliminated when cells are treated with NaB and FAB, indicating that *F. nucleatum* metabolites can inhibit the damage caused to the mitochondrial membrane by NaB (Figure 6A and B).

ROS levels are a significant indicator of cell damage induced by normal physiological functions and environmental influences. When HCT116 and DLD-1 cells were treated with NaB, ROS levels significantly increased ($P < 0.001$) and the peak level shifted to the right. When cells were treated with FAB, there was a small reduction in ROS levels, but no significant difference when compared to the control group. When cells were co-treated with FAB and NaB, the effect of NaB was reversed (Figure 6C and D). This suggests that *F. nucleatum* metabolites have a protective impact on CRC cells, possibly by reducing the damage caused by NaB to mitochondria.

NaB damages the mitochondrial morphology of CRC cells

We assessed the amount of ATP present in HCT116 and DLD-1 cells to further test whether NaB had an impact on energy metabolism in CRC cells. Cells treated with NaB showed a substantial drop in ATP levels compared to the control group, but this impact was mitigated by FAB. Transmission electron microscopy showed that the mitochondria of the control group were largely undamaged, with distinct cristae and no visible damage. However, following NaB treatment, the mitochondrial matrix and cristae start to vanish, and in extreme situations, matrix overflow and mitochondrial membrane damage occurred. After the addition of FAB, the shape of the mitochondria was improved and the damage caused by

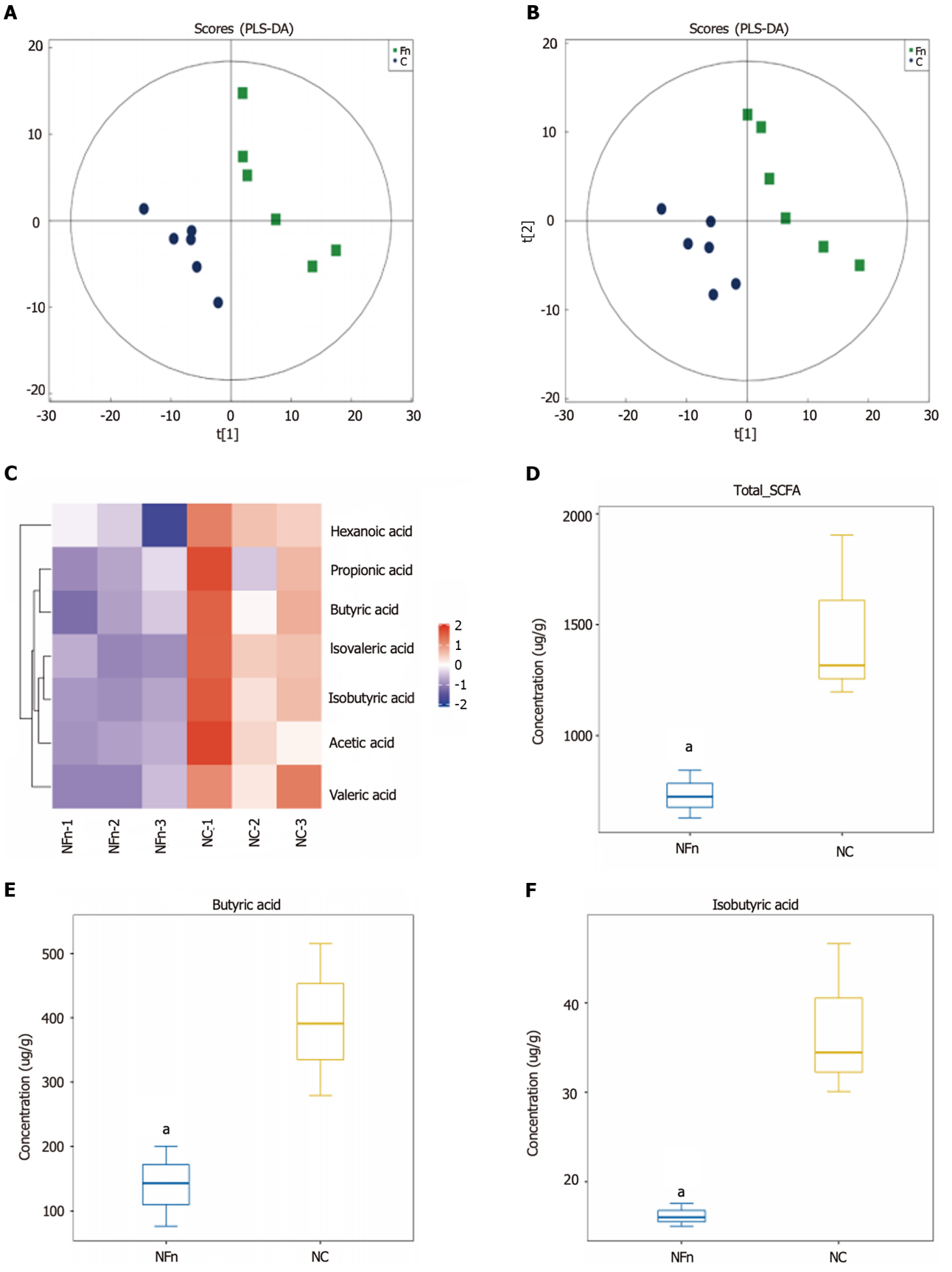

Figure 4 *Fusobacterium nucleatum* inhibits the formation of the short chain fatty acid butyric acid. A and B: Positive ion mode PLS-DA analysis diagram and negative ion mode PLS-DA analysis diagram show that there is a significant difference between the feces of mice treated with *Fusobacterium nucleatum* (*F. nucleatum*) and the control group (NC) in the PC1 direction (n = 6 for each group); C-F: The total amount of short-chain fatty acids (SCFAs), butyric acid, and isobutyric acid was significantly lower in the treatment group of *F. nucleatum* than the untreated group (n = 3 for each group). NFn: *F. nucleatum* treatment group. $^{a}P < 0.05$.

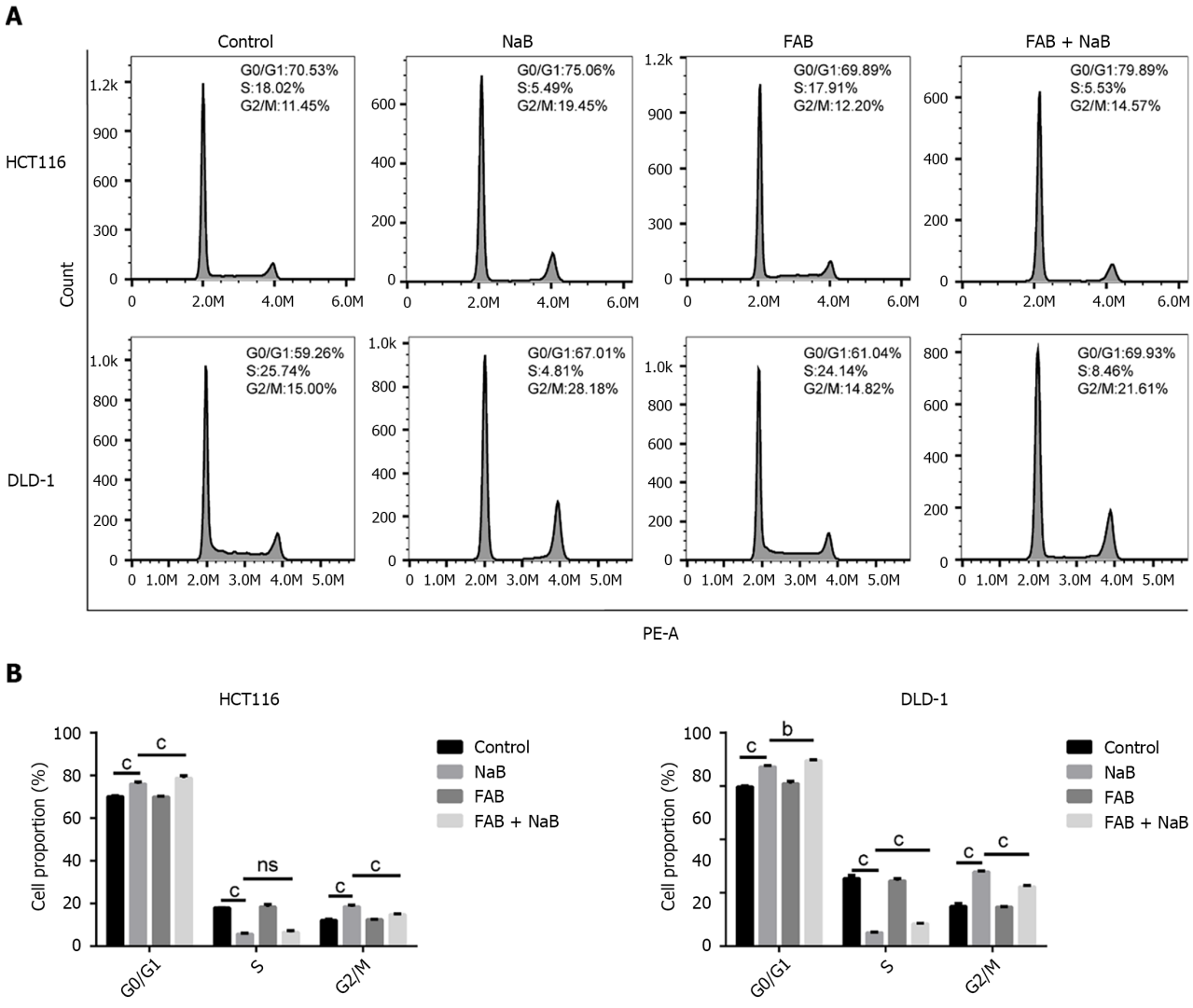

Figure 5 Effects of sodium butyrate and *Fusobacterium nucleatum* on the cell cycle of HCT116 and DLD-1 cells. A: Sodium butyrate (NaB) blocks the cell cycle at G2/M phase, while treatment with *Fusobacterium nucleatum* has no significant effect on the cell cycle; B: Statistical analysis of flow cytometry results. ns: $P > 0.05$, $^{b}P < 0.01$, $^{c}P < 0.001$. FAB: *Fusobacterium nucleatum* supernatant.

NaB was diminished (Figure 7).

NaB and F. nucleatum regulate CRC cell proliferation through AMPK signal pathway

According to our findings, NaB affects energy metabolism of CRC cell lines. The serine/threonine kinase AMPK is a significant energy sensor in cells and is essential for preserving energy balance. AMPK activation results in cell cycle arrest and inhibition of tumor development and will therefore be essential to cancer prevention. We investigated the expression levels of cycle-related proteins in the AMPK signaling pathway. Protein analysis revealed that AMPK was activated, p-AMPK expression increased, proliferation proteins such as CDK1, C-myc, and cyclin B1 were decreased, and cycle arrest protein P21 expression increased after NaB treatment of DLD-1 and HCT116 cells. In contrast, *F. nucleatum* treatment reduced AMPK phosphorylation and promoted the expression of cyclic-related proteins CDK1 and C-myc, indicating that *F. nucleatum* treatment promoted cell cycle progression in CRC cells. However, *F. nucleatum* and NaB were administered together, the effect of *F. nucleatum* was significantly attenuated (Figure 8), which is consistent with the findings that early NaB blocked the CRC cell cycle.

AMPK is necessary for NaB to inhibit CRC cell proliferation

To establish the role of AMPK in NaB-induced cell inhibition, we used AMPK-specific siRNA to knock down AMPK expression. In HCT116 and DLD-1 cells (Figure 9), AMPK-specific siRNA prevented AMPK phosphorylation and increased the expression of downstream associated proliferative proteins following NaB treatment (Figure 10). Flow cytometry analysis also revealed that AMPK-specific siRNA prevented the cycle arrest caused by NaB (Figure 11). These findings indicate that AMPK is required for NaB to inhibit CRC cell proliferation.

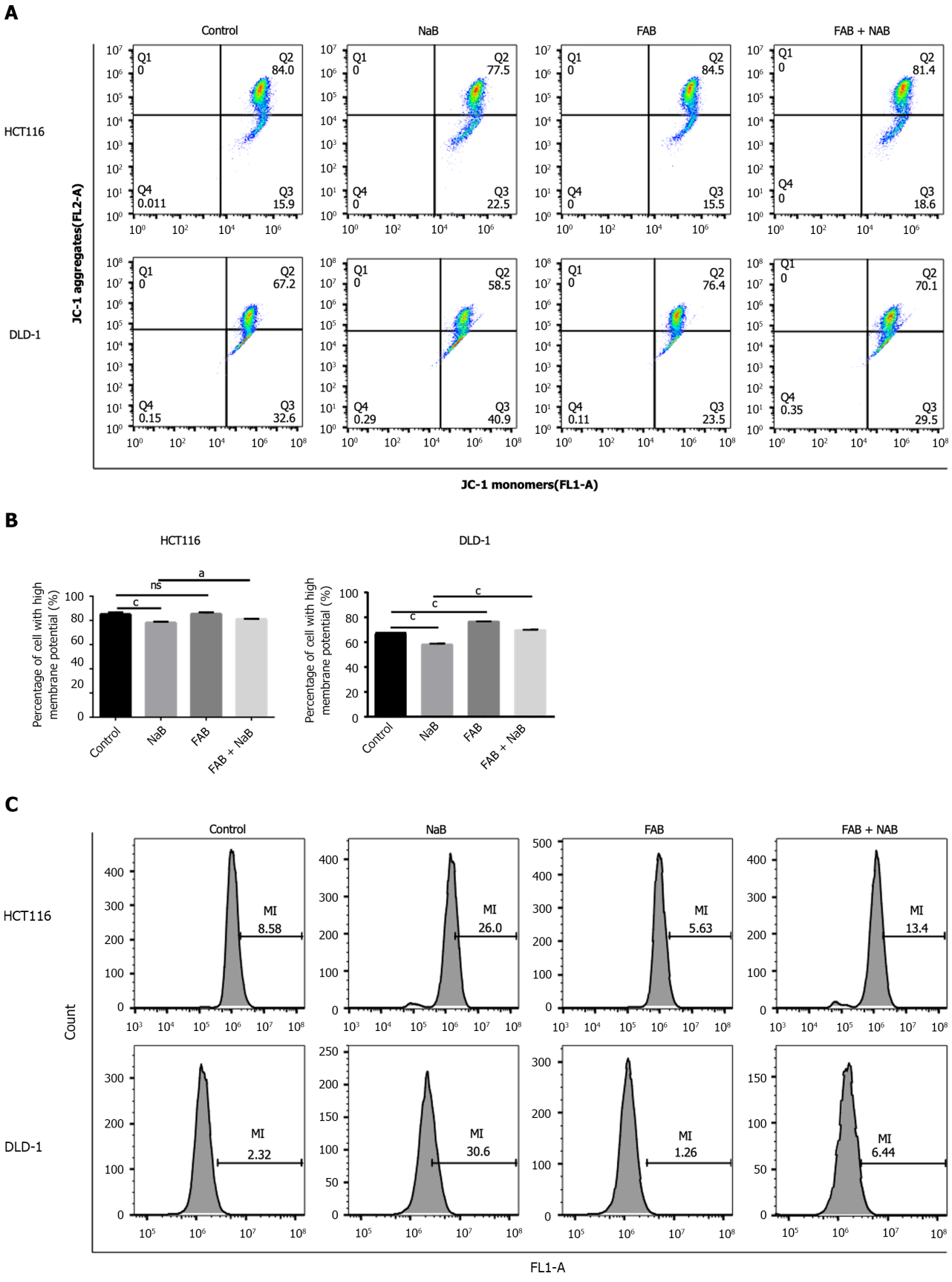
A
Control
NaB
FAB
FAB + NAB
HCT116
DLD-1
JC-1 aggregates(FL2-A)
JC-1 monomers(FL1-A)
Q1 0
Q2 84.0
Q4 0.011
Q3 15.9
Q2 77.5
Q4 0
Q3 22.5
Q2 84.5
Q4 0
Q3 15.5
Q2 81.4
Q4 0
Q3 18.6
Q2 67.2
Q4 0.15
Q3 32.6
Q2 58.5
Q4 0.29
Q3 40.9
Q2 76.4
Q4 0.11
Q3 23.5
Q2 70.1
Q4 0.35
Q3 29.5
B
HCT116
DLD-1
Percentage of cell with high membrane potential (%)
ns
a
c
Control
NaB
FAB
FAB + NaB
C
HCT116
DLD-1
Count
FL1-A
MI 8.58
MI 26.0
MI 5.63
MI 13.4
MI 2.32
MI 30.6
MI 1.26
MI 6.44

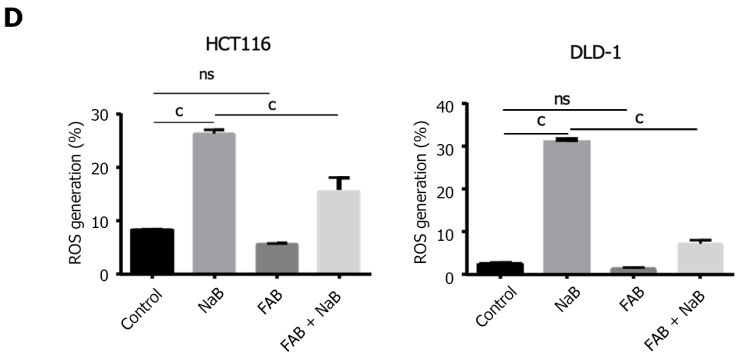

Figure 6 Effects of *Fusobacterium nucleatum* and sodium butyrate on mitochondrial membrane potential and reactive oxygen species in colorectal cancer cells. A: Sodium butyrate (NaB) decreased the mitochondrial membrane potential of colorectal cancer cells; however, the mitochondrial membrane potential of the cells recovered after treatment with NaB and *Fusobacterium nucleatum* supernatant (FAB); B: Statistical results of mitochondrial membrane potential experiments. Data are presented as mean ± standard deviation (SD) from at least three independent experiments; C: NaB stimulates the generation of reactive oxygen species (ROS) in colorectal cancer cells, FAB decreased the effect of NaB and reduced NaB damage to mitochondria; D: Statistical results of ROS. Data from at least three independent experiments are expressed as mean ± SD. ns: $P > 0.05$, $^{a}P < 0.05$, $^{c}P < 0.001$.

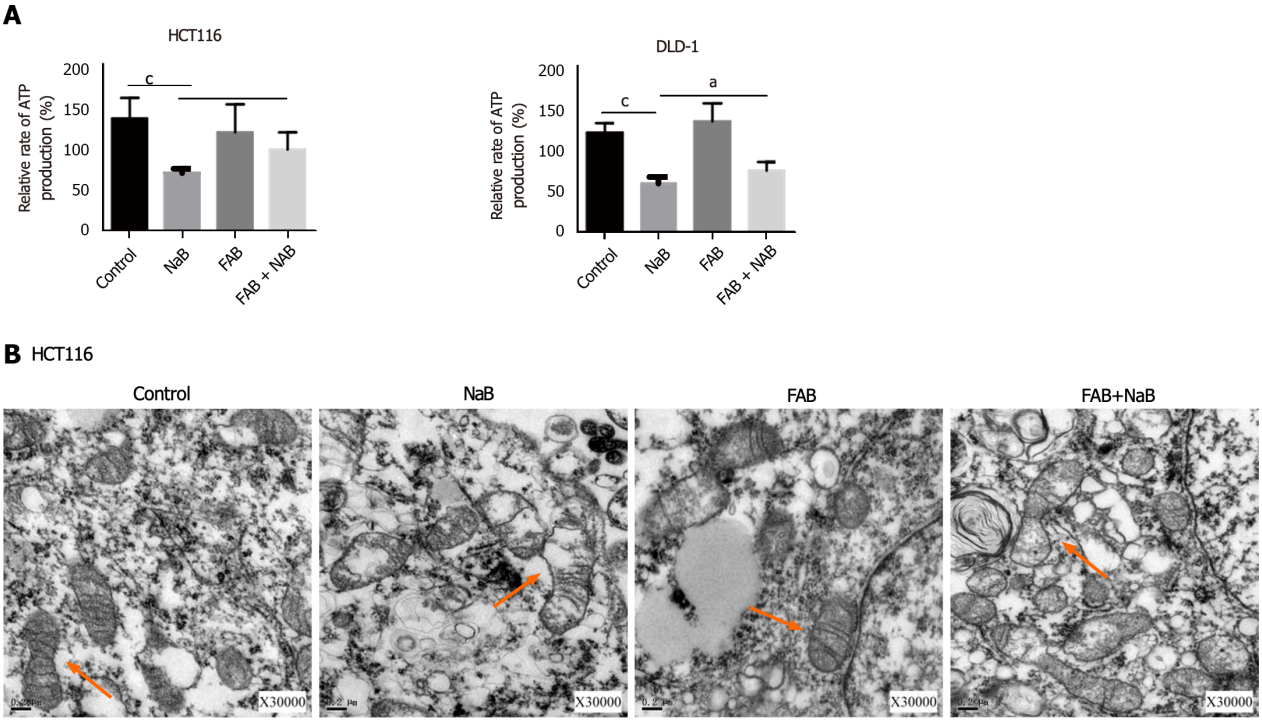

Figure 7 Sodium butyrate damages the mitochondrial morphology of colorectal cancer cells. A: Sodium butyrate (NaB) inhibits adenosine triphosphate synthesis, but treatment with *Fusobacterium nucleatum* supernatants (FAB) suppresses this effect; B: After treatment with NaB and FAB, morphological changes of mitochondria were observed under transmission electron microscopy. $^{a}P < 0.05$, $^{c}P < 0.001$.

DISCUSSION

There is a close relationship between the intestinal microecology and the occurrence and development of CRC. Dysregulation of microbial balance is often observed in CRC patients. According to some studies, *F. nucleatum* is abundant in the tumor microenvironment and fecal samples of CRC patients, thus its presence is regarded as one of the risk factors for the incidence and progression of CRC[24]. Yu *et al*[25] discovered that *F. nucleatum* content is prevalent in CRC tissues of patients whose cancer recurs after chemotherapy. 16S rDNA sequencing was employed in this experiment to detect bacterial diversity between CRC tissues and normal/paracancerous tissues. *Fusobacteriaceae* was discovered to be primarily concentrated in CRC tissues, whereas *Clostrididae* was shown to be abundant in normal tissues (Figure 1A). Using FISH technology to detect *F. nucleatum* content in CRC tissue and normal tissue samples, we found that the abundance of *F. nucleatum* in CRC tissue was significantly higher than that in normal tissue (Figure 1B), consistent with previous sequencing results. This indicates that *F. nucleatum* plays an important role in the occurrence and development of CRC.

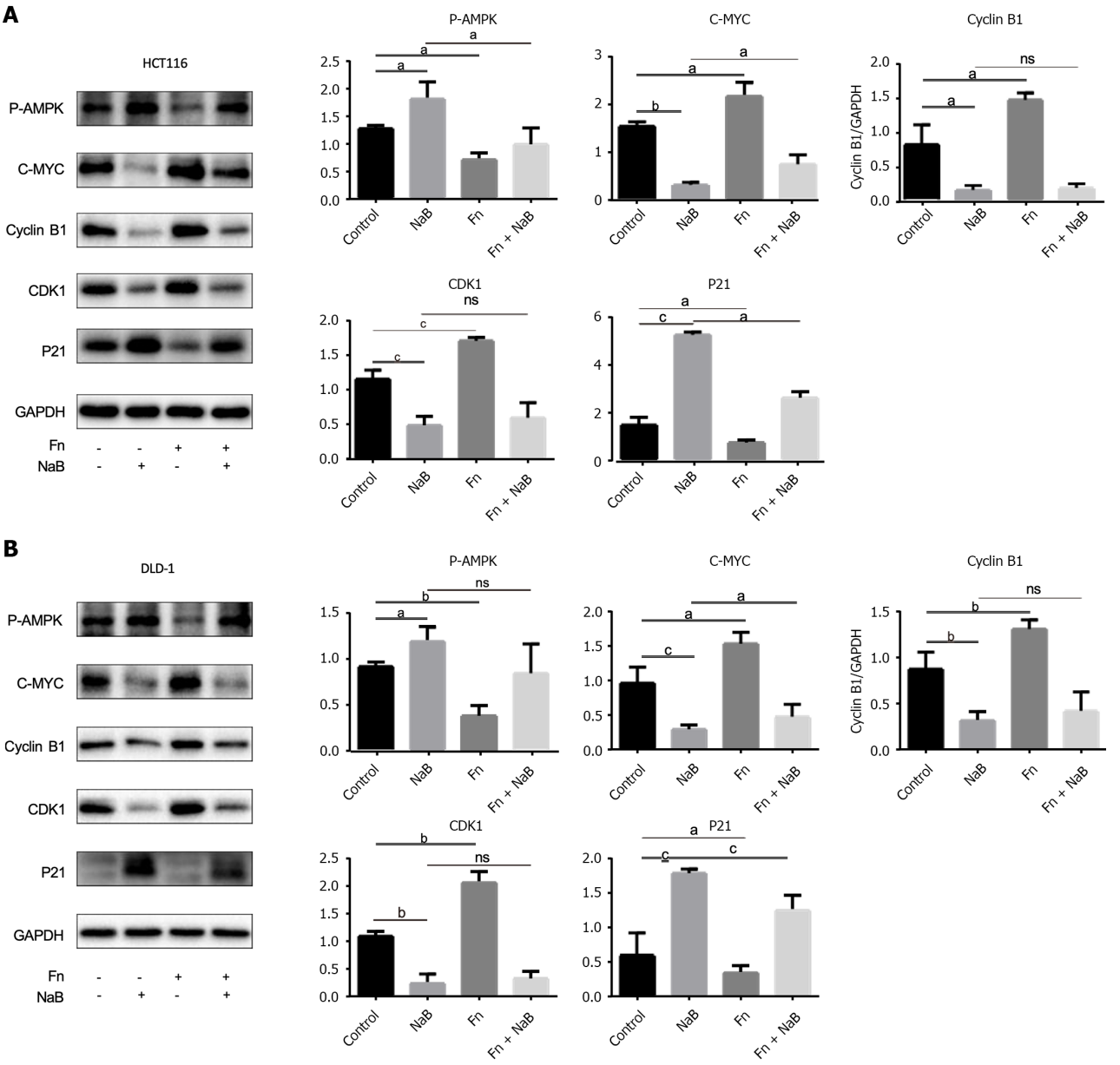

Figure 8 Sodium butyrate and *Fusobacterium nucleatum* regulates the proliferation of colorectal cancer cells through the adenosine monophosphate-activated protein kinase signal pathway. A and B: Adenosine monophosphate-activated protein kinase (AMPK) was activated in DLD-1 and HCT116 cells by treatment with sodium butyrate (NaB), leading to increased expression of phosphorylated AMPK (p-AMPK), decrease in expression of proliferation proteins such as CDK1, C-myc, and cyclin B1, and increase in expression of cycle arrest protein P21. However, treatment with *Fusobacterium nucleatum* inhibited the expression of p-AMPK. Data are expressed as mean ± standard deviation, from at least three independent experiments. $^{a}P < 0.05$, $^{b}P < 0.01$, $^{c}P < 0.001$, ns: $P > 0.05$.

This experiment used 16S rDNA sequencing on fecal samples from CRC patients and healthy individuals to further investigate the relationship between intestinal flora and CRC and found significant differences between the flora of CRC tissue and normal/paracancerous tissue (Figure 2A and B). Among these bacteria, butyric acid generating bacteria such as *Lac_Lachnospira*, *Lac_Roseburia*, and *Rum_Faecalibacterium* are common in feces of healthy patients (Figure 2C). Our research also found that the abundance of *Lac_Lachnospira*, *Lac_Roseburia*, and *Rum faecalibacterium* decreased significantly as CRC progressed from stage I to later stages (Figure 2D), indicating that butyric acid-producing bacteria play an important role in the progression of CRC.

After administering *F. nucleatum* intragastrically to BALB/c mice, their feces were analyzed to assess variations in bacterial populations and metabolic processes. The feces of mice treated with *F. nucleatum* contained much lower levels of butyric acid generating bacteria (*Lac_Rosebaria* and *Clo_Closteriales*) (Figure 3A and B). Interestingly, changes in the intestinal flora caused changes in intestinal metabolic patterns (Figure 4A and B), as well as changes in the production of SCFAs, such as butyric acid (Figure 4C-F). This finding implies that *F. nucleatum* may promote CRC progression by changing intestinal metabolites *in vitro* and *in vivo*.

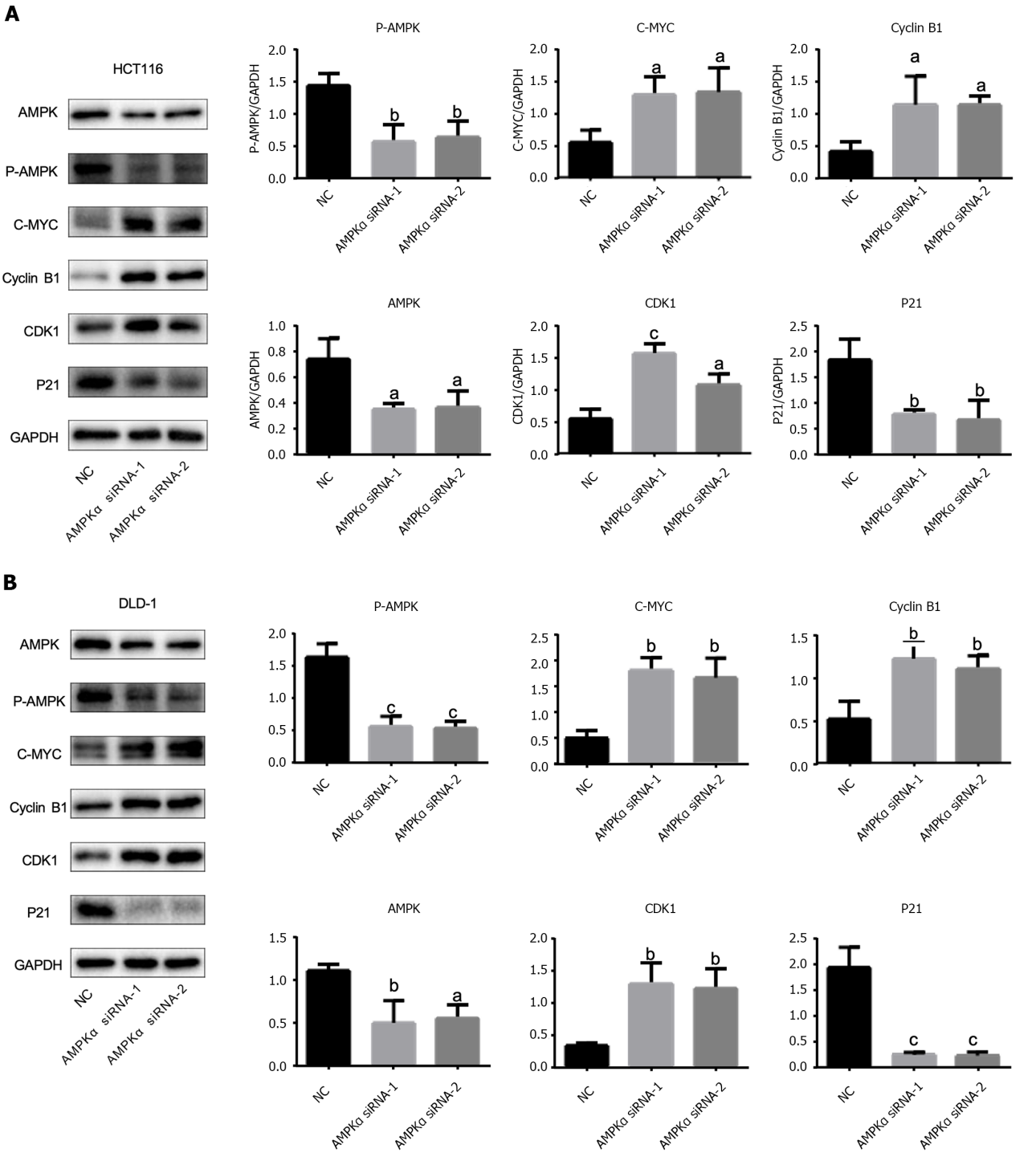

Figure 9 Adenosine monophosphate-activated protein kinaseα-specific small interfering RNA effectively reduced the expression of adenosine monophosphate-activated protein kinase and its phosphorylation in DLD-1 and HCT116 cells. A and B: Adenosine monophosphate-activated protein kinase (AMPK)α-specific small interfering RNA (siRNA) reduces AMPK phosphorylation, increases the expression of proteins such as C-myc, CDK1, and Cyclin B1, and reduces the expression of P21. Data are expressed as mean ± standard deviation, from at least three independent experiments. $^{a}P < 0.05$, $^{b}P < 0.01$, $^{c}P < 0.001$. NC: Control; p-AMPK: Phosphorylated-adenosine monophosphate-activated protein kinase.

Furthermore, studies have shown that *F. nucleatum* competes with the beneficial butyrate-producing *Clostridium butyricum* units, and that an abundance of *F. nucleatum* leads to a decrease in *Clostridium butyricum* abundance[26]. Therefore, it is vital to understand the association between *F. nucleatum* and butyric acid. We have previously treated DLD-1 cells with *F. nucleatum* and collected metabolites for nuclear magnetic resonance analysis. The results showed that after treating CRC cells with *F. nucleatum*, the extracellular concentration of butyrate significantly decreased[27]. Therefore, we speculate that *F. nucleatum* can actively consume butyric acid, promoting CRC development. In the future, we will further explore the relationship between *F. nucleatum* and *Clostridium butyricum*.

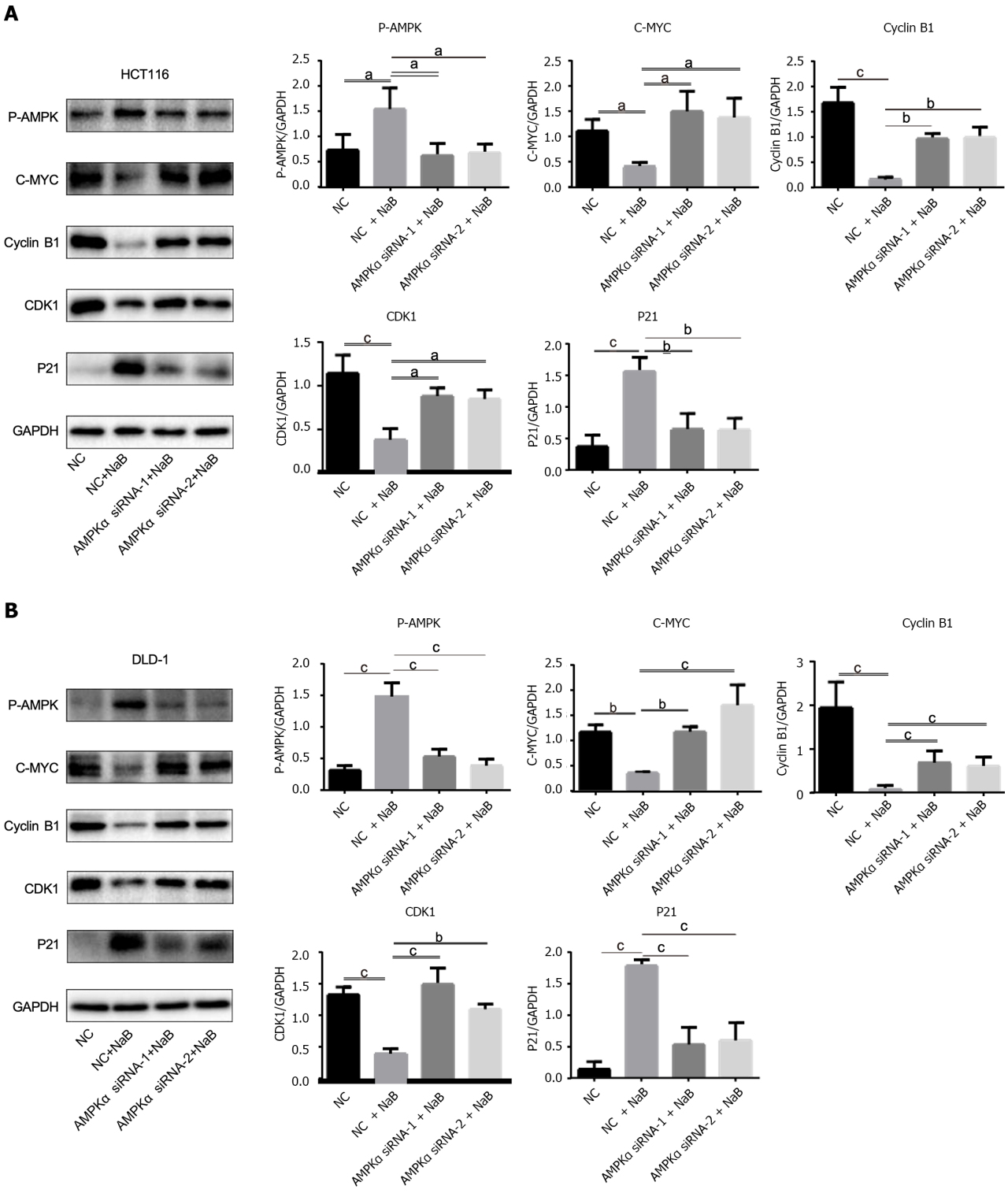

Figure 10 Adenosine monophosphate-activated protein kinaseα-specific small interfering RNA inhibits the anticancer effect of sodium butyrate. A and B: Sodium butyrate (NaB) activates adenosine monophosphate-activated protein kinase (AMPK), inhibits proliferative protein expression. However, after transfection with AMPK small interfering RNA (siRNA), AMPK is knocked down, and the inhibitory function of NaB on cancer is weakened. Data are expressed as mean ± standard deviation, from at least three independent experiments. $^{a}P < 0.05$, $^{b}P < 0.01$, $^{c}P < 0.001$. NC: Control; p-AMPK: Phosphorylated adenosine monophosphate-activated protein kinase.

Butyrate is the preferred energy source for colonic cells and has been shown to inhibit tumor development through a variety of mechanisms[28], including anti-inflammatory and immunomodulatory effects, down-regulation of the Wnt signaling pathway[29], inhibition of tumor cell proliferation and migration[21], limitation of tumor angiogenesis[22], induction of apoptosis[30], and promotion of tumor cell differentiation[31]. In this study, we used flow cytometry to investigate the effect of NaB on the cell cycle in DLD-1 and HCT116 CRC cell lines. Our findings showed that NaB arrested the cell cycle at the G2/M phase. When CRC cells were co-treated with *F. nucleatum* supernatant and NaB, there was a significant drop in the number of cells in the G2/M phase, demonstrating that *F. nucleatum* can mitigate the effect

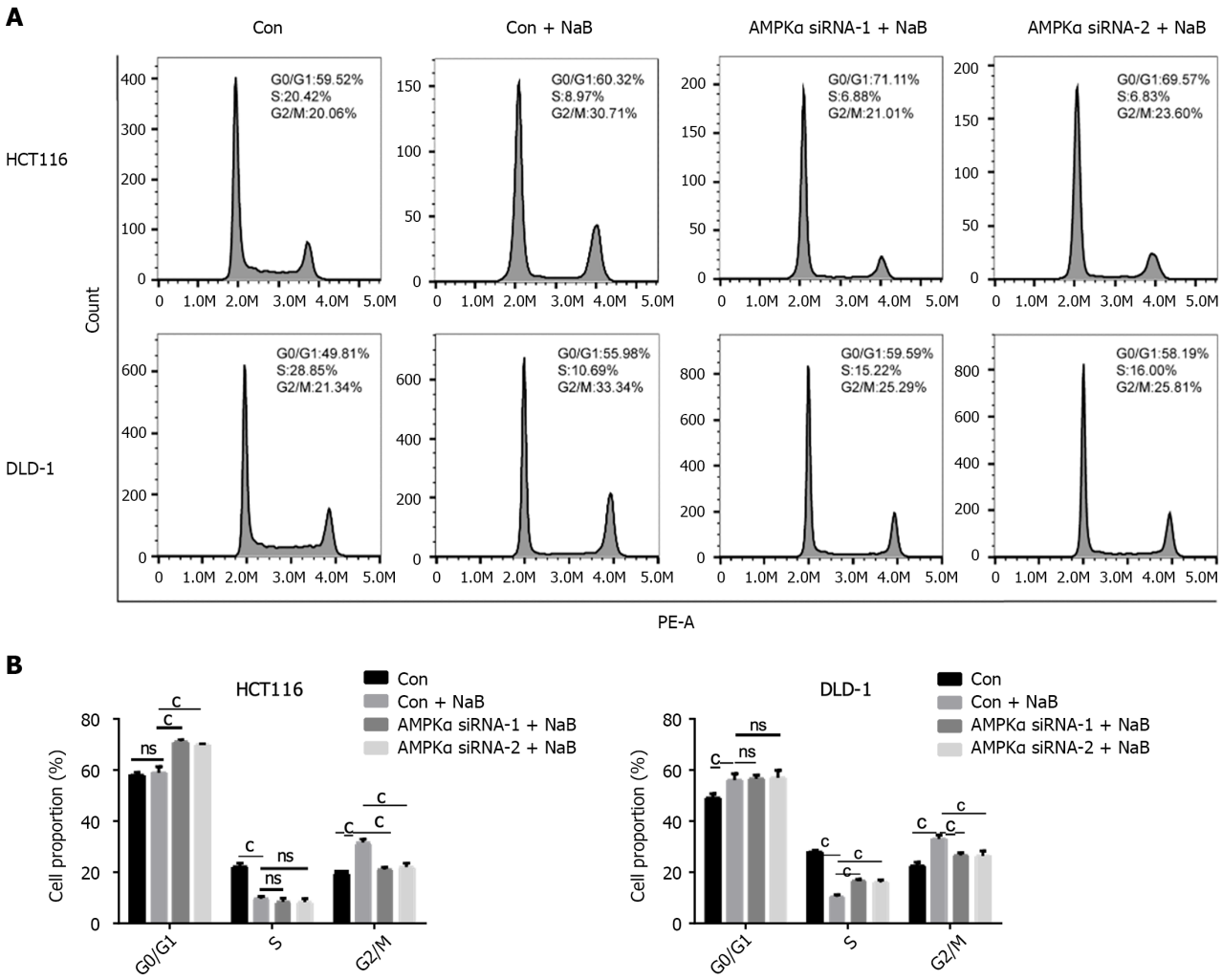

Figure 11 Adenosine monophosphate-activated protein kinase-specific small interfering RNA prevented cycle arrest caused by sodium butyrate. A and B: Sodium butyrate (NaB) arrested the cell cycle of DLD-1 and HCT116 cells in the G2/M phase, while adenosine monophosphate-activated protein kinase small interfering RNA (siRNA) transfection inhibited this phenomenon. ns: $P > 0.05$, $^{c}P < 0.001$. p-AMPK: Phosphorylated adenosine monophosphate-activated protein kinase.

of NaB on the cell cycle (Figure 5A and B).

ATP is the most direct source of energy in organisms, acting as the driving force for numerous biological operations. The mitochondrion is at the heart of cellular energy metabolism, producing the majority of ATP[32]. ROS are byproducts of aerobic respiration as well as signaling molecules that affect numerous cellular activities[33], and they play an important role in regulating various physiological functions in animals. In this study, we discovered that NaB treatment reduced ATP generation while increasing ROS production in CRC cells. The effect of NaB was partially inhibited when treated with *F. nucleatum* (Figures 6C, D, and 7A).

Furthermore, we used transmission electron microscopy to assess alterations in mitochondrial membrane potential and examined mitochondrial morphology in CRC cell lines. The mitochondrial membrane potential was shown to decrease after NaB treatment. In addition, the mitochondrial membrane was disrupted, the matrix began to melt, and the crista began to blur. When compared to the NaB group, the mitochondrial membrane potential increased in cells co-treated with NaB and *F. nucleatum* supernatants (FAB), as did the mitochondrial morphology. These findings reveal that NaB can disrupt energy metabolism by altering mitochondrial structure, whereas *F. nucleatum* metabolites have a protective impact and can mitigate NaB damage (Figure 7B).

AMPK is a highly conserved serine/threonine protein kinase that regulates cell cycle checkpoints in cancer cells in response to energy stress to coordinate proliferation and energy availability[34]. Because our experimental results show that NaB and *F. nucleatum* can impact ATP generation in CRC cells, we hypothesize that both affect CRC development *via* the AMPK pathway. After 24 h of treatment with *F. nucleatum*, the expression of p-AMPK was reduced, showing a relationship between *F. nucleatum* and the AMPK pathway. We evaluated the expression levels of cell cycle-related proteins in the AMPK pathway to further analyze the relationship between *F. nucleatum*, NaB, and the AMPK pathway. Western blotting revealed that NaB increased the expression of Thr172 p-AMPK and activated AMPK in both CRC cell lines (HCT116 and DLD-1) (Figure 8A and B). Furthermore, the AMPK-related proliferative proteins c-Myc, CDK1 and cyclin B1 were downregulated, whereas the cycle inhibitory protein P21 was upregulated. *F. nucleatum* treatment increased the expression of cyclin-related proteins c-Myc, CDK1 and cyclin B1, while inhibiting the production of

phosphorylated AMPK and P21. These findings suggest that *F. nucleatum* and NaB can both regulate the proliferation of CRC cells *via* AMPK.

We employed AMPK-specific siRNA to knock down AMPK expression and then co-treated HCT116 and DLD-1 cells with NaB to explore the role of AMPK in CRC cell proliferation. AMPK-specific siRNA substantially decreases AMPK phosphorylation and the expression of its downstream proteins c-Myc, cyclinB1, and CDK1 (Figure 9A and B). When cells were co-treated with AMPK-specific siRNA and NaB, AMPK-specific siRNA prevented the induction of cell cycle arrest observed with NaB alone (Figures 10 and 11). These data suggest that NaB requires AMPK to inhibit CRC cell proliferation.

CONCLUSION

In conclusion, *F. nucleatum* can regulate the intestinal metabolite butyrate, and NaB can regulate energy metabolism and prevent CRC proliferation *via* the AMPK pathway. The findings of this study may provide a better understanding of CRC pathogenesis , thereby facilitating the development of more effective therapeutic approaches.

ARTICLE HIGHLIGHTS

Research background

Colorectal cancer (CRC) ranks among the most prevalent malignant neoplasms globally. *Fusobacterium nucleatum (F. nucleatum)* has been implicated in the initiation, progression, and prognostic outcomes of CRC. Butyrate, a short-chain fatty acid (SCFA) derived from the bacterial fermentation of soluble dietary fiber, exhibits inhibitory effects on several types of cancers.

Research motivation

Recent research has demonstrated that the SCFA butyrate can suppress the proliferation, enrichment, and adherence of *F. nucleatum* in CRC tissues. This suppression is achieved by the downregulation of adhesion-associated outer membrane proteins, including RadD, FomA, and FadA. Consequently, this leads to a decrease in the colonization and invasion of *F. nucleatum* and mitigates its contribution to chemoresistance. Therefore, this study aims to investigate whether *F. nucleatum* can influence the synthesis of the intestinal metabolite butyric acid, thereby facilitating the development of CRC.

Research objectives

Exploring whether *F. nucleatum* affects the production of intestinal metabolite butyrate to promote CRC development.

Research methods

Fecal samples were collected from mice in the treatment group following oral administration of *F. nucleatum* for the analysis of SCFAs and 16S rDNA. Concurrently, CRC cells underwent co-treatment with *F. nucleatum* and sodium butyrate (NaB) *in vitro* to assess alterations in the cell cycle, mitochondrial functionality, and the expression of pertinent proteins.

Research results

The abundance of *F. nucleatum* is markedly elevated in fecal specimens and CRC tissues from patients with CRC. *F. nucleatum* suppresses the synthesis of the SCFA butyric acid. NaB impairs mitochondrial functionality and impedes the cell cycle in CRC cells. Both NaB and *F. nucleatum* modulate the growth of CRC cells *via* the adenosine monophosphate-activated protein kinase (AMPK) signaling pathway. The presence of AMPK is essential for NaB's effectiveness in inhibiting CRC cell proliferation.

Research conclusions

Our findings showed that the abundance of *F. nucleatum* is significantly high in fecal samples and CRC tissues from CRC patients. *F. nucleatum* impedes the synthesis of the SCFA butyric acid. NaB compromises mitochondrial functionality and obstructs the cell cycle in CRC cells. The growth of CRC cells is modulated by both NaB and *F. nucleatum via* the AMPK signaling pathway. The presence of AMPK is critical for the ability of NaB to curb CRC cell proliferation.

Research perspectives

The outcomes of this research could enhance our comprehension of CRC pathogenesis, potentially leading to the formulation of more efficacious therapeutic strategies.

ACKNOWLEDGEMENTS

The author thanks Dr. Xu Chang from the First Affiliated Hospital of Wenzhou Medical University for providing cancer pathological sections.

FOOTNOTES

Co-corresponding authors: Yong-Liang Lou and Xiang Li.

Author contributions: Lou YL and Li X are responsible for funding acquisition; Wu QL, Fang XT, and Li X contributed to study conceptualization; Ji L, Lou YL and Li X supervised the study; Li X wrote, reviewed and edited the manuscript and performed project management; Wu QL, Fang XT, Wan XX, Ding QY, and Zhang YJ participated in the data curation and investigation; Wu QL and Fang XT contributed to the methodology of this study; Wu QL is responsible for original draft preparation; Ji L is responsible for resources; Ji L and Lou YL were involved in project administration, Li X and Lou YL contributed equally to this work as co-corresponding authors; All authors were involved in the critical review of the results and have contributed to, read, and approved the final manuscript.

Supported by the Key Discipline of Zhejiang Province in Medical Technology (First Class, Category A) and the Health Project of the Science and Technology Department of Wenzhou, No. Y20220029.

Institutional review board statement: This work was approved by the First Affiliated Hospital of Wenzhou Medical University.

Institutional animal care and use committee statement: All animal studies were conducted in compliance with the animal experiment guidelines of Wenzhou Medical University. The protocols were approved by the Animal Experimental Ethics Committee, No. wydw2022-0217).

Conflict-of-interest statement: All the authors report having no relevant conflicts of interest for this article.

Data sharing statement: The datasets presented in this study can be found in online repositories. The names of the repository/repositories and accession number(s) can be found below: National Center for Biotechnology Information (NCBI) BioProject, https://www.ncbi.nlm.nih.gov/bioproject/, PRJNA799208: National Center for Biotechnology Information (NCBI) SRA, https://www.ncbi.nlm.nih.gov/sra/, PRJNA1015171 and National Genomics Data Center (NGDC) China National Center for Bioinformation (CNCB)/Beijing Institute of Genomics (BIG), Chinese Academy of Sciences (CAS) Open Archive for Miscellaneous Data (OMIX), https://ngdc.cncb.ac.cn/omix/, PRJCA019758.

ARRIVE guidelines statement: The authors have read the ARRIVE guidelines, and the manuscript was prepared and revised according to the ARRIVE guidelines.

Country/Territory of origin: China

ORCID number: Ling Ji 0000-0002-2867-3755; Yong-Liang Lou 0000-0003-4198-0001; Xiang Li 0000-0001-6346-1574.

S-Editor: Wang JJ
L-Editor: Filipodia
P-Editor: Chen YX

REFERENCES

1 **Wong MCS**, Huang J, Huang JLW, Pang TWY, Choi P, Wang J, Chiang JI, Jiang JY. Global Prevalence of Colorectal Neoplasia: A Systematic Review and Meta-Analysis. *Clin Gastroenterol Hepatol* 2020; **18**: 553-561.e10 [PMID: 31323383 DOI: 10.1016/j.cgh.2019.07.016]
2 **Chen W**, Zheng R, Baade PD, Zhang S, Zeng H, Bray F, Jemal A, Yu XQ, He J. Cancer statistics in China, 2015. *CA Cancer J Clin* 2016; **66**: 115-132 [PMID: 26808342 DOI: 10.3322/caac.21338]
3 **Seol JE**, Kim J, Lee BH, Hwang DY, Jeong J, Lee HJ, Ahn YO, Lee JE, Kim DH. Folate, alcohol, ADH1B and ALDH2 and colorectal cancer risk. *Public Health Nutr* 2020; 1-8 [PMID: 32223781 DOI: 10.1017/S136898001900452X]
4 **Carr PR**, Weigl K, Edelmann D, Jansen L, Chang-Claude J, Brenner H, Hoffmeister M. Estimation of Absolute Risk of Colorectal Cancer Based on Healthy Lifestyle, Genetic Risk, and Colonoscopy Status in a Population-Based Study. *Gastroenterology* 2020; **159**: 129-138.e9 [PMID: 32179093 DOI: 10.1053/j.gastro.2020.03.016]
5 **Park EM**, Chelvanambi M, Bhutiani N, Kroemer G, Zitvogel L, Wargo JA. Targeting the gut and tumor microbiota in cancer. *Nat Med* 2022; **28**: 690-703 [PMID: 35440726 DOI: 10.1038/s41591-022-01779-2]

6 **Kim J**, Lee HK. Potential Role of the Gut Microbiome In Colorectal Cancer Progression. *Front Immunol* 2021; **12**: 807648 [PMID: 35069592 DOI: 10.3389/fimmu.2021.807648]

7 **Wong CC**, Yu J. Gut microbiota in colorectal cancer development and therapy. *Nat Rev Clin Oncol* 2023; **20**: 429-452 [PMID: 37169888 DOI: 10.1038/s41571-023-00766-x]

8 **Dove WF**, Clipson L, Gould KA, Luongo C, Marshall DJ, Moser AR, Newton MA, Jacoby RF. Intestinal neoplasia in the ApcMin mouse: independence from the microbial and natural killer (beige locus) status. *Cancer Res* 1997; **57**: 812-814 [PMID: 9041176]

9 **Yu J**, Feng Q, Wong SH, Zhang D, Liang QY, Qin Y, Tang L, Zhao H, Stenvang J, Li Y, Wang X, Xu X, Chen N, Wu WK, Al-Aama J, Nielsen HJ, Kiilerich P, Jensen BA, Yau TO, Lan Z, Jia H, Li J, Xiao L, Lam TY, Ng SC, Cheng AS, Wong VW, Chan FK, Yang H, Madsen L, Datz C, Tilg H, Wang J, Brünner N, Kristiansen K, Arumugam M, Sung JJ. Metagenomic analysis of faecal microbiome as a tool towards targeted non-invasive biomarkers for colorectal cancer. *Gut* 2017; **66**: 70-78 [PMID: 26408641 DOI: 10.1136/gutjnl-2015-309800]

10 **Pleguezuelos-Manzano C**, Puschhof J, Rosendahl Huber A, van Hoeck A, Wood HM, Nomburg J, Gurjao C, Manders F, Dalmasso G, Stege PB, Paganelli FL, Geurts MH, Beumer J, Mizutani T, Miao Y, van der Linden R, van der Elst S; Genomics England Research Consortium, Garcia KC, Top J, Willems RJL, Giannakis M, Bonnet R, Quirke P, Meyerson M, Cuppen E, van Boxtel R, Clevers H. Mutational signature in colorectal cancer caused by genotoxic pks(+) E. coli. *Nature* 2020; **580**: 269-273 [PMID: 32106218 DOI: 10.1038/s41586-020-2080-8]

11 **Motamedi H**, Ari MM, Shahlaei M, Moradi S, Farhadikia P, Alvandi A, Abiri R. Designing multi-epitope vaccine against important colorectal cancer (CRC) associated pathogens based on immunoinformatics approach. *BMC Bioinformatics* 2023; **24**: 65 [PMID: 36829112 DOI: 10.1186/s12859-023-05197-0]

12 **Kong C**, Liang L, Liu G, Du L, Yang Y, Liu J, Shi D, Li X, Ma Y. Integrated metagenomic and metabolomic analysis reveals distinct gut-microbiome-derived phenotypes in early-onset colorectal cancer. *Gut* 2023; **72**: 1129-1142 [PMID: 35953094 DOI: 10.1136/gutjnl-2022-327156]

13 **Lee MH**. Harness the functions of gut microbiome in tumorigenesis for cancer treatment. *Cancer Commun (Lond)* 2021; **41**: 937-967 [PMID: 34355542 DOI: 10.1002/cac2.12200]

14 **Seely KD**, Morgan AD, Hagenstein LD, Florey GM, Small JM. Bacterial Involvement in Progression and Metastasis of Colorectal Neoplasia. *Cancers (Basel)* 2022; **14** [PMID: 35205767 DOI: 10.3390/cancers14041019]

15 **Castellarin M**, Warren RL, Freeman JD, Dreolini L, Krzywinski M, Strauss J, Barnes R, Watson P, Allen-Vercoe E, Moore RA, Holt RA. Fusobacterium nucleatum infection is prevalent in human colorectal carcinoma. *Genome Res* 2012; **22**: 299-306 [PMID: 22009989 DOI: 10.1101/gr.126516.111]

16 **Yachida S**, Mizutani S, Shiroma H, Shiba S, Nakajima T, Sakamoto T, Watanabe H, Masuda K, Nishimoto Y, Kubo M, Hosoda F, Rokutan H, Matsumoto M, Takamaru H, Yamada M, Matsuda T, Iwasaki M, Yamaji T, Yachida T, Soga T, Kurokawa K, Toyoda A, Ogura Y, Hayashi T, Hatakeyama M, Nakagama H, Saito Y, Fukuda S, Shibata T, Yamada T. Metagenomic and metabolomic analyses reveal distinct stage-specific phenotypes of the gut microbiota in colorectal cancer. *Nat Med* 2019; **25**: 968-976 [PMID: 31171880 DOI: 10.1038/s41591-019-0458-7]

17 **Tunsjø HS**, Gundersen G, Rangnes F, Noone JC, Endres A, Bemanian V. Detection of Fusobacterium nucleatum in stool and colonic tissues from Norwegian colorectal cancer patients. *Eur J Clin Microbiol Infect Dis* 2019; **38**: 1367-1376 [PMID: 31025134 DOI: 10.1007/s10096-019-03562-7]

18 **Wang N**, Fang JY. Fusobacterium nucleatum, a key pathogenic factor and microbial biomarker for colorectal cancer. *Trends Microbiol* 2023; **31**: 159-172 [PMID: 36058786 DOI: 10.1016/j.tim.2022.08.010]

19 **Kim SM**, Vetrivel P, Ha SE, Kim HH, Kim JA, Kim GS. Apigetrin induces extrinsic apoptosis, autophagy and G2/M phase cell cycle arrest through PI3K/AKT/mTOR pathway in AGS human gastric cancer cell. *J Nutr Biochem* 2020; **83**: 108427 [PMID: 32559585 DOI: 10.1016/j.jnutbio.2020.108427]

20 **Chattopadhyay I**, Gundamaraju R, Jha NK, Gupta PK, Dey A, Mandal CC, Ford BM. Interplay between Dysbiosis of Gut Microbiome, Lipid Metabolism, and Tumorigenesis: Can Gut Dysbiosis Stand as a Prognostic Marker in Cancer? *Dis Markers* 2022; **2022**: 2941248 [PMID: 35178126 DOI: 10.1155/2022/2941248]

21 **Zeng H**, Briske-Anderson M. Prolonged butyrate treatment inhibits the migration and invasion potential of HT1080 tumor cells. *J Nutr* 2005; **135**: 291-295 [PMID: 15671229 DOI: 10.1093/jn/135.2.291]

22 **Zgouras D**, Wächtershäuser A, Frings D, Stein J. Butyrate impairs intestinal tumor cell-induced angiogenesis by inhibiting HIF-1alpha nuclear translocation. *Biochem Biophys Res Commun* 2003; **300**: 832-838 [PMID: 12559948 DOI: 10.1016/s0006-291x(02)02916-9]

23 **Yu T**, Ji L, Lou L, Ye S, Fang X, Li C, Jiang F, Gao H, Lou Y, Li X. Fusobacterium nucleatum Affects Cell Apoptosis by Regulating Intestinal Flora and Metabolites to Promote the Development of Colorectal Cancer. *Front Microbiol* 2022; **13**: 841157 [PMID: 35369440 DOI: 10.3389/fmicb.2022.841157]

24 **Hashemi Goradel N**, Heidarzadeh S, Jahangiri S, Farhood B, Mortezaee K, Khanlarkhani N, Negahdari B. Fusobacterium nucleatum and colorectal cancer: A mechanistic overview. *J Cell Physiol* 2019; **234**: 2337-2344 [PMID: 30191984 DOI: 10.1002/jcp.27250]

25 **Yu T**, Guo F, Yu Y, Sun T, Ma D, Han J, Qian Y, Kryczek I, Sun D, Nagarsheth N, Chen Y, Chen H, Hong J, Zou W, Fang JY. Fusobacterium nucleatum Promotes Chemoresistance to Colorectal Cancer by Modulating Autophagy. *Cell* 2017; **170**: 548-563.e16 [PMID: 28753429 DOI: 10.1016/j.cell.2017.07.008]

26 **Zheng DW**, Dong X, Pan P, Chen KW, Fan JX, Cheng SX, Zhang XZ. Phage-guided modulation of the gut microbiota of mouse models of colorectal cancer augments their responses to chemotherapy. *Nat Biomed Eng* 2019; **3**: 717-728 [PMID: 31332342 DOI: 10.1038/s41551-019-0423-2]

27 **Huang JP**, Yang LN, Fang XT, Yu TT, Li X, Lou YL. [Fusobacterium nucleatum and Cdk5 promote colorectal cancer cell migration]. *Chinese J Microecol* 2020; **32**: 889-892,896 [DOI: 10.13381/j.cnki.cjm.202008005]

28 **O'Keefe SJ**. Diet, microorganisms and their metabolites, and colon cancer. *Nat Rev Gastroenterol Hepatol* 2016; **13**: 691-706 [PMID: 27848961 DOI: 10.1038/nrgastro.2016.165]

29 **Bordonaro M**, Lazarova DL, Sartorelli AC. Butyrate and Wnt signaling: a possible solution to the puzzle of dietary fiber and colon cancer risk? *Cell Cycle* 2008; **7**: 1178-1183 [PMID: 18418037 DOI: 10.4161/cc.7.9.5818]

30 **Chirakkal H**, Leech SH, Brookes KE, Prais AL, Waby JS, Corfe BM. Upregulation of BAK by butyrate in the colon is associated with increased Sp3 binding. *Oncogene* 2006; **25**: 7192-7200 [PMID: 16732318 DOI: 10.1038/sj.onc.1209702]

31 **Comalada M**, Bailón E, de Haro O, Lara-Villoslada F, Xaus J, Zarzuelo A, Gálvez J. The effects of short-chain fatty acids on colon epithelial proliferation and survival depend on the cellular phenotype. *J Cancer Res Clin Oncol* 2006; **132**: 487-497 [PMID: 16788843 DOI: 10.1007/s00432-006-0092-x]

32 **Zhang J**, Qiao W, Luo Y. Mitochondrial quality control proteases and their modulation for cancer therapy. *Med Res Rev* 2023; **43**: 399-436

[PMID: 36208112 DOI: 10.1002/med.21929]

33 **Kasai S**, Shimizu S, Tatara Y, Mimura J, Itoh K. Regulation of Nrf2 by Mitochondrial Reactive Oxygen Species in Physiology and Pathology. *Biomolecules* 2020; **10** [PMID: 32079324 DOI: 10.3390/biom10020320]

34 **Steinberg GR**, Hardie DG. New insights into activation and function of the AMPK. *Nat Rev Mol Cell Biol* 2023; **24**: 255-272 [PMID: 36316383 DOI: 10.1038/s41580-022-00547-x]

World Journal of Gastroenterology

Submit a Manuscript: https://www.f6publishing.com

World J Gastroenterol 2024 April 14; 30(14): 2038-2058

DOI: 10.3748/wjg.v30.i14.2038

ISSN 1007-9327 (print) ISSN 2219-2840 (online)

ORIGINAL ARTICLE

Basic Study

Comparative transcriptomic analysis reveals the molecular changes of acute pancreatitis in experimental models

Pan Zheng, Xue-Yang Li, Xiao-Yu Yang, Huan Wang, Ling Ding, Cong He, Jian-Hua Wan, Hua-Jing Ke, Nong-Hua Lu, Nian-Shuang Li, Yin Zhu

Specialty type: Gastroenterology and hepatology

Provenance and peer review: Unsolicited article; Externally peer reviewed.

Peer-review model: Single blind

Peer-review report's scientific quality classification

Grade A (Excellent): 0
Grade B (Very good): B, B
Grade C (Good): 0
Grade D (Fair): 0
Grade E (Poor): 0

P-Reviewer: Hakim GD, Turkey; Rodrigo L, Spain

Received: December 8, 2023
Peer-review started: December 8, 2023
First decision: January 4, 2024
Revised: January 19, 2024
Accepted: March 1, 2024
Article in press: March 1, 2024
Published online: April 14, 2024

Pan Zheng, Xue-Yang Li, Xiao-Yu Yang, Huan Wang, Ling Ding, Cong He, Jian-Hua Wan, Hua-Jing Ke, Nong-Hua Lu, Nian-Shuang Li, Yin Zhu, Department of Gastroenterology, Digestive Disease Hospital, The First Affiliated Hospital, Jiangxi Medical College, Nanchang University, Nanchang 330006, Jiangxi Province, China

Corresponding author: Yin Zhu, MD, PhD, Chief Doctor, Department of Gastroenterology, Digestive Disease Hospital, The First Affiliated Hospital, Jiangxi Medical College, Nanchang University, No. 17 Yongwaizheng Street, Donghu District, Nanchang 330006, Jiangxi Province, China. ndyfy01977@ncu.edu.cn

Abstract

BACKGROUND

Acute pancreatitis (AP) encompasses a spectrum of pancreatic inflammatory conditions, ranging from mild inflammation to severe pancreatic necrosis and multisystem organ failure. Given the challenges associated with obtaining human pancreatic samples, research on AP predominantly relies on animal models. In this study, we aimed to elucidate the fundamental molecular mechanisms underlying AP using various AP models.

AIM

To investigate the shared molecular changes underlying the development of AP across varying severity levels.

METHODS

AP was induced in animal models through treatment with caerulein alone or in combination with lipopolysaccharide (LPS). Additionally, using *Ptf1α* to drive the specific expression of the *hM3* promoter in pancreatic acinar cells transgenic C57BL/6J- *hM3/Ptf1α(cre)* mice were administered Clozapine N-oxide to induce AP. Subsequently, we conducted RNA sequencing of pancreatic tissues and validated the expression of significantly different genes using the Gene Expression Omnibus (GEO) database.

RESULTS

Caerulein-induced AP showed severe inflammation and edema, which were exacerbated when combined with LPS and accompanied by partial pancreatic tissue necrosis. Compared with the control group, RNA sequencing analysis

revealed 880 significantly differentially expressed genes in the caerulein model and 885 in the caerulein combined with the LPS model. Kyoto Encyclopedia of Genes and Genomes enrichment analysis and Gene Set Enrichment Analysis indicated substantial enrichment of the *TLR* and *NOD*-like receptor signaling pathway, TLR signaling pathway, and *NF-κB* signaling pathway, alongside elevated levels of apoptosis-related pathways, such as apoptosis, *P53* pathway, and phagosome pathway. The significantly elevated genes in the *TLR* and *NOD*-like receptor signaling pathways, as well as in the apoptosis pathway, were validated through quantitative real-time PCR experiments in animal models. Validation from the GEO database revealed that only *MYD88* concurred in both mouse pancreatic tissue and human AP peripheral blood, while *TLR1*, *TLR7*, *RIPK3*, and *OAS2* genes exhibited marked elevation in human AP. The genes *TUBA1A* and *GADD45A* played significant roles in apoptosis within human AP. The transgenic mouse model *hM3/Ptf1α(cre)* successfully validated significant differential genes in the *TLR* and *NOD*-like receptor signaling pathways as well as the apoptosis pathway, indicating that these pathways represent shared pathological processes in AP across different models.

CONCLUSION

The *TLR* and *NOD* receptor signaling pathways play crucial roles in the inflammatory progression of AP, notably the *MYD88* gene. Apoptosis holds a central position in the necrotic processes of AP, with *TUBA1A* and *GADD45A* genes exhibiting prominence in human AP.

Key Words: Acute pancreatitis; RNA-sequencing; Experimental acute pancreatitis models; Inflammatory; Apoptosis; TLR and NOD-like signaling pathways

Core Tip: AP is a critical emergency condition with no effective targeted therapeutic interventions currently available. Therefore, RNA sequencing (RNA-seq) was employed to investigate the molecular alterations in acute pancreatitis (AP), aiming to identify novel therapeutic strategies. The RNA-seq analysis showed a significant upregulation of *TLR* and *NOD*-like signaling pathways in AP, with crucial involvement of genes such as *TLR7*, *IRF7*, and *MYD88*. Notably, the *TUBA1A* and *GADD45A* genes were identified as key players in the apoptosis signaling pathway. Substantial evidence was provided through comprehensive validation using Gene Expression Omnibus Series datasets from human peripheral blood and mouse pancreatic tissues, as well as transgenic mouse models to examine inflammation and apoptosis-related molecules. This study offers fresh insights for future therapeutic approaches in managing AP and establishes new directions for subsequent fundamental investigations.

Citation: Zheng P, Li XY, Yang XY, Wang H, Ding L, He C, Wan JH, Ke HJ, Lu NH, Li NS, Zhu Y. Comparative transcriptomic analysis reveals the molecular changes of acute pancreatitis in experimental models. *World J Gastroenterol* 2024; 30(14): 2038-2058
URL: https://www.wjgnet.com/1007-9327/full/v30/i14/2038.htm
DOI: https://dx.doi.org/10.3748/wjg.v30.i14.2038

INTRODUCTION

Acute pancreatitis (AP), defined as an inflammatory disorder of the pancreas, is characterized by early activation of digestive enzymes followed by self-digestion of the pancreas[1]. The disease ranges from a mild and self-limiting condition to severe AP (SAP), which is associated with high mortality due to pancreatic necrosis and persistent organ failure[2]. Although the etiology varies in different countries and regions, gallstone disease, alcohol intake, and hyperglyceridemia are common causes of AP. Generally, the initial management of AP is nutritional support, and effective treatment strategies are limited[3].

Currently, the exact pathogenic mechanism remains unclear. Due to the unpredictable progression of this disease and limited access to human pancreatic tissues, there are still great challenges in research on the molecular mechanism of AP. Therefore, experimental animal models have been extensively used to explore the pathogenic mechanism of AP, which could be helpful for the development of novel preventive and therapeutic strategies for AP.

In 1977, Lampel and Kern were the first to report that the intravenous administration of high concentrations of the gut hormone cholecystokinin homolog caerulein could induce a mild and reversible form of AP in rats[4]. Since then, the caerulein model has emerged as one of the most extensively employed experimental models for investigating the molecular mechanisms underpinning AP[5,6]. The premature activation of digestive enzymes, such as trypsinogen, and their intrapancreatic activation are distinctive traits of pancreatic hyperstimulation, which are also fundamental mechanisms underlying the caerulein model.

Furthermore, the caerulein model aids in unraveling processes related to autophagic dysfunction, aberrant calcium signaling, and endoplasmic reticulum stress, all of which constitute the central pathogenic mechanisms of AP[7]. Key characteristics of the caerulein-induced AP model include prominent pancreatic edema, extensive inflammation, and a

degree of acinar cell necrosis. Notably, this model exhibits a pronounced self-limiting nature, with recovery typically occurring within approximately one week. However, it is firmly established clinically that the severity of AP is linked to significantly different clinical outcomes. While mild cases may spontaneously resolve, severe cases are associated with high mortality rates.

To investigate the shared molecular changes underlying the development of AP across varying severity levels, a combination of caerulein and lipopolysaccharide (LPS) has been employed to induce SAP[5]. The inclusion of LPS treatment was linked to substantial damage to the intestinal barrier, resembling peripheral organ injuries observed in patients. This exacerbated the pancreatic inflammatory responses and acinar cell injuries[2].

The *TLR* and *NOD*-like receptor signaling pathways are widely recognized as playing pivotal roles in the inflammatory immune response. Activation of these signaling pathways results in the release of various inflammatory mediators, fostering the advancement of tissue inflammation. Additionally, the release of chemokines facilitates the migration of immune cells from the bloodstream into tissues[8,9]. The discovery of crucial genes within *TLR* and *NOD*-like receptor signaling pathways offered fresh perspectives on mitigating the inflammatory response in AP and introduced novel therapeutic targets.

Apoptosis is a regulated cell death process critical for preserving tissue and organ stability and overall health[10]. In the progression of AP, apoptosis plays a role in the elimination of damaged pancreatic cells, thereby averting additional inflammation and tissue damage. This function can be perceived as a protective mechanism that curtails the disease's severity[11]. However, excessive apoptosis may lead to severe damage to pancreatic tissues[12]. Hence, comprehending the molecular mechanisms governing acinar cell apoptosis in AP is of paramount significance, as it has the potential to open up novel avenues and therapeutic strategies aimed at halting the progression of necrotic alterations in AP or obstructing its necrotic pathways.

To explore the molecular biological changes in pancreatic tissue as AP progresses, we conducted RNA sequencing (RNA-seq) on AP animal models exposed to both caerulein alone and in conjunction with LPS. This analysis unveiled the extensive activation of inflammatory and apoptotic signaling pathways, along with the genes implicated in the progression of AP. RNA-seq data from AP mouse pancreatic tissue and AP patient blood samples in the Gene Expression Omnibus (GEO) database corroborated the transcriptional changes in these key genes. *Ptf1a* serves as a pancreatic acinar-specific promoter[13], whereas *hM3* is a subtype of human cloned muscarinic receptors[14]. Specific activation of *hM3* within the pancreatic acini of mice triggers excessive secretion of pancreatic enzymes, leading to the onset of AP. The transgenic mouse *hM3/Ptf1α*$^{(Cre)}$ AP model further emphasized the key role of the apoptosis pathway in the development of AP. These molecular biological changes provide comprehensive insights and evidence, offering directions for future disease treatment and fundamental research.

MATERIALS AND METHODS

Experimental animals

Male wild-type mice at the age of 6-8 wk were obtained from Nanjing Gempharmatech Co. Ltd. *Ptf1α*$^{(cre)}$ mice and *hM3*$^{-/-}$ mice were both acquired from Shanghai Southern Model Biological Technology Co., Ltd. *hM3/Ptf1α* $^{(cre)}$ mice were generated by breeding *hM3*$^{-/-}$ mice and *Ptf1α*$^{(cre)}$ mice. All animal experiments were approved by the Institutional Animal Care and Use Committee of The First Affiliated Hospital of Nanchang University and complied with the national and international guidelines for the Care and Use of Laboratory Animals. In each group of every batch of animal models, there were at least 6 mice included.

Construction of AP experimental models

The induction of AP was achieved by administering ten consecutive intraperitoneal injections of caerulein (Sigma-Aldrich, St. Louis, Missouri, United States, at a dose of 50 μg/kg), with one-hour intervals between each injection, followed immediately by a single dose of LPS (Sigma-Aldrich, St. Louis, Missouri, United States, at a dose of 10 mg/kg). The control group received intraperitoneal injections of saline. *hM3/Ptf1α*$^{(cre)}$ mice were pre-treated one month in advance by daily intragastric administration of tamoxifen (Sigma-Aldrich, 10 mg/kg) for one week to activate *Ptf1α*$^{(cre)}$ expression. Subsequently, a single intraperitoneal injection of Clozapine N-oxide (Sigma-Aldrich, 1 mg/kg) was administered to induce spontaneous AP.

Histopathology

The mice were euthanized 24 h after AP modeling, and fresh pancreatic tissue was retrieved. The pancreatic tissues were fixed in 4% formalin for 24 h, followed by embedding in paraffin and sectioning into 4 μm slices for *H&E* staining. Pancreatic injury was blindly assessed by two pathologists according to previously described criteria. In brief, the pancreatic histopathological assessment included four categories: edema, inflammatory cell infiltration, necrosis, each scored from 0-3[15].

RNA isolation

The RNA was extracted using the MolPure® Cell Tissue Kit (Yeasen Biotechnology Shanghai Co., Ltd., 19221ES50). Add the processed homogenate into Mol Pure DNA Removal/RNA Binding Column A2 (column placed in a 2 mL Collection Tube), then centrifuge and collect the filtrate containing RNA. Proceed to protein removal, clear away proteins through protein removal solution, wash the column twice with wash solution, and elute the collected RNA using RNase-free H_2O.

Real-time PCR analysis

The quantitative real-time PCR (qRT-PCR) assay was performed to measure the mRNA expression levels of the target genes using the Hifair® III 1st Strand cDNA Synthesis SuperMix (Yeasen Biotechnology Shanghai Co., Ltd., 11141ES10) for qPCR Kit and the Hieff UNICON® Universal Blue qPCR SYBR Green Master Mix Kit (Yeasen Biotechnology Shanghai Co., Ltd., 11211ES03). GAPDH was employed as the internal reference. The primer sequences used are listed in Supplementary Table 1.

Database

The validation data were sourced from the GEO database, with GSE109227 comprising RNA-seq data from pancreatic samples of normal mice and pancreatitis-induced mice[16], and GSE194331 containing RNA-seq data from peripheral blood of healthy individuals and AP patients[17].

RNA-seq

The libraries were constructed using VAHTS Universal V6 RNA-seq Library Prep Kit according to the manufacturer's instructions. The transcriptome sequencing and analysis were conducted by OE Biotech Co., Ltd. (Shanghai, China). The libraries were sequenced on a llumina Novaseq 6000 platform and 150 bp paired-end reads were generated. About 55 raw reads for each sample were generated. Raw reads of fastq format were firstly processed using fastp and the low-quality reads were removed to obtain the clean reads. Then about 50 clean reads for each sample were retained for subsequent analyses. The clean reads were mapped to the reference genome using HISAT2 FPKM3 of each gene was calculated and the read counts of each gene were obtained by HT Seq-count principal component analysis (PCA) analysis were performed using R (v 3.2.0) to evaluate the biological duplication of samples.

Differential expression analysis was performed using the DESeq2 Q value < 0.05 and foldchange > 2 or foldchange < 0.5 was set as the threshold for significantly differential expression genes (DEGs). Hierarchical cluster analysis of DEGs was performed using R (v 3.2.0) to demonstrate the expression pattern of genes in different groups and samples. The radar map of top 30 genes was drawn to show the expression of up-regulated or down-regulated DEGs using R packet ggradar.

Based on the hypergeometric distribution, Gene Ontology (GO), Kyoto Encyclopedia of Genes and Genomes (KEGG) pathway, Reactome and Wiki Pathways enrichment analysis of DEGs were performed to screen the significant enriched term using R (v 3.2.0), respectively. R (v 3.2.0) was used to draw the column diagram, the chord diagram and bubble diagram of the significant enrichment term.

Gene Set Enrichment Analysis analysis

Gene Set Enrichment Analysis (GSEA) was performed using GSEA software. The analysis was used a predefined gene set, and the genes were ranked according to the degree of differential expression in the two types of samples. Then it is tested whether the predefined gene set was enriched at the top or bottom of the ranking list.

Statistical analysis

The data were expressed as the mean ± SEM. Statistical analysis was performed using the SPSS 13.0 software. Differences between two groups with normal distributions were assessed by Student's t test, and one-way analysis of variance was used to compare differences between more than two groups. The least significant difference post hoc test was performed when analysis of variance indicated significance. The value of $P < 0.05$ was regarded as the cutoff for statistical significance.

RESULTS

Treatment with caerulein alone or in combination with LPS induced varying degrees of experimental AP

The drug AP models mainly include the caerulein model and the arginine model, among which the caerulein model has become the most widely used AP model due to its close similarity to human pancreatitis pathogenesis and its feasibility. To investigate the common characteristics of AP, treatment with caerulein alone or in combination with LPS was performed to induce the AP model (Figure 1A). After stimulation with caerulein, pancreatic acinar cell edema was markedly evident, manifesting as a significant increase in the pancreas-to-body weight ratio. This edema was even more pronounced when caerulein was combined with LPS (Figure 1B).

H&E staining analysis showed an increased interstitial space between pancreatic acini in mice with AP, with infiltration of inflammatory cells and pronounced pancreatic necrosis following the coadministration of caerulein with LPS (Figure 1C). Edema and inflammation were notably enhanced when caerulein was combined with LPS, as reflected in the pathological scoring (Figure 1D).

qRT-PCR analysis was used to assess the expression of the proinflammatory cytokines *TNF-α*, Interleukin-6, and Interleukin-1beta (Figure 1E-G). These inflammatory factors were significantly elevated in AP, with a more pronounced increase observed in mice treated with LPS. This finding aligned well with the clinical features of AP, especially in patients with concurrent intestinal dysfunction, who had a higher risk of pancreatic necrosis[18,19]. Despite variations in the severity of the AP model, the observed pancreatic inflammatory characteristics remain consistent with the clinical manifestations, featuring prominent edema, inflammation, and necrosis.

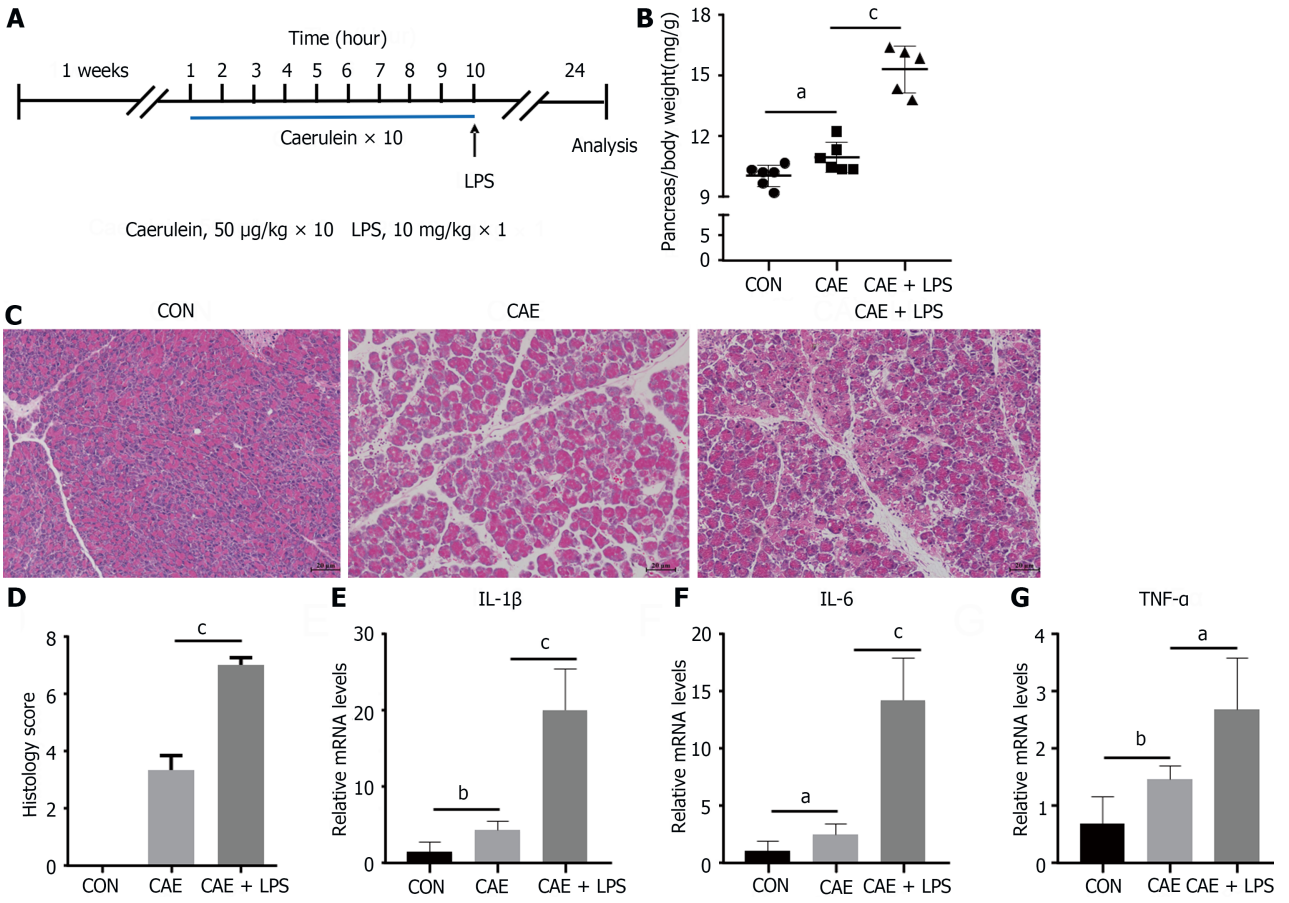

Figure 1 Treatment with caerulein alone or in combination with lipopolysaccharide induced varying degrees of experimental acute pancreatitis. Modeling methods for the control group, caerulein (CAE) group, and CAE combined with lipopolysaccharide (LPS; CAE + LPS) group, evaluation of pancreatic tissue changes, and relevant parameters. A: Schematic representation of the modeling methods for the CAE group and CAE + LPS group; B: Pancreatic weight ratios in the three groups; C: H&E staining of pancreatic tissue; D: Scores for edema, inflammation, and necrosis in pancreatic pathology; E-G: Quantitative real-time PCR expression values of pancreatic inflammatory factors. n = 6 per group, $^{a}P < 0.05$, $^{b}P < 0.01$, $^{c}P < 0.001$. CAE: Caerulein; CON: Control; LPS: Lipopolysaccharide.

RNA-seq identified the molecular changes during the development of AP

To investigate the molecular changes during the onset of AP, RNA-seq was performed on pancreatic tissues from normal pancreas and two AP models. PCA and bar charts revealed significant differentially expressed (SDE) gene expression at the transcriptional level among the three groups (Supplementary Figure 1). In comparison to normal pancreas, there were 2268 upregulated and 1787 downregulated genes in the AP experimental model induced by caerulein alone. There were 2400 upregulated and 1878 downregulated genes compared to normal pancreas in the AP model induced by caerulein in conjunction with LPS. The number of differentially expressed genes between the two AP models was relatively low. Using volcano plots and heatmaps, we displayed the SDE genes between the two AP models and the normal pancreas (Figure 2A and B).

In comparison to a normal pancreas, the AP induced solely by caerulein contained 880 SDE genes, while the AP model induced by caerulein combined with LPS had 885 SDE genes. It was noteworthy that there were 644 common SDE genes between the two AP models, indicating a high degree of overlap. This high overlap in SDE genes suggested that although these models differ in severity, their pathogenic mechanisms are remarkably similar (Figure 2C).

GO enrichment analysis revealed that AP mice were enriched in biological processes related to immune system pathways and inflammatory responses. The cytoplasm and cytoskeleton were the major cellular components affected. In terms of molecular function, there was a significant influence on protein binding (Figure 2D). KEGG analysis showed that pathways associated with apoptosis processes in AP showed significant enrichment. Consistent with previous studies, both groups were enriched in immune- and inflammation-related signaling pathways, such as the *NOD*-like receptor, *TLR*, and *NF-κB* signaling pathways (Figure 2E)[8,20]. GSEA also showed upregulation of the *NOD*-like receptor, *TLR*, *NF-κB*, apoptosis, and *P53* signaling pathways in both AP models. Taken together, these data suggest that inflammation, immune response and cell apoptosis play crucial roles during the onset of AP.

NOD-like receptor and TLR signaling pathways play a crucial role in the progression of AP

The *TLR* and *NOD*-like receptor signaling pathways, which are critical for the regulation of immune and inflammatory responses, have been reported to play important roles in AP pathogenesis[20-22]. As shown in Figure 3A and B, the SDE genes in these two pathways were identified. *TLR7*, *IRF7*, *SPP1*, *OAS2*, and *RIPK3* were the common SDE genes observed

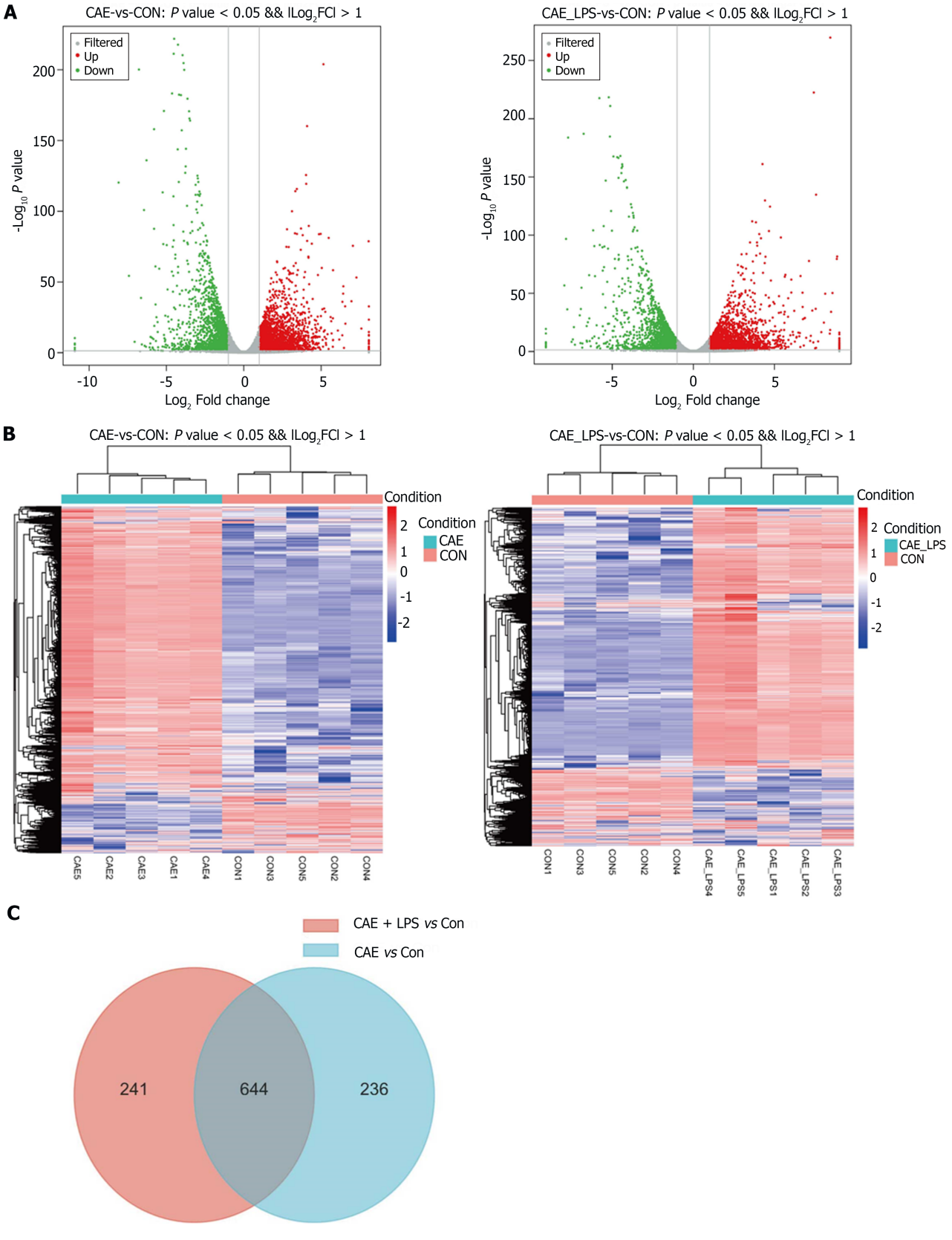
A
CAE-vs-CON: P value < 0.05 && |Log2FCl > 1
Filtered
Up
Down
-Log10 P value
Log2 Fold change
CAE_LPS-vs-CON: P value < 0.05 && |Log2FCl > 1
B
CAE-vs-CON: P value < 0.05 && |Log2FCl > 1
Condition
CAE
CON
CAE_LPS-vs-CON: P value < 0.05 && |Log2FCl > 1
CAE_LPS
C
CAE + LPS vs Con
CAE vs Con
241
644
236

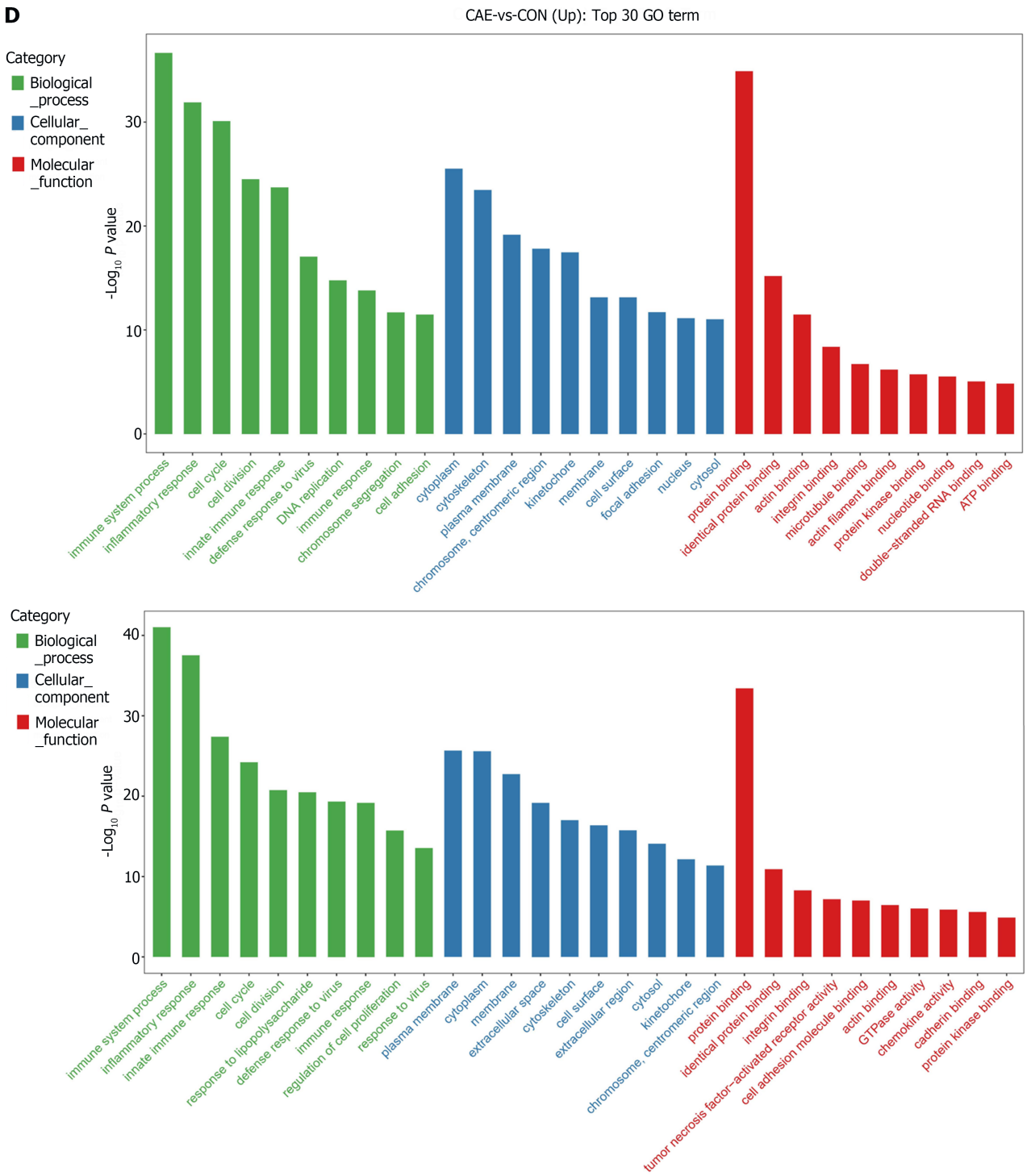
D
CAE-vs-CON (Up): Top 30 GO term
Category
Biological _process
Cellular_ component
Molecular _function
-Log10 P value
0
10
20
30
immune system process
inflammatory response
cell cycle
cell division
innate immune response
defense response to virus
DNA replication
immune response
chromosome segregation
cell adhesion
cytoplasm
cytoskeleton
plasma membrane
chromosome, centromeric region
kinetochore
membrane
cell surface
focal adhesion
nucleus
cytosol
protein binding
identical protein binding
actin binding
integrin binding
microtubule binding
actin filament binding
protein kinase binding
nucleotide binding
double-stranded RNA binding
ATP binding
Category
Biological _process
Cellular_ component
Molecular _function
-Log10 P value
0
10
20
30
40
immune system process
inflammatory response
innate immune response
cell cycle
cell division
response to lipopolysaccharide
defense response to virus
immune response
regulation of cell proliferation
response to virus
plasma membrane
cytoplasm
membrane
extracellular space
cytoskeleton
cell surface
extracellular region
cytosol
kinetochore
chromosome, centromeric region
protein binding
identical protein binding
integrin binding
tumor necrosis factor-activated receptor activity
cell adhesion molecule binding
actin binding
GTPase activity
chemokine activity
cadherin binding
protein kinase binding

E

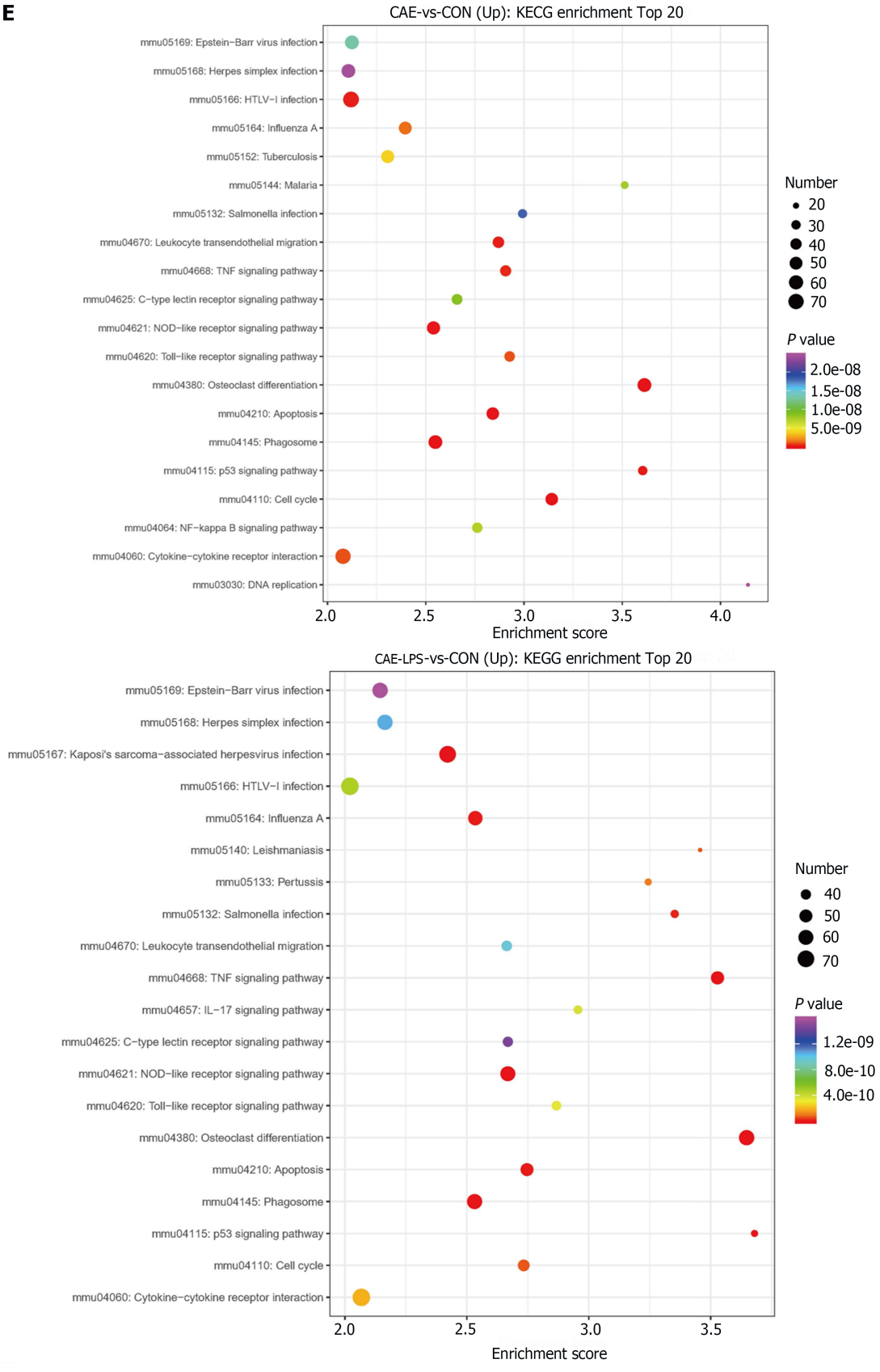
CAE-vs-CON (Up): KECG enrichment Top 20
mmu05169: Epstein-Barr virus infection
mmu05168: Herpes simplex infection
mmu05166: HTLV-I infection
mmu05164: Influenza A
mmu05152: Tuberculosis
mmu05144: Malaria
mmu05132: Salmonella infection
mmu04670: Leukocyte transendothelial migration
mmu04668: TNF signaling pathway
mmu04625: C-type lectin receptor signaling pathway
mmu04621: NOD-like receptor signaling pathway
mmu04620: Toll-like receptor signaling pathway
mmu04380: Osteoclast differentiation
mmu04210: Apoptosis
mmu04145: Phagosome
mmu04115: p53 signaling pathway
mmu04110: Cell cycle
mmu04064: NF-kappa B signaling pathway
mmu04060: Cytokine-cytokine receptor interaction
mmu03030: DNA replication
2.0
2.5
3.0
3.5
4.0
Enrichment score
Number
20
30
40
50
60
70
P value
2.0e-08
1.5e-08
1.0e-08
5.0e-09
CAE-LPS-vs-CON (Up): KEGG enrichment Top 20
mmu05169: Epstein-Barr virus infection
mmu05168: Herpes simplex infection
mmu05167: Kaposi's sarcoma-associated herpesvirus infection
mmu05166: HTLV-I infection
mmu05164: Influenza A
mmu05140: Leishmaniasis
mmu05133: Pertussis
mmu05132: Salmonella infection
mmu04670: Leukocyte transendothelial migration
mmu04668: TNF signaling pathway
mmu04657: IL-17 signaling pathway
mmu04625: C-type lectin receptor signaling pathway
mmu04621: NOD-like receptor signaling pathway
mmu04620: Toll-like receptor signaling pathway
mmu04380: Osteoclast differentiation
mmu04210: Apoptosis
mmu04145: Phagosome
mmu04115: p53 signaling pathway
mmu04110: Cell cycle
mmu04060: Cytokine-cytokine receptor interaction
2.0
2.5
3.0
3.5
Enrichment score
Number
40
50
60
70
P value
1.2e-09
8.0e-10
4.0e-10

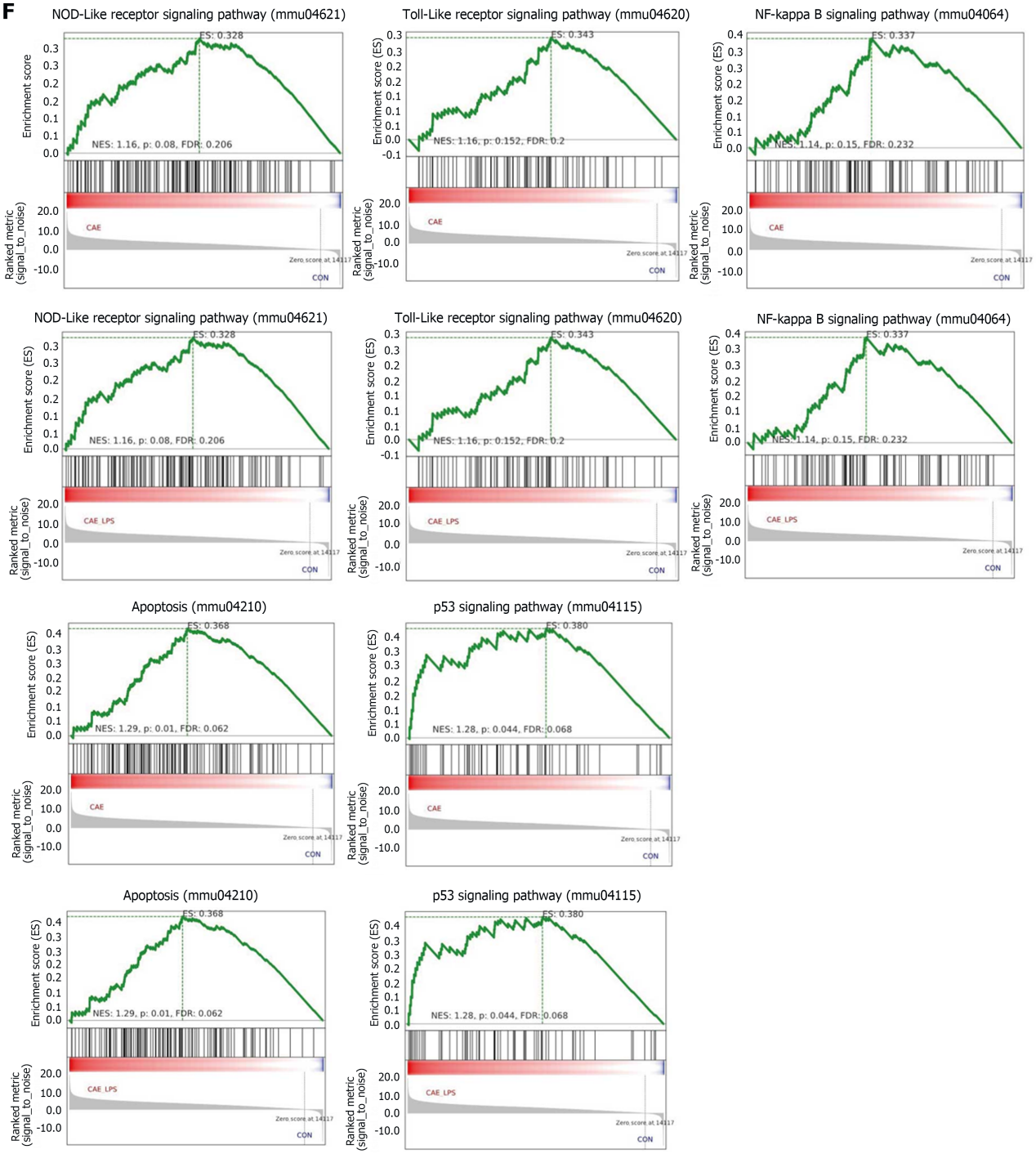

Figure 2 RNA-seq identified the molecular changes during the development of acute pancreatitis. Comparative analysis of the caerulein (CAE) group and CAE + lipopolysaccharide (LPS) group with the control (Con) group. A: Volcano plot of significant differentially expressed (SDE) genes (*P* value < 0.05 and |log2FC| > 1), with red indicating significant upregulation and green indicating significant downregulation; B: Venn diagram, where blue represents CAE group *vs* Con group, and red represents CAE + LPS group *vs* Con group, with the gray area representing commonly differentially expressed genes in both groups compared to the Con group; C: Heatmap displaying the expression of SDE genes in each pancreatic sample, with red indicating upregulated genes and blue indicating downregulated genes; D: Gene Ontology (GO) functional annotation of the top 30 significantly different genes, with the GO classification chart showing the distribution of entries related to biological processes, cellular components, and molecular functions; E: Enrichment analysis results of the top 20 significantly different Kyoto Encyclopedia of Genes and Genomes pathways; F: Gene Set Enrichment Analysis for the *NOD*-like receptor, *TLR*, *NF-κB*, and *P53* signaling pathways, as well as apoptosis. CAE: Caerulein; CON: Control; LPS: Lipopolysaccharide.

when comparing the two models to normal pancreas. Among these genes, *TLR7* is often reported in conjunction with IL22 to mitigate various diseases and is thought to have a similar role in AP[23]. Furthermore, interferon *IRF7* may play a crucial role in anti-inflammation and immune activation[24], while *SPP1* is often reported for its central role in modulating the immunological microenvironment of cancer[25].

To confirm that these genes are involved in AP pathogenesis, we generated two experimental AP animal models with caerulein or in combination with LPS treatment. qRT-PCR analysis showed that the mRNA levels of *TLR7*, *IRF7*, and

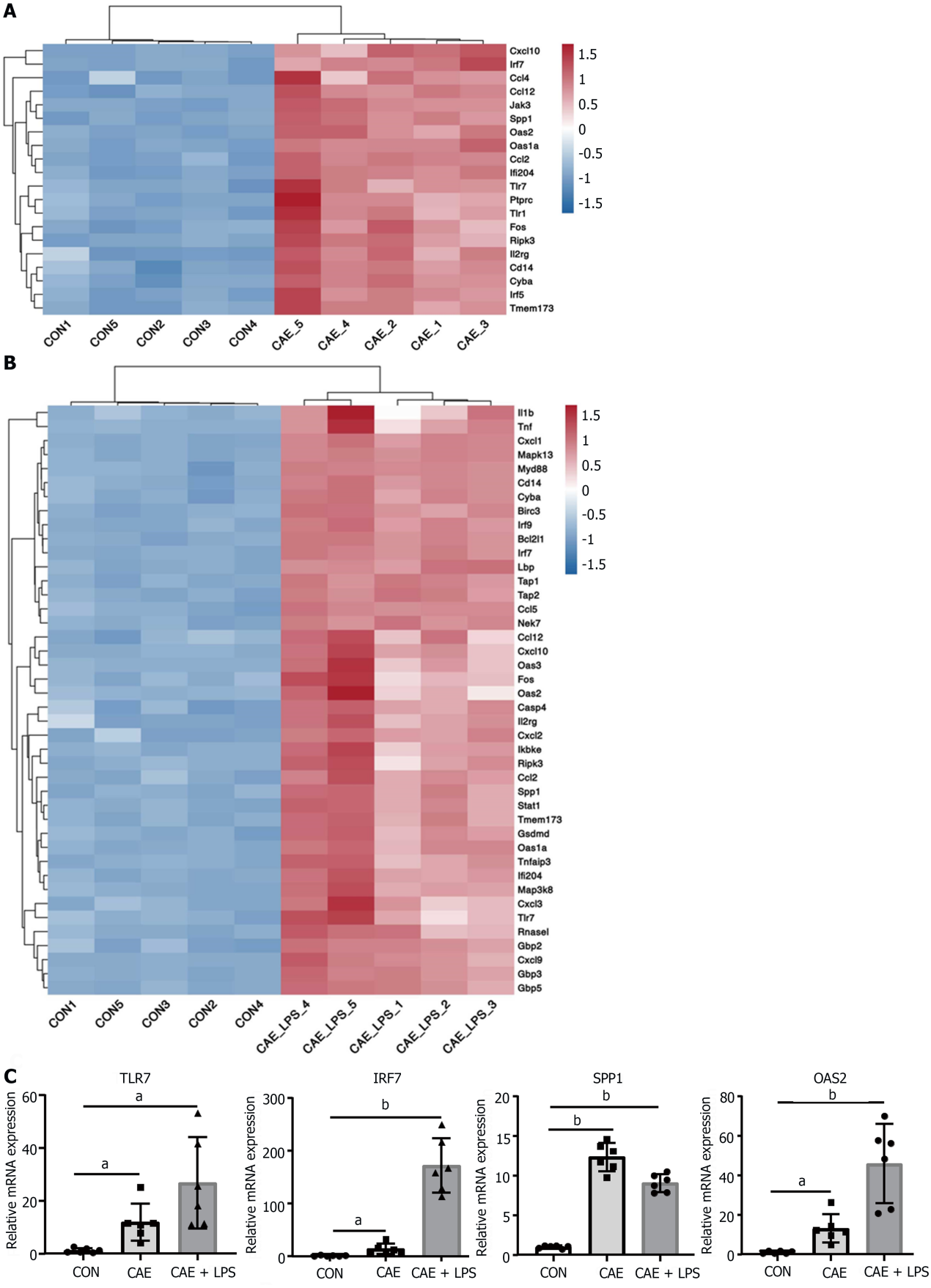
A
Cxcl10
Irf7
Ccl4
Ccl12
Jak3
Spp1
Oas2
Oas1a
Ccl2
Ifi204
Tlr7
Ptprc
Tlr1
Fos
Ripk3
Il2rg
Cd14
Cyba
Irf5
Tmem173
1.5
1
0.5
0
-0.5
-1
-1.5
CON1
CON5
CON2
CON3
CON4
CAE_5
CAE_4
CAE_2
CAE_1
CAE_3
B
Il1b
Tnf
Cxcl1
Mapk13
Myd88
Cd14
Cyba
Birc3
Irf9
Bcl2l1
Irf7
Lbp
Tap1
Tap2
Ccl5
Nek7
Ccl12
Cxcl10
Oas3
Fos
Oas2
Casp4
Il2rg
Cxcl2
Ikbke
Ripk3
Ccl2
Spp1
Stat1
Tmem173
Gsdmd
Oas1a
Tnfaip3
Ifi204
Map3k8
Cxcl3
Tlr7
Rnasel
Gbp2
Cxcl9
Gbp3
Gbp5
1.5
1
0.5
0
-0.5
-1
-1.5
CON1
CON5
CON3
CON2
CON4
CAE_LPS_4
CAE_LPS_5
CAE_LPS_1
CAE_LPS_2
CAE_LPS_3
C
TLR7
IRF7
SPP1
OAS2
Relative mRNA expression
CON
CAE
CAE + LPS

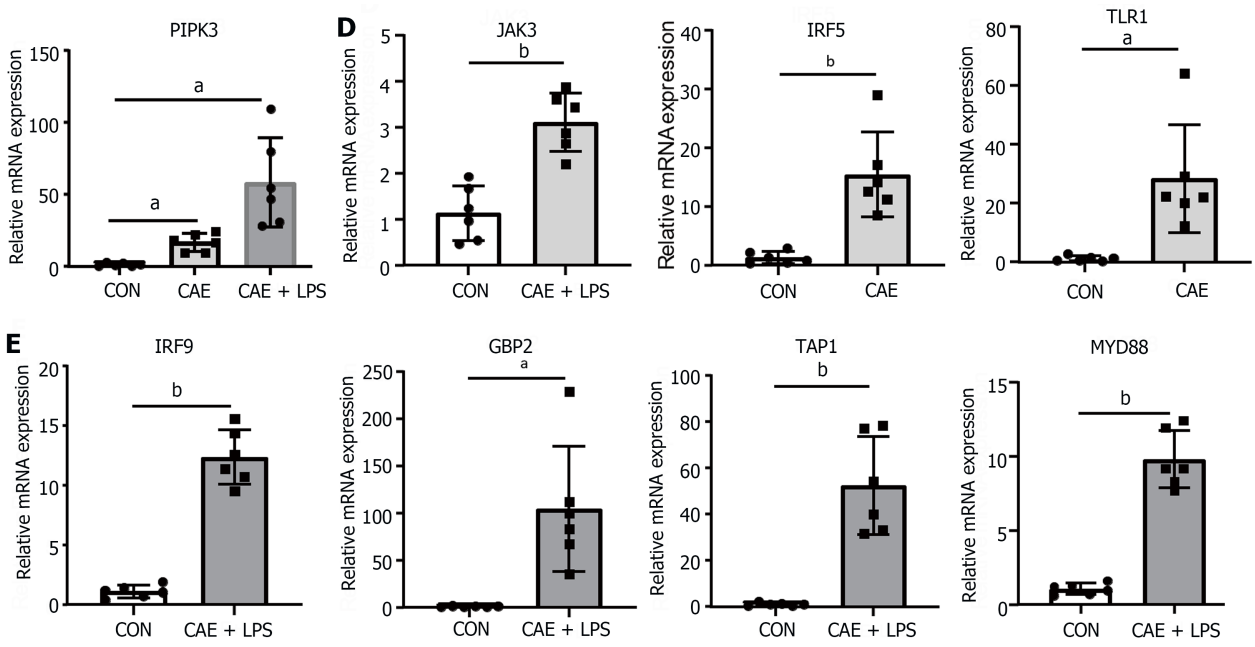

Figure 3 *NOD*-like receptor and *TLR* signaling pathway played a crucial role in the progression of acute pancreatitis. Significant differentially expressed genes in the *NOD*-like receptor and *TLR* signaling pathways after comparing the caerulein (CAE) group and CAE + lipopolysaccharide (LPS) group to the control (Con) group. A: Heatmap of significant differentially expressed (SDE) genes in the CAE Group compared to the Con group; B: Heatmap of SDE genes in the CAE + LPS group compared to the Con group; C: Quantitative real-time PCR (qRT-PCR) expression values of commonly significantly different genes in both groups; D: qRT-PCR expression values of specifically significantly different genes in the CAE Group compared to the Con group; E: qRT-PCR expression values of specifically significantly different genes in the CAE + LPS group compared to the Con group. n = 6 per group, $^{a}P < 0.01$, $^{b}P < 0.001$. CAE: Caerulein; CON: Control; LPS: Lipopolysaccharide.

SPP1 were significantly upregulated in both AP models compared with the control group (Figure 3C). Interestingly, not all genes showed an association with disease severity. In the model involving caerulein and LPS, *TLR7*, *IRF7*, *OAS2*, and *RIPK3* exhibited more pronounced upregulation, possibly linked to the intestinal damage caused by LPS. *SPP1* did not show a similar trend, possibly due to its close association with ductal growth and development in the pancreas[26]. Additionally, the unique SDE genes in each of the two AP models were validated. Some genes, including *JAK3*, *IRF5*, and *TLR1*, were uniquely upregulated in the experimental model treated with caerulein alone, while other genes, including *IRF9*, *GBP2*, *TAP1* and *MYD88*, were upregulated in the model treated with caerulein combined with LPS (Figure 3D and E). In conclusion, these data suggested that genes in the *TLR* and *NOD*-like receptor signaling pathways, including *TLR7*, *IRF7*, *OAS2*, and *RIPK3*, may be involved in the progression of AP and are strongly associated with the severity of AP.

Public RNA-seq data reveal the significant role of TLR and NOD-like signaling pathways in AP pathogenesis

To validate the RNA-seq results, two GSE datasets (GSE109227, GSE194331) from the GEO database were downloaded. The GSE109277 dataset comprised RNA sequencing results of mouse pancreatic tissue. Wild-type C57BL6J mice were injected intraperitoneally with 9 hourly injections of 50 mg/kg caerulein (n = 6) to induce experimental AP, while sodium chloride was used as a control (n = 4). The data from GSE194331 consists of human peripheral blood RNA sequencing, encompassing 32 healthy volunteers and samples taken within 24 h of presentation from 87 patients admitted to the hospital with AP. These data indicated that the mRNA levels of *MYD88* were upregulated, both in AP experimental models and in serum from patients with AP (Figure 4A). This observation suggested a significant degree of similarity in AP development between different species, with *MYD88* genes playing key roles in the development of AP in animal models and in humans. However, the *IRF7, IRF9,* and *SPP1* genes were only validated in the mouse pancreatic tissue sequencing (Figure 4B-D). Interestingly, despite not being successfully validated in mouse pancreatic tissue sequencing data, *TLR1*, *TLR7*, *RIPK3* and *OAS2* were validated in human peripheral blood sequencing data (Figure 4E-H). This may be attributed to the limited sample size of mouse pancreatic tissue and substantial individual variations. Unfortunately, GBP2 was slightly elevated in both humans and mice, but there was no statistical difference (Figure 4I). In summary, these data further indicated that the *TLR* and *NOD*-like receptor signaling pathways play an important role in the development of AP through the regulation of some key genes, such as *MYD88*.

Apoptosis serves as a crucial pathway mediating pancreatic necrosis in AP

Apoptosis, a programmed cell death process, has been reported to play a key role in AP and can clear damaged cells in the early stages of inflammation. However, it can also become excessively activated in the later stages, leading to significant acinar cell death[7,11]. Given that the apoptosis pathway was significantly activated in the AP mouse models (Figure 2F), we further identified the SDE genes involved in this pathway. The heatmap plot showed SDE genes in the two AP models *vs* normal pancreatic tissue, including apoptosis-related genes such as *BAK1*, *BAX*, *PIDD1*, the *FOS* and the factor *TNF* (Figure 5A and B).

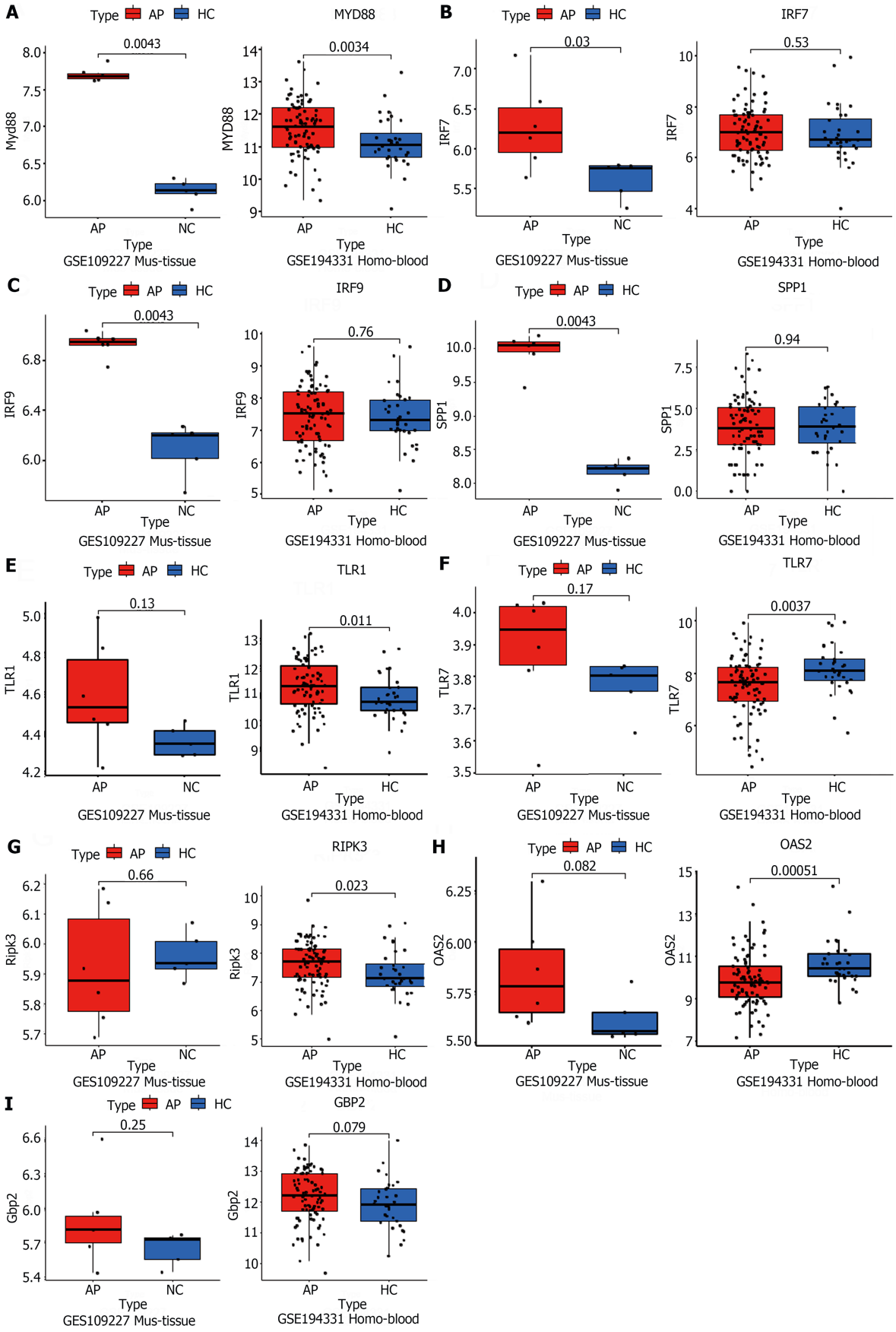

Figure 4 Public RNA-seq data reveals that the significant role of *TLR* and *NOD*-like signaling pathways in acute pancreatitis pathogenesis. A-I: The acute pancreatitis (AP) animal RNA-seq dataset (GSE109227) and human AP patient blood RNA-seq dataset (GSE194331) were downloaded from the Gene Expression Omnibus database for the external validation of significant differentially expressed genes in the successfully validated *NOD*-like receptor and *TLR* signaling pathways in the animal model, using quantitative real-time PCR. n = 6 per group.

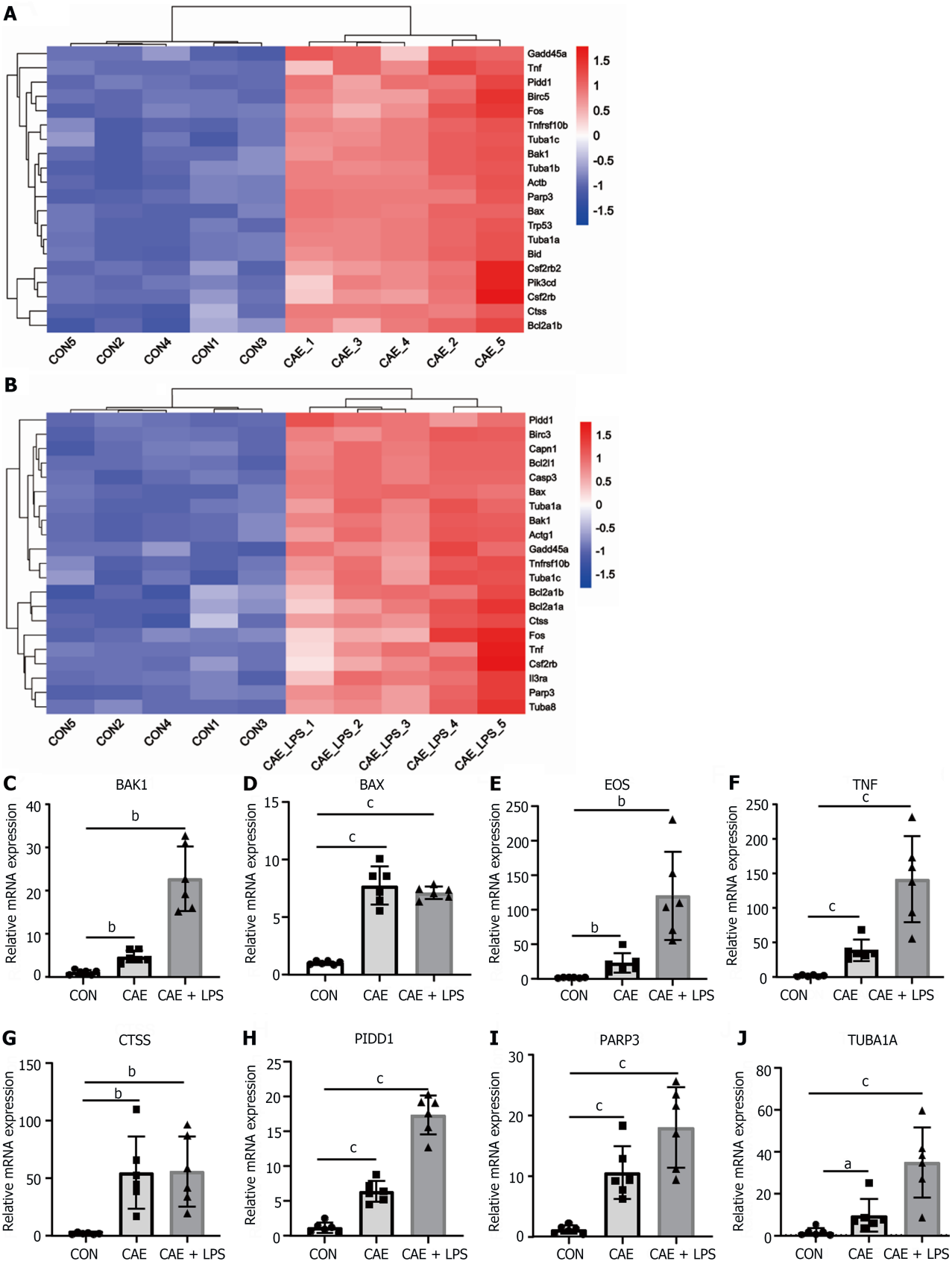
A
Gadd45a
Tnf
Pidd1
Birc5
Fos
Tnfrsf10b
Tuba1c
Bak1
Tuba1b
Actb
Parp3
Bax
Trp53
Tuba1a
Bid
Csf2rb2
Pik3cd
Csf2rb
Ctss
Bcl2a1b
1.5
1
0.5
0
-0.5
-1
-1.5
CON5
CON2
CON4
CON1
CON3
CAE_1
CAE_3
CAE_4
CAE_2
CAE_5
B
Pidd1
Birc3
Capn1
Bcl2l1
Casp3
Bax
Tuba1a
Bak1
Actg1
Gadd45a
Tnfrsf10b
Tuba1c
Bcl2a1b
Bcl2a1a
Ctss
Fos
Tnf
Csf2rb
Il3ra
Parp3
Tuba8
1.5
1
0.5
0
-0.5
-1
-1.5
CON5
CON2
CON4
CON1
CON3
CAE_LPS_1
CAE_LPS_2
CAE_LPS_3
CAE_LPS_4
CAE_LPS_5
C
BAK1
Relative mRNA expression
CON
CAE
CAE + LPS
D
BAX
Relative mRNA expression
CON
CAE
CAE + LPS
E
EOS
Relative mRNA expression
CON
CAE
CAE + LPS
F
TNF
Relative mRNA expression
CON
CAE
CAE + LPS
G
CTSS
Relative mRNA expression
CON
CAE
CAE + LPS
H
PIDD1
Relative mRNA expression
CON
CAE
CAE + LPS
I
PARP3
Relative mRNA expression
CON
CAE
CAE + LPS
J
TUBA1A
Relative mRNA expression
CON
CAE
CAE + LPS

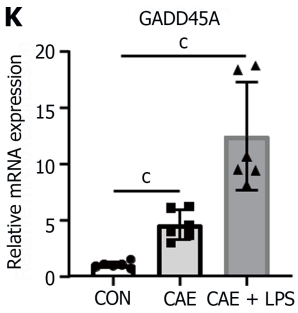

Figure 5 Apoptosis served as a crucial pathway mediating pancreatic necrosis in acute pancreatitis. Significant differentially expressed (SDE) genes in the apoptotic signaling pathway after comparing the caerulein (CAE) group and CAE + lipopolysaccharide (LPS) group to the control (Con) group. A: Heatmap of SDE genes in the CAE group compared to the Con group; B: Heatmap of SDE genes in the CAE + LPS group compared to the Con group; C-K: Quantitative real-time PCR expression values of commonly significantly different genes in both groups, n = 6 per group, $^{a}P < 0.05$, $^{b}P < 0.01$, $^{c}P < 0.001$. CAE: Caerulein; CON: Control; LPS: Lipopolysaccharide.

To validate the RNA-seq results, two additional batches of AP animal models were generated. Consistently, compared with the normal group, the mRNA levels of these genes were significantly upregulated in the experimental model of AP treated with caerulein or in combination with LPS treatment, as detected by qRT-PCR (Figure 5C-K). Notably, several apoptosis-related genes, such as *BAK1*, *FOS*, and *TNF*, showed a more pronounced increase in expression in the group with AP induced by the combination of caerulein and LPS, indicating a close correlation between apoptosis genes and the severity of AP. These data indicated that apoptosis is considered an important biological feature of AP.

TUBA1A and GADD45A are genes closely associated with apoptosis in AP

Similarly, the validation of apoptosis-related genes was conducted using RNA-seq data from both animal pancreatic tissue and human peripheral blood samples. In contrast to the confirmation of inflammation and immune-related genes mentioned earlier, most apoptosis-related genes were not confirmed in the human peripheral blood sequencing results. Only two genes, *TUBA1A* and *GADD45A*, were successfully validated (Figure 6A and B). This discrepancy may be attributed to species differences and variations in the sequenced samples. Apoptosis primarily acts on cells within tissues and has a smaller impact on the entire systemic circulation, making it challenging to detect in peripheral blood samples.

As expected, the mouse pancreatic sequencing results were highly consistent with our results, such as *BAX*, *BAK1*, *FOS* , *CTSS*, *TUBA1A*, and *GADD45A* (Figure 6A-E). Unfortunately, while the expression of the *PARP3* gene aligned with our anticipated trend, it did not exhibit significant differences (Figure 6F). Further exploration revealed that the *TNF* and *PIDD1* genes demonstrated a completely contrary expression pattern to our expectations (Figure 6G and H). Unfortunately, PIDD1 had the exact opposite trend, suggesting that it may not be representative of the variation in AP (Figure 6I). Therefore, we believe that further efforts are warranted in the exploration of apoptosis-related processes in AP to identify targets that also play roles in humans.

Inflammatory response in hM3/Ptf1α$^{(cre)}$ transgenic animal models consistent with the caerulein model

To gather further evidence to substantiate the significance and universality of apoptosis in AP, we decided to employ a transgenic animal model for validation. The *hM3/Ptf1α$^{(cre)}$* model involves the activation of *M3* receptors in acinar cells of the pancreas, induced by a pancreas-specific promoter, *Ptf1α*, leading to spontaneous pancreatitis. The *hM3* cholinergic receptor is a component of the cholinergic nervous system and is widely distributed across various organs and tissues. Within the digestive system, the *hM3* receptor plays a significant role in the contraction of gastrointestinal smooth muscles, secretion of digestive fluids, and gastrointestinal motility[27]. The *Ptf1α* gene functions as a transcription factor that is crucial in regulating the development of pancreatic acinar cells. The cre recombinase driven by the *Ptf1α* gene promoter marked the *hM3* gene specifically expressed in acinar cells[28]. Transgenic mice were administered tamoxifen orally to activate *Ptf1α$^{(cre)}$*, followed by intraperitoneal injection of Clozapine N-oxide (CNO) after a one-month interval to activate the *Ptf1α* gene (Figure 7A).

Activation of the *hM3* gene led to excessive secretion of pancreatic enzymes, causing AP. More severe than the caerulein model, the mice exhibited extensive diffuse necrosis and abundant inflammatory infiltration in the pancreas (Figure 7B). After inducing pancreatitis, qRT-PCR was utilized to assess the inflammatory genes mentioned above. The results revealed that despite variations in modeling approaches, all genes exhibited a consistent trend with the caerulein model: notably elevated during AP (Figure 7C-K). This underscores once more the pivotal role of the genes we have identified as key players in AP inflammation.

The apoptosis in AP in the hM3/Ptf1α$^{(cre)}$ transgenic animal model was consistent with the caerulein models

To further investigate the expression changes in apoptotic genes after AP induction in transgenic mice, qRT-PCR was employed to assess their expression. Surprisingly, apoptotic gene expression was confirmed in the *hM3/Ptf1α$^{(cre)}$* mouse model and these findings confirmed the similarity in the regulatory mechanisms of the apoptotic pathway across different AP models (Figure 8). Identifying key targets that influence apoptosis and promote a positive role in AP could aid in reducing pancreatic necrosis.

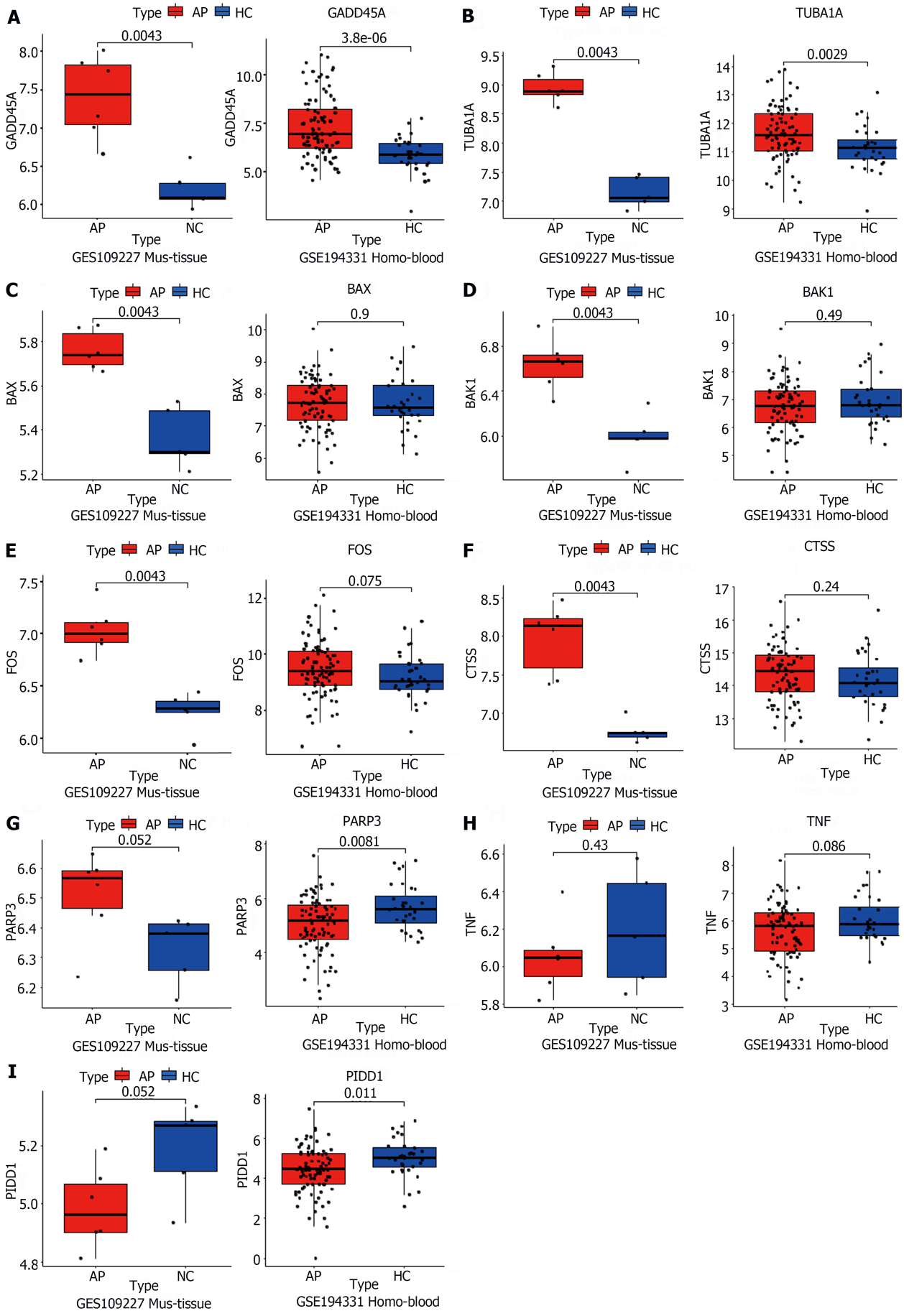

Figure 6 TUBA1A and GADD45A were genes closely associated with apoptosis in acute pancreatitis. A-I: The acute pancreatitis (AP) animal

RNA-seq dataset (GSE109227) and human AP patient blood RNA-seq dataset (GSE194331) were downloaded from the Gene Expression Omnibus database for the external validation of the genes successfully validated in the animal model and related to the apoptotic signaling pathway, using quantitative real-time PCR. AP: Acute pancreatitis; HC: Healthy control.

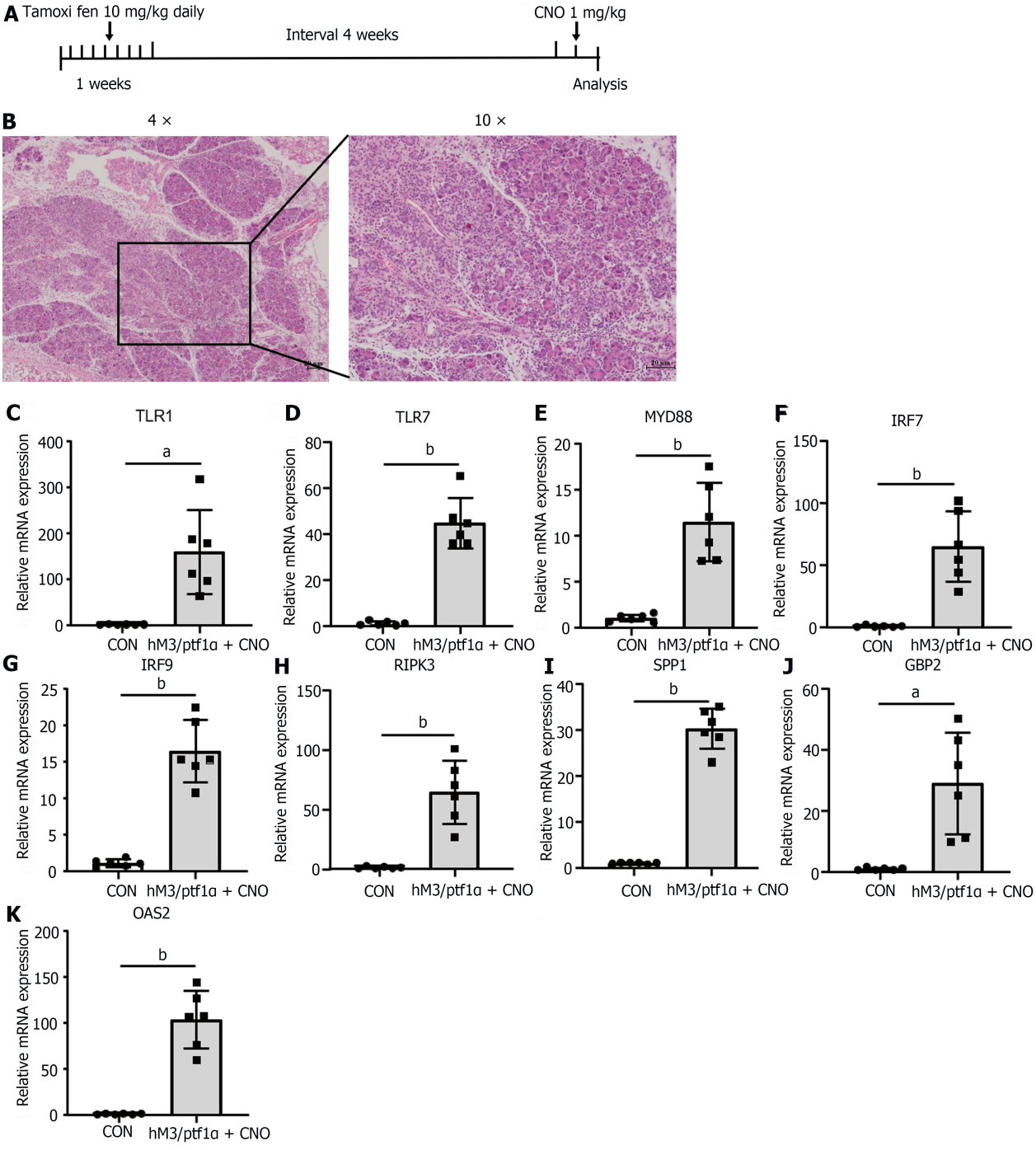

Figure 7 Inflammatory response in *hM3/Ptf1α(cre)* transgenic animal models consistent with the caerulein model. *hM3/Ptf1α(cre)* model and its pathological images with inflammatory gene validation. A: Schematic representation of the *hM3/Ptf1α(cre)* model; B: H&E staining of pancreatic tissue schematic representation of the modeling methods; C-K: Validation of the significant differentially expressed genes in the transgenic animal *hM3/Ptf1α(cre)* model after inducing acute pancreatitis, which were found in the *NOD*-like receptor and *TLR* signaling pathways. n = 6 per group, $^{a}P < 0.01$, $^{b}P < 0.001$. CON: Control; CNO: Clozapine N-oxide.

DISCUSSION

In our effort to unravel the molecular changes underlying the development of AP, we adopted the widely recognized and physiologically relevant caerulein model. To closely mimic clinical scenarios and to avoid the limitations of a single severity model, we employed a combination of caerulein and LPS to induce SAP. Transcriptome analysis utilizing RNA-seq revealed dynamic transcriptional alterations in AP. Comparative analysis between the caerulein group and the caerulein combined with LPS group revealed a highly congruent set of SDE genes. GO and KEGG analyses highlighted the enrichment of pathways predominantly associated with inflammation, immunity, and apoptosis. Notably, the *NOD*-like receptor and *TLR* signaling pathways exhibited robust concordance of SDE genes in our induced animal samples, bolstering the internal validity of our experimental results. However, this congruence was not fully recapitulated in external datasets. Importantly, genes including *TLR1*, *MYD88*, *RIPK3*, and *GBP2*, which were differentially expressed in our model, were also validated in human blood samples, underscoring the reliability of our findings and offering novel therapeutic targets for future studies in the realms of inflammation and immunity. Within the apoptosis-related pathways, the atypical expression of the *TUBA1A* and *GADD45A* genes stood out remarkably. Their dysregulation not only held true in our animal model but also withstood scrutiny in publicly available GEO datasets and transgenic animal experiments. This presents a promising outlook for *TUBA1A* and *GADD45A* as novel intervention targets for the necrosis of AP in future clinical treatment.

In our quest to decipher the intricate mechanisms underlying AP, we judiciously opted not to employ all available modeling approaches. This decision was rooted in the realization that certain models fail to faithfully represent the pathophysiological mechanisms and exhibit unique, albeit nonrepresentative, conditions associated with AP. For instance, the AP model induced by intraperitoneal injection of L-arginine, while being informative in specific contexts, does not provide clear mechanistic insights into AP and may be related to amino acid imbalances and oxidative stress[29-31]. Importantly, this model does not closely mimic the etiology observed in clinical AP patients, thus limiting its translational relevance. Similarly, the retrograde ductal infusion-induced AP model primarily manifests lesions in the pancreatic head characterized by extensive necrosis, with the pancreatic tail displaying primarily edematous changes[32]. The non-uniform distribution of pathological alterations in this model, while recapitulating certain aspects of gallstone-induced pancreatitis, deviates from the clinical course of AP[33]. Nevertheless, this model bears semblance to the mechanistic underpinnings of biliary pancreatitis, offering a prospective avenue for investigating the molecular mechanisms underlying the development of gallstone-induced pancreatitis.

The early-phase inflammatory response in AP plays a pivotal role in exacerbating disease progression[34]. Consequently, our study placed particular emphasis on the major inflammatory signaling pathways: the *TLR* and *NOD*-like receptor signaling pathways. High-quality research has reported a close association between *TLR*-like receptors and inflammatory damage in AP[19]. Notably, the absence of the toll-like receptor 2 receptor effectively alleviates AP in animal models[17], while the *TLR4* receptor is closely linked to lung injury in AP[18]. Evidently, *TLR*-like receptor signaling pathways are intricately linked to the progression of AP.

This study verified key genes, such as *TLR1*, *MYD88*, *RIPK3*, and *GBP2*, through multiple models and datasets, offering valuable insights and directions for future research endeavors. *MYD88* functions as a downstream molecule of *TLR*-like receptors, participating jointly in the regulation of immunity and inflammatory responses while also having the capability to modulate *RIPK3* involvement in cellular apoptosis pathways[35,36]. *GBP2* is a highly regarded molecule within the field of oncology research, as it has the capacity to enhance tumor invasion and proliferation abilities[37]. *NOD* receptors often play a supplementary role alongside *TLR*-like receptors, and numerous reports have associated them with intestinal injury in AP. For instance, they can assist Paneth cells in mitigating intestinal damage in the absence of *TLR4* [38]. Therefore, these two crucial inflammatory signaling pathways warrant further exploration, as they may serve as critical points of initiation in the inflammatory cascade of AP.

Apoptosis, a form of programmed cell death, is critically important for the development and maintenance of the immune system, as well as its response to external and internal stimuli[11]. In the course of AP, apoptosis of acinar cells is often closely associated with oxidative stress and inflammation. Numerous reports have highlighted genes that can modulate and influence the progression of apoptosis, including recent research findings implicating genes such as those involved in the *ATF6/P53/IFM2* and *Sirt1/Nrf2/TNF* pathways[39,40]. Many reviews have emphasized the role of key genes such as caspases; however, significant differential expression of caspases at the transcriptional level was not observed in our study, possibly due to minimal changes in their transcription and more pronounced alterations at the protein level[7,41]. *TNF-α*, an apoptosis-responsive protein present in pancreatic acinar cells, exhibited notable transcriptional changes[40]. Among the successfully validated genes, *TUBA1A* and its association with apoptosis have received limited attention[42], while *GADD45A*, as a critical apoptosis-related gene, plays a significant role in promoting apoptosis through interactions with various molecules[43,44]. Subsequent research efforts may shift the focus toward *TUBA1A* to explore novel avenues of investigation. This research underscores the intricate regulatory mechanisms of apoptosis in the context of AP, shedding light on key genes and their transcriptional dynamics, with potential implications for therapeutic intervention.

The etiology of AP was diverse, and we have yet to explore other causative factors leading to AP, such as hyperlipidemic pancreatitis and alcoholic pancreatitis. Furthermore, there was a wide range of animal models available for AP, including models induced by L-arginine, pancreatic duct ligation, and retrograde ductal infusion, but comparative experiments in this area were lacking. Despite the identification of numerous genes playing important roles in inflammation and apoptosis, further validation experiments in animal models and in-depth exploration of their mechanisms will be finished in future work. Transgenic mouse models of AP certainly exhibit unique molecular changes, but we have not extensively investigated the differences between these models and the commonly used caerulein model. The aforementioned unfinished aspects will be the focus of our subsequent work. Nonetheless, our study provides insights

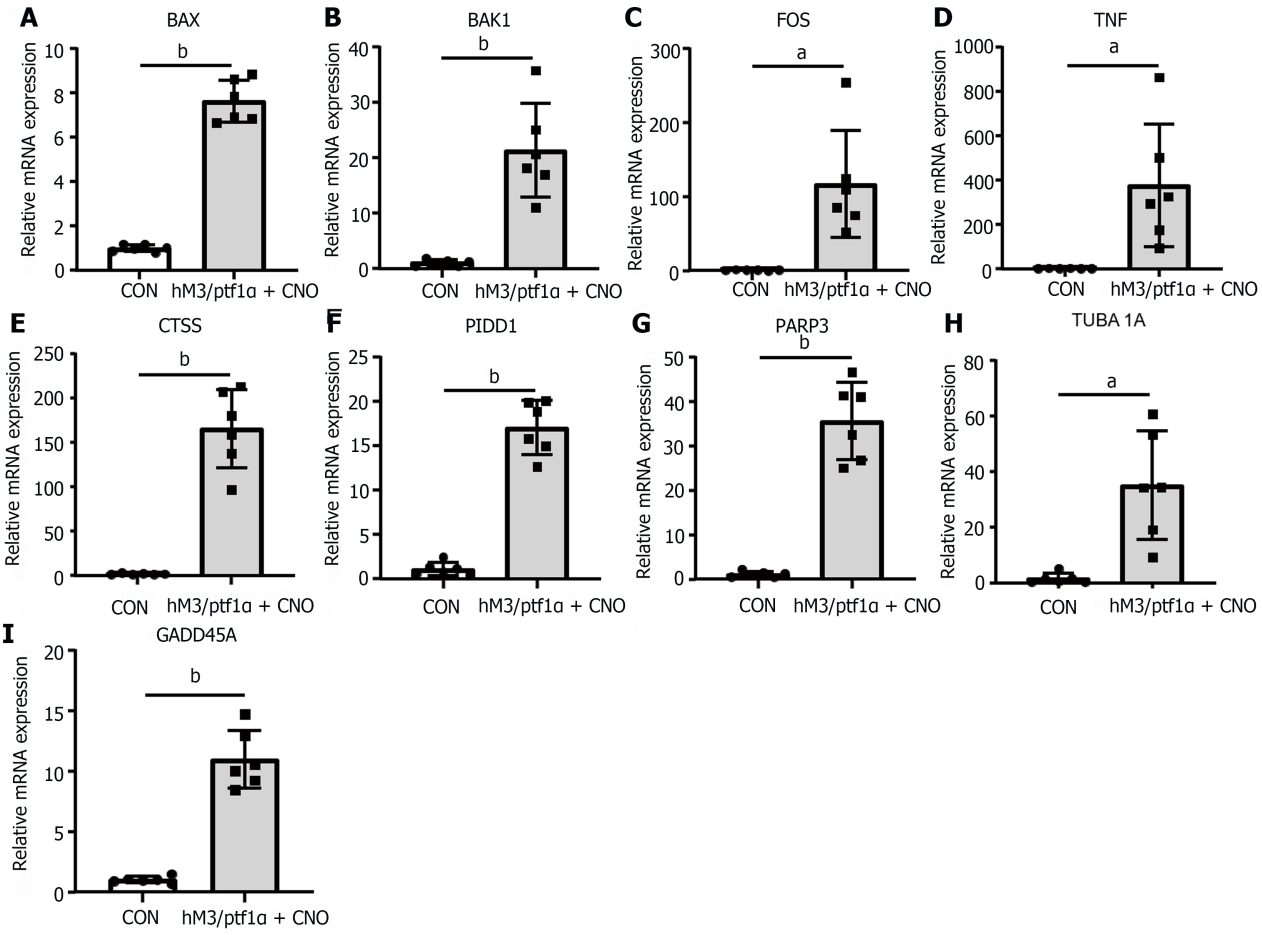

Figure 8 The apoptosis in acute pancreatitis in the *hM3/Ptf1α(cre)* transgenic animal model was consistent with the caerulein models. A-I: Validation of the significant differentially expressed genes in the *NOD*-like receptor and *TLR* signaling pathways in the transgenic animal *hM3/Ptf1α(cre)* model after inducing acute pancreatitis. n = 6 per group, $^{a}P < 0.01$, $^{b}P < 0.001$. CON: Control; CNO: Clozapine N-oxide.

into the molecular alterations in AP and identifies genes that play crucial roles in inflammation and apoptosis processes, offering potential therapeutic targets.

CONCLUSION

This study investigated the molecular changes associated with the development of AP. RNA-seq analysis identified a significant overlap in the gene expression patterns between AP and normal pancreas, primarily involving inflammatory, immune, and apoptotic pathways. The validation of the *TLR* and *NOD*-like receptor signaling pathways using animal tissues and two GEO datasets highlighted several potential key genes, including *TLR7*, *IRF7*, *SPP1*, *OAS2*, and *RIPK3*. Moreover, we emphasized the importance of apoptotic pathways in AP. By incorporating transgenic animal models into the validation process, *TUBA1A* and *GADD45A* were identified as the most important expressed genes, suggesting their potential as critical targets for future interventions and therapies in AP. Both wild type and the *hM3/Ptf1α*$^{(cre)}$ mice shared the same pattern of inflammation. These discoveries provide new avenues for the treatment of necrosis in AP.

ARTICLE HIGHLIGHTS

Research background

Acute pancreatitis (AP) is a severe abdominal condition with an increasing incidence rate. Currently, there are no specific therapeutic approaches targeting the underlying causes of this disease. Research on AP is still in its early stages, and this study focuses on the molecular changes associated with inflammation and apoptosis, two major pathological events in AP. The aim is to identify new potential targets for treatment interventions.

Research motivation

This study primarily focused on the molecular changes in AP, indicating significant alterations in inflammation and

apoptosis. The research also identified key genes involved in the *TLR* and *NOD* signaling pathways, as well as in the apoptotic signaling pathway, highlighting new research and intervention targets for future investigations in this field.

Research objectives

The purpose of this research was to investigate the parthenogenesis and molecular changes associated with AP. In fact, we have identified genes that play important roles in the inflammatory and apoptotic signaling pathways. These findings provide directions for future studies aimed at reducing inflammation and alleviating pancreatic necrosis in AP, as well as discovering new therapeutic approaches for AP.

Research methods

In this study, RNA sequencing analysis was employed to investigate the molecular changes associated with AP and identify key genes involved. Additionally, external GSE from human peripheral blood samples and mouse pancreatic tissues were downloaded and used for validation purposes. Transgenic mice models were also utilized to further validate the findings after induction of AP.

Research results

The molecular changes in inflammation and apoptosis are consistent between different animal models of AP and transgenic AP models. The *TLR* and *NOD* signaling pathways play important roles in the inflammatory response of AP, with key genes identified as *TLR1*, *TLR7*, *RIPK3*, and *OAS2*. *TUBA1A* and *GADD45A* have been identified as crucial molecules involved in regulating acinar cell apoptosis in AP. However, further analysis is still needed to investigate AP associated with various etiologies and different modeling method.

Research conclusions

New theories: (1) *TUBA1A* and *GADD45A* are key molecules involved in regulating apoptosis of vesicular cells in AP; and (2) Transgenic mice, *hM3/Ptf1a*$^{(cre)}$ with AP induced by caerulein, exhibit similar molecular changes. New method: Transgenic mice carrying the *hM3/Ptf1α*$^{(cre)}$ construct were generated and successfully developed AP.

Research perspectives

Using the latest single-cell sequencing technology to investigate the pathogenic mechanisms of AP in-depth.

FOOTNOTES

Co-corresponding authors: Yin Zhu and Nian-Shuang Li.

Author contributions: Zhu Y and Li NS designed and coordinated the study; Zheng P and Li XY completed the experimental testing and wrote the article; Wan JH and Yang XY were in charge of animal modeling; He C and Ke HJ were responsible for data download and analysis in GEO database; Ding L and Wang H bred transgenic mouse; Zhu Y, Lu NH and Li NS revised and verified the article; all authors were involved in the critical review of the results and have contributed to, read, and approved the final manuscript. The reason for choosing Zhu Y and Li NH as co-corresponding authors is that Zhu Y and Li NH have made equal efforts in the whole research process, played a common important role in the design and guidance of the paper, and ensured the quality and reliability of the paper. Pan Z and Li XY contributed equally to this article.

Supported by National Natural Science Foundation of China, No. 82260133 and No. 82370661; the Academic and Technical Leader of major disciplines in Jiangxi Province, No. 20225BCJ23021; the Jiangxi Medicine Academy of Nutrition and Health Management, No. 2022-PYXM-01; the Natural Science Foundation of Jiangxi Province, No. 20224ACB216004; and the Technological Innovation Team Cultivation Project of the First Affiliated Hospital of Nanchang University, No. YFYKCTDPY202202.

Institutional animal care and use committee statement: The First Affiliated Hospital of Nanchang University approved experimental animal welfare ethics Approved by the Experimental Animal Welfare Ethics Committee of the First Affiliated Hospital of Nanchang University, Zhu Yin, Gastroenterology Department of our Hospital, "Research on the mechanism of Bifidobacterium pseudolongum Protecting intestinal mucosal Barrier in acute pancreatitis by activating NOD2-autophagy signal axis" (Approval number: CDYFYIACUC-202306QR022), does not violate the ethical principles of experimental animal welfare, and agrees to carry out the research under the approved protocol. Experimental animal Welfare Ethics Committee of the First Affiliated Hospital of Nanchang University

Conflict-of-interest statement: The authors declare that they have no competing interests.

Data sharing statement: The first author obtained two files, GSE109227 and GSE194331, from the public database GEO for validation purposes.

ARRIVE guidelines statement: The authors have read the ARRIVE Guidelines, and the manuscript was prepared and revised according to the ARRIVE Guidelines.

Country/Territory of origin: China

ORCID number: Xue-Yang Li 0000-0001-8161-4781; Ling Ding 0000-0002-2655-5616; Cong He 0000-0002-1185-5456; Nong-Hua Lu 0000-0003-4373-551X; Nian-Shuang Li 0000-0001-7343-9311; Yin Zhu 0000-0002-7561-2306.

S-Editor: Lin C
L-Editor: A
P-Editor: Cai YX

REFERENCES

1 **Habtezion A**, Gukovskaya AS, Pandol SJ. Acute Pancreatitis: A Multifaceted Set of Organelle and Cellular Interactions. *Gastroenterology* 2019; **156**: 1941-1950 [PMID: 30660726 DOI: 10.1053/j.gastro.2018.11.082]
2 **Garg PK**, Singh VP. Organ Failure Due to Systemic Injury in Acute Pancreatitis. *Gastroenterology* 2019; **156**: 2008-2023 [PMID: 30768987 DOI: 10.1053/j.gastro.2018.12.041]
3 **Boxhoorn L**, Voermans RP, Bouwense SA, Bruno MJ, Verdonk RC, Boermeester MA, van Santvoort HC, Besselink MG. Acute pancreatitis. *Lancet* 2020; **396**: 726-734 [PMID: 32891214 DOI: 10.1016/S0140-6736(20)31310-6]
4 **Lampel M**, Kern HF. Acute interstitial pancreatitis in the rat induced by excessive doses of a pancreatic secretagogue. *Virchows Arch A Pathol Anat Histol* 1977; **373**: 97-117 [PMID: 139754 DOI: 10.1007/BF00432156]
5 **Lerch MM**, Gorelick FS. Models of acute and chronic pancreatitis. *Gastroenterology* 2013; **144**: 1180-1193 [PMID: 23622127 DOI: 10.1053/j.gastro.2012.12.043]
6 **Zhan X**, Wang F, Bi Y, Ji B. Animal models of gastrointestinal and liver diseases. Animal models of acute and chronic pancreatitis. *Am J Physiol Gastrointest Liver Physiol* 2016; **311**: G343-G355 [PMID: 27418683 DOI: 10.1152/ajpgi.00372.2015]
7 **Lee PJ**, Papachristou GI. New insights into acute pancreatitis. *Nat Rev Gastroenterol Hepatol* 2019; **16**: 479-496 [PMID: 31138897 DOI: 10.1038/s41575-019-0158-2]
8 **Santoni M**, Andrikou K, Sotte V, Bittoni A, Lanese A, Pellei C, Piva F, Conti A, Nabissi M, Santoni G, Cascinu S. Toll like receptors and pancreatic diseases: From a pathogenetic mechanism to a therapeutic target. *Cancer Treat Rev* 2015; **41**: 569-576 [PMID: 26036357 DOI: 10.1016/j.ctrv.2015.04.004]
9 **Caruso R**, Warner N, Inohara N, Núñez G. NOD1 and NOD2: signaling, host defense, and inflammatory disease. *Immunity* 2014; **41**: 898-908 [PMID: 25526305 DOI: 10.1016/j.immuni.2014.12.010]
10 **Han J**, Zhong CQ, Zhang DW. Programmed necrosis: backup to and competitor with apoptosis in the immune system. *Nat Immunol* 2011; **12**: 1143-1149 [PMID: 22089220 DOI: 10.1038/ni.2159]
11 **Bhatia M**. Apoptosis versus necrosis in acute pancreatitis. *Am J Physiol Gastrointest Liver Physiol* 2004; **286**: G189-G196 [PMID: 14715516 DOI: 10.1152/ajpgi.00304.2003]
12 **Wang G**, Qu FZ, Li L, Lv JC, Sun B. Necroptosis: a potential, promising target and switch in acute pancreatitis. *Apoptosis* 2016; **21**: 121-129 [PMID: 26514558 DOI: 10.1007/s10495-015-1192-3]
13 **Ogawa S**, Fukuda A, Matsumoto Y, Hanyu Y, Sono M, Fukunaga Y, Masuda T, Araki O, Nagao M, Yoshikawa T, Goto N, Hiramatsu Y, Tsuda M, Maruno T, Nakanishi Y, Hussein MS, Tsuruyama T, Takaori K, Uemoto S, Seno H. SETDB1 Inhibits p53-Mediated Apoptosis and Is Required for Formation of Pancreatic Ductal Adenocarcinomas in Mice. *Gastroenterology* 2020; **159**: 682-696.e13 [PMID: 32360551 DOI: 10.1053/j.gastro.2020.04.047]
14 **Ruiz de Azua I**, Gautam D, Guettier JM, Wess J. Novel insights into the function of β-cell M3 muscarinic acetylcholine receptors: therapeutic implications. *Trends Endocrinol Metab* 2011; **22**: 74-80 [PMID: 21106385 DOI: 10.1016/j.tem.2010.10.004]
15 **Tian R**, Tan JT, Wang RL, Xie H, Qian YB, Yu KL. The role of intestinal mucosa oxidative stress in gut barrier dysfunction of severe acute pancreatitis. Eur Rev Med Pharmacol Sci 2013; 17: 349-355 [PMID: 23426538]
16 **Norberg KJ**, Nania S, Li X, Gao H, Szatmary P, Segersvärd R, Haas S, Wagman A, Arnelo U, Sutton R, Heuchel RL, Löhr JM. RCAN1 is a marker of oxidative stress, induced in acute pancreatitis. Pancreatology 2018; 18: 734-741 [PMID: 30139658 DOI: 10.1016/j.pan.2018.08.005]
17 **Nesvaderani M**, Dhillon BK, Chew T, Tang B, Baghela A, Hancock RE, Eslick GD, Cox M. Gene Expression Profiling: Identification of Novel Pathways and Potential Biomarkers in Severe Acute Pancreatitis. J Am Coll Surg 2022; 234: 803-815 [PMID: 35426393 DOI: 10.1097/XCS.0000000000000115]
18 **Zhu Y**, He C, Li X, Cai Y, Hu J, Liao Y, Zhao J, Xia L, He W, Liu L, Luo C, Shu X, Cai Q, Chen Y, Lu N. Gut microbiota dysbiosis worsens the severity of acute pancreatitis in patients and mice. J Gastroenterol 2019; 54: 347-358 [PMID: 30519748 DOI: 10.1007/s00535-018-1529-0]
19 **Li XY**, He C, Zhu Y, Lu NH. Role of gut microbiota on intestinal barrier function in acute pancreatitis. World J Gastroenterol 2020; 26: 2187-2193 [PMID: 32476785 DOI: 10.3748/wjg.v26.i18.2187]
20 **Li L**, Liu Q, Le C, Zhang H, Liu W, Gu Y, Yang J, Zhang X. Toll-like receptor 2 deficiency alleviates acute pancreatitis by inactivating the NF-κB/NLRP3 pathway. Int Immunopharmacol 2023; 121: 110547 [PMID: 37356124 DOI: 10.1016/j.intimp.2023.110547]
21 **Sharif R**, Dawra R, Wasiluk K, Phillips P, Dudeja V, Kurt-Jones E, Finberg R, Saluja A. Impact of toll-like receptor 4 on the severity of acute pancreatitis and pancreatitis-associated lung injury in mice. Gut 2009; 58: 813-819 [PMID: 19201771 DOI: 10.1136/gut.2008.170423]
22 **Hoque R**, Farooq A, Ghani A, Gorelick F, Mehal WZ. Lactate reduces liver and pancreatic injury in Toll-like receptor- and inflammasome-mediated inflammation via GPR81-mediated suppression of innate immunity. Gastroenterology 2014; 146: 1763-1774 [PMID: 24657625 DOI: 10.1053/j.gastro.2014.03.014]
23 **Abt MC**, Buffie CG, Sušac B, Becattini S, Carter RA, Leiner I, Keith JW, Artis D, Osborne LC, Pamer EG. TLR-7 activation enhances IL-22-mediated colonization resistance against vancomycin-resistant enterococcus. Sci Transl Med 2016; 8: 327ra325 [PMID: 26912904 DOI: 10.1126/scitranslmed.aad6663]
24 **Minaga K**, Watanabe T, Arai Y, Shiokawa M, Hara A, Yoshikawa T, Kamata K, Yamashita K, Kudo M. Activation of interferon regulatory

factor 7 in plasmacytoid dendritic cells promotes experimental autoimmune pancreatitis. J Gastroenterol 2020; 55: 565-576 [PMID: 31960143 DOI: 10.1007/s00535-020-01662-2]

25 **Storrs EP**, Chati P, Usmani A, Sloan I, Krasnick BA, Babbra R, Harris PK, Sachs CM, Qaium F, Chatterjee D, Wetzel C, Goedegebuure SP, Hollander T, Anthony H, Ponce J, Khaliq AM, Badiyan S, Kim H, Denardo DG, Lang GD, Cosgrove ND, Kushnir VM, Early DS, Masood A, Lim KH, Hawkins WG, Ding L, Fields RC, Das KK, Chaudhuri AA. High-dimensional deconstruction of pancreatic cancer identifies tumor microenvironmental and developmental stemness features that predict survival. NPJ Precis Oncol 2023; 7: 105 [PMID: 37857854 DOI: 10.1038/s41698-023-00455-z]

26 **Hendley AM**, Rao AA, Leonhardt L, Ashe S, Smith JA, Giacometti S, Peng XL, Jiang H, Berrios DI, Pawlak M, Li LY, Lee J, Collisson EA, Anderson MS, Fragiadakis GK, Yeh JJ, Ye CJ, Kim GE, Weaver VM, Hebrok M. Single-cell transcriptome analysis defines heterogeneity of the murine pancreatic ductal tree. Elife 2021; 10 [PMID: 34009124 DOI: 10.7554/eLife.67776]

27 **Tolaymat M**, Sundel MH, Alizadeh M, Xie G, Raufman JP. Potential Role for Combined Subtype-Selective Targeting of M(1) and M(3) Muscarinic Receptors in Gastrointestinal and Liver Diseases. Front Pharmacol 2021; 12: 786105 [PMID: 34803723 DOI: 10.3389/fphar.2021.786105]

28 **Datta J**, Dai X, Bianchi A, De Castro Silva I, Mehra S, Garrido VT, Lamichhane P, Singh SP, Zhou Z, Dosch AR, Messaggio F, Ban Y, Umland O, Hosein PJ, Nagathihalli NS, Merchant NB. Combined MEK and STAT3 Inhibition Uncovers Stromal Plasticity by Enriching for Cancer-Associated Fibroblasts With Mesenchymal Stem Cell-Like Features to Overcome Immunotherapy Resistance in Pancreatic Cancer. Gastroenterology 2022; 163: 1593-1612 [PMID: 35948109 DOI: 10.1053/j.gastro.2022.07.076]

29 **Siriviriyakul P**, Sriko J, Somanawat K, Chayanupatkul M, Klaikeaw N, Werawatganon D. Genistein attenuated oxidative stress, inflammation, and apoptosis in L-arginine induced acute pancreatitis in mice. *BMC Complement Med Ther* 2022; **22**: 208 [PMID: 35927726 DOI: 10.1186/s12906-022-03689-9]

30 **Kaur J**, Sidhu S, Chopra K, Khan MU. Calendula officinalis ameliorates l-arginine-induced acute necrotizing pancreatitis in rats. *Pharm Biol* 2016; **54**: 2951-2959 [PMID: 27339751 DOI: 10.1080/13880209.2016.1195848]

31 **Perides G**, Laukkarinen JM, Vassileva G, Steer ML. Biliary acute pancreatitis in mice is mediated by the G-protein-coupled cell surface bile acid receptor Gpbar1. *Gastroenterology* 2010; **138**: 715-725 [PMID: 19900448 DOI: 10.1053/j.gastro.2009.10.052]

32 **Gardner TB**. Acute Pancreatitis. *Ann Intern Med* 2021; **174**: ITC17-ITC32 [PMID: 33556276 DOI: 10.7326/AITC202102160]

33 **Jakkampudi A**, Jangala R, Reddy R, Mitnala S, Rao GV, Pradeep R, Reddy DN, Talukdar R. Acinar injury and early cytokine response in human acute biliary pancreatitis. *Sci Rep* 2017; **7**: 15276 [PMID: 29127325 DOI: 10.1038/s41598-017-15479-2]

34 **Chen L**, Zheng L, Chen P, Liang G. Myeloid Differentiation Primary Response Protein 88 (MyD88): The Central Hub of TLR/IL-1R Signaling. *J Med Chem* 2020; **63**: 13316-13329 [PMID: 32931267 DOI: 10.1021/acs.jmedchem.0c00884]

35 **Lawlor KE**, Feltham R, Yabal M, Conos SA, Chen KW, Ziehe S, Graß C, Zhan Y, Nguyen TA, Hall C, Vince AJ, Chatfield SM, D'Silva DB, Pang KC, Schroder K, Silke J, Vaux DL, Jost PJ, Vince JE. XIAP Loss Triggers RIPK3- and Caspase-8-Driven IL-1β Activation and Cell Death as a Consequence of TLR-MyD88-Induced cIAP1-TRAF2 Degradation. *Cell Rep* 2017; **20**: 668-682 [PMID: 28723569 DOI: 10.1016/j.celrep.2017.06.073]

36 **Ren Y**, Yang B, Guo G, Zhang J, Sun Y, Liu D, Guo S, Wu Y, Wang X, Wang S, Zhang W, Guo X, Li X, Li R, He J, Zhou Z. GBP2 facilitates the progression of glioma *via* regulation of KIF22/EGFR signaling. *Cell Death Discov* 2022; **8**: 208 [PMID: 35436989 DOI: 10.1038/s41420-022-01018-0]

37 **Yu S**, Yu X, Sun L, Zheng Y, Chen L, Xu H, Jin J, Lan Q, Chen CC, Li M. GBP2 enhances glioblastoma invasion through Stat3/fibronectin pathway. *Oncogene* 2020; **39**: 5042-5055 [PMID: 32518375 DOI: 10.1038/s41388-020-1348-7]

38 **Qi-Xiang M**, Yang F, Ze-Hua H, Nuo-Ming Y, Rui-Long W, Bin-Qiang X, Jun-Jie F, Chun-Lan H, Yue Z. Intestinal TLR4 deletion exacerbates acute pancreatitis through gut microbiota dysbiosis and Paneth cells deficiency. *Gut Microbes* 2022; **14**: 2112882 [PMID: 35982604 DOI: 10.1080/19490976.2022.2112882]

39 **Tan JH**, Cao RC, Zhou L, Zhou ZT, Chen HJ, Xu J, Chen XM, Jin YC, Lin JY, Zeng JL, Li SJ, Luo M, Hu GD, Yang XB, Jin J, Zhang GW. ATF6 aggravates acinar cell apoptosis and injury by regulating p53/AIFM2 transcription in Severe Acute Pancreatitis. *Theranostics* 2020; **10**: 8298-8314 [PMID: 32724472 DOI: 10.7150/thno.46934]

40 **Abdelzaher WY**, Ahmed SM, Welson NN, Marraiki N, Batiha GE, Kamel MY. Vinpocetine ameliorates L-arginine induced acute pancreatitis *via* Sirt1/Nrf2/TNF pathway and inhibition of oxidative stress, inflammation, and apoptosis. *Biomed Pharmacother* 2021; **133**: 110976 [PMID: 33202281 DOI: 10.1016/j.biopha.2020.110976]

41 **Wang X**, Cai H, Chen Z, Zhang Y, Wu M, Xu X, Yang L. Baicalein alleviates pyroptosis and inflammation in hyperlipidemic pancreatitis by inhibiting NLRP3/Caspase-1 pathway through the miR-192-5p/TXNIP axis. *Int Immunopharmacol* 2021; **101**: 108315 [PMID: 34785144 DOI: 10.1016/j.intimp.2021.108315]

42 **Zenón-Meléndez CN**, Carrasquillo Carrión K, Cantres Rosario Y, Roche Lima A, Meléndez LM. Inhibition of Cathepsin B and SAPC Secreted by HIV-Infected Macrophages Reverses Common and Unique Apoptosis Pathways. *J Proteome Res* 2022; **21**: 301-312 [PMID: 34994563 DOI: 10.1021/acs.jproteome.1c00187]

43 **Zhang Y**, Wu J, Fu Y, Yu R, Su H, Zheng Q, Wu H, Zhou S, Wang K, Zhao J, Shen S, Xu G, Wang L, Yan C, Zou X, Lv Y, Zhang S. Hesperadin suppresses pancreatic cancer through ATF4/GADD45A axis at nanomolar concentrations. *Oncogene* 2022; **41**: 3394-3408 [PMID: 35551503 DOI: 10.1038/s41388-022-02328-4]

44 **Wang M**, Tian B, Shen J, Xu S, Liu C, Guan L, Guo M, Dou J. Bavachin induces apoptosis in colorectal cancer cells through Gadd45a *via* the MAPK signaling pathway. *Chin J Nat Med* 2023; **21**: 36-46 [PMID: 36641231 DOI: 10.1016/S1875-5364(23)60383-8]

World Journal of Gastroenterology

Submit a Manuscript: https://www.f6publishing.com

World J Gastroenterol 2024 April 14; 30(14): 2059-2067

DOI: 10.3748/wjg.v30.i14.2059

ISSN 1007-9327 (print) ISSN 2219-2840 (online)

CASE REPORT

Outcomes of endoscopic sclerotherapy for jejunal varices at the site of choledochojejunostomy (with video): Three case reports

Jun Liu, Peng Wang, Li-Mei Wang, Jing Guo, Ning Zhong

Specialty type: Gastroenterology and hepatology

Provenance and peer review: Unsolicited article; Externally peer reviewed.

Peer-review model: Single blind

Peer-review report's scientific quality classification

Grade A (Excellent): 0
Grade B (Very good): B, B
Grade C (Good): 0
Grade D (Fair): 0
Grade E (Poor): 0

P-Reviewer: Salvadori M, Italy; Yoshida H, Japan

Received: January 2, 2024
Peer-review started: January 2, 2024
First decision: January 30, 2024
Revised: February 9, 2024
Accepted: March 26, 2024
Article in press: March 26, 2024
Published online: April 14, 2024

Jun Liu, Peng Wang, Li-Mei Wang, Jing Guo, Ning Zhong, Department of Gastroenterology, Qilu Hospital of Shandong University, Jinan 250012, Shandong Province, China

Corresponding author: Ning Zhong, MD, PhD, Professor, Department of Gastroenterology, Qilu Hospital of Shandong University, No. 107 Wenhua West Road, Jinan 250012, Shandong Province, China. nathan.zhongning@foxmail.com

Abstract

BACKGROUND

Hemorrhage associated with varices at the site of choledochojejunostomy is an unusual, difficult to treat, and often fatal manifestation of portal hypertension. So far, no treatment guidelines have been established.

CASE SUMMARY

We reported three patients with jejunal varices at the site of choledochojejunostomy managed by endoscopic sclerotherapy with lauromacrogol/α-butyl cyanoacrylate injection at our institution between June 2021 and August 2023. We reviewed all patient records, clinical presentation, endoscopic findings and treatment, outcomes and follow-up. Three patients who underwent pancreaticoduodenectomy with a Whipple anastomosis were examined using conventional upper gastrointestinal endoscopy for suspected hemorrhage from the afferent jejunal loop. Varices with stigmata of recent hemorrhage or active hemorrhage were observed around the choledochojejunostomy site in all three patients. Endoscopic injection of lauromacrogol/α-butyl cyanoacrylate was carried out at jejunal varices for all three patients. The bleeding ceased and patency was observed for 26 and 2 months in two patients. In one patient with multiorgan failure and internal environment disturbance, rebleeding occurred 1 month after endoscopic sclerotherapy, and despite a second endoscopic sclerotherapy, repeated episodes of bleeding and multiorgan failure resulted in eventual death.

CONCLUSION

We conclude that endoscopic sclerotherapy with lauromacrogol/α-butyl cyanoacrylate injection can be an easy, effective, safe and low-cost treatment option for jejunal varicose bleeding at the site of choledochojejunostomy.

Key Words: Endoscopic sclerotherapy; Jejunal varices; Choledochojejunostomy; Portal vein hypertension; Case report

Core Tip: This is the first series of case reports on endoscopic sclerotherapy for venous varices at the choledochojejunostomy, including videos. From the experiences of our center, endoscopic sclerotherapy with lauromacrogol/α-butyl cyanoacrylate injection may be considered as an easy, cost-effective and efficient treatment option for hemorrhage from venous varices at the choledochojejunostomy site. For patients without complications, underlying diseases, and significant organ dysfunction, as well as those who have undergone pancreaticoduodenectomy for benign diseases, endoscopic sclerotherapy tends to have better outcomes.

Citation: Liu J, Wang P, Wang LM, Guo J, Zhong N. Outcomes of endoscopic sclerotherapy for jejunal varices at the site of choledochojejunostomy (with video): Three case reports. *World J Gastroenterol* 2024; 30(14): 2059-2067
URL: https://www.wjgnet.com/1007-9327/full/v30/i14/2059.htm
DOI: https://dx.doi.org/10.3748/wjg.v30.i14.2059

INTRODUCTION

The prevalence of gastrointestinal hemorrhage from ectopic varices is relatively low, ranging from 1% to 5%[1,2]. Bilioenteric anastomosis is an uncommonly affected site of ectopic variceal bleeding[3]. Hemorrhage associated with varices at the site of choledochojejunostomy is an unusual, difficult to treat, and often fatal manifestation of portal hypertension (PHT). The possible cause of hemorrhage from ruptured jejunal varices could be extrahepatic portal vein obstruction or stenosis at the site where choledochojejunostomy was previously carried out, which leads to the development of hepatopetal portal collaterals through the anastomosis and PHT[4,5].

Diagnosis of ectopic variceal hemorrhage at a bilioenteric anastomosis can be difficult because varices are located deep within the jejunal loop and factors such as postsurgical adhesions make early detection of the bleeding source more difficult[6]. Treatment of ectopic variceal hemorrhage at bilioenteric anastomoses can be challenging because of their hemodynamic complexity. So far, no treatment guidelines have been established, so it may require a multidisciplinary approach and depend on the patient's conditions[7]. There are two treatment choices: Portal decompression and obliteration of the varices[8-11]. Endoscopic sclerotherapy has been reported as a minimally invasive therapeutic method for jejunal varices[12-14].

We report three patients with jejunal varices at the site of choledochojejunostomy managed by endoscopic sclerotherapy with lauromacrogol/α-butyl cyanoacrylate injection. We highlight the outcomes of endoscopic sclerotherapy for such rare causes of bleeding, and analyze the possible factors affecting treatment effectiveness.

CASE PRESENTATION

Chief complaints

Case 1: A 25-year-old woman was admitted to hospital because of hematemesis, melena and hematochezia for 1 wk (Table 1).

Case 2: A 55-year-old man was admitted to our hospital with hematochezia for 1 month and hematemesis for 12 d (Table 1).

Case 3: A 68-year-old man presented to our hospital with intermittent melena, dizziness and fatigue for 1 month (Table 1).

History of present illness

Case 1: Local laboratory tests showed a minimum hemoglobin level of 45 g/L, which necessitated blood transfusions for 8 months. The location of the bleeding could not be definitively identified by repeated gastroscopy and colonoscopy.

Case 2: Gastroscopy and angiography at the local hospital did not definitively identify the site of bleeding.

Case 3: Gastroscopy at the local hospital revealed esophageal and gastric varices, no signs of bleeding.

History of past illness

Case 1: The patient had undergone pancreaticoduodenectomy with a Whipple anastomosis for a solid pseudopapillary tumor of the pancreas 29 months prior to the current visit. Eighteen days after surgery, follow-up computed tomography (CT) revealed formation of thrombosis in the portal vein and superior mesenteric vein, and anticoagulation therapy was administered.

Table 1 The patients' basic information and clinical data

Patient No.	Age (yr)	Sex	Primary disease	Duration from operation to admission	Injection mixture composition	Pre-Clipping	Carvedilol intake	Rebleeding
1	25	Female	Solid pseudopapillary tumor of pancreas	29 months	Auromacrogol/α-butyl cyanoacrylate (5.0/0.5 mL)	No	No	No
2	55	Male	Cholangio; carcinoma	14 months	Lauromacrogol/α-butyl cyanoacrylate (12/1 mL)	Yes	No	Yes
3	68	Male	Cholangio; carcinoma	47 months	Lauromacrogol/α-butyl cyanoacrylate (30/3 mL)	No	Yes	No

Case 2: He had undergone pancreaticoduodenectomy 14 months previously with a Whipple anastomosis for moderately to poorly differentiated adenocarcinoma of the bile duct. The portal vein and the right wall of the superior mesenteric vein were affected by tumor invasion and were partially resected during the operation.

Case 3: He had undergone pancreaticoduodenectomy with a Whipple-Braun anastomosis for moderately differentiated adenocarcinoma of the bile duct (pathological staging pT2N0) 47 months previously.

Personal and family history

All the three patients denied any family history of genetic disease and malignant tumours.

Physical examination

Case 1: The vital sign were as follows: Blood pressure, 104/72 mmHg; heart rate, 104 beats per min.

Case 2: On physical examination, the vital sign were as follows: Blood pressure, 121/63 mmHg; heart rate, 83 beats per min. Furthermore, anemic appearance and right abdominal tenderness were detected.

Case 3: On physical examination, the vital sign were as follows: Blood pressure, 121/74 mmHg; heart rate, 75 beats per min.

Laboratory examinations

Case 1: Hemoglobin: 77.0 g/L; white blood counts (WBC): 19.94 × 10^9/L; platelet (PLT): 97 × 10^9/L.

Case 2: After admission, laboratory assessments revealed that the patient had heart failure, kidney failure and severe internal environment disorder. Hemoglobin: 73.0 g/L; PLT: 98 × 10^9/L; blood urea nitrogen: 42.70 mmol/L; serum creatinine: 367 μmol/L; carbon dioxide combining power: 6.5 mmol/L; carbohydrate antigen 19-9: 42.85 U/mL.

Case 3: Hemoglobin: 84.0 g/L; WBC: 3.46 × 10^9/L; PLT: 104 × 10^9/L.

Imaging examinations

Case 1: After another episode of hematochezia, emergency gastroscopic examination the afferent loop revealed tortuous dilated blood vessels around the choledochojejunostomy site (Figure 1A), along with mucosal rupture (Figure 1B). Endoscopic ultrasonography confirmed the presence of numerous varicose veins near the choledochojejunostomy site, with abundant blood flow (Figure 1C).

Case 2: A nonenhanced abdominal CT scan revealed liver cirrhosis and PHT. With adequate adjustment of the internal environment and continuous renal replacement therapy, we performed emergency endoscopy on the afferent loop, which revealed a significant number of tortuous dilated varicose veins near the choledochojejunostomy site, along with several sites of active bleedings (Figure 1D).

Case 3: CT showed prehepatic PHT, suspicious tumor recurrence in the hepatic hilum area, and varices around the choledochojejunostomy site (Figure 1E). Gastroscopy and colonoscopy detected no particular bleeding point, and only detected nonbleeding signs of esophageal and gastric fundus varices. From these findings, his condition was suspected to be due to repeated rupturing of jejunal varices of the afferent loop, which had developed because of extrahepatic portal venous obstruction at the hepatic hilum area. Colonoscopy was undertaken to assess the possible varices around the choledochojejunostomy site at the afferent loop. There were three varicose veins visible with signs of erythema (Figure 1F) and thrombus head (Figure 1G), along with spontaneous bleeding (Figure 1H).

FINAL DIAGNOSIS

The final diagnosis of the three patients were jejunal varices at the site of choledochojejunostomy.

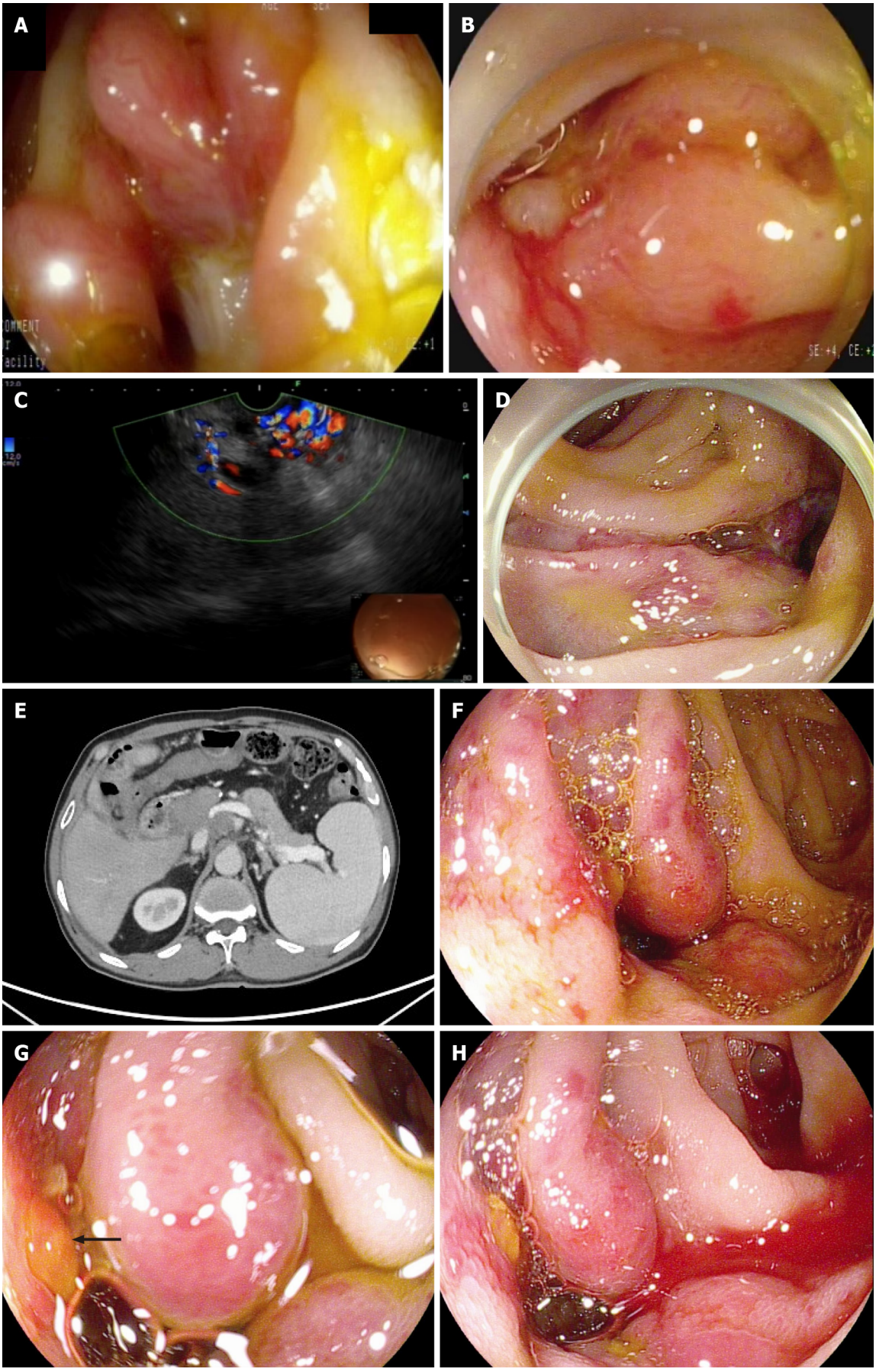

Figure 1 Emergency endoscopy confirmed the presence of numerous varicose veins before endoscopic sclerotherapy and was validated by endoscopic ultrasonography. A: Emergency gastroscopy revealed tortuous dilated blood vessels around the choledochojejunostomy site (Case 1); B: A

mucosal rupture was detected with spontaneous bleeding (Case 1); C: Endoscopic ultrasonography confirmed the presence of numerous varicose veins with abundant blood flow (Case 1); D: Emergency gastroscopy revealed a significant number of tortuous dilated varicose veins near the choledochojejunostomy site, along with several active bleedings. Hemostatic clips were used before endoscopic sclerotherapy (Case 2); E: Computed tomography showed prehepatic portal hypertension, suspicious tumor recurrence in the hepatic hilum area and the formation of varices around the choledochojejunostomy site (Case 3); F: Colonoscopy revealed three varicose veins visible with signs of erythema (Case 3); G: Thrombus head (arrow) was detected (Case 3); H: Spontaneous bleeding was observed at the site of varicose veins (Case 3).

TREATMENT

Case 1

Injection sclerotherapy with lauromacrogol/α-butyl cyanoacrylate (5.0/0.5 mL) was carried out at the mucosal rupture (Figure 2A). Vascular angiography showed a patent portal vein and segmental occlusion of the superior mesenteric vein with old mural thrombus (arrow, Figure 2B). Therefore, balloon angioplasty of the superior mesenteric vein was not feasible. Considering the risk of bleeding, anticoagulant medication was not administered.

Case 2

Hemostatic clips were used to close off the bleeding points. Subsequently, combined injection of lauromacrogol/α-butyl cyanoacrylate (12/1 mL) was administered to the varicose veins (Figure 2C).

Case 3

A sandwich method was used to inject a mixture of lauromacrogol/α-butyl cyanoacrylatepoly (30/3 mL) at multiple points for endoscopic sclerotherapy (Figure 2D and Video).

OUTCOME AND FOLLOW-UP

Case 1

Hemorrhage has remained stable for 27 months of follow-up.

Case 2

Rebleeding occurred 1 month after endoscopic sclerotherapy, and despite two further endoscopic sclerotherapy procedures, repeated episodes of bleeding and multi-organ failure resulted in eventual death.

Case 3

The patient developed moderate abdominal discomfort that disappeared within 2 d. He declined further examinations regarding tumor recurrence and was discharged with 6.25 mg carvedilol orally once daily after sclerotherapy to reduce portal vein pressure. One month later, the patient returned to the hospital for a follow-up examination. Enhanced CT revealed increased soft tissue density in the hepatic hilum, suggesting metastasis. There was also localized narrowing of the portal vein, with increased pressure on the right side of the narrowed segment. The peritoneum was thickened, and abdominal lymph nodes were enlarged (Figure 3A). The endoscopic follow-up revealed adhesive clumps and exudative ulcers near the choledochojejunostomy site, with no signs of bleeding (Figure 3B). The patient underwent endoscopic ultrasound-guided fine needle aspiration (EUS-FNA) of the hepatic hilum mass, which was confirmed to be high-grade intraepithelial neoplasia, suggesting metastasis. However, the patient declined portal vein stenting intervention and was subsequently discharged. Two months after undergoing endoscopic sclerotherapy, a follow-up call revealed the patient had no further gastrointestinal bleeding and continued to take carvedilol consistently.

DISCUSSION

Anastomotic jejunal varices are a rare and often easily ignored cause of bleeding from the gastrointestinal tract and are typically diagnosed in patients with portal vein hypertension due to cirrhotic or extrahepatic PHT[15,16]. In some patients who have previously undergone cholangiojejunostomy, portal vein hypertension may occur as a result of extrahepatic portal venous stenosis or obstruction, leading to the development of hepatopetal portal collaterals through the anastomosis in the afferent loop[17]. Extrahepatic portal venous stenosis or obstruction can result from thrombophlebitis of the portal or superior mesenteric vein associated with an infection, compression or invasion of the portal vein by benign and malignant tumor, radiation-induced portal vein stenosis, thrombosis caused by portal stasis associated with hepatic cirrhosis, or surgical adhesions[18,19]. The most likely causes in our patients were as follows. Case 1 was considered to have a long-segment occlusion in the superior mesenteric vein due to an obsolete thrombus associated with potential infection. Case 2 had a tumor invading the right wall of the portal vein and superior mesenteric vein, leading to an intraoperative vascular wall resection. In case 3, it was believed to have resulted from local stenosis of the portal vein caused by recurrence of a tumor at the hepatic portal region, leading to portal vein hypertension on the

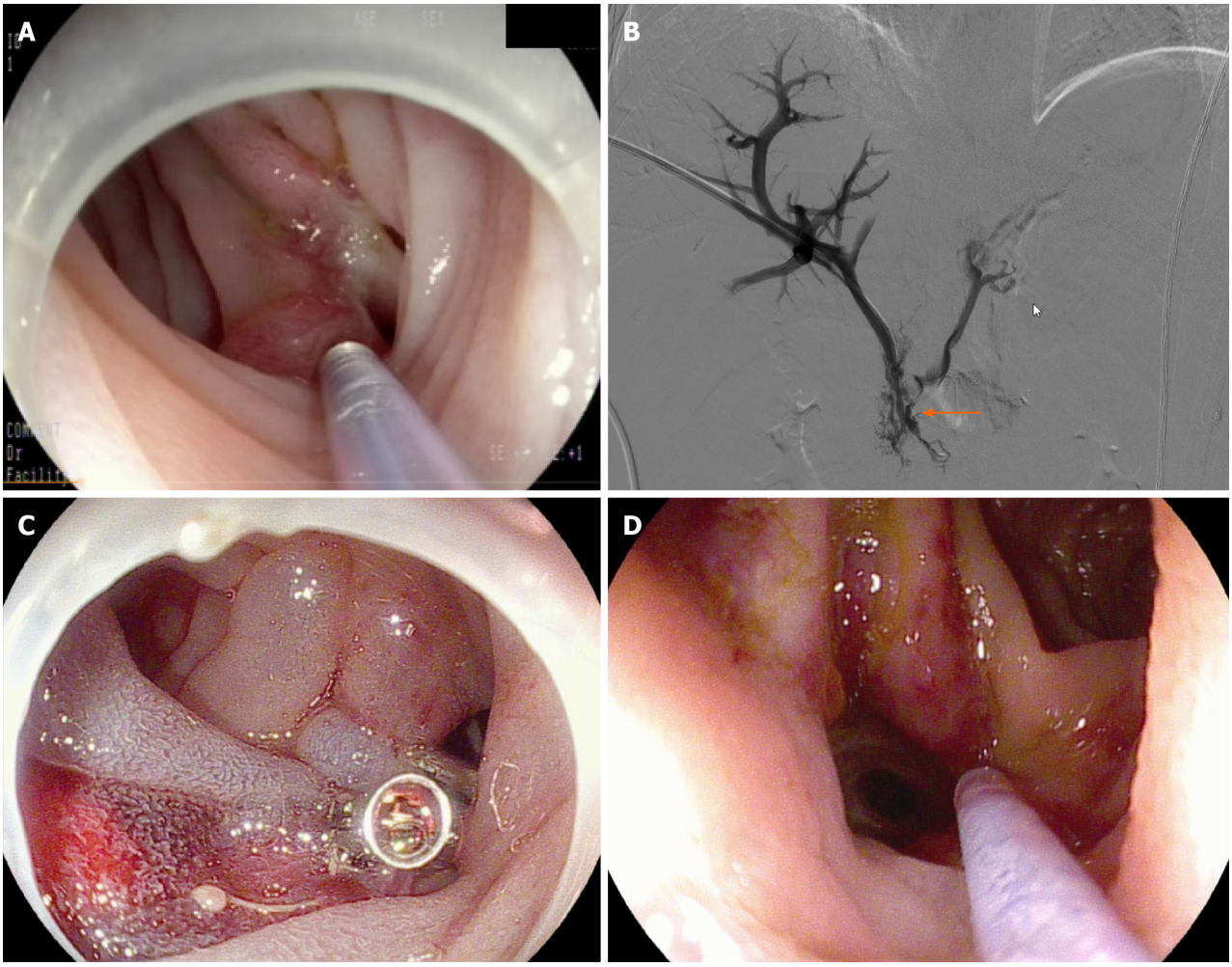

Figure 2 Hemostatic clips were used to close off the bleeding points. A: Injection sclerotherapy mixture of lauromacrogol/α-butyl cyanoacrylate (5.0/0.5 mL) (Case 1); B: Vascular angiography showed a patent portal vein, but a segment occlusion of the superior mesenteric vein with old mural thrombus (arrow) (Case 1); C: A combined injection of lauromacrogol/α-butyl cyanoacrylate (12/1 mL) was administered at the varicose veins (Case 2); D: Endoscopic sclerotherapy with lauromacrogol/α-butyl cyanoacrylate (30/3 mL) injection for jejunal varices were carried out immediately (Case 3).

right side of the stenotic segment.

Although the number of long-term survival cases after cholangiojejunostomy has increased, only a few have so far been reported. Despite the low incidence, jejunal varices should be considered in the differential diagnosis of digestive bleeding in patients with a history of pancreaticoduodenectomy. Clinical features for variceal bleeding are similar to those of typical varices. Depending on the bleeding rate, venous varices at the site of cholangiojejunostomy can present with hematemesis, melena or hematochezia. Based on previous reports, venous varices at the site of cholangiojejunostomy can lead to hemorrhagic shock, often requiring multiple blood transfusions during the treatment process. All three patients we reported received multiple blood transfusions during treatment.

Ectopic varices at the site of cholangiojejunostomy, which can trigger life-threatening bleeding, are usually overlooked in the differential diagnosis when hemorrhage occurs, owing to the length of small bowel, tortuosity and the intermittent nature of bleeding[3]. Enteroscopy can serve as an effective interventional diagnostic tool with therapeutic capabilities [14]. For patients who have undergone the Whipple procedure, experienced endoscopists can also reach the site of choledochojejunostomy using conventional gastroscopy and colonoscopy, and endoscopic treatment can also be performed. Capsule endoscopy cannot show the anastomosis because it is in the afferent limb[20].

Treatment of jejunal loop varices is difficult and has no definitive conclusion because of their hemodynamic complexity. Two treatment options are available: Obliteration of the varices (by endoscopic sclerotherapy or ligation, embolization using interventional radiology, surgery for re-anastomosis); and portal decompression (by portal venous dilatation and stent placement, splenectomy, and shunt operation)[9,21-26]. A multidisciplinary approach with the cooperation of endoscopists, interventional radiologists, and surgeons is critical for timely treatment of these patients [27]. The choice of treatment strategy depends on the patient's overall condition, and the physician's skill and equipment available at the institution. Norton *et al*[12]. used an algorithmic approach for treatment, and endoscopic therapy was recommended as the primary option. Embolization, surgical shunt or transjugular intrahepatic portosystemic shunt should be taken into consideration if the hemorrhage cannot be successfully controlled by endoscopic therapy and the portal vein is patent. Surgical ligation should be selected if the portal vein is obstructed. In summary, endoscopic therapy should be the first-choice management for ectopic variceal bleeding. Additionally, second or third rounds of treatment

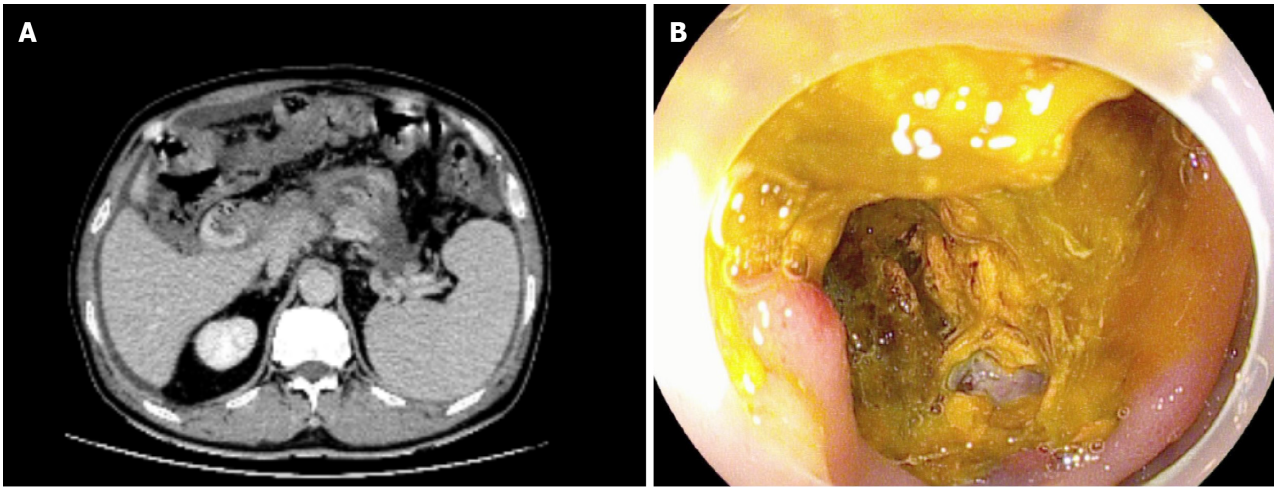

Figure 3 Endoscopic re-examination confirmed no signs of bleeding after endoscopic sclerotherapy (Case 3). A: Follow-up enhanced computed tomography revealed increased soft tissue density in the hepatic hilum, suggesting metastasis; B: Follow-up endoscopy revealed adhesive clumps and exudative ulcers near the choledochojejunostomy site, with no signs of bleeding observed.

should be taken into consideration, because control of ectopic bleeding is sometimes difficult[5].

In case 1, vascular angiography showed patent portal vein blood flow, but the superior mesenteric vein was occluded due to chronic thrombosis, making balloon angioplasty with stent placement impossible. For case 2, the previous surgical records indicated that the primary tumor had a wide-ranging involvement, affecting the portal vein and superior mesenteric vein. The patient's poor general physical condition and cardiac and renal functions led him ultimately to decide upon repeated endoscopic sclerotherapy as the treatment option. For case 3, CT confirmed the presence of a soft tissue mass in the hepatic hilum area, which encased and compressed the portal vein, resulting in significant narrowing. EUS-FNA was inclined towards a possible recurrence. However, the patient ultimately refused the placement of a portal vein stent.

Some factors may affect the clinical outcomes of endoscopic sclerotherapy for variceal bleeding at the site of cholangiojejunostomy. The severity of varices can affect the difficulty and success rate of treatment. More severe varices may require more treatment sessions or a greater amount of sclerosant, increasing the risk and complexity of the treatment. The overall condition of the patient can influence the risk and recovery of the procedure. Some patients may have failure of other organs that could increase the risk of treatment. The endoscopist's expertise and skill can directly affect the success rate of treatment and the incidence of complications. Post-treatment follow-up and strategies to prevent recurrence are also crucial factors. From the prospective of pathophysiology, beta-blockers make sense in patients with ectopic varices[28]. Case 3 has been regularly taking carvedilol after sclerotherapy to reduce portal vein pressure; however, large-scale clinical data are still needed to evaluate the benefits of using carvedilol in patients with varices at the biliary-enteric anastomosis.

There were some limitations to the current study. First, the results were obtained retrospectively, and the number of cases was small. However, due to the short survival period caused by the underlying neoplastic disease and post-pancreaticoduodenectomy, as well as the low incidence of venous varices at the choledochojejunostomy site, there are a small number of reports of these patients. Further studies with larger sample size or prospective cohort studies are needed to confirm the safety and effectiveness. Second, all endoscopic sclerotherapeutic procedures were performed by an endoscopist at a single center. Therefore, it is difficult to generalize the current results. Despite these limitations, to our knowledge, this is the first series of case reports on endoscopic sclerotherapy for venous varices at the choledochojejunostomy site, including videos.

CONCLUSION

Endoscopic sclerotherapy with lauromacrogol/α-butyl cyanoacrylate injection may be considered as an easy, cost-effective and efficient treatment option for hemorrhage from venous varices at the choledochojejunostomy site in patients who have undergone pancreaticoduodenectomy. For patients without complications, underlying diseases, and significant organ dysfunction, as well as those who have undergone pancreaticoduodenectomy for benign diseases, endoscopic sclerotherapy tends to have better outcomes. The treatment of this rare cause of bleeding will increasingly require a multidisciplinary approach and personalized treatment choices in the future.

FOOTNOTES

Author contributions: Liu J designed the research study; Liu J and Wang P analyzed the data and wrote the manuscript; Wang LM and

Guo J performed the primary literature and data extraction; Zhong N was responsible for revising the manuscript; and all authors read and approved the final version.

Informed consent statement: All study participants or their legal guardian provided informed written consent about personal and medical data collection prior to study enrolment.

Conflict-of-interest statement: The authors declare no conflicts of interest for this article.

CARE Checklist (2016) statement: The authors have read the CARE Checklist (2016), and the manuscript was prepared and revised according to the CARE Checklist (2016).

Country/Territory of origin: China

ORCID number: Ning Zhong 0009-0002-5315-8197.

S-Editor: Fan JR
L-Editor: A
P-Editor: Zheng XM

REFERENCES

1 **Wilson SE**, Stone RT, Christie JP, Passaro E Jr. Massive lower gastrointestinal bleeding from intestinal varices. *Arch Surg* 1979; **114**: 1158-1161 [PMID: 314792 DOI: 10.1001/archsurg.1979.01370340064011]
2 **Sato T**, Akaike J, Toyota J, Karino Y, Ohmura T. Clinicopathological features and treatment of ectopic varices with portal hypertension. *Int J Hepatol* 2011; **2011**: 960720 [PMID: 21994879 DOI: 10.4061/2011/960720]
3 **Watanabe N**, Toyonaga A, Kojima S, Takashimizu S, Oho K, Kokubu S, Nakamura K, Hasumi A, Murashima N, Tajiri T. Current status of ectopic varices in Japan: Results of a survey by the Japan Society for Portal Hypertension. *Hepatol Res* 2010; **40**: 763-776 [PMID: 20649816 DOI: 10.1111/j.1872-034X.2010.00690.x]
4 **Hiraoka K**, Kondo S, Ambo Y, Hirano S, Omi M, Okushiba S, Katoh H. Portal venous dilatation and stenting for bleeding jejunal varices: report of two cases. *Surg Today* 2001; **31**: 1008-1011 [PMID: 11766071 DOI: 10.1007/s005950170013]
5 **Sasamoto A**, Kamiya J, Nimura Y, Nagino M. Successful embolization therapy for bleeding from jejunal varices after choledochojejunostomy: report of a case. *Surg Today* 2010; **40**: 788-791 [PMID: 20676866 DOI: 10.1007/s00595-009-4129-z]
6 **Hekmat H**, Al-toma A, Mallant MP, Mulder CJ, Jacobs MA. Endoscopic N-butyl-2-cyanoacrylate (Histoacryl) obliteration of jejunal varices by using the double balloon enteroscope. *Gastrointest Endosc* 2007; **65**: 350-352 [PMID: 17259003 DOI: 10.1016/j.gie.2006.07.001]
7 **Wakasugi M**, Tsujie M, Goda S, Ohnishi K, Koga C, Tei M, Kawabata R, Hasegawa J. Laparotomy-assisted transcatheter variceal embolization for bleeding jejunal varices formed at the site of choledochojejunostomy: Report of a case and review of the literature. *Int J Surg Case Rep* 2020; **77**: 554-559 [PMID: 33395844 DOI: 10.1016/j.ijscr.2020.11.091]
8 **Sato T**, Yasui O, Kurokawa T, Hashimoto M, Asanuma Y, Koyama K. Jejunal varix with extrahepatic portal obstruction treated by embolization using interventional radiology: report of a case. *Surg Today* 2003; **33**: 131-134 [PMID: 12616377 DOI: 10.1007/s005950300029]
9 **Sakai M**, Nakao A, Kaneko T, Takeda S, Inoue S, Yagi Y, Okochi O, Ota T, Ito S. Transhepatic portal venous angioplasty with stenting for bleeding jejunal varices. *Hepatogastroenterology* 2005; **52**: 749-752 [PMID: 15966197]
10 **Sone M**, Arai Y, Morita S, Tomimatsu H, Sugawara S, Ishii H, Takeuchi Y. Percutaneous creation of an extraanatomic splenoportal shunt in a patient with bleeding ectopic varices. *J Vasc Interv Radiol* 2014; **25**: 1301-1303 [PMID: 25085063 DOI: 10.1016/j.jvir.2014.05.006]
11 **Abdalla AO**, Abdallah MA, Calvo LA. Successful Treatment of a Case of Ectopic Jejunal Varices with Portal Venous Stenting. *Am J Case Rep* 2019; **20**: 948-952 [PMID: 31266933 DOI: 10.12659/AJCR.916003]
12 **Norton ID**, Andrews JC, Kamath PS. Management of ectopic varices. *Hepatology* 1998; **28**: 1154-1158 [PMID: 9755256 DOI: 10.1002/hep.510280434]
13 **Prachayakul V**, Aswakul P, Kachintorn U. Bleeding hepaticojejunostomy anastomotic varices successfully treated with Histoacryl injection, using single-balloon enteroscopy. *Endoscopy* 2011; **43** Suppl 2 UCTN: E153 [PMID: 21563058 DOI: 10.1055/s-0030-1256233]
14 **Takashima K**, Matsui S, Komeda Y, Nagai T, Toshiharu S, Kashida H, Kudo M. Endoscopic sclerotherapy under balloon-assisted enteroscopy for hemorrhagic jejunal varices after choledocho-jejunostomy. *Endoscopy* 2020; **52**: E41-E42 [PMID: 31434157 DOI: 10.1055/a-0987-9780]
15 **Akhter NM**, Haskal ZJ. Diagnosis and management of ectopic varices. *Gastrointest Interv* 2012; **1**: 3-10 [DOI: 10.1016/j.gii.2012.08.001]
16 **Kastanakis M**, Anyfantakis D, Katsougris N, Bobolakis E. Massive gastrointestinal bleeding due to isolated jejunal varices in a patient without portal hypertension. *Int J Surg Case Rep* 2013; **4**: 439-441 [PMID: 23528981 DOI: 10.1016/j.ijscr.2013.01.029]
17 **Heiberger CJ**, Mehta TI, Yim D. Jejunal varices: an unconsidered cause of recurrent gastrointestinal haemorrhage. *BMJ Case Rep* 2019; **12** [PMID: 30850571 DOI: 10.1136/bcr-2018-228680]
18 **Moncure AC**, Waltman AC, Vandersalm TJ, Linton RR, Levine FH, Abbott WM. Gastrointestinal hemorrhage from adhesion-related mesenteric varices. *Ann Surg* 1976; **183**: 24-29 [PMID: 1082310 DOI: 10.1097/00000658-197601000-00005]
19 **Sakurai K**, Amano R, Yamamoto A, Nishida N, Matsutani S, Hirata K, Kimura K, Muguruma K, Toyokawa T, Kubo N, Tanaka H, Yashiro M, Ohira M, Hirakawa K. Portal vein stenting to treat portal vein stenosis in a patient with malignant tumor and gastrointestinal bleeding. *Int Surg* 2014; **99**: 91-95 [PMID: 24444277 DOI: 10.9738/INTSURG-D-13-00128.1]

20 **Ali S**, Asad Ur Rahman, Navaneethan U. An Unusual Cause of Recurrent Gastrointestinal Bleeding After Whipple's Surgery. *Gastroenterology* 2017; **153**: e1-e2 [PMID: 28672119 DOI: 10.1053/j.gastro.2016.12.046]

21 **Saeki Y**, Ide K, Kakizawa H, Ishikawa M, Tashiro H, Ohdan H. Controlling the bleeding of jejunal varices formed at the site of choledochojejunostomy: report of 2 cases and a review of the literature. *Surg Today* 2013; **43**: 550-555 [PMID: 22777133 DOI: 10.1007/s00595-012-0243-4]

22 **Taniguchi H**, Moriguchi M, Amaike H, Fuji N, Murayama Y, Kosuga T. Hemorrhage from varices in hepaticojejunostomy in the fifth and tenth year after surgery for hepatic hilar bile duct cancer: a case report. *Cases J* 2008; **1**: 59 [PMID: 18652705 DOI: 10.1186/1757-1626-1-59]

23 **Rezende-Neto JB**, Petroianu A, Santana SK. Subtotal splenectomy and central splenorenal shunt for treatment of bleeding from Roux en Y jejunal loop varices secondary to portal hypertension. *Dig Dis Sci* 2008; **53**: 539-543 [PMID: 17597406 DOI: 10.1007/s10620-007-9878-1]

24 **Ota S**, Suzuki S, Mitsuoka H, Unno N, Inagawa S, Takehara Y, Sakaguchi T, Konno H, Nakamura S. Effect of a portal venous stent for gastrointestinal hemorrhage from jejunal varices caused by portal hypertension after pancreatoduodenectomy. *J Hepatobiliary Pancreat Surg* 2005; **12**: 88-92 [PMID: 15754107 DOI: 10.1007/s00534-004-0941-4]

25 **Maeda N**, Maruyama H, Higashimori A, Ominami M, Fukunaga S, Nagami Y, Fujiwara Y. Successful treatment using balloon-assisted enteroscopy for jejunal loop variceal bleeding after pancreaticoduodenectomy. *Endoscopy* 2023; **55**: E536-E537 [PMID: 36931298 DOI: 10.1055/a-2037-5581]

26 **Nasr S**, Dahmani W, Jaziri H, Becheikh Y, Ameur WB, Elleuch N, Jmaa A. Massive hematochezia due to jejunal varices successfully treated with coil embolization. *Clin Case Rep* 2022; **10**: e6339 [PMID: 36188043 DOI: 10.1002/ccr3.6339]

27 **Kohli DR**, Levy MF, Smallfield GB. Laparotomy-Assisted Endoscopic Injection of Jejunal Varices for Overt Small Bowel Bleeding. *ACG Case Rep J* 2017; **4**: e79 [PMID: 28670593 DOI: 10.14309/crj.2017.79]

28 **Biecker E**. Portal hypertension and gastrointestinal bleeding: diagnosis, prevention and management. *World J Gastroenterol* 2013; **19**: 5035-5050 [PMID: 23964137 DOI: 10.3748/wjg.v19.i31.5035]

Published by **Baishideng Publishing Group Inc**
7041 Koll Center Parkway, Suite 160, Pleasanton, CA 94566, USA
Telephone: +1-925-3991568
E-mail: office@baishideng.com
Help Desk: https://www.f6publishing.com/helpdesk
https://www.wjgnet.com